12-2014

Reliability-Based Design and Acceptance Protocol for Driven Piles

Joseph Jabo
University of Arkansas, Fayetteville

Reliability-Based Design and Acceptance Protocol for Driven Piles

Reliability-Based Design and Acceptance Protocol for Driven Piles

A dissertation submitted in partial fulfillment
of the requirements for the degree of
Doctor of Philosophy in Civil Engineering

by

Joseph Jabo
PSG College of Technology affiliated to the University of Bharathiar
Bachelor of Engineering in Civil Engineering, 2002
University of Hannover
Master of Science for Geotechniques and Infrastructure in Civil Engineering and Geodetic Science, 2005

December 2014
University of Arkansas

This dissertation is approved for recommendation to the Graduate Council.

_____
Dr. Norman D. Dennis
Dissertation Director

_____
Dr. Richard A. Coffman
Committee Member

_____
Dr. Michelle L. Bernhardt
Committee Member

_____
Dr. Edward A. Pohl
Committee Member

Abstract

The current use of the Arkansas Standard Specifications for Highway Construction Manuals (2003, 2014) for driven pile foundations faces various limitations which result in designs of questionable reliability. These specifications are based on the Allowable Stress Design method (ASD), cover a wide range of uncertainties, do not take into account pile and soil types, and were developed for general use. To overcome these challenges it is deemed necessary to develop a new design and acceptance protocol for driven piles. This new protocol incorporates locally calibrated RLFD resistance factors for accounting for local design and construction experiences and practices, as well as specific soil conditions and pile types.

In that perspective, this dissertation focuses on the design and acceptance of driven pile foundations (predominately for bridge projects) using an LRFD protocol. A great deal of insight is gained into the factors that contribute to the performance of deep foundations by conducting an extensive literature review. The research assembled a relatively large database of pile load tests where both static and dynamic load testing was performed and sufficient soils information existed to perform static design calculations. A MATLAB® based program was developed to use the information contained in the database to compute resistance factors for driven piles using the First Order Second Moment Method (FOSM), Improved FOSM, the First Order Reliability Method (FORM), and Monte Carlo Simulations (MCS). The research also addressed a technique to update resistance factors using Bayesian techniques when new load tests are added to the database. More importantly the dissertation formulated a design and acceptance protocol that seeks to unify the level of reliability for deep foundations through both the design and construction phases.

As a verification mechanism to the developed design and acceptance protocol, a full-scale pile load testing program was recommended. The testing program would be composed of ten driven piles that had been dynamically and statically load tested. It was found that, for the same required reliability level, acceptance criteria could be lowered if more piles are tested on a jobsite. Subsequently, a non-contact instrument–such as Pile Driving Monitoring device–is recommended to verify in situ pile capacity of each and every pile on construction site. The results from in situ pile capacity verification could be employed to update the calibrated resistance factors and to refine future designs.

Acknowledgments

Special thanks are directed to my supervisor, Dr. Norman D. Dennis for his enthusiastic guidance, invaluable financial support and encouragement throughout my PhD program and in all aspects of this work. His numerous comments and suggestions during the preparation of this dissertation are gratefully acknowledged. His patience and availability for any help whenever needed with his heavy workload are appreciated.

Also, special thanks go out to the faculty and staff at the University of Arkansas for their commitment to the University and to the students. I would like to thank my advisory committee for its invaluable comments and suggestions, especially at the beginning of this dissertation.

My appreciation is also extended to fellow graduate students in Civil Engineering for their discussions, support and social interaction during my study. I would like to thank all academic and non-academic members of Civil Engineering, for their warm-hearted cooperation during my stay at the University of Arkansas.

Heartfelt acknowledgements are expressed to my late father and mother. Without their sacrifices, guidance and support, I may never have come this long journey in my studies. Very special and sincere gratitude is offered to my wife, Liliose, and my son, Kenny, for their love, patience and support during my graduate program. They are the source of strength behind this study.

Dedication

To my wife Liliose and my son Kenny

To all my family

Table of Contents

List of Tables

List of Figures

Chapter 1 Introduction

1.1 Overview on Implementation of LRFD Specifications

To ensure uniform reliability throughout the structure of a bridge, AASHTO LRFD bridge design specifications were developed. The intended benefits of these LRFD specifications include: an effective reliability approach of handling enormous amount of uncertainties encountered in geotechnical field, a consistent design approach for the entire bridge, optimum and cost effective design/acceptance procedures. Because of these intended advantages, the FHWA mandated on June 28, 2000 that all new bridges initiated after October 1, 2007 be designed using LRFD approach. Many DOTs and other design agencies have started to implement these specifications. Furthermore, local LRFD calibrations are underway to minimize the conservatism built in to the design process and to account for local construction experiences and practices.

The overall objectives of this research are to improve pile capacity agreement between design and monitoring phases and improve the current design and acceptance protocol through local calibration of resistance factors of driven piles. The study consists of evaluating the most utilized design and acceptance approaches for driven piles to unify the approach for each; collecting high quality data on driven piles in Arkansas, and performing robust statistical analyses on all collected data which lead to refined and hopefully higher, resistance factors.

To achieve the overall objectives a high quality database containing soil properties, pile driving records, and load test data for a large number of driven piles is developed. In the process of collecting designs, driving and testing data for this series of driven piles, guidance is developed for a pile monitoring program that allows future updates and improvements in resistance factors. In the future, this database can be supplemented with load test data from full-

scale production piles at various locations around the state of Arkansas.

1.2 Problem Definition

Following the FHWA memorandum issued on June 28, 2000 that all new bridges initiated after October 1, 2007 be designed using LRFD approach, the Arkansas Highway and Transportation Department (AHTD) recently adopted the AASHTO LRFD design procedures for designing its bridge foundations. However, the current methods utilized to design and accept pile construction work result in the use of very low resistance factors for driven piles. As a result, bridge foundations designed using LRFD procedures are significantly more expensive than those designed and constructed under the older allowable stress procedures (ASD). The low resistance factors currently used by the AHTD are those recommended by AASHTO LRFD Bridge design specifications (2004) for the particular design and acceptance procedures employed by the Department. These resistance factors are the result of a statistical calibration of measured to predict pile capacities based on a national, or international, database of pile load tests (Paikowsky et al., 2004). Recently, Dennis (2012) showed that this calibration at the national level produced resistance factors that were lower than those produced by data generated from piles that were driven in geological settings similar to Arkansas. The use of these low resistance factors in bridge design have resulted in either oversized piles, more piles in a bridge foundation, or showed a poor agreement between design and in-situ capacity values which led to a significant increase in cost for the entire structure.

Prediction of pile capacity using static design methods yields capacities that are often different from the capacities observed on site during pile driving. The main cause for this disparity is due to the wide range of uncertainties that are encountered in the geotechnical realm. The variability involved with sampling and soil property determination, along with the choice of

the design method, are the major sources of uncertainty during the design phase. The highest level of uncertainty during construction is associated with monitoring of the pile driving operation and the choice of method used to arrive at a driven pile capacity. Depending on the procedure or type of device used to measure or predict field capacity a wide number of factors could impact the prediction or measurement. These factors include the degree of disturbance of the soil during driving, soil - pile interaction, and changes in pile capacity over time due to setup or relaxation. These sources of uncertainty can lead to unacceptably high probabilities of service failure, which explains why very low resistance factors are being used in driven pile design. For instance, the AHTD traditionally used a factor of safety (FOS) of 4.0 during static capacity prediction design to account for all possible uncertainties. Current field verification procedures utilize the Engineering News Record Formula (ENR) which has a resistance factor of 0.1. This resistance factor, in combination with recommended load factors, yields an equivalent FOS of 14, which is more than three times the old FOS used during design and pile acceptance.

In addition to the uncertainties identified above there is non-agreement between pile capacities predicted during the design and monitoring phases due to the inherently different approaches used for design and acceptance. Because of the differing approaches used with design and acceptance procedures, it is inevitable that the predicted capacities will likely be different for given piles. During the design phase, static analysis methods are used to determine preliminary pile lengths and quantities. These prediction methods are often empirically based and require that all parameters relating to the capacity prediction (soil properties, driving methods, pile type, etc.) be similar to those encountered in the data set that was used to create the method to have an accurate prediction. During the construction phase, static load tests are seldom scheduled, most of the measures of pile capacity are semi-empirical and use dynamic

approaches, such as wave equation approach, signal matching technique, and dynamic formulas. Despite the use of these advanced prediction approaches, the capacity determination and drivability predictions for driven piles are often not in agreement with static design methods and still are far from satisfactory.

Given the serious nature of the problem caused by the lack of agreement between design and monitoring phases, it is imperative that a structurally sound and cost effective design and monitoring strategy be put in place. There is a need to recalibrate the AASHTO recommended resistance factors by incorporating local experiences that will reduce the amount of uncertainties introduced in LRFD-based design process and improve the pile capacity prediction, and possibly reduce the cost of the foundation. Much higher resistance factors can be locally adopted in design after a large-scale and high quality database is built. This database should be composed of local or regional static and dynamic pile load tests to facilitate the calibration.

1.3 Organization of the Dissertation

This dissertation includes 6 chapters. Chapter 1 introduces the implementation of the LRFD specifications, definition of the problem, research objectives, scope, and general research methodology and sequence of tasks involved in the research. Chapter 2 is a literature review pertaining to LRFD calibration, and includes discussion of the different reliability approaches, a typical framework for LRFD calibration, different pile analysis methods, and several nationwide case histories of the LRFD calibration. Chapter 3 deals with preliminary calibration of resistance factors based on reliability theory and using a database developed with local pile load tests data. In this chapter, methodologies for collecting pile information amassed in the database for pile capacity predictions and for data analysis are stated. Chapter 3 concludes with preliminary recommendations based only on the available information in the database. Chapter 4 introduces a

methodology for updating resistance factors based on a Bayesian approach. Factors affecting the updating process are identified through simulation studies and relevant conclusions are made. Chapter 5 deals with development of design and acceptance protocol by integrating the calibrated resistances factors and other findings into the process—where construction control methods impact the designs, and number of piles tested on a job site influences the acceptance criterion. Chapter 6 summarizes the major findings of the research and gives an overview of suggested future study.

1.4 Objectives of the Research

The purpose of the research is to create a well-structured framework for pile design and a construction monitoring and acceptance program that minimizes uncertainty and promotes agreement in predicting pile capacity between the two phases. A decrease in the level of uncertainty for a particular design approach to estimate the pile capacity is associated with an increase in the value of the resistance factor for a given level of reliability. Increases in resistance factors can reduce the high cost of piled foundations which currently result from high levels of uncertainty associated with both static design procedures and field acceptance procedures. The specific objectives are to:

Objective 1: Through a review of the literature, quantify the level of need for calibrating the resistance factors to account for different design and inspection methods allowed in the AASHTO LRFD Bridge Design Manual.

Objective 2: Calibrate resistance factors for design and field acceptance through the use of an improved pile load test database consisting of local load tests and improved soils information.

Objective 3: Unify static design predictions and dynamic field acceptance procedures so that a consistent and reliable driven pile capacity is obtained.

Objective 4: Produce a pile design and a driving monitoring protocol that guarantees the same level of reliability established during the local calibration process.

1.5 Scope, Methodology, and Tasks of the Research

The study examines the possibility of increasing the resistance factors in the LRFD design method for driven piles. This can be achieved by reducing the level of uncertainty, thus enhancing the accuracy in estimating the pile capacity. To achieve the overall objectives, the research focuses on strength limit states, reliability theory, and reconciling design and construction processes and incorporating pile data from local static and dynamic load testing into the process. Additional data from regional pile load tests are also incorporated into analysis to supplement the locally collected data. Figure 1-1 plots a flow chart that summarizes the research methodology and its different tasks. After a thoroughly comprehensive documentation of the existing LRFD calibration framework, a preliminary calibration of resistance factors was performed utilizing locally collected pile data. Preliminary recommendations were made. Generally, a series of full-scale pile load tests are recommended to verify the validity of the preliminary results. In the process of collecting pile data, the LRFD literature was reviewed, a local calibration was completed and a design and acceptance protocol is developed.

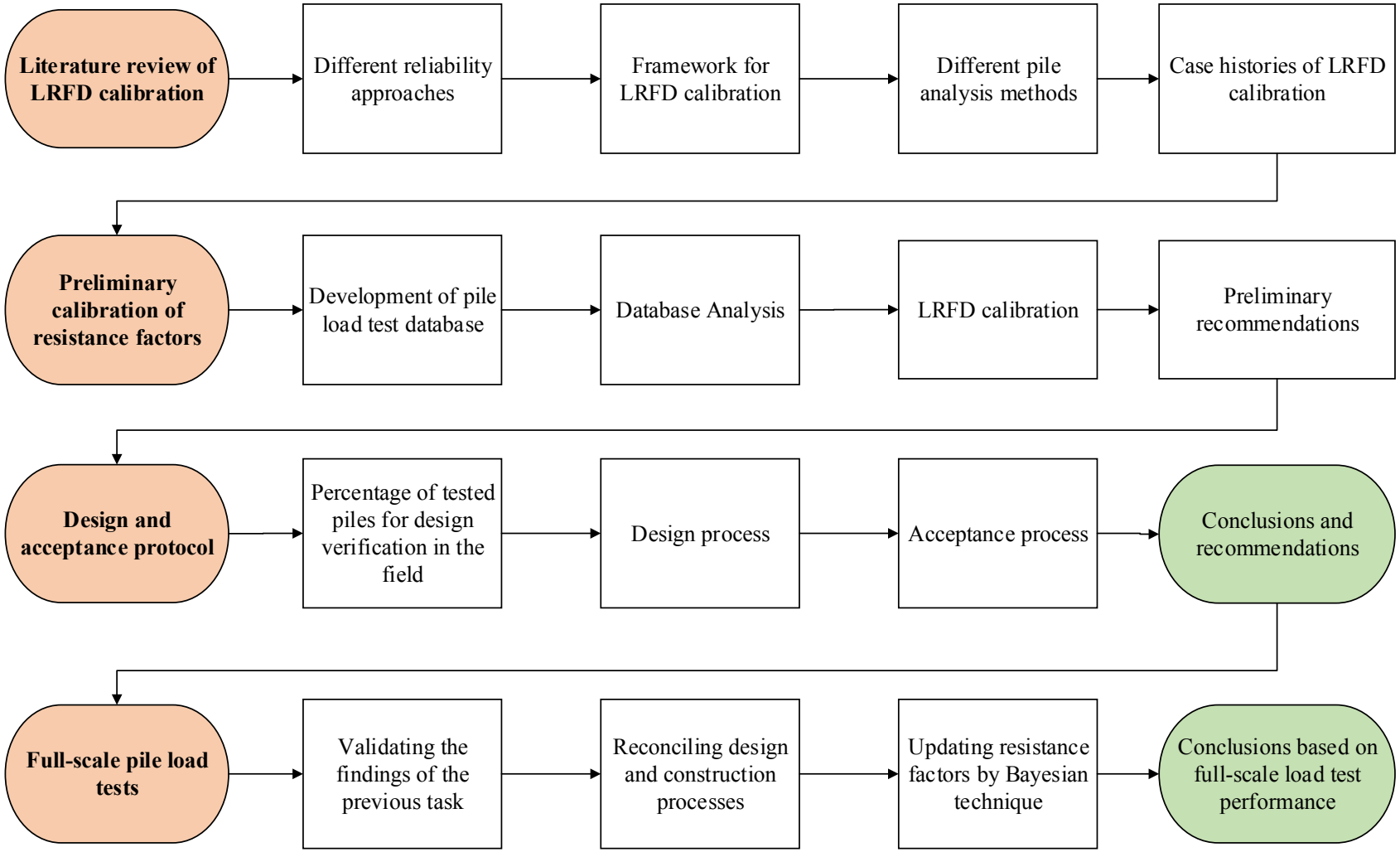

Figure 1-1 Flow Chart for Research Methodology and Supporting Tasks.

The research methodology illustrated in Figure 1-1 presents a logical sequence of tasks which lead to accomplishment of the specific objectives of the research. The research progressed as described in the following sequence:

Task 1. Literature Review and Development of Pile Database

Specific objectives in this task are the acquisition of LRFD knowledge, quantification of the level of need for calibrating resistance factors to account different design and inspection methods within the LRFD method, and development of a reliable pile database. Task 1 involves the following steps:

1. Carry out a comprehensive literature review for different pile foundation design approaches such as ASD and LRFD methods.
2. Investigate the evolution and application of LRFD. This step explores how resistance factors in the AASHTO LRFD bridge manual for predicting capacity of driven piles were developed, and the level of reliability used to develop these factors.
3. Investigate a typical calibration framework in NCHRP report 507 by Paikowsky et al.(2004) used to establish the current AASHTO LRFD bridge specifications.
4. Evaluate the work previously conducted by various State DOTs. In this step a review of several case studies of recent LRFD resistance factor calibrations from different states is conducted and areas of concern encountered in these various cases are identified.
5. Identify different analytical methods for predicting the capacity of driven piles. This step involves identification of different sources of uncertainty in various pile prediction and measurement approaches recommended by the AASHTO bridge manual or technical literature. An assessment of pile design, pile installation methods, and construction quality evaluation methodologies that are routinely in use in the State of Arkansas is conducted

through a thorough assessment of the Arkansas Standard Specification for Highway Construction by the AHTD (2003, 2014).

6. Retrieve pile load test data from bridge construction reports in Arkansas and surrounding areas.
7. Create database of the retrieved pile information. An electronic pile database is developed in Microsoft Access™2013.

Task 2. Data Analysis and Calibration of Preliminary Resistance Factors

The targeted objective is to develop a more reliable design approach by calibrating the resistance factors based on local experience. In this task, a baseline calibration of resistance factors is performed using data from various regional locations that are believed to have geological settings similar to Arkansas. This task involves the compilation and analysis of data from the database developed in Task 1. The steps are described below:

1. Sort database into several categories based on different pile types (concrete, steel pipes, and H piles), and soil types (cohesive, non-cohesive, and mixed). This action is performed in order to separate and reduce uncertainties in the data.
2. Study static design and dynamic driving biases. Pile data are analyzed using statistical analyses. Statistical data parameters such as average, standard deviation, coefficient of variation (COV), coefficient of regression, coefficient of determination, Cook's distance, etc., are utilized to quantify the level of agreement between various quantities involved. With capacity measurements from static load tests (SLT) taken as the reference value, static design and dynamic driving biases are studied.
3. Develop preliminary resistance factors based on different reliability approaches. The implementation of several reliability models such as First Order Second Moment Method

(FOSM), First Order Reliability Method (FORM), and Monte Carlo Simulation (MCS) is achieved through the use of the MATLAB program to deploy a standalone program (ReliaPile) for pile data analyses.

4. Compare results yielded by different reliability approaches to the AASHTO LRFD recommended resistance factors and draw conclusions about these different reliability approaches.

Task 3. Establish Preliminary Recommendations

The objective of this task is to come up with a reliable, simple, and cost-effective design and construction procedures based on the preliminary resistance factors developed in Task 2. Involved steps are:

1. Compare most utilized static design methods and dynamic prediction methods based on their preliminary resistance factors, and their corresponding efficient factors.
2. Choose simple and cost-effective design and construction control procedures.

Task 4. Pile Design Verification and Updating of Resistance Factors

The main objective of Task 4 is to verify the applicability of the developed resistance factors by conducting full-scale pile load tests in the state of Arkansas. While the performance of the calibrated resistance factors could be studied and verified by conducting full-scale load testing, due to the time frame of this research the full-scale pile load testing was not performed. However, such verification phase is highly recommended before conclusive LRFD recommendations are made. If it is performed, Task 4 could be achieved in the following sequence:

1. Conduct full-scale pile load tests at bridge sites (Arkansas). This step involves data collection and reduction. In this step, full-scale static and dynamic load tests are

performed on driven piles. The number of tests depends on the availability of pile construction projects. Since the tests are to be of high quality for calibration verification and updating, the testing and monitoring procedures should be very well documented. For this purpose static load tests together with the signal matching coupled with the Pile Driving Monitoring device (PDM) are recommended to monitor the piling process.

2. Evaluate the performance of the locally-calibrated resistance factors. Based on soil profiles and driving records for the piles tested in the field, nominal capacities are calculated. From these nominal values the factored design capacities are determined based on the preliminary resistance factors. Recommendations are made by comparing the factored design capacities to the actual measured capacities from static load tests interpreted using Davisson's criterion.
3. Perform a Bayesian update of the locally calibrated resistance factors. After quality assessment of the full-scale pile load test results and validity evaluation of the usage of preliminary calibrated resistance factors, a Bayesian technique is employed together with high quality data from full-scale testing to update the preliminary resistance factors. In that context the results of full-scale load testing constitute new information that is the basis of estimating a likelihood function. This new function is utilized to update the prior distribution (current predictive distribution used to calibrate preliminary resistance factors) in order to get updated information that is used to obtain new (updated) resistance factors.

Task 5. Final Recommendations on Pile Selection, Design, and Evaluation

The main purpose of this task is to establish a pile design and driving monitoring program including recommendations related to the technical issues involved during pile capacity

measurements, such as dynamic or static load testing. This final stage summarizes all the research findings. The production of the recommendation report involves the following steps:

1. Compare the locally calibrated resistance factors and the AASHTO recommendations.
2. Develop final LRFD recommendations based on the available information in the database.
3. Summarize different procedures that the research followed and present various conditions in which the research was conducted. The summary is structured in the form of a protocol for future reference.
4. Produce a well-structured pile monitoring program for future implementation. This program contains guidance on reconciling differences in static design predictions and field monitoring predictions.
5. Integrate final recommendations into design, construction, and acceptance protocols.

1.6 Benefits of the Research (Deliverables)

The direct outcomes of this research are grouped into 4 direct benefits:

1. A calibrated and cost effective pile design protocol that ensures uniform reliability and consistency in the design and construction phases; and a clear, concise, and reliable framework that can be utilized to recalibrate and refine resistance factors for local LRFD pile design.
2. A monitoring program to increase the accuracy of estimates of the actual in-situ capacity of pile foundations from observations during driving.
3. A methodology to properly compare predicted static pile capacity to driving resistance.

Chapter 2 Literature Review

2.1 Introduction to Pile Foundation Design: ASD versus LRFD

This section gives an overview on the Allowable Stress Design (ASD) also known as working stress design, and a detailed review of the principles and development of the Load and Resistance Factor Design (LRFD) approach for bridge foundation design.

2.1.1 Overview of an Allowable Stress Design (ASD)

For over two centuries, the ASD approach has been in use in the design of superstructures and substructures. Under ASD method, the actual loads to act on the structures are compared to strength through a factor of safety (FS). The process requires an experienced engineer and subjective judgment to ensure an adequate FS. In the earlier version of Standard Specifications for Highway Bridges (AASHTO, 1997), the traditional factors of safety are proposed, and a multiplier is adopted to account for different levels of control in analysis and construction. However, a major shortcoming of the ASD approach is that the method does not consider the different degrees of uncertainties associated with applied loads and resistance performance. Thus, ASD cannot ensure consistent and reliable performance of the foundations, and the economy of this design method becomes questionable. Since loads and resistances are not deterministic in nature, rather they are probabilistic, the artificial factor of safety approach must be replaced by a probability-based design approach that better deals with rational geotechnical properties (Becker & Devata, 2005).

2.1.2 LRFD Approach

Because of the drawbacks in the ASD approach, the Load and Resistance Factor Design (LRFD) approach was developed in the mid-1950s to ensure a uniform degree of reliability throughout the structure. Because of this advantage of the LRFD, AASHTO has been in the

process of replacing the ASD method with LRFD for foundation design since 1994. In the LRFD approach, the factored loads should not exceed the factored resistances. The ability of the LRFD approach in handling the uncertainties associated with design parameters is achieved by employing a rational framework of probability theory, resulting in a constant degree of reliability and a consistent design approach for the super- and sub-structures. Another advantage of using LRFD over the ASD approach is that the LRFD approach makes the design engineers more confident because its design process does not require the same amount of experience and engineering judgment as the ASD does (AbdelSalam, Ng, Sritharan, Suleiman, & Roling, 2012).

2.1.2.1 Basic Principles of LRFD Approach

In the LRFD approach, loads are multiplied by load factors, typically greater than one, while resistances are multiplied by resistance factors which are typically less than one. At the limit state equilibrium the factored loads are equal to the factored capacities as expressed in Equation 2-1:

$$\phi R_n = \sum \eta_i \gamma_i Q_i \qquad \text{Equation 2-1}$$

where R_n is the nominal resistance, ϕ is the resistance factor, Q_i is structural load, γ_i is the load factor, and a modifier factor $\eta_i = \eta_D \eta_R \eta_I \geq 0.95$ and η_D = effects of ductility; η_R = redundancy; η_I = operational importance.

The uncertainties within loads and resistances may be fully defined through their Probability Density Functions (PDFs) as shown in Figure 2-1. The overlap area between the PDFs defines the probability of failure, where loads may exceed the resistances. For a safe design approach, LRFD calibration adjusts design factors to minimize the overlap area without compromising the underlying risk within the constrained economy. This overlap depends on the relative position of the PDFs determined by their mean biases (μ_Q, μ_R) for loads and resistances,

the dispersion of the two curves is represented by their standard deviations (σ_Q, σ_R), and the shape of the PDFs (Rahman, 2002).

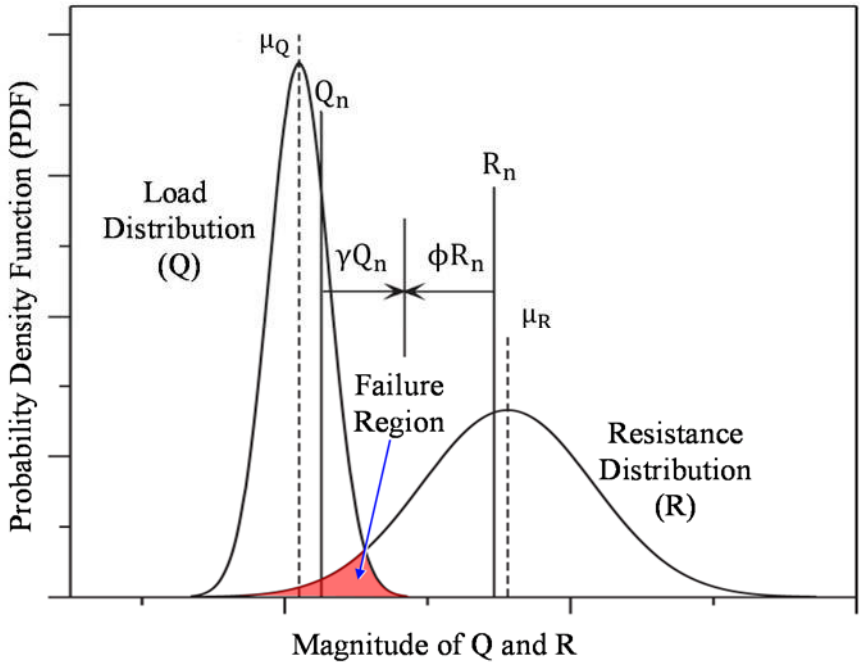

Figure 2-1 An Illustration of Probability Density Functions, PDFs, for Loads and Resistances and their Overlap Area for RLFD Calibration Purposes as Adapted from Paikowsky et al. (2010).

2.1.2.2 Overview of Uncertainties in Geotechnical Field

Whether pile capacity is established by static analyses, dynamic testing in the field at the time of driving, or static load test methods, it is governed by the shear strength of soil layers around the pile perimeter and at the pile tip (T. Smith & Dusicka, 2009). The determination of these shear-strengths requires evaluation of soil and rock properties. Due to the complicated nature of soil deposition and the complexity of soil-structure interaction behavior, many uncertainties are found in geotechnical engineering. However, due to time and economic constraints only limited geotechnical sampling, testing, and logging of boreholes are performed. Primary sources of geotechnical uncertainties can be classified in three categories: (a) inherent variability, (b) measurement uncertainties, and (c) transformation uncertainties (Kulhawy &

Phoon, 2002). The first source results largely from the natural geologic processes that produced and continually modify the soil mass in-situ. The second source arises from (i) sampling methods used to obtain soil/rock specimens (e.g., a standard penetration test, SPT); (ii) field or laboratory testing techniques used to evaluate soil/rock properties (e.g., SPT blow count or triaxial tests); and (iii) models used to interpret and predict soil/rock properties (e.g., Mohr- Coulomb model). Measurements of soil/rock properties in the field and laboratory produce random errors that are typical of all measurements (Withiam et al., 1998) . In general, tests that are highly operator-dependent and have complicated test procedures will have greater variability than those with simple procedures and little operator dependency (Kulhawy & Trautmann, 1996). However, there exists random testing error, which refers to the remaining scatter in the test results that is not assignable to specific testing parameters and is not caused by inherent soil variability. Collectively, as depicted in Figure 2-2, the first two sources can be described as data scatter. In-situ or laboratory measurements could also be influenced by statistical uncertainty or sampling error resulting from limited information. This uncertainty can be minimized with increased testing, but it is commonly included within the measurement error. The third component of uncertainty is introduced when field or laboratory measurements are transformed into design soil properties using empirical or other correlation models (e.g., correlating the standard penetration test N value with the undrained shear strength). Transformation uncertainty may also occur due to differences between estimated properties and the actual properties of the constructed structure as a result of differing construction methods or insufficient construction quality control and assurance (Lazarte, 2011).

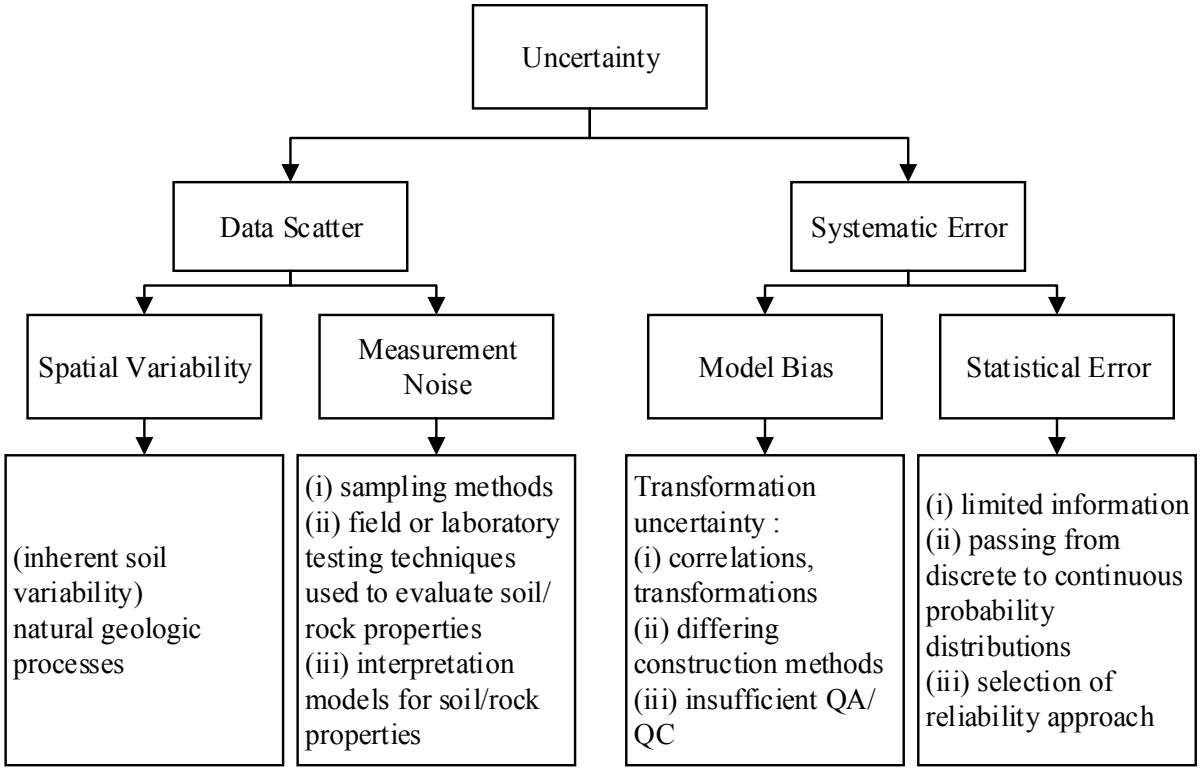

Figure 2-2 Chart Summarizing Different Sources of Uncertainty in Geotechnical Reliability Analysis.

2.1.2.3 Reliability Theory in LRFD

2.1.2.3.1 LRFD Development for Driven Pile Foundations

In the late 1980's, several studies focused on the development and applicability of the LRFD approach in geotechnical engineering. The first geotechnical LRFD manual was developed in 1989 by the American Association of State Highway and Transportation Officials (AASHTO). The FHWA released the FHWA Manual for the Design of Bridge Foundations in early 1990, followed by the National Corporative Highway Research Program (NCHRP) Report 343 by Barker et al. (1991). The NCHRP Report 343 later became the basis for the foundation section of the 1994 AASHTO Bridge Design Specifications.

2.1.2.3.1.1 Calibration Approach used by Barker et al. (1991)

NCHRP Report 343 by Barker, et al. (1991) is the source of the AASHTO (2004) LRFD resistance factors for driven pile foundation design. This report only evaluated the reliability of static analysis methods in predicting the bearing capacity of driven piles. While the report did not evaluate dynamic prediction methods it included a parameter, λ_V, which accounted the effect of quality control procedures during pile driving, such as the use of the ENR (Engineering News-Record) driving formula for pile capacity acceptance. Calibrations using reliability theory were performed for the λ-Method (Vijayvergiya & Focht Jr., 1972), the CPT Method (Nottingham & Schmertmann, 1975), the SPT Method (Meyerhof, 1976), the ß-Method (Esrig & Kirby, 1979), and the α-Method (Tomlinson, 1987). In general, Barker's calibrations attempted to replicate the design capacities that matched those created by using Allowable Stress Design (ASD) procedures. This resulted in using reliability theory with a target reliability index ß of between 2.0 and 2.5. Barker et al. (1991) provided statistics for model error, systematic error in the measurement of the soil parameters, and error due to inherent spatial variability.

Because the level of safety represented by the resistance factors determined by a calibration fitted to ASD safety factors may not be consistent with the level of safety represented by those determined using reliability theory,., Barker et al. (1991) considered the results of previous studies to make the final selection of resistance factors. The α-Method was found the most reliable, followed by the λ-Method. The ß-Method was found to be the least reliable of the five static analysis methods. The selected resistance factor for the α-Method heavily depended on the reliability of theory results, and was higher than the resistance factor implied by fitting to ASD. Similarly, for the λ-method, the reliability theory calibration resulted in a resistance factor that was slightly lower than the resistance factor implied by past practice.

2.1.2.3.1.2 Calibration Approach used by Paikowsky, et al. (2004)

The LRFD calibration conducted by Paikowsky et al. (2004) in NCHRP report 507 was based on 338 pile case histories amassed in a more robust database of pile load tests. There was no need to make any assumptions of spatial variability and systematic error as separate sources of error because the size of the database was large enough to adequately account for all sources of error. Although pile data was grouped in the database according to soil type, resistance prediction method, and pile type, the details of the characteristics of each subgroup were not provided. The study found that the resistance data followed a lognormal distribution. The LRFD calibrations were performed for the α-, the λ-, the ß-, the SPT, the CPT, and the Nordlund/Thurman Methods using two reliability methods. The two methods were the, First Order Reliability Method (FORM) and First Order Second Moment Method (FOSM). However, the final results relied more heavily on the FORM results. To select the target reliability indices, Paikowsky, et al. referenced past work including NCHRP Report 343 by Barker, et al. (1991) among others. They assigned a target reliability index of 3.0 for pile groups that contain fewer than five piles, and a target reliability index of 2.3 for pile groups that contained five or more piles (Allen, Laboratory, & Institute, 2005). In general, the resistance factors obtained in NCHRP report 507 were more conservative than the values obtained in the NCHRP report 343 for all methods of capacity prediction except for the Schmertmann CPT method. To take into account the lack of redundancy in the foundation systems the study proposed a reduction of 20 percent of the resistance factors.

The study also conducted a calibration of resistance factors for dynamic analysis methods. These methods involve pile tests that are carried out during pile driving and monitoring to verify the accomplishment of design pile capacity, and to avoid pile damage

during driving due to hammer impact. During calibration for dynamic tests the pile database was divided into subgroups based on the method of analysis and driving conditions at the time of analysis such as end of driving (EOD) or beginning of restrike (BOR). The hammer used for the load testing was assumed to be the same as the hammer used for the production pile driving. The number of load test in each subgroup varied from 99 to 384. The study showed that the number of piles which should be dynamically tested on a project depended on the size of the project, degree of variability in the subsurface conditions, amount of SLT information available on the project, as well as reasons for performing dynamic tests. Thus they provided recommendations for the number of piles to be dynamically tested as well as the acceptance criterion for a driven pile project. An average capacity was set to a minimum of 85 percent of the nominal ultimate capacity as an acceptance criterion for a set of driven piles.

2.1.2.3.1.3 State-Specific Projects (LRFD Calibration Case Histories)

Different states conducted similar study to establish state-specific recalibration of resistance factors for driven piles. Those states faced similar challenges and converged to similar trends and conclusions as Paikowsky et al., which are summarized below.

Based on a database of 218 pile cases, McVay et al. (2000) reported the statistical parameters and the corresponding resistance factors for various dynamic methods used in LRFD procedures for driven piles in Florida,. In total, eight dynamic methods were studied including the ENR, modified ENR, Florida DOT method, Gates driving formulas, CAPWAP, Case method for PDA, Paikowsky's energy method, and Sakai's energy method. It was demonstrated that the modern methods based on wave mechanics, such as signal matching, are about two times more cost effective in reaching target reliability indices of 2.0 to 2.5 than the ENR and modified ENR driving formulas. Similar to previous studies, this study demonstrated

that static analysis methods used in most design practice over-predicted the observed capacities as determined by static load testing; whereas, most dynamic capacity evaluation methods used for quality control were found to under-predict measured pile capacities. The study proposed an efficiency measurement index to objectively assess the performance of pile analysis methods in order to overcome the shortcomings of economy evaluation based on absolute values of the resistance factors.

The Bridge Section of the Oregon Department of Transportation (ODOT) conducted a similar project of recalibration of resistance factor (T. Smith, Banas, Gummer, & Jin, 2011). However, it was solely limited to establishing a resistance factor for the GRLWEAP. In that study, existing national databases were assessed and used together with new cases from the literature to build a comprehensive database. It was reported that the information in these databases was not always correct. There were a number of anomalous load test and many load test which were missing critical data such as blow count, especially at the BOR condition. The FHWA static capacity software program, DRIVEN, was used for the capacity prediction and the GRLWEAP program was adopted for creation of the bearing graph (T. Smith et al., 2011). These predictions generated a bias λ and COV statistics for a range of ODOT selected scenarios. A reliability index ß of 2.33 associated with the case of redundant piles in groups was used to establish resistance factors and efficiency measures (ϕ/λ). The FOSM reliability method was used for the calibration of resistance factor at EOD and BOR. The results of the FOSM analysis served as the basis for further analysis with the Monte Carlo Simulations (MCS) method. The MCS was based on probabilistic procedures using random number generation and the resistance bias factor of (λ) found by lognormal tail fits of the data from EOD and BOR predictions. The

study recommended the use of field measured hammer performance, CAPWAP based soil input parameters, and pile type into design.

D'Andrea et al. (2009) reported that the Louisiana Department of Transportation (LA DOTD), in conjunction with Louisiana Transportation Research Center (LTRC), conducted a similar calibration research project and completed the driven pile calibration in 2006. The pile load test database used for the calibration was created by conducting an extensive search in projects library of the LA DOTD. Only pre-cast, pre-stressed concrete (PPC) piles that had been statically tested to failure and had adequate soil information were included in the study. A total of 42 PPC pile load tests met these criteria. In addition to the load test results, all other relevant information, including soil borings, pile driving logs, dynamic testing and analysis, and CPT data, were collected. It was reported that more than 90 percent of the pile load test data were from southern Louisiana, where the soil is weaker than that from northern Louisiana. The majority of the soil profiles in the database consisted of clay, although approximately 25 percent of them were in mixed soils of sand and clay. Statistical analyses were used to evaluate the different pile design methods which included previously mentioned static design methods, direct CPT design methods, and dynamic measurement methods. The resistance factors from the calibration using FOSM were about 10 percent lower than those from the calibrations where more sophisticated methods such as FORM or Monte Carlo Simulation were used. Due to limitations of information relative to soil type the reported resistance factors for the static methods lumped all soil types together. The study proposed a separate calibration of resistance factors for northern Louisiana because that region presents stiffer soils than southern region. In general, the LA DOTD calibration resulted in resistance factors approximately 25 percent to 60 percent greater than the resistance factors presented in the AASHTO (2004) calibration. However, the resistance factor

obtained for dynamic analysis was much lower than the value provided by the AASHTO calibration. The potential reason postulated was that the dynamic analyses are less effective in clay soils.

Wainaina et al. (2009) reported that North Carolina State University (NCSU) used pile load test data from the North Carolina Department of Transportation (NCDOT) highway construction projects to perform a reliability based calibration of resistance factors for axially loaded driven pile. A total of 140 piles with capacity predicted using signal matching via the driving analyzer (PDA) and 35 static load tests data were compiled and grouped into different design categories and different geological regions. Resistance statistics were evaluated for each design category in terms of bias factors and coefficient of variation. Bayesian updating was employed to improve the statistics of the resistance bias factors, which were derived from a limited number of pile load tests. Load statistics presented in the AASHTO LRFD bridge design specifications were used in the reliability analysis during the calibration of the resistance factors. The calibration was performed for three methods of static pile capacity analysis commonly used by the NCDOT, namely the Vesic, the Nordlund, and the Meyerhof methods. FOSM and FORM were employed for the reliability analysis. During analysis the NCSU grouped data into 7 different categories of pile type and geologic region. The analysis showed that the difference between the resistance factors for the Vesic and Nordlund methods was insignificant. However, the resistance factors for the Nordlund method were approximately 20 percent higher than those for the Meyerhof method. The NCDOT Nordlund resistance factor for pre-stressed concrete piles was found to be 0.45, for a reliability index of 2.5. Therefore, there was close agreement between the AASHTO and NCDOT resistance factors for the Nordlund method for pre-stressed concrete piles. On the other hand, the NCDOT Meyerhof resistance factors are considerably higher than

those recommended by AASHTO. Also, the NCDOT resistance factors derived for all three static analysis methods for steel H-piles were significantly higher than the AASHTO resistance factors. This observation led to the conclusion that there is a need to differentiate between high and low displacement piles because the current AASHTO resistance factors do not differentiate between pile types.

2.1.2.3.1.4 Summary on the LRFD Development

Several case histories of recalibration of resistance factors show that the estimation of pile resistance is not an easy or straightforward task, and it can involve considerable engineering judgment which is difficult to quantify statistically. Furthermore, the data upon which the needed input statistics were based were limited in terms of quantity and, in some cases, quality. Therefore, the final selection of resistance factors considered both the statistical reliability of the method and the level of safety implied by past successful design practice. To deviate from substantially conservative practices of the past, a large and reliable local/state-specific database coupled with reliability theory is needed. The presented case histories have shown that the recalibration of the LRFD resistance factors is beneficial and can be made possible through reliability approach. Moreover, updating databases and refining resistance factors is required in order to minimize the level of uncertainty and cost of the entire structure.

2.1.2.3.2 Calibration by Fitting to ASD

Calibration by fitting to ASD is recommended only when data required for the statistical analysis are not available. The resistance factors obtained through ASD fitting serve only as benchmark to provide a similar degree of safety that was provided by the ASD method. However, resistance factors derived in this fashion do not satisfy the LRFD reliability based requirements. A direct approach of fitting resistance factor to the ASD can be accomplished using the following equation:

$$\phi = \frac{\gamma_{DL}(DL/LL) + \gamma_{LL}}{(DL/LL + 1)FS} \qquad \text{Equation 2-2}$$

where

ϕ = Resistance factor

γ_{DL} = Load factor for Dead Loads (DL), assumed according to Table 2-1

γ_{LL} = Load factor for Live Loads (LL) assumed according to Table 2-1

DL/LL = Dead load to live load ratio

FS = Factor of Safety associated with The ASD method

The DL/LL ratio ranges between 1.0 and 4.0 for bridge structures depending on the bridge span and other factors (Paikowsky et al., 2004). Recommended values of the ratio DL/LL are included in Table 2-1.

Table 2-1 Dead Load Factors, Live Load Factors, and Dead to Live Load Ratios used for the Purpose of the LRFD resistance factors calibration by fitting to ASD Approach.

Load type	Recommended LFD load factors (Barker et al., 1991)	Recommended LRFD load factors (AASHTO, 2004)
Dead Load	1.30	1.25
Live Load	2.17	1.75
DL/LL	3.0 (Allen, 2005)	2.0 to 2.5 (Paikowsky et al., 2004)

2.1.2.3.3 Calibration using Reliability Theory

Reliability based design focuses on the most important aspect of performance, which is the probability of failure. The probability of failure depends on both parametric and model uncertainties. The probability of failure is a more consistent and complete measure of safety since it is invariant to all mechanically equivalent definitions of safety, and incorporates additional uncertainty information. The main advantage of reliability analysis is the ability to carry out a much broader range of parametric studies without actually performing thousands of design checks with different inputs one at a time (Phoon, 2008). Calibration using reliability theory consists of limiting the probability of failure (p_f) of structures to a certain acceptable extent. The intersection of the two PDFs defining loads Q and resistance R is shown in Figure 2-1. The area of overlap between the two PDFs is considered the failure zone. A better way to quantify this overlap zone is to define a performance function (g) by subtracting the two PDFs. This performance function (g) also known as the limit state function corresponding to the margin of safety. The probability of failure (p_f) is the area to the left of the zero axis as shown on Figure 2-3. In this regard, the reliability of the structure is evaluated using the reliability index, β. The reliability index has a geometric meaning, which is the number of standard deviations (σ_g), separating the mean safety margin from the mean value of the performance function, g (Baecher & Christian, 2003).

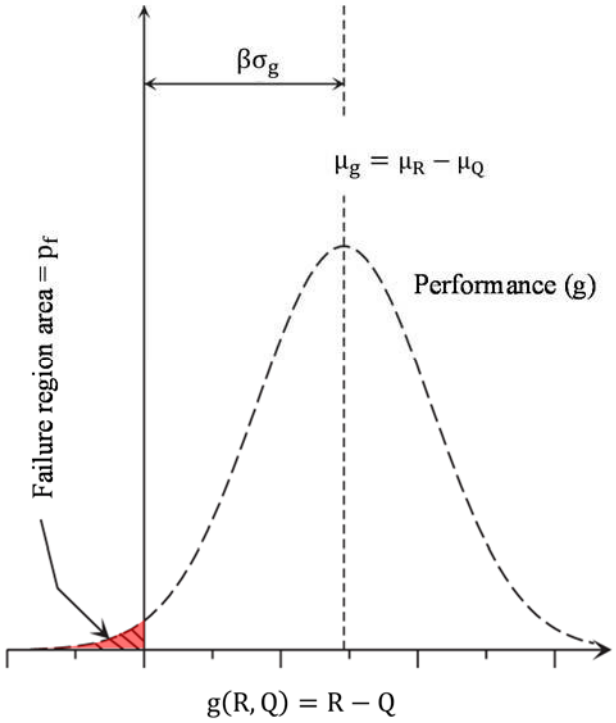

Figure 2-3 Illustration of Probability of Failure and Geometrical Meaning of the Reliability Index for the Performance Function (g). (Baecher & Christian, 2003).

There are several statistical methods that can be used for calibrating the LRFD resistance factors. They differ from their degrees of sophistication and accuracy. The following section describes three methods of reliability; First Order Second Moment (FOSM), the Monte Carlo simulation (MCS) and First Order Reliability Method (FORM), which are widely used for calibrating the LRFD design methods for driven pile foundations.

2.1.2.3.3.1 Closed-Form Solution - First Order Second Moment (FOSM) Method

Since FOSM is considered to be easy to use and valid for preliminary analyses, it is initially used for preliminary calibration of resistance factors. In the FOSM method, a Taylor series expansion is used to linearize the limit state function about the mean value of the variable. Since only the mean and the variance are used in the expansion, it is called First Order (Mean) Second Moment (variance). The analysis considers pile design problems involving a random capacity (R) and a random load (Q). The limit state is defined as that in which the capacity is

equal to the applied load. Clearly, the pile will fail if the capacity is less than this applied load. Conversely, the pile should perform satisfactorily if the applied load is less than the capacity. These three situations can be described concisely by a single performance function (g), as follows:

$$g = R - Q \qquad \text{Equation 2-3}$$

Mathematically, the above three situations simply correspond to the conditions of g = 0, g < 0, and g > 0, respectively.

The basic objective of reliability based design is to ensure that the probability of failure does not exceed an acceptable threshold level. This objective can be stated using the performance function as follows:

$$p_f = Prob(g < 0) \leq p_T \qquad \text{Equation 2-4}$$

in which Prob(·) = probability of an event, p_f = probability of failure, and p_T = acceptable target probability of failure. A more convenient alternative to the probability of failure is the reliability index (β), which is defined as:

$$\beta = -\Phi^{-1}(p_f) \qquad \text{Equation 2-5}$$

in which $\Phi^{-1}(\cdot)$ = inverse of the standard normal cumulative function, Φ. In this study the function $\Phi^{-1}(\cdot)$ was obtained in MATLAB using norminv (p_f).

The basic reliability problem is to evaluate p_f from some pertinent statistics of Q and R, which typically include the mean (μ_Q or μ_R) and the standard deviation (σ_Q or σ_R), and possibly the probability density function. A simple closed-form solution for p_f is available if R and Q follow a bivariate normal distribution. For this condition, the solution to Equation 2-4 is:

$$p_f = \Phi\left(-\frac{\mu_R - \mu_Q}{\sqrt{\sigma_R^2 + \sigma_Q^2 - 2\rho_{RQ}\sigma_R\sigma_Q}}\right) = \Phi(-\beta)$$ Equation 2-6

in which ρ_{RQ} = product-moment correlation coefficient between R and Q. Numerical values for $\Phi(\cdot)$ are obtained using the MATLAB function normcdf $(-\beta)$.

2.1.2.3.3.1.1 Target Reliability Indices for the Research:

NCHRP report 507 (Paikowsky et al., 2004) recommended a target reliability index (β) of 2.33 corresponding to a probability of failure of 1% for driven piling in pile groups of 5 or more piles. A reliability index of 3.0, corresponding to a probability of failure of 0.1%, .is recommended for single piles and pile groups containing 4 or less piles

In general, loads and resistances were found to follow a lognormal distribution, thus Equation 2-6 was modified to translate lognormals, i.e. ln(R) and ln(Q), to follow a bivariate normal distribution with mean of ln(R) = λ_R , mean of ln(Q) = λ_Q , standard deviation of ln(R) = ξ_R , standard deviation of ln(Q) = ξ_{RQ}, and a correlation between ln(R) and ln(Q) = ρ'_{RQ}:

$$p_f = \Phi\left(-\frac{\lambda_R - \lambda_Q}{\sqrt{\xi_R^2 + \xi_Q^2 - 2\rho'_{RQ}\xi_R\xi_Q}}\right)$$ Equation 2-7

The relationships between the mean (μ) and standard deviation (σ) of a lognormal and the mean (λ) and standard deviation (ξ) of the equivalent normal are given in Equation 2-8 and Equation 2-9 (Zhang & Tang, 2002):

$$\xi^2 = ln[1 + (\sigma/\mu)^2$$ Equation 2-8

$$\lambda = ln(\mu) - 0.5\xi^2$$ Equation 2-9

In this case R and Q are considered to be independent lognormals. Therefore, the correlation between them is zero. Consequently, Equation 2-7 reduces to the following expression:

$$\beta = \frac{ln\left(\frac{\mu_R}{\mu_Q}\sqrt{\frac{1+COV_Q{}^2}{1+COV_R{}^2}}\right)}{\sqrt{ln[(1+COV_R^2)(1+COV_Q^2)]}}$$ Equation 2-10

in which $COV_R = \sigma_R/\mu_R$ and $COV_Q = \sigma_Q/\mu_Q$.

For LRFD calibration purposes, this equation was modified by introducing load and resistance factors and then rearranging to express a relation to the resistance factor (ϕ). The calculations followed steps outlined below:

Step1. Identifying the typical LRFD design equation, which is the expansion of Equation 2-1:

$$\phi R_n = \gamma_{DL} DL_n + \gamma_{LL} LL_n$$ Equation 2-11

in which ϕ = resistance factor, γ_{DL} and γ_{LL} = dead and live load factors respectively, and R_n, DL_n and LL_n are nominal values of capacity, dead load, and live load respectively. The AASHTO LRFD bridge design specifications recommended $\gamma_{DL} = 1.25$ and $\gamma_{LL} = 1.75$ (Paikowsky et al., 2004) as shown in Table 2-1.

Step2. The nominal values are related to the mean values as: $\mu_R = b_R R_n$, $\mu_{DL} = b_{DL} DL_n$, $\mu_{LL} = b_{LL} LL_n$, in which b_R ,b_{DL} , and b_{LL} are bias factors and μ_R , μ_{DL} , and μ_{LL} are mean values for the resistance, dead load, and live load respectively. NCHRP report 507 recommends bias factors for dead and live load of 1.05 and 1.15 respectively. These values are also in close agreement with the values recommended in NCHRP report 368 (Nowak, 1999) and were used in several DOT related projects. The same references recommend values of coefficients of variation for the dead load, and live load as, COV_{DL} = 0.1, and COV_{LL} = 0.2. For capacity, the COV_R varies depending on the pile capacity prediction methods in use. The value of resistance bias factor, b_Q can be smaller or larger than one.

Step3. Assume a value for the load ratio (DL_n/LL_n). A reasonable range for (DL_n/LL_n) is 1 to 4 as reported in Table 2-1. Since the choice of load ratio depends on the span of the structure, NCHRP report 507 recommends the use of a DL_n to LL_n ratio ranging from 2 to 2.5 as mentioned earlier, which is, by and large, applicable for long span bridges. As part of this dissertation, the impact of the dead to live load ratio on the resistance factor was established by using a more sophisticated reliability method, FORM. The results of that analysis are presented in Figure 2-4. That Figure illustrates that the load ratio has little influence on resistance factors when the ratio is greater than 2.

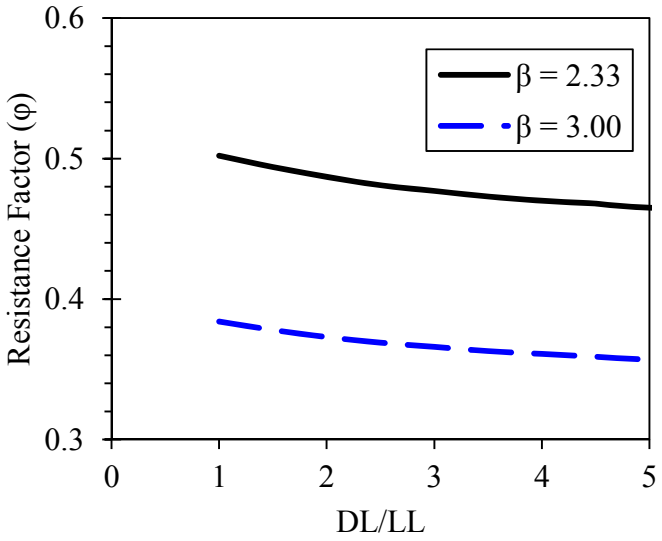

Figure 2-4 Influence of Dead-to-Live Load Ratio on Resistance Factor for Reliability Indices of 2.33 and 3.00: Resistance Factors are Calculated using First Order Reliability Method for $b_R = 1.0$ and $COV_R = 0.4$.

The mean live load and mean dead load are calculated as follows:

$$\mu_{LL} = \frac{\phi}{\gamma_{DL}\frac{DL_n}{LL_n} + \gamma_{LL}} \cdot \frac{\mu_R b_{LL}}{b_R} \qquad \text{Equation 2-12}$$

$$\mu_{DL} = \frac{DL_n}{LL_n} \cdot \frac{\mu_{LL} b_{DL}}{b_{LL}} \qquad \text{Equation 2-13}$$

Step4. Calculate the reliability index using Equation 2-10 with $\mu_Q = \mu_{DL} + \mu_{LL}$ and:

$$COV_Q = \frac{\sqrt{(\mu_{DL} COV_{DL})^2 + (\mu_{LL} COV_{LL})^2}}{\mu_{DL} + \mu_{LL}}$$ Equation 2-14

An alternate and direct approximation of COV_Q is presented in Equation 2-15

$$COV_Q \approx \sqrt{COV_{DL}^2 + COV_{LL}^2}$$ Equation 2-15

According to Phoon (2008), the expression in Equation 2-15 is erroneous , but it is popular because the resistance factor in LRFD can be easily back-calculated from a target reliability index (β_T) with a closed formed expression given in Equation 2-16, where all input parameters are dimensionless:

$$\phi = \frac{b_R(\gamma_D \frac{DL_n}{LL_n} + \gamma_{LL}) \sqrt{\frac{1 + {COV_Q}^2}{1 + {COV_R}^2}}}{(b_{DL} \frac{DL_n}{LL_n} + b_{LL}) exp\left\{\beta_T \sqrt{ln[(1 + COV_R^2)(1 + COV_Q^2)]}\right\}}$$ Equation 2-16

Equation 2-16 was used in a closed form by Piakowsky, et.al.2004. Resistance factors were calculated for different values of bias resistance factors. It can be seen that the use of this formula does not involve the assumption of any nominal value of any force in action. In this research the statistics of the resistance, R, are determined by comparing load test results with predicted values as:

$$b_{Ri} = \frac{R_{measured(i)}}{R_{predicted(i)}}$$ Equation 2-17

2.1.2.3.3.2 Iterative Procedures

Many studies had found that the statistics of resistance R are primarily influenced by model errors, rather than uncertainties in the soil parameters (Phoon, 2008). Hence, it is likely that Equation 2-16 would only accommodate a very narrow range of coefficient of variation of parametric uncertainties. To accommodate larger uncertainties in the soil parameters, such as

medium and high COV ranges, R must be expanded as a function of the governing soil parameters. By doing so, the above closed-form solution in Equation 2-16 is no longer applicable (Phoon & Kulhawy, 2005).

The general reliability problem consists of a performance function $P(y_1, y_2, \ldots, y_n)$ and a multivariate probability density function $f(y_1, y_2, \ldots, y_n)$. As stated previously, the performance function is defined to be zero at the limit state, less than zero when the limit state is exceeded— fail, and larger than zero otherwise— safe. The performance function is nonlinear for most practical problems, and it specifies the likelihood of realizing any one particular set of input parameters $(y_1, y_2, \ldots, y_n)$, which may include material, load, and geometrical parameters. The objective of reliability analysis is to calculate the probability of failure, which can be expressed formally as follows:

$$p_f = \int_{P<0} f(y_1, y_2, \ldots, y_n)\, dy_1\, dy_1 \ldots dy_n \qquad \text{Equation 2-18}$$

The domain of integration is illustrated by a shaded region in Figure 2-5 (a). Exact closed form solutions are not available even if the multivariate probability density function is normal, unless the performance function is linear or quadratic. Therefore, more advanced and sophisticated reliability procedures, such as Monte Carlo Simulations and First Order Reliability Methods, are used to evaluate the solution of the Equation 2-18.

2.1.2.3.3.2.1 Monte Carlo Simulation (MCS)

Monte Carlo Simulation (MCS) uses randomly generated numbers for the component variables to determine the probability distribution of the design variable, i.e., the resistance factor in this current research. Devroye (1986) shows several ways to transform these random numbers into suitable numbers needed for a specific problem. The MCS method requires the statistical distribution of selected input variables to be known (Jones, Kramer, & Arduino, 2002). The

general procedure for implementing MCS is adapted from Hammersley and Handscomb (1964), and the various steps of the procedure are outlined by Phoon (2008). For the purpose of this research the following steps were carried out and computational program (named ReliaPile) was written in MATLAB:

Step1. Estimate the minimum number of simulations (N) required to achieve a specified level of coefficient of variation (COV_{pf}) of p_f using:

$$N = \frac{1 - p_f}{COV_{pf}^2 * (p_f)} \qquad \text{Equation 2-19}$$

For example, for a COV_{pf} of 10% a minimum number of N = 100,000 simulations is required for a reliability index of 3.00 corresponding to a probability of failure of 0.1%.

Step2. Determine $(y_1, y_2, \ldots, y_n)$ using Monte Carlo simulations by simulating normal random vectors. The MATLAB function "normrnd" was used to generate these random vectors.

Step3. The performance function can take the form of either the Equation 2-3 in case of normal distribution of the variables or the following Equation 2-20 in case of lognormal distribution.

$$P = ln(R) - ln(Q) \qquad \text{Equation 2-20}$$

Step4. Substitute $(y_1, y_2, \ldots, y_n)$ into the performance function using the Equation 2-8 and Equation 2-9 using $x_i^* = \exp(\lambda + y_i\xi)$, where x_i^* corresponds to the design point in the original physical space.

Step5. Count the number of cases, N_f where the performance function P < 0, i.e., failure.

Step6. For a range of resistance factors, ϕ estimate the probabilities of failure, $\hat{p}_f$ using:

$$\hat{p}_f = \frac{N_f}{N} \qquad \text{Equation 2-21}$$

Step7. Pick the value of (ϕ)that corresponds to β = 2.33 ($\hat{p}_f$ = 1.0%) and 3.00 ($\hat{p}_f$ =0.1%).

Linear interpolation can be used if necessary.

2.1.2.3.3.2.2 First-Order Reliability Method (FORM)

As noted by Rackwitz (2001), when computing small probabilities of failure having a high dimensional space which is spanned by the random variables in the problem, the first order reliability method (FORM) provides an accurate and practical scheme,. The basic theoretical procedure and results were provided by Hasofer and Lind (1974). If the actual limit state function (P = 0) is replaced by an approximate linear limit state function (P_L = 0 as illustrated in Figure 2-5) that passes through the most likely failure point (design point or β-point), the following relationship is obtained:

$$p_f \approx \Phi(-\beta) \qquad \text{Equation 2-22}$$

The problem in Equation 2-18 reduces to a constrained nonlinear optimization problem:

$$\beta = min\sqrt{z^t z} \ \ for \ \ z: P(z) \ \leq 0 \qquad \text{Equation 2-23}$$

in which $z = (z_1, z_2, z_3)^t$, where z_i stand for resistance, live load, and dead load; and z^t is the transpose of z.

Optimization performed in the standard space (z(i)) is more stable than optimization in the original physical space (R,Q), and the β-point is the best linearization point because the probability density is highest at that point (Phoon, 2008). The solution of a constrained optimization problem in the current study followed six steps in MATLAB:

Step1. Specify the number of variables (z(i)) in standard space.

Step2. Define the objective function as the geometric mean of the reliability index, objfun $=\sqrt{z^t z}$, which is the distance from the origin. It was written as norm(z) in MATLAB.

Step3. Define the performance function of the problem, (P), as Equation 2-24 which is obtained by combining Equation 2-12, Equation 2-13, and Equation 2-20.

$$P = ln\frac{b_R(\gamma_{DL}\frac{DL_n}{LL_n} + \gamma_{LL})}{\phi(b_{DL}\frac{DL_n}{LL_n} + b_{LL})}$$ Equation 2-24

Step4. Substitute (z_1, z_2, z_3) into the performance function, changing from original physical space (R,Q) to standard space (z(i)) taking into account of lognormal distribution of R and Q.

Step5. Perform the optimization $\beta = \min\sqrt{z^t z}$ for z: $P(z) \leq 0$, for a range of ϕ values, and

Step6. Pick the values of ϕ that correspond to $\beta = 2.33$ and 3.00.

The approximate solution obtained from FORM is easier to visualize in a standard space spanned by uncorrelated Gaussian random variables with zero mean and a unit standard deviation as illustrated in Figure 2-5 (b). In such a coordinate system, the reliability index is directly measured from origin to the design point.

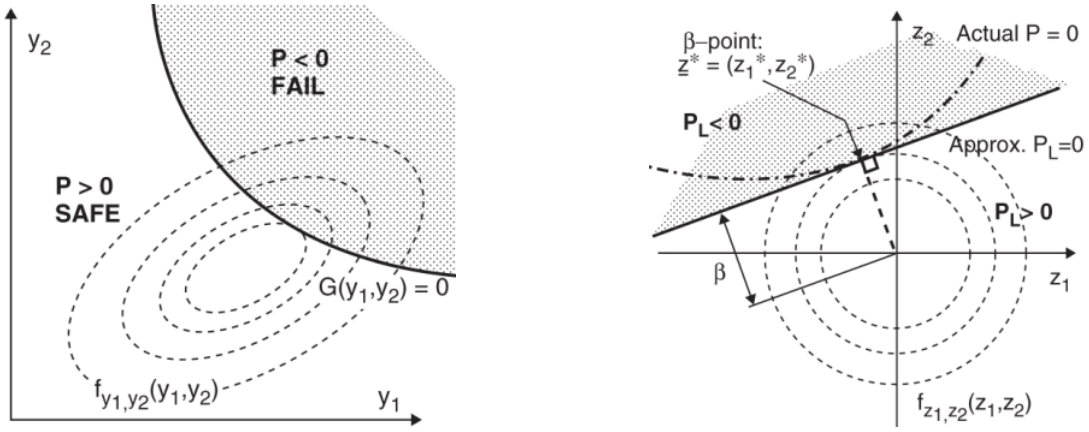

(a) (b)

Figure 2-5 Presentation of (a) General Reliability Problem with Constrained Nonlinear Optimization in Original Physical Space, and (b) Solution using FORM with an Approximate Linear Limit State Function in Standard Space (Phoon, 2008).

2.1.2.4 Methods for Testing Goodness of Fit of a given Distribution

Statistically, pile resistances are random variables. The calibration framework of the LRFD resistance factor requires assumptions on the shape of PDF which describes the

distribution of the resistances. Data recorded for resistances are fitted to specific distributions such as normal or lognormal distribution. Since these distributions are assumed, the data set has to be tested for goodness of fit to the specified distribution. Many statistical tests can be conducted on the PDFs in order to ensure that they are following an assumed distribution. For a given significance level these tests show how well the selected distribution fits the data. Among these tests are: Chi-Square goodness of fit (Chi2), Kolmogorov-Smirnov test (K-S) for upper and lower tail tests, Lilliefors composite goodness-of-fit test that uses Monte Carlo simulation, and Anderson Darling test (AD). The following section describes the methods used in the current study.

2.1.2.4.1 Chi-Squared Test

The Chi-Squared test (Chi2) determines if a sample comes from a population with a specific distribution. This test is applied to categorical or binned data, so the value of the test statistic depends on how the data is grouped into bins (Ebeling, 1997). The statistic of the Chi-Square is mathematically defined as:

$$\chi^2 = \sum_{i=1}^{k} \frac{(O_i - E_i)^2}{E_i} \qquad \text{Equation 2-25}$$

where O_i and E_i are the observed and expected frequencies respectively for bin i, and the latter frequency is given by $E_i = F(x_2) - F(x_1)$, where F(x) is the CDF of the probability distribution being tested, and x_1, x_2 are the limits for bin i.

The null and alternative hypotheses are H_0 for the data that follow the specified distribution; and H_1 for the data that do not follow the specified distribution. The hypothesis regarding the distributional form is rejected at the chosen significance level (α) if the test statistic is greater than the critical value defined as $\chi^2_{1-\alpha,k-1}$ meaning the Chi-Squared inverse CDF with

k-1 degrees of freedom and a significance level of α.

2.1.2.4.2 Kolmogorov-Smirnov Test

The Kolmogorov-Smirnov Test (K-S) helps in deciding if a sample comes from a hypothesized continuous distribution. It is based on the empirical cumulative distribution function. For a given random sample $x_1, x_2 \ldots, x_n$ from some continuous distribution with CDF, F(x), the empirical CDF is denoted by:

$$F_n(x) = \frac{1}{n}.[Number\ of\ observations\ \leq x] \qquad \text{Equation 2-26}$$

According to Conover (1999) the Kolmogorov-Smirnov statistic (D) is based on the supremum vertical difference between the hypothesized theoretical F(x), and the empirical cumulative distribution function Fn(x):

$$D = \sup_x |F_n(x) - F(x)| \qquad \text{Equation 2-27}$$

If D exceeds the 1- α quantile as given by the table of quantiles for the K-S test statistic, the hypothesis regarding the distributional form H_0 is rejected at the chosen significance level (α). A value of α equal to 0.05 is typically utilized for most applications to evaluate the null hypothesis (H_0). The shortcoming of the K-S test is that the predetermined critical values in the standard tables for this test are only valid when testing whether a data set is from a completely specified distribution. The result of the test are conservative when one or more distribution parameters are estimated: the probability that the fit is rejected in error becomes lower than the actual significance level given by the standard tables. Therefore, the Lilliefors' or Anderson-Darling tests are preferred over K-S test when the statistical parameters of the hypothesized distribution are not known or have to be estimated.

2.1.2.4.3 Lilliefors'Test

It is common practice to assume a distribution with an unknown mean and standard deviation for a given dataset. In that scenario K-S tests can be applied to evaluate the goodness-of-fit hypotheses after estimating the unknown parameters. Unfortunately, the null distribution of the K-S test statistic when parameters are estimated is far more complicated (Gibbons & Chakraborti, 2003). Liliefors (1967) showed that using the usual critical points developed for K-S tests gives extremely conservative results. Therefore, he used Monte Carlo simulations to compute accurate critical values for the Kolmogorov-Smirnov statistic in cases where the distribution parameters must be estimated from sample data. For a given sample of n observations, Lilliefors'statistic is defined as,

$$D = \max_x |F_n(x) - F(x)| \qquad \text{Equation 2-28}$$

where $F_n(x)$ is the sample cumulative distribution function and $F(x)$ is the cumulative normal distribution function with $\mu = \bar{X}$, the sample mean and s^2, the sample variance, defined with denominator $n - 1$. If D exceeds the corresponding critical value determined using MCS, then the null hypothesis is rejected.

2.1.2.4.4 Anderson-Darling Test

The Anderson-Darling (AD) test is a modification of the Kolmogorov-Smirnov (K-S) test and gives more weight to the tails of distribution than does the K-S test (Razali & Wah, 2011). While the critical values for K-S test do not depend on the specific distribution being tested, the Anderson-Darling test makes use of the hypothesized distribution in calculating critical values. This offers the possibility of conducting a more sensitive test with a disadvantage that critical values have to be determined for each hypothesized distribution. The AD uses a statistical p-value, which is a measure of the risk associated with false rejection of the null hypothesis and

offers indications that the data fits a specified distribution. If the p-value is less than the critical value, such as 0.05, then there is a greater than 95% chance that the specified distribution is incorrect and the null hypothesis can be rejected without risk. The Anderson-Darling general procedure is to compare the fit of an observed cumulative distribution function $F_n(x)$ to an expected cumulative distribution function F(x) by computing the AD statistic (A^2).

$$A^2 = \int_{-\infty}^{+\infty} \frac{[F_n(x) - F(x)]^2}{F(x)[1 - F(x)]} dF(x) \qquad \text{Equation 2-29}$$

It was shown in Anderson and Darling (1954) that the above statistic can be written as:

$$A^2 = -n - \frac{1}{n}\sum_{i=1}^{n}(2i-1).\left[lnF(x_i) + ln\left(1 - F(x_{n-i+1})\right)\right] \qquad \text{Equation 2-30}$$

For small sample sizes (n), A^2 requires correction (D'Agostino, 1986) as follows:

$$A^* = A^2\left(1.0 + \frac{0.75}{n} + \frac{2.25}{n^2}\right) \qquad \text{Equation 2-31}$$

If the value for A^2 or A^* is too large, the hypothesis is to be rejected. Equation 2-30 and Equation 2-31 are written in MATLAB to conduct AD test for analyzing data sample distribution. The results of the test are compared with Chi2, K-S, and Lilliefors tests for accepting the fitted distribution.

2.1.2.5 Bayesian Updating of Resistance Factors

2.1.2.5.1 Introduction

Static pile load test results are considered the benchmark when calibrating and reducing uncertainty in capacity prediction methods for piles. The generally accepted practice in pile design calls for the use of a higher resistance factor when pile load tests are to be performed; and a low resistance factor is needed when the load test is not prescribed (AASHTO, 2012). Zhang (2004) suggests that load tests provide new information that could be used to enhance the

reliability of a pile design using the traditional static analysis method. To enhance pile analysis methods Kay (1976) used a Bayesian statistical approach by combining prior information of estimated pile capacity with load test results for single piles in sand. Sidi and Tang (1985) used the same approach to enhance pile capacity predictions in clay and considered model error that was associated with the prediction. Five years latter Lacasse, Guttormsen, and Goulois (1990) outlined a Bayesian updating technique to effectively update the reliability of pile design methods given the results of pile load test. On the basis of pile driving records, Lacasse, Tan, and Keaveny (1992) used the Bayesian technique to update the prediction of driven pile axial capacity. The Bayesian approach proved its importance when Zhang and Tang (2002) used it to reduce pile length on the basis of the same target reliability index by incorporating the results of pile load tests into pile design.

Based upon these previous successful case histories the Bayesian updating technique is included in this study to improve/refine the LRFD resistance factor of pile capacity prediction on the basis of the same target reliability index. The values of bias factor determined from existing data are treated as the prior distribution, and results obtained from full scale static pile load testing are treated as the likelihood distribution.

2.1.2.5.2 Bayesian Framework – Parameter Estimation and Bayesian Statistics

2.1.2.5.2.1 Estimation of Parameters

This section provides an insight into Bayesian theory and summarizes some key principles that are involved in this technique. More details on the related classical reliability theory can be found in Ang and Tang (1975), and Ayyub and McCuem (2002).

For the purpose of establishing parameters, if Θ represents an unknown random variable, with a prior density function $f'(\Theta)$, the prior probability that Θ will fall between θ_j and $\theta_j + \Delta\theta$

can objectively be written as $f'(\theta_j)\Delta\theta$ as illustrated in Figure 2-6.

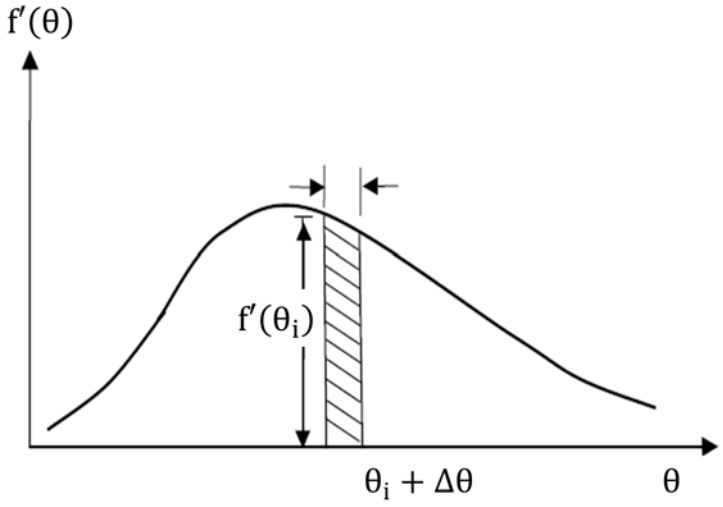

Figure 2-6 Example of Continuous Prior Distribution of Parameter θ for the Purpose of Updating the Distribution based on Bayesian Technique (Ang & Tang, 1975).

For an observed outcome, ε, of the experiment the posterior probability that θ is located within the interval $[\theta_j \;\; \theta_j + \Delta\theta]$ can be obtained by applying Bayes' theorem, as follows:

$$f''(\theta_j)\Delta\theta = \frac{P(\varepsilon|\theta_j)f'(\theta_j)\Delta\theta}{\sum_{j=1}^{n} P(\varepsilon|\theta_j)f'(\theta_j)\Delta\theta} \qquad \text{Equation 2-32}$$

where $P(\varepsilon|\theta_j) = P(\varepsilon|\theta_j < \theta \leq \theta_j + \Delta\theta)$, as $\Delta\theta$ approaches zero, Equation 2-32 becomes:

$$f''(\theta_j) = \frac{P(\varepsilon|\theta_j)f'(\theta_j)\Delta\theta}{\int_{-\infty}^{+\infty} P(\varepsilon|\theta)f'(\theta)d\theta} \qquad \text{Equation 2-33}$$

where the term $P(\varepsilon|\theta)$ is the condition probability. It is referred to as the likelihood function of θ. If that likelihood function is symbolized as $L(\theta)$, and $K = \left[\int_{-\infty}^{+\infty} P(\varepsilon|\theta)f'(\theta)d\theta\right]^{-1}$, the Equation 2-33 becomes:

$$f''(\theta) = K\, L(\theta)\, f'(\theta) \qquad \text{Equation 2-34}$$

where K= the normalizing constant, $L(\theta)$ = the likelihood function, $f'(\theta)$ = the prior distribution, and $f''(\theta)$ = the posterior density function.

To adapt the above Bayesian updating approach to a pile capacity prediction, a set of pile load tests is required to get the actual pile capacity values. If the test outcome with a set of n observed values follows a normal distribution with a known standard deviation σ and a mean of $\overline{x}$, then the existing distribution of the pile capacity can be updated directly using the Bayesian approach. For a known prior normal distribution $f' = N_{\mu}(\mu', \sigma')$, the posterior density function of the mean pile capacity, f'', is also normal as reported by Ang and Tang (2007) and elsewhere, such as Kay (1976). If f'' is characterized as $f'' = N_{\mu}(\mu'', \sigma'')$, by solving Equation 2-34, the updated or posterior parameters for the mean capacity distribution are given by the following relationships:

$$\mu'' = \frac{\overline{x}(\sigma')^2 + \mu'(\frac{\sigma^2}{n})}{(\sigma')^2 + (\frac{\sigma^2}{n})} \qquad \text{Equation 2-35}$$

$$(\sigma'')^2 = \frac{(\sigma')^2(\frac{\sigma^2}{n})}{(\sigma')^2 + (\frac{\sigma^2}{n})} \qquad \text{Equation 2-36}$$

To obtain the updated distribution of the population, the predictive density $N_X(\mu_X'', \sigma_X'')$ for next observation is determined. Such a distribution combines uncertainties to give a future observation $\overline{x}$ given the observations $x_1, \ldots, x_n$. The resulting joint distribution is also normal when the prior and likelihood are normal. The parameters of the predictive distribution are given as:

$$\mu_X'' = \mu'' \qquad \text{Equation 2-37}$$

$$\sigma_X'' = \sigma\sqrt{1 + \frac{(\frac{\sigma'^2}{n})}{(\sigma')^2 + (\frac{\sigma^2}{n})}} \qquad \text{Equation 2-38}$$

where μ_X'' and σ_X'' are the updated mean and standard deviation of the population respectively. The predictive uncertainty will increase if there is uncertainty in the parameter values. It is clear that when the sample size (n) increases the influence of the prior mean (μ') diminishes, but when n is small, the posterior mean is close to the prior mean.

2.1.2.5.3 Steps for Updating Resistance Factors Based on Bayesian Theory

The technique for updating resistance is based on the Bayesian updating procedure that combines a prior distribution of the bias factor of the resistance with its likelihood distribution. The updated distribution of the resistance is obtained through the following procedure:

Step1. When pile capacity and loads are assumed to follow a lognormal distribution, the first two moment parameters, mean and standard deviation, of a corresponding normal distribution are first calculated from that of the lognormal distributions for both prior and likelihood functions. Equation 2-8 and Equation 2-9 are used for these calculations.

Step2. Based on the converted normal distributions of the prior information and the likelihood information, the Bayesian updating rule for multiple observations yields the mean and standard deviation of the posterior distributions using Equation 2-37 and Equation 2-38. The following expressions are obtained:

$$\mu_u = \frac{\mu_p(\sigma_l^2/n) + \mu_l\sigma_p^2}{\sigma_p^2 + (\sigma_l^2/n)}$$

$$\sigma_u^2 = \sigma_l\sqrt{1 + \frac{(\sigma_p^2/n)}{\sigma_p^2 + (\sigma_l^2/n)}}$$

where, μ = the normal mean value, σ = the normal standard deviation, n = sample size, subscript p, l, and u stand for prior, likelihood and updated estimates. Note that the test outcome with a set of n observed values is assumed to have a known standard deviation σ_l. This standard deviation is estimated from the site variability determined

among test piles at one site. The average σ_l corresponding to a coefficient of variation of COV=0.25 for medium within-site variability was chosen for the analysis in this study.

Step3. To obtain the corresponding lognormal parameters ($\mu_{\lambda_u}, \sigma_{\lambda_u}$) the normal posterior statistics are transformed back to lognormal using the following expressions (Zhang & Tang, 2002):

$$\mu_{\lambda_u} = exp(\mu_u + 0.5\sigma_u^2)$$

$$\sigma_{\lambda_u}^2 = (\mu_{\lambda_u}^2)[exp(\sigma_u) - 1]$$

Step4. Based on FOSM, FORM, or MCS reliability analysis, the updated resistance factors (ϕ_u) are recalculated using the obtained posterior statistical parameters (μ_{λ_u} and $cov_{\lambda_u} = \sigma_{\lambda_u}/\mu_{\lambda_u}$) of the variable λ_R, resistance bias factor.

2.2 Methods of Pile Analysis

Designing deep foundations requires subsurface investigations that yield important soil information such as stratification, location of the water table and engineering properties of the soil and rock at the pile location. However, the piling process disturbs the soil, thus changing the theoretical pile capacity predicted using the soil properties measured before the installation. Different methods for predicting capacity of driven piles were developed to account for the soil disturbance during driving. This section provides a detailed review of some of pile analysis methods used to predict static axial pile capacity in the design of deep foundations.

2.2.1 Static Analysis Methods

Various methods exist to predict nominal axial capacity of driven piles. These methods include the static capacity methods, which are employed during the design phase to produce a preliminary length of the pile. Static capacity prediction methods are empirically or semi-empirically based and were developed on the basis of field load test data. Although the use of

these static analysis methods seems to be a straightforward process, they require the design to have similar setting as the dataset utilized in developing the methods. When an axial load is applied to a vertical pile, the pile transfers it to the soil through end bearing and side friction. At static equilibrium state applied load is equal to the sum of the resistance forces mobilized by soil as shown in the following general equations (Dennis, 1982):

$Q + W_p = Q_s + Q_p$ (In compression) Equation 2-39

$Q = Q_s + Q_p + W_p$ (In tension) Equation 2-40

where, Q is the pile capacity, Q_s is the total load transfer from pile to soil in side friction, Q_p is load transfer in end bearing, and W_p is the weight of the pile. The submerged weight of piles is oftentimes ignored, and for piles in tension the term $Q_p$disappears. The above expressions constitute the basis for the following static capacity prediction methods.

2.2.1.1 Pile Capacity in Cohesive Soils

The methods include the Alpha (α) methods, Beta (β) method, Lambda (λ) methods, and CPT-method.

2.2.1.1.1 The Alpha (α) method (Tomlinson, 1957, 1971)

The Tomlinson method (1957, 1971) for designing piles driven into clay soils is based on the methodology of predicting the unit side resistance (f_s) of piles. In this method, also known as the alpha method, the unit side resistance is expressed as f_s also called as C_a.

$C_a = \alpha \, . \, c_u$ Equation 2-41

where $f_s$or C_a = unit side resistance, c_u = mean undrained shear strength along the length of the pile and α = an adhesion factor that is a function of c_u. Tomlinson determined that α decreases as c_u increases. However, his database included measurements of c_u obtained from lower-quality strength testing, such as the unconfined compression (UC) or unconsolidated undrained (UU)

triaxial tests. He analyzed loading tests on steel pipe and shell piles, tapered and untapered precast concrete piles, and timber piles driven into clays and silts. All these piles were axially loaded in compression. The failure load was taken from the load-settlement curve at a deflection of one-tenth of the pile diameter. The set-up time between pile driving and loading varied between 5 days to 3 years. The measured side capacity (Q_s) was obtained by subtracting the calculated tip capacity from the measured pile capacity. Tomlinson used the following relationships to compute the adhesion factor (α).

$$Q_s = Q_f - N_C A_b c_b = Q_f - 9. A_b c_b \qquad \text{Equation 2-42}$$

$$\alpha = \frac{C_a}{c_u} = \frac{Q_s}{C.L.c_u} \qquad \text{Equation 2-43}$$

where Q_s = measured side capacity, Q_f = ultimate carrying capacity of pile, N_C = bearing capacity factor, A_b = area of base of pile, c_b = cohesion at base of pile, C = circumference of pile, L =embedded length of pile. During design unit side resistance $C_a, or\ f_s$ is obtained from Figure 2-7, which plots pile unit side resistance versus undrained shear strength for piles embedded in cohesive soils. If adhesion factor (α) is required, Figure 2-8 is used.

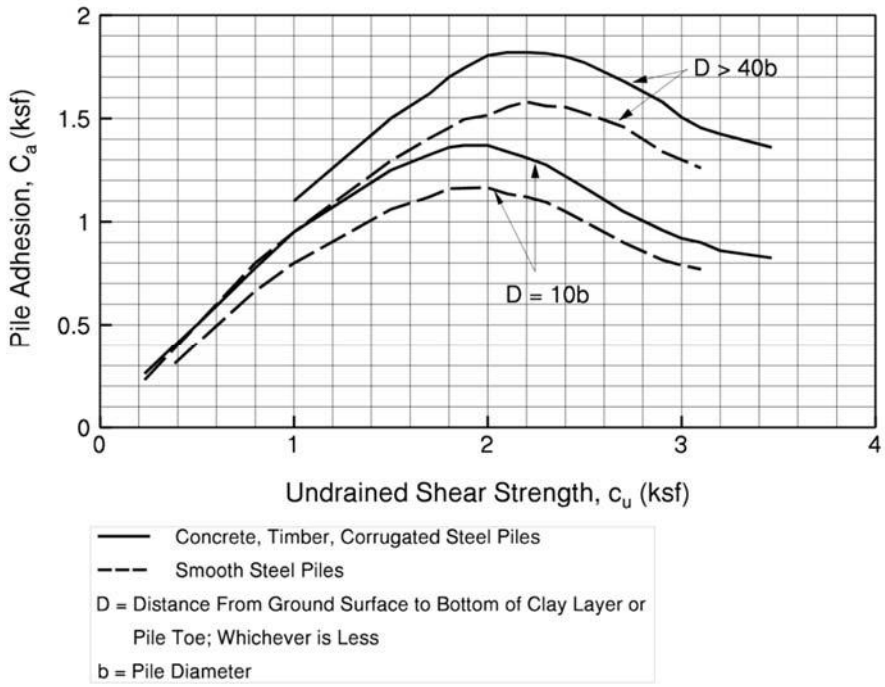

Figure 2-7 Pile Adhesion versus Undrained Shear Strength for Piles Embedded into Cohesive Soils; adapted from Mathias and Cribbs (1998).

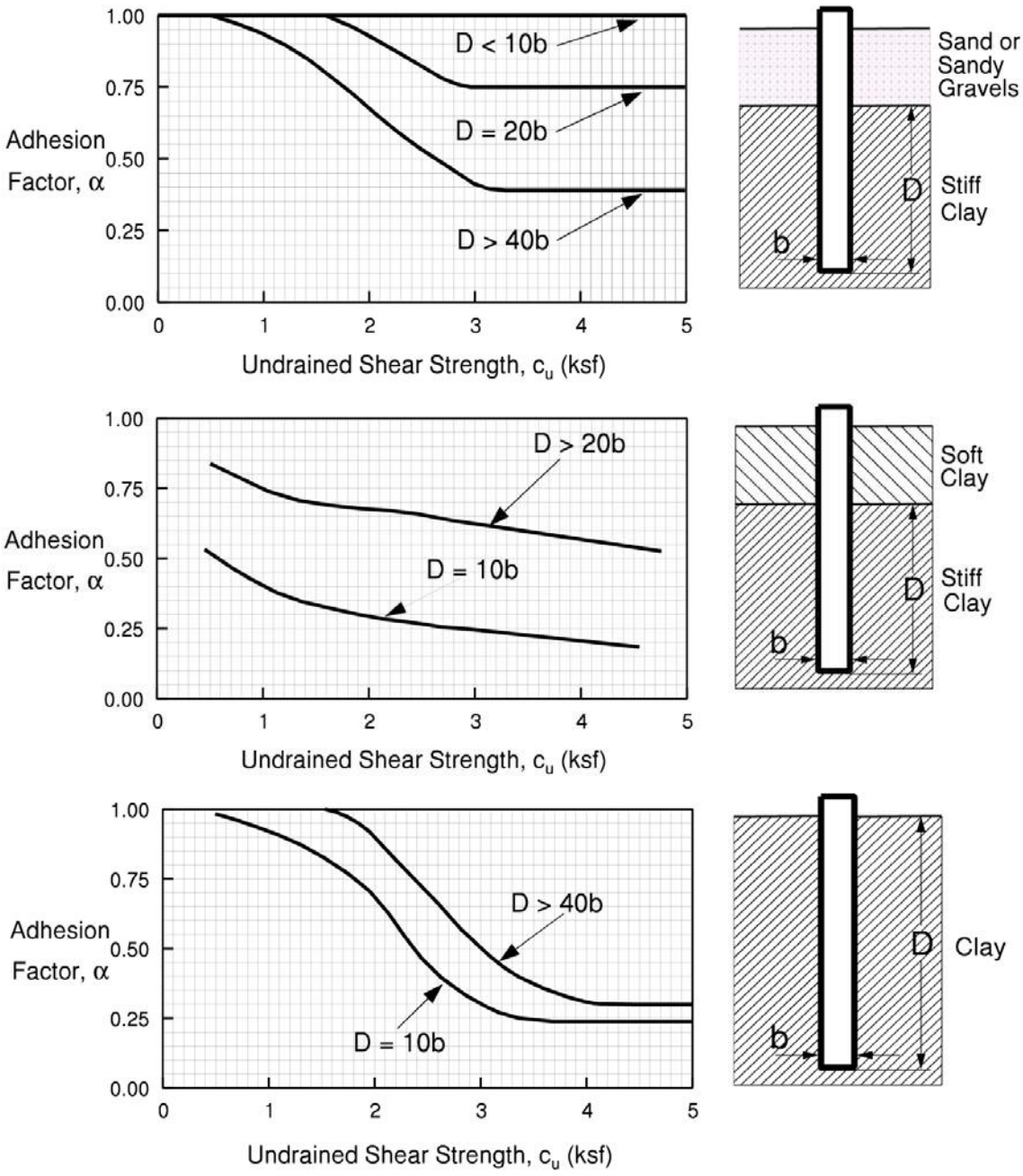

Figure 2-8 Relation between Adhesion Factors and Undrained Shear Strength for Piles driven into Predominantly Cohesive Soils (Tomlinson, 1971) as adapted from Mathias and Cribbs (1998).

2.2.1.1.2 The α-API Method

The α-API-I Method was developed by the American Petroleum Institute (API) in 1974. Like Tomlinson's approach, the API method is also based on total stress analysis and is a semi-empirical procedure. The alpha factor was back calculated from pile load tests. However, pile load tests were better documented and more reliable than those used by Tomlinson. Most of the pile tests took place in the offshore or near offshore environment. Using the undrained shear strength (c_u) of the soil, the side capacity of the pile is calculated. To determine side unit resistance of the pile Equation 2-41 is employed, but the developed α -values are given by the following relationships:

$$\alpha = 1 \qquad for\ c_u \leq 500\ psf \qquad \text{Equation 2-44}$$

$$\alpha = 1.25 - 0.5\left(\frac{c_u - 500\ psf}{2000}\right) \qquad for\ 500\ psf < c_u < 1500\ psf \qquad \text{Equation 2-45}$$

$$\alpha = 0.5 \qquad for\ c_u \geq 1500\ psf \qquad \text{Equation 2-46}$$

API-II method is an improvement of API-I, and it incorporates the influence of c_u/p' ratio in α expression for Siliceous and Carbonate soils. According to API RP 2A-WSD (2000) :

$$\alpha = 0.5(c_u/p')^{-0.5} \leq 1.0 \qquad for\ (c_u/p') \leq 1.0 \qquad \text{Equation 2-47}$$

$$\alpha = 0.5(c_u/p')^{-0.25} \leq 1.0 \qquad for\ (c_u/p') > 1.0 \qquad \text{Equation 2-48}$$

where p′ is the effective overburden pressure at the point of consideration. The procedure to compute the unit end bearing q, in cohesive soils, as recommended by API RP 2A (2000), is as follows:

$q = 9.c_b$ where c_b is the cohesion at base of pile Equation 2-49

2.2.1.1.3 The β Method

The β-method is used for predicting side friction of piles based on effective stress. The use of effective stress attempts to model the long-term drained shear strength of the soil

surrounding the pile. The method is based on a semi-empirical approach, and the effective stress is derived from the free-field vertical effective overburden stress. Fellenius (1991) established β values to be used for different soil types such as clay, silt, sand, or gravel. The method can be adapted to even be used for layered soil profiles. The beta factor (β) is affected by the soil type, mineralogy, density, strength, pile insulation technique, and other factors. The values of β range normally range between 0.23 and 0.8, and may exceed 1.0 for over-consolidated soils , but cannot exceed 2.0 (Esrig & Kirby, 1979). The AASHTO LRFD Bridge Design Guide, (2012) reports that the β-method works best for piles in normally consolidated and lightly over-consolidated soils. The unit skin friction of the pile with this effective stress method is calculated as follows:

$$f_s = \beta \,.\, \bar{p}_o \qquad \text{Equation 2-50}$$

where

β = Bjerrum-Burland beta coefficient $\beta = k_s tan\ \delta$ (or Table 2-2)

$\bar{p}_o$ = Average effective free-field overburden pressure along the pile shaft

k_s = Earth pressure coefficient, and δ = Friction angle between pile and soil

The unit end bearing q_t is given by:

$$q_t = N_t \,.\, p_t \qquad \text{Equation 2-51}$$

where N_t is the end bearing capacity coefficient (Table 2-2), and p_t is the effective overburden pressure at pile toe.

Table 2-2 Approximate Range of Beta Coefficient, β and End Bearing Capacity Coefficient, N_t for various Ranges of Internal Friction Angle of the Soil, after Fellenius (1991).

Soil type	ϕ' (deg.)	β	N_t
Clay	25 – 30	0.23 – 0.40	3 – 30
Silt	28 – 34	0.27 – 0.50	20 – 40
Sand	32 – 40	0.30 – 0.60	30 – 150
Gravel	35 – 45	0.35 – 0.80	60 – 300

2.2.1.1.4 Lambda (λ-I) method (Vijayvergiya & Focht Jr., 1972)

The λ-method is an empirical approach and was developed from a combination of both total and effective stress concepts. The effect of depth on cohesion was also considered in the relationship. Piles were driven into the cohesive soils at various depths and their side capacities were evaluated. The design factor λ was calculated based on the following relationship for a specified pile tip depth:

$$\lambda = Q_s/[(\sigma'_v + 2c_u)(C.L)] \quad or \quad Q_s = \lambda[(\sigma'_v + 2c_u)(C.L)] \qquad \text{Equation 2-52}$$

$$Q_{tot} = Q_s + 9.A_b c_b \qquad \text{Equation 2-53}$$

where Q_s = measured side capacity; Q_{tot} = ultimate carrying capacity of pile; λ = dimensioless coefficient that characterizes the friction between pile and soil as presented in Figure 2-9; σ'_v = mean effective vertical stress between the ground surface and the pile tip; C = circumference of pile; L = length of pile; c_u = mean undrained shear strength along the pile; c_b = undrained strength at the base of the pile; and A_b = area of the base of the pile.

Some judgment is required in selecting values for geometry and strength when using this method for pile types other than pipe piles, as the method was originally developed for straight sided steel pipe piles in clay (Dennis, 1982).

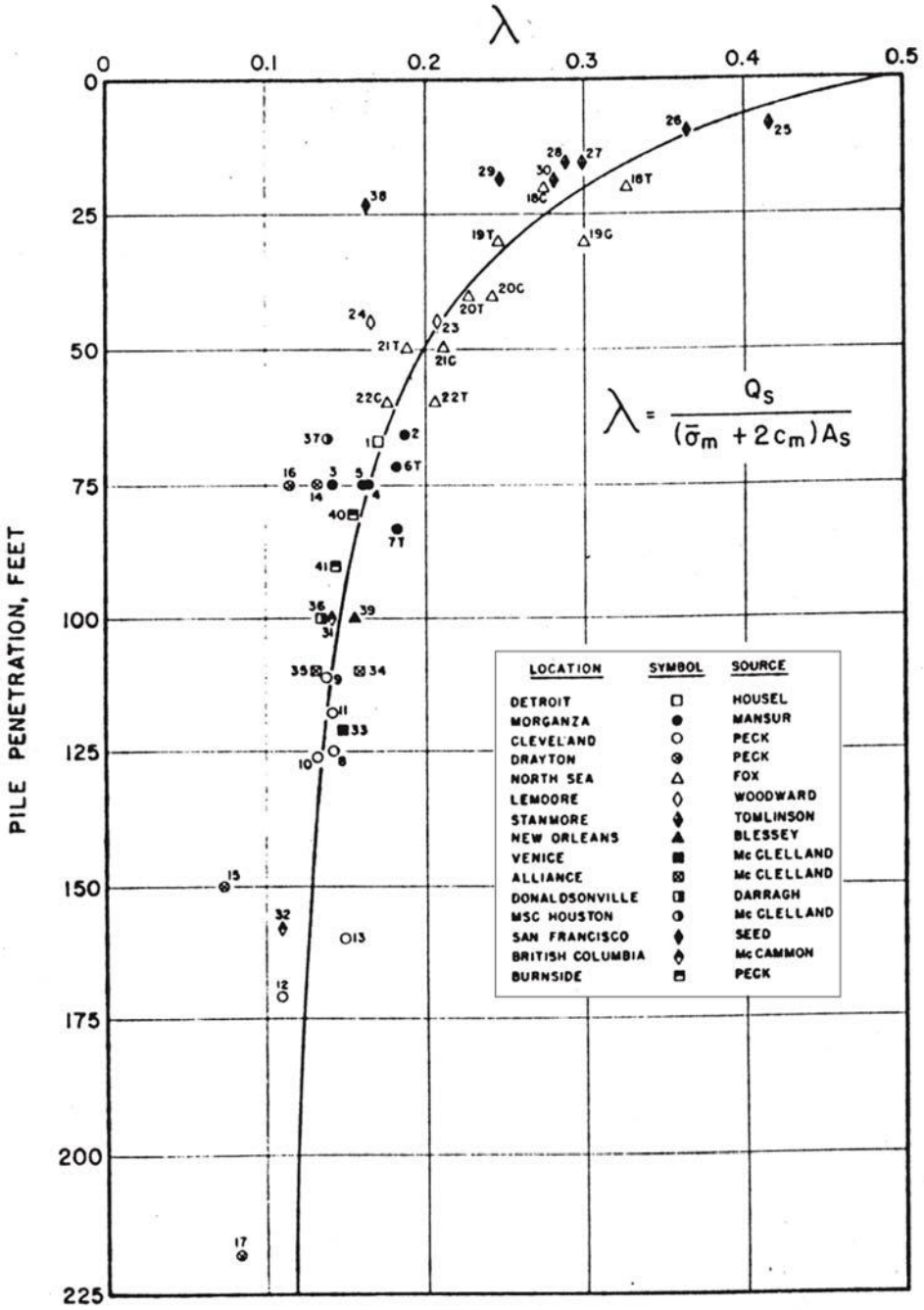

Figure 2-9 Values of Lambda, λ, versus Pile Penetration in Cohesive Soils (Vijayvergiya & Focht Jr., 1972).

2.2.1.1.5 Lambda (λ -II) method (Kraft, Amerasinghe, & Focht, 1981)

The λ-II-method is an improved λ–method. The λ coefficient is improved by incorporating a pile-soil stiffness factor π_3 in the design. This factor π_3 was introduced based on full scale pile load testing (pile load tests with strain gages installed on the pile skin to measure shaft friction along the pile skin). The factor π_3 takes into account pile stiffness E and the amount of movement, u, between pile and soil necessary to mobilize the full unit side capacity. The method uses Equation 2-52 and Equation 2-53 as λ –method. However, λ is calculated using Equations 2-55 and 2-56 and is a function of pile-soil stiffness and the consolidation state of the soil. The pile-soil stiffness, π_3, is established using the following relationship:

$$\pi_3 = \pi D f_{max} L^2/(AEu^*) \qquad \text{Equation 2-54}$$

where D = pile diameter; f_{max} = peak soil-pile friction ≈ c_u; A = cross sectional area of the pile adhesion between pile and soil; E = pile modulus; L = embedded pile length; u^* = relative soil-pile movement at which f_{max} is developed (normally taken as 0.1 in.).

The value of λ is a function of the c_u/p' ratio of the soil and π_3 as illustrated in the following equations:

$$\lambda = 0.178 - 0.016\, ln(\pi_3) \quad for\ c/p' \leq 0.4 \textit{ (normally consolidated soils)} \qquad \text{Equation 2-55}$$

$$\lambda = 0.232 - 0.032\, ln(\pi_3) \quad for\ c/p' > 0.4 \textit{ (overconsolidated soils)} \qquad \text{Equation 2-56}$$

These values of λ are subjected to a minimum value of 0.14 as reported by Kraft et al., (1972).

2.2.1.1.6 The CPT-Method

The Cone Penetration Test (CPT) method used in the current study for predicting pile capacity was originally developed by Nottingham and Schmertmann (1975). The method is empirically based and uses CPT values to calculate the pile capacity. Since the CPT provides continuous readings for the soil profile, this CPT method leads to a more accurate pile design

capacities. For driven piles, the cone method accurately models the system, where cone tip resistance (q_c) is used to determine the tip resistance of piles, while the sleeve friction ($\bar{f}_s$) is used to calculate the skin friction along the pile shaft. For non-cohesive soils, the ultimate shaft resistance R_s is computed as (Hannigan, Goble, Thendean, Likins, & Rausche, 1998):

$$R_s = k\left[\frac{1}{2}\left(\bar{f}_s A_s\right)_{0-8b} + \left(\bar{f}_s A_s\right)_{8b-D}\right] \quad \text{Equation 2-57}$$

If $\bar{f}_s$ is not available, R_s can be calculated from the cone tip resistance as follows:

$$R_s = C_f \sum q_c \,.A_s \quad \text{Equation 2-58}$$

For cohesive soils, the shaft resistance is computed as follows:

$$R_s = \alpha'.\bar{f}_s.A_s \quad \text{Equation 2-59}$$

where:

k = Ratio of unit pile shaft resistance to unit cone sleeve friction in sands (Figure 2-10)

D = Embedded pile length

b = Pile width or diameter

$\bar{f}_s$ = Average unit sleeve friction from CPT at the point considered

A_s = Pile-soil surface area over the point considered

C_f = Factor obtained from Table 2-3

q_c = Average cone tip resistance along the pile length

α' = Ratio of pile shaft resistance to cone sleeve friction (Figure 2-11)

The ultimate tip resistance q_t is calculated as follows:

$$q_t = (q_{c1} + q_{c2})/2 \quad \text{Equation 2-60}$$

where q_{c1} = Average of cone tip resistance over the distance xb as shown in Figure 2-12, b = Pile diameter, q_{c2} = Average of cone tip resistance over the distance 8b above the pile.

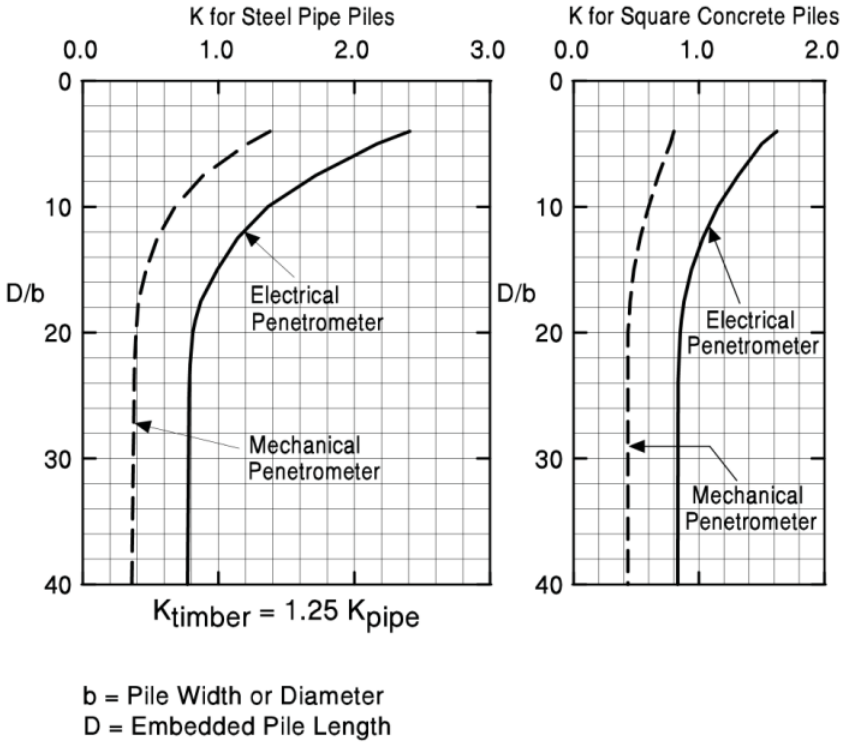

Figure 2-10 Penetrometer Design Curves for Side Friction Estimation for Different Types of Pile Driven into Sands (Hannigan et al., 1998).

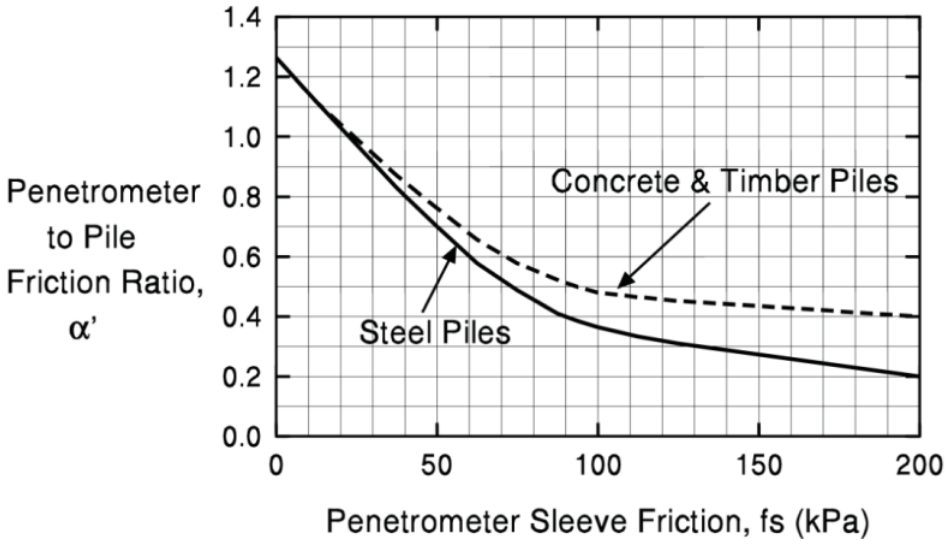

Figure 2-11 Design Curve for Estimating Side-Friction for Different Types of Pile Driven in Clay Soils (Schmertmann, 1978).

Table 2-3 Values of CPT- C_f Factor for Different Types of Piles (Hannigan et al., 1998).

Type of piles	**C_f**
Precast concrete	0.012
Timber	0.018
Steel displacement	0.012
Open end steel pipe	0.008

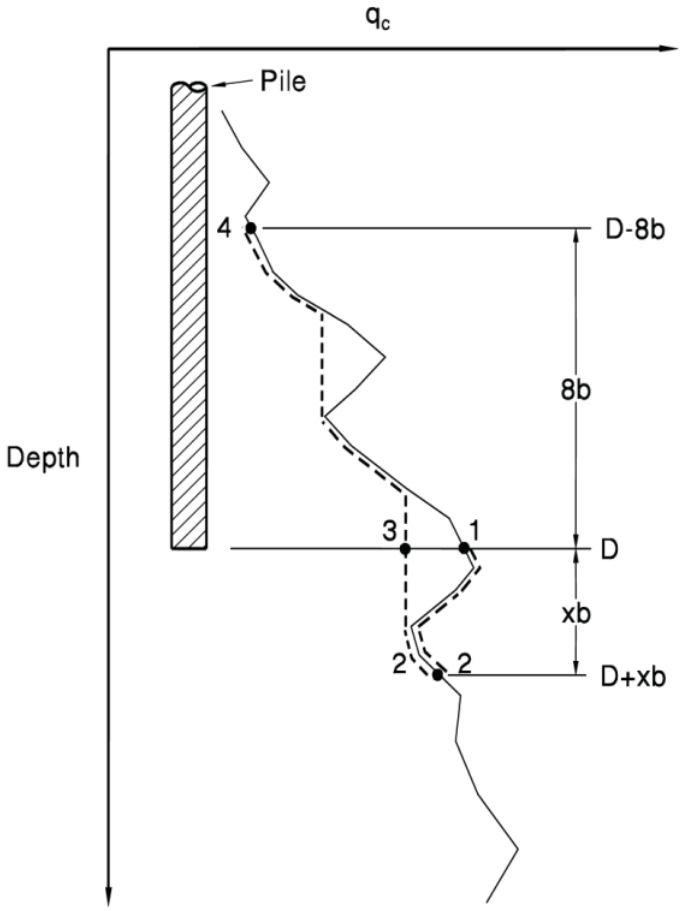

q_{c1}: Average q_c over a distance x_b below the pile tip (path 1-2-3). Sum q_c values in both the downward (path 1-2) and upward (path 2-3) direction. Use actual q_c values along path 1-2 and the minimum path rule along path 2-3. Compute q_{c1} for x-values from 0.7 to 3.75 below the pile toe and use the minimum q_{c1} value obtained.

q_{c2}: Average q_c over a distance 8b above the pile toe (path 3-4) using the minimum path rule as for path 2-3 in q_{c1} computations. D: Embedded pile length.

Figure 2-12 Illustration of Nottingham and Schmertman Procedure for Estimating Pile Toe Capacity as Reported by Hannigan et al.(2006).

2.2.1.2 Pile Capacity in Cohesionless Soils

2.2.1.2.1 The SPT-Meyerhof Method (1956, 1976)

Prediction of pile capacity based on SPT N-values was first reported by Meyerhof (1956). He first correlated N-values with the cone tip resistances From CPT that had been correlated with pile resistances. He further enhanced the results of the predictions in (1976). The method is an empirical approach used in cohesionless soils, such as sands and non-plastic silts. Due to the non-reproducibility of SPT N-values and simplified assumptions contained in the method, the FHWA-HI 97-013 (Hannigan et al., 1998) suggests the method only be used for preliminary estimates of the pile capacity, not for final design recommendations. For piles driven to a depth D_b in cohesionless soil, the unit end bearing capacity, q_t, is given by:

$$q_t = \frac{0.4\ \bar{N}'_b . D_b}{b} \quad \leq \overline{4N}'_b\ tsf \ \textit{for sands or}\ \ 3\bar{N}'_b\ tsf \ \ \textit{for non-plastic silts} \qquad \text{Equation 2-61}$$

where $\bar{N}'_b$= average SPT blow counts (blows/1ft) of the bearing stratum extended to 3b below pile tip and corrected for overburden pressure, b = Pile diameter, and D_b= Pile embedment depth in the bearing stratum.

The average value of side shear f_s, in tsf, in cohesionless soils for the SPT-Meyerhof method, is calculated using the following equations:

$$f_s = \frac{\bar{N}'}{50} \leq 1.0\ tsf \qquad \textit{for displacement (e.g., closed end pipe) piles} \qquad \text{Equation 2-62}$$

$$f_s = \frac{\bar{N}'}{100} \leq 0.5\ tsf \qquad \textit{for non-displacement (e.g., Open End Pipes, H) piles} \qquad \text{Equation 2-63}$$

where $\bar{N}'$ is the average SPT blow counts along the pile and corrected for overburden pressure.

2.2.1.2.2 The Nordlund Method (1963)

Nordlund (1963) developed a semi-empirical method for predicting pile capacity in cohesionless soils, such as sandy and gravelly soils. The method was developed based on field observations from static pile load tests. The general relationship between pile resistance and soil shear parameters suggested by Nordlund accounts for different pile shapes as well as pile types and materials, such as H-piles, closed and open-ended pipe piles, and timber piles. FHWA-NHI-05-042 (Hannigan et al., 2006) provides a more detailed pile design procedure using the Nordlund method. Special judgment should be used when applying the method to piles greater than 500 mm in diameter/width as the piles used to establish the method were smaller than that. The general equation for tapered piles for total ultimate pile capacity is given by the following equation:

$$Q_u = \sum_{d=o}^{d=D} K_\delta \cdot C_f \cdot P_d \cdot \frac{sin(\delta + \omega)}{cos\,\omega} C_d \cdot \Delta d + \alpha_t \cdot N_q' \cdot A_t \cdot P_t \qquad \text{Equation 2-64}$$

For piles with uniform cross sections, the capacity is calculated using the equation:

$$Q_u = K_\delta \cdot C_f \cdot P_d \cdot sin\,\delta \cdot C_d \cdot D + \alpha_t \cdot N_q' \cdot A_t \cdot P_t \qquad \text{Equation 2-65}$$

or, it can be written as: $$Q_u = K_\delta \cdot C_f \cdot P_d \cdot sin\,\delta \cdot C_d \cdot D + q_L \cdot A_t \qquad \text{Equation 2-66}$$

where:

d = Depth

D = Embedded pile length

K_δ = Coefficient of lateral earth pressure at depth d (Table 2-4)

C_f = Correlation factor for K_δ when $\delta \neq \varphi$ in Figure 2-13

P_d = Effective overburden pressure at the mid-depth of pile increment, d

δ = Friction angle between soil and pile

ω = Angle of pile taper from vertical

C_d = Pile perimeter at depth d

Δd = Length of pile segment

α_t = Factor depending on pile depth-width relationship as presented in Figure 2-14

N_q' = Bearing capacity factor presented in Figure 2-15 (Hannigan et al., 2006)

A_t = Pile toe area

P_t = Effective overburden pressure at the pile toe ≤ 150 kPa, ≤ 3.2 ksf

q_L = Limiting unit tip resistance in Figure 2-16

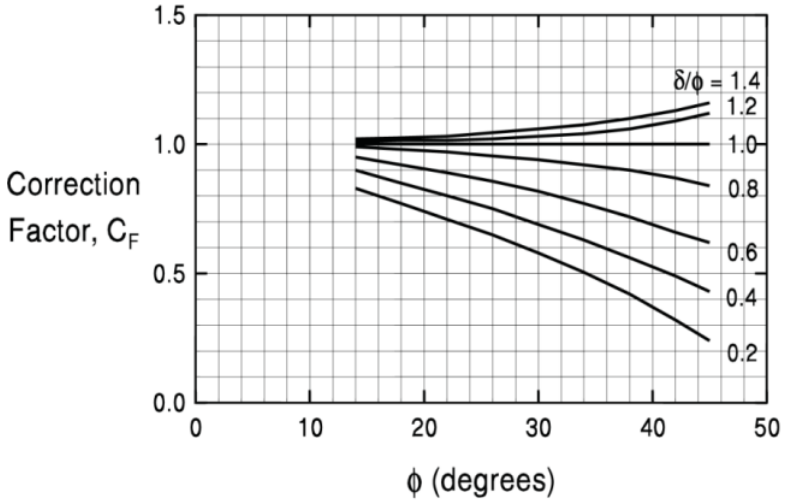

Figure 2-13 Correction Factor C_f for K_δ when Friction Angle between Pile and Soil, δ is Different from Internal Friction Angle ϕ of the Soil (Hannigan et al., 2006).

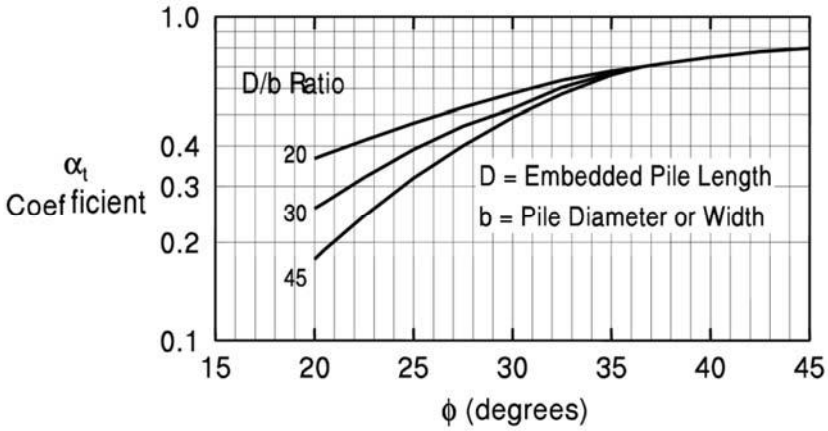

Figure 2-14 Chart for Estimating the Values of α_t Coefficient from Internal Friction Angle ϕ

Table 2-4 Design Table for Evaluating Values of K_δ for Piles when $\omega = 0^o$ and V= 0.10 to 10.0 ft^3/ft. as adapted from FHWA-NHI-05-042 (Hannigan et al., 2006).

ϕ[°]	Displaced volume (V), from 0.10 to 1.00 ft^3/ft (0.0093 to 0.0930 m^3/m)									
	0.10	0.20	0.30	0.40	0.50	0.60	0.70	0.80	0.90	1.00
25	0.70	0.75	0.77	0.79	0.80	0.82	0.83	0.84	0.84	0.85
26	0.73	0.78	0.82	0.84	0.86	0.87	0.88	0.89	0.90	0.91
27	0.76	0.82	0.86	0.89	0.91	0.92	0.94	0.95	0.96	0.97
28	0.79	0.86	0.90	0.93	0.96	0.98	0.99	1.01	1.02	1.03
29	0.82	0.90	0.95	0.98	1.01	1.03	1.05	1.06	1.08	1.09
30	0.85	0.94	0.99	1.03	1.06	1.08	1.10	1.12	1.14	1.15
31	0.91	1.02	1.08	1.13	1.16	1.19	1.21	1.24	1.25	1.27
32	0.97	1.10	1.17	1.22	1.26	1.30	1.32	1.35	1.37	1.39
33	1.03	1.17	1.26	1.32	1.37	1.40	1.44	1.46	1.49	1.51
34	1.09	1.25	1.35	1.42	1.47	1.51	1.55	1.58	1.61	1.63
35	1.15	1.33	1.44	1.51	1.57	1.62	1.66	1.69	1.72	1.75
36	1.26	1.48	1.61	1.71	1.78	1.84	1.89	1.93	1.97	2.00
37	1.37	1.63	1.79	1.90	1.99	2.05	2.11	2.16	2.21	2.25
38	1.48	1.79	1.97	2.09	2.19	2.27	2.34	2.40	2.45	2.50
39	1.59	1.94	2.14	2.29	2.40	2.49	2.57	2.64	2.70	2.75
40	1.70	2.09	2.32	2.48	2.61	2.71	2.80	2.87	2.94	3.00

ϕ	Displaced volume (V), from 1.0 to 10.0 ft^3/ft (0.093 to 0.930 m^3/m)									
	1.0	2.0	3.0	4.0	5.0	6.0	7.0	8.0	9.0	10.0
25	0.85	0.90	0.92	0.94	0.95	0.97	0.98	0.99	0.99	1.00
26	0.91	0.96	1.00	1.02	1.04	1.05	1.06	1.07	1.08	1.09
27	0.97	1.03	1.07	1.1	1.12	1.13	1.15	1.16	1.17	1.18
28	1.03	1.10	1.14	1.17	1.2	1.22	1.23	1.25	1.26	1.27
29	1.09	1.17	1.22	1.25	1.28	1.3	1.32	1.33	1.35	1.36
30	1.15	1.24	1.29	1.33	1.36	1.38	1.40	1.42	1.44	1.45
31	1.27	1.38	1.44	1.49	1.52	1.55	1.57	1.60	1.61	1.63
32	1.39	1.52	1.59	1.64	1.68	1.72	1.74	1.77	1.79	1.81
33	1.51	1.65	1.74	1.80	1.85	1.88	1.92	1.94	1.97	1.99
34	1.63	1.79	1.89	1.96	2.01	2.05	2.09	2.12	2.15	2.17
35	1.75	1.93	2.04	2.11	2.17	2.22	2.26	2.29	2.32	2.35
36	2.00	2.22	2.35	2.45	2.52	2.58	2.63	2.67	2.71	2.74
37	2.25	2.51	2.67	2.78	2.87	2.93	2.99	3.04	3.09	3.13
38	2.50	2.81	2.99	3.11	3.21	3.29	3.36	3.42	3.47	3.52
39	2.75	3.10	3.3	3.45	3.56	3.65	3.73	2.80	3.86	3.91
40	3.00	3.39	3.62	3.78	3.91	4.01	4.10	4.17	4.24	4.30

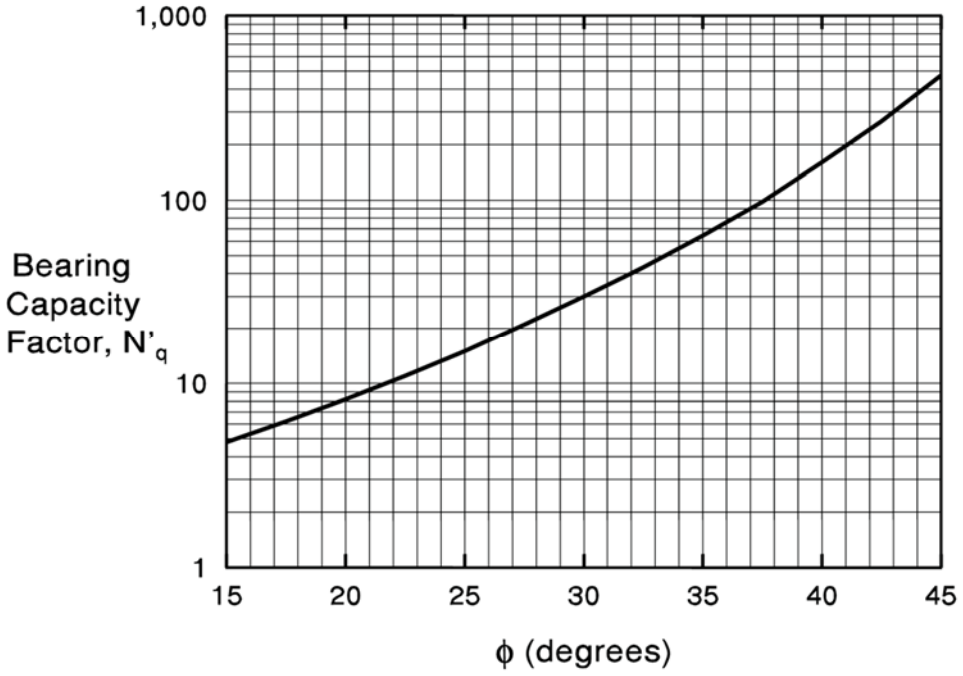

Figure 2-15 Chart for Estimating Bearing Capacity Coefficient N'_q from Internal Friction Angle ϕ of the Soil (Hannigan et al., 2006).

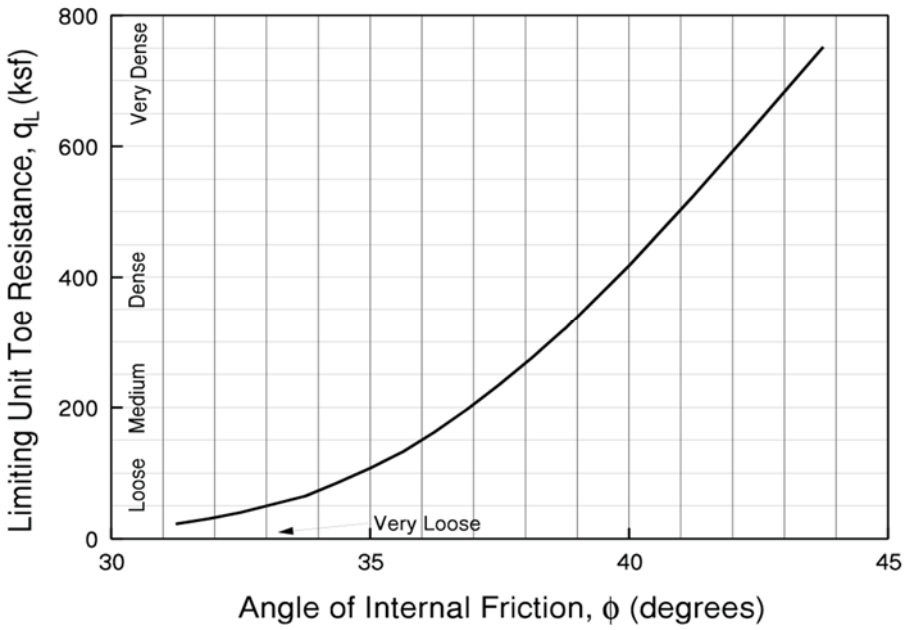

Figure 2-16 Relationship Between Toe Resistance and Internal Friction Angle ϕ in Sand as Reported by Meyerhof (1976).

2.2.1.2.3 The DRIVEN Computer Program

The program DRIVEN was developed by the FHWA to calculate pile resistance. The software implements the static capacity prediction methods using the procedures presented by Nordlund (1963), Thurman (1964), Meyerhof (1976), Cheney and Chassie (1982), Tomlinson (1971, 1987), and Hannigan, et. al. (1998). The capability of this program extends to open and closed end pipe piles, steel H-piles, concrete piles, and other pile types. Pile capacity calculation requires inputting the soil layers, unit weights, and strength parameters. The program gives an option to include the percentage of strength loss during driving into the analysis. Thus, pile capacity can be calculated at the EOD, as well as at BOR. DRIVEN can accommodate several analysis options such as downdrag, scour, pile plugging; and it can simulate multiple phreatic surfaces. The program can create an input file formatted for the GRLWEAP program for further capacity analysis using stress wave analysis (Mathias & Cribbs, 1998). However, some challenges still exist in the use of the DRIVEN program.

DRIVEN only accepts a maximum of five SPT-N values, creating a limitation in a soil profile which might include many more than five blow counts. If soil layer has more than five N values, the user needs the engineering judgment in picking five representative N values for input. In order to overcome this barrier, the user could use an N-value to friction angle correlation to calculate effective friction angle values using the full set of reported SPT-N values for each layer. This can allow a more accurate representation of a layer which has highly variable SPT test results. DRIVEN does not allow the direct use of N-values for cohesive soils. Although the FHWA recommends the SPT N values solely for use with cohesionless soils, in many instances there is no other measure of resistance available for clay or silt layers. In the absence of other soil data, N values can be utilized to estimate undrained shear strength using existing

correlations, such as those presented in Table 2-5, published by Terzaghi and Peck (1961). Terzaghi listed a range of uncorrected N values corresponding to a range of unconfined compressive strength values. AASHTO (2012) recommends an improved correlation between SPT-N value and undrained cohesion as suggested by Hara et al. (1974), but several other correlations also exist e.g., Bowles (1996). This process of determining shear strength values for cohesive soils based on N values requires the judgment of an experienced engineer who is familiar with the local soil conditions.

Table 2-5 Relation of Consistency of Clay, Number of Blows N on Sampling Spoon and Unconfined Compressive Strength (Terzaghi & Peck, 1961).

Consistency	Very Soft	Soft	Medium	Stiff	Very Stiff	Hard
N	< 2	2 - 4	4 - 8	8 - 15	15 - 30	> 30
q_u (tons/ft^2)	< 0.25	0.25-0.50	0.50-1.00	1.00-2.00	2.00-4.00	> 4.00

The DRIVEN program does not allow the export of open ended pipe piles to GRLWEAP. The user must assume that the open ended pipe piles are closed-ended and has to check for plugging before exporting the data to GRLWEAP format. For H-Piles, the user must know when to use the H or Box perimeter/area for calculating side and tip areas. Only square shapes are supported in the DRIVEN program for concrete piles. If non-square concrete piles are to be analyzed the non-square shape must be transformed into an equivalent square pile with the same cross sectional area to retain proper side area for side friction development during DRIVEN analysis.

2.2.1.3 Comparison of Different Static Methods

Selecting an appropriate static analysis method for a specific pile design problem depends on several factors, such as the degree of accuracy needed from the design analysis, the soil and pile types, as well as the extent of measured soil properties. The commonly used static analysis

methods are presented in Table 2-6 along with a brief description of the general implementation approach and characteristics of each method

Table 2-6 Comparison Between Commonly Used Static Analysis Methods for Predicting Capacity of Driven Piles as adapted from AbdelSalam et al.(2012) and Hannigan et al.(2006).

Method	Approach	Recommended soil type	Design Parameters needed	Advantages	Limitations
SPT	Empirical	Non-cohesive soils	Results from SPT test. (i.e., N-value blow counts)	Commonly used SPT test, and availability of N-values for most construction projects, also it is a simple and easy method to use	The SPT test is not a reliable test compared to other lab and/or in-situ tests.
CPT	Empirical	Cohesive and Non-cohesive soils	Results of CPT test. (Sleeve friction and cone tip resistance)	CPT is an accurate test, and CPT method is very satisfactory especially for driven piles. It could be used in layered soils.	The CPT test is considered an expensive test. Difficult to advance cone in very hard cohesive soils.
Nordlund	Semi-empirical	Non-cohesive soils	Charts provided by Nordlund and Thurman (Hannigan et al., 2006)	It accounts for pile shape (i.e. tapered piles), as well as pile material and type (i.e. Steel H-piles, closed and open-end piles, timber piles).	The angle of soil internal friction is calculated using the SPT test N-values. The method over predicts the capacity for piles with widths larger than 600 mm.
α −methods	Semi-empirical	Cohesive soils	Undrained shear strength soil parameter (c_u). Adhesion factor (α).	Simple calculation from laboratory undrained shear strength values to adhesion. Widely used method especially in cohesive soils. It proved to give reasonable results for displacement and non-displacement piles.	There are several types of relations for α factor that give a large scatter and require engineering judgment and local experience when choosing the suitable relation.
β-method	Semi-empirical	Cohesive and Non-cohesive soils	Effective stresses calculated from the vertical effective overburden stress	Good design approach theoretically better than undrained analysis. It was developed to model the long-term drainage shear strength and can be used for different soil types and for layered soil profiles	The method tends to overestimate the pile capacity for heavily over consolidated soils.

2.2.2 Dynamic Formulas

2.2.2.1 Introduction

Dynamic pile driving formulas are used to determine the load carrying capacity of the pile based on observations of pile penetration obtained during the piling process. These dynamic formulas are empirically based, and the majority of them were derived from Newton's law of impact and conservation of energy principles. The records show that dynamic formulas have been in use well over 190 years, Eytelwein (Dutch) presented his driving formula in 1820 (Fragaszy, Higgins, & Lawton, 1985). Over the years many dynamic formulas have been presented in an attempt to develop more accurate and reliable prediction methods. In the early 1960s the editors of Engineering News Record (ENR) had 450 such formulas on file (E. A. Smith, 1962), and Chellis (1951) had collected thirty-eight dynamic pile driving formulas in his textbook. Equation 2-67 is the basis of all driving formulas. It equates the kinetic energy of the hammer to the work generated by the resistance of the pile as it penetrates the soil:

$$W_R \times h = R \times S \qquad \text{Equation 2-67}$$

where W_R= Weight of the pile driving ram, h = Drop height (stroke) of the ram, R = Resistance to pile penetration, and S = Pile penetration distance under one hammer blow, i.e., pile set.

The main differences that exists among various driving formulas resides in the way they handle energy losses that occur during hammer impact. Some of the formulas incorporate the energy losses due to only the temporary elastic compressions of the cap, pile, and soil (quake); others use the energy losses associated with only the Newtonian theory of impact, as described by the coefficient of restitution; and a few formulas consider both energy losses in their expressions. Despite the existence of many of these driving formulas, only a few of them are widely used. AASHTO LRFD Bridge Design Specifications (2012) only recommends the

FHWA Gates Formula for establishing pile driving criteria. The following section introduces 5 different driving formulas.

2.2.2.2 Engineering News Record (ENR Formula)

The Engineering News Record (ENR) formula was first published by A. M. Wellington in (1888). This formula was a simplified case of the rational formula developed earlier by J. F. Redtenbacher and presented in 1857. The formula is based on impulse-momentum theory. Initially, the ENR formula was developed to be used only for gravity hammers and timber piles, and it included a constant term, C which was given a value of 1.0 inch per blow to account for energy losses due to temporary elastic compression of the pile, pile cap, and soil. With introduction of more advanced driving equipment such as single- and double-acting steam hammers, Wellington proposed modifications of the constant term, C to compensate for the lubricating action of the soil that occurred as a result of the more rapid strokes of the new hammers. He further recommended a factor of safety of 6 to be used in the formula. The resulting ENR formula, as reported by Peck, et al. (1974), is presented in Equation 2-68.

$$R_u = \frac{W_R \times h}{s + C} \qquad \text{Equation 2-68}$$

where

R_u = Ultimate pile resistance measured during driving

W_R = Weight of the hammer ram, expressed in the same units as R_u

h = Height of fall of the ram (i.e., its stroke), expressed in the same units as s C

s = Pile penetration distance under one hammer blow, i.e., pile permanent set

C = Energy loss per hammer blow, (1.0 in. for drop hammers, and 0.1 in. for all other hammers)

The expression $W_R \times h$ can be replaced by E_h, which is rated hammer energy per blow for diesel, air-steam, or hydraulic hammers.

2.2.2.3 Janbu Formula

The Janbu driving formula was introduced in 1953 by Nilmar Janbu. The formula neglects the temporary elastic compressions in the system (Janbu, 1953). However, Fragaszy et al. (1985) report that Janbu incorporated a driving coefficient, K_u in the formula, which in turn contains terms representing the difference between static and dynamic capacity, the ratio is associated with the transfer of load into the soil as a function of depth, and hammer efficiency. Moreover, the driving coefficient is correlated with the ratio of the pile weight, W_p, to the weight of the pile driving hammer, W_R, in an effort to account for the variability in the energy available at the end of the period of restitution. The Janbu formula is expressed as follows:

$$R_u = \left(\frac{e_h \times W_R \times h}{s}\right)\left(\frac{1}{K_u}\right) \qquad \text{Equation 2-69}$$

$$K_u = C_d\left[1 + \left(1 + \frac{\lambda_e}{C_d}\right)^{1/2}\right]$$

$$C_d = 0.75 + 0.15\left(\frac{W_p}{W_R}\right)$$

$$\lambda_e = \frac{e_h \times W_R \times h \times L}{A \times E \times s^2}$$

2.2.2.4 Gates Formula

The Gates formula was proposed by Marvin Gates in 1957. The formula modeled a strictly empirical relationship between hammer energy, final pile set, and the measured capacity from static pile load test. Through statistical analysis and curve-fitting practice, Gates (1957) arrived at the final form of his formula as presented in Equation 2-70, and recommended that a factor of safety of 4 be applied to account for the uncertainties in the dataset.

$$R_u = \left(\frac{6}{7}\right)\sqrt{e_h \cdot E_h} \cdot log\left(\frac{10}{s}\right)$$ Equation 2-70

where R_u is the ultimate resistance to pile penetration expressed in tons, E_h is the rated hammer energy per blow expressed in foot-pounds per blow, and s = pile set in inches per blow.

2.2.2.5 FHWA Modified Gates Formula

As the name implies, the FHWA Modified Gates Formula originated from an enhancement to the original Gates formula presented in Equation 2-70. The fact that the original formula tended to over-predict pile capacity at low driving resistances and under-predict pile capacity at high driving resistances motivated the FHWA to update the formula. By performing statistical correlations on an extended database of static pile load tests, Richard Cheney of the FHWA arrived at the FHWA Modified Gates formula (Paikowsky et al., 2004) which is presented in Equation 2-71. Because of the high quality of the dataset used in establishing this formula, it is recommended that this dynamic pile driving formula be used before all other dynamic pile driving formulas in the construction control of driven pile in the 2007 through 2012 editions of the AASHTO-LRFD Bridge Design Specifications.(AASHTO, 2007, 2012).

$$R_u = 1.75\ \sqrt{W_R \cdot h} \cdot log_{10}(10 \cdot N_b) - 100$$ Equation 2-71

where R_u= Ultimate resistance to pile penetration (kips), W_R = Weight of the pile driving ram expressed in pounds, h= Drop height of the ram expressed in feet, and N_b = Number of hammer blows for one inch of pile permanent set.

2.2.2.6 WSDOT Driving Formula

The Washington State Department of Transportation (WSDOT) conducted an in-house study to develop its own version of a pile driving formula similar to the Gates formula. Allen (2005) developed the WSDOT formula based on an expanded database established by Paikowsky et al. (2004). This database was comprised of data from numerous static pile load

tests conducted throughout the US. Allen (2005) followed procedures similar to those used by Richard Cheney of the FHWA and also departed from Gates formula to statistically enhance the prediction of the in-house formula. The final form of formula is presented in Equation 2-72.

$$R_u = 6.6\, F_{eff} \cdot W_R \cdot h \cdot ln\ (10 \cdot N_b) \qquad \text{Equation 2-72}$$

where

R_u = Ultimate bearing resistance, in kips

F_{eff} = Hammer efficiency factor, equal to 0.55 for air/steam hammers with all pile types, 0.37 for open-ended diesel hammers with concrete or timber piles, 0.47 for open-ended diesel hammers with steel piles, 0.35 for closed-ended diesel hammers with all pile types, 0.58 for hydraulic hammers with all pile types, and 0.28 for gravity hammers with all pile types,

W_R = Weight of ram, in kips

h = Vertical drop of hammer or stroke of ram, in feet

N_b = Average penetration resistance in blows per inch for the last 4 inches of driving

ln = The natural logarithm, in base "e"

2.2.2.7 Comparison of Different Driving Formulas

As stated earlier many pile driving formulas exist for the construction control of driven piles, which makes it difficult to select one formula that best suits a particular case. Many comparative studies have been carried out in the past to identify the best performing formulas. The general trend is that when specific combinations of pile, hammer, and soil type are considered, none of the dynamic formulas is consistently better than all of the others. For many driving formulas that existed in the late 40s, Chellis (1949) showed that it was extremely difficult to compare their performance because each formula performed well in only specific conditions.

Nonetheless, Olson and Flaate (1967) concluded that the ENR was inferior to the other studied formulas based solely on its remarkably low correlation coefficient. This was later confirmed by Fragaszy et al. (1989) who found the ENR formula to be the least accurate method with a COV of the predicted to measured ultimate pile capacity being approximately two to three times higher than that for the Gates formula. The Gates formula was the most accurate formula among all formulas on the comparative list. AASHTO LRFD Bridge Design Specifications (2007, 2012) recommends its derivative, FHWA-Gates Formula.

2.2.3 Dynamic Analysis Methods

2.2.3.1 Introduction

Dynamic analysis methods model the hammer-pile-soil system better than the dynamic pile driving formulas do. In addition to predicting pile capacity during construction, the dynamic analysis methods possess extended advantages over static analysis methods, as they can be used to control pile construction, detect pile damage, evaluate driving hammer performance, assess soil resistance distribution, determine dynamic soil parameters and evaluate the setup/relaxation effect. The working principles of the dynamic analysis methods are based on wave propagation theory, which was first proposed by A.J.C Barre de Saint Venant in the 1860's. This Frenchman developed the differential equation governing one dimensional wave propagation in an elastic rod and also proposed its theoretical solution. Saint Venant's equation was applied to pile driving analyses around the world in the 1930's, e.g., L.H. Donnell in the United States, D.V. Isaacs in Australia, and W.H. Glanville in England (Goble & Rausche, 1980). The application of the method has progressively evolved in the United States. There are different dynamic methods that are now being routinely used, such as signal matching and wave equation analysis programs. Dynamic analysis using principles of stress wave analysis has been incorporated into a standard

specification for deep pile foundations by the American Society for Testing and Materials (ASTM Standard D4945-12, 2012) under the title of high-strain dynamic testing of deep foundations.

2.2.3.2 Pile Driving Analyzer (PDA)

The Pile Driving Analyzer (PDA)is a data acquisition system which conditions and converts signals from strain gauges and accelerometers attached to the pile during driving to records of force and velocity versus time (Hannigan et al., 1998). Pile Driving Analyzer, as it is known today, was developed in the 1960s by George Goble and his students at the Case Western Reserve University, and uses the Case method of signal matching to analyze stress waves and predict pile capacity. The first comprehensive study using signal matching was conducted by W.H. Glanville, et al., in 1938. The focus of the study was to understand why concrete piles cracked at both the top and the bottom during pile driving. As part of his study, measurements were taken during pile driving using what was considered, at that time, portable equipment which needed to be housed in a construction trailer (Glanville, Grime, Fox, Davies, & Institution of Civil Engineers, 1938). Glanville was truly the pioneer in the field of signal matching, as it would take some 18 years before similar work was done in the Netherlands by A. Verduin in 1956 and some 25 years before it was done in the United States (Goble & Rausche, 1980).

The PDA performs integrations and all other required computations to analyze the dynamic records for transferred energy, driving stresses, structural integrity, and pile capacity during pile driving. Analyses can be conducted at the end of driving, and during pile restrike. The force in the pile is computed from the measured strain, ε, times the product of the pile elastic modulus, E, and cross sectional area, A, or: $F(t) = EA\varepsilon(t)$. The velocity is obtained by integrating the measured acceleration, record, a(t), or: $V(t) = \int a(t)dt$. A typical PDA-dynamic

testing system consists of the data acquisition system (Figure 2-17a) and a pair of strain gages and accelerometers bolted to diametrically opposite sides of the pile (Figure 2-17b) to monitor strain and acceleration and account for nonuniform hammer impacts and pile bending.

(a) (b)

Figure 2-17 A typical PDA-system Consisting of (a) PDA-data Acquisition System and (b) a Pair of Strain Transducers and Accelerometers Bolted to Pile (Rausche, Nagy, Webster, & Liang, 2009).

Signal matching has alleviated some shortcomings associated with dynamic formulas. Signal matching addresses the assumption of a rigid pile that neglects pile axial stiffness effects on driveability, the assumption that the soil resistance is constant and instantaneous to the impact force. The PDA collects measurements during pile driving and numerical results for each blow for dynamic quantities are electronically stored for later production of graphical and numerical summary outputs. In the PDA, force and velocity records are viewed on a graphic LCD computer screen (Figure 2-17a) during pile driving to evaluate data quality, soil resistance distribution, and pile integrity. Using the force and velocity records, the PDA estimates the total soil resistance (RTL) using Equation 2-73. This equation is based on the Case method, which assumes the dynamic soil resistance as a linear function of a viscous damping coefficient and velocity at the pile toe. The total soil resistance is assumed to be a combination of static and dynamic resistances. Hannigan et al. (2006) specified that the viscous damping coefficient is a product of

a Case damping factor (J_c) and a pile impedance ($Z = EA/C$) as it was defined by Goble et al. (1975).

Table 2-7 shows the recommended Case damping factor (J_c) values. The static soil resistance (RSP) is derived from Equation 2-74, by subtracting the dynamic soil resistance from the total soil resistance. To estimate pile capacity, the PDA uses the maximum static resistance (RMX) by searching for time t_1 in the force and velocity records that gives the largest value of static soil resistance (RSP).

$$RTL = \frac{1}{2}[F(t_1) + F(t_2)] + \frac{1}{2}[V(t_1) - V(t_2)] \quad \text{Equation 2-73}$$

$$RSP = RTL - J_c[\frac{EA}{C}V(t_1) + F(t_1) - RTL] \quad \text{Equation 2-74}$$

where

RTL = Total soil resistance at time t_1 of initial hammer impact, kip;

RSP = Static soil resistance at time t_1 of initial hammer impact, kip;

$F(t_1)$ = Force measured at transducer location at time t_1, kip;

$F(t_2)$ = Force measured at transducer location at time $t_2 = t_1 + 2L/C$, kip;

$V(t_1)$ = Velocity measured at accelerometer location at time t_1, ft/s;

$V(t_2)$ = Velocity measured at accelerometer location at time $t_2 = t_1 + 2L/C$, ft/s;

E = Modulus of elasticity of the pile (ρC^2) , ksi;

A = Cross sectional area of the pile, in2;

C = Speed of the stress wave, ft/s;

L = The pile length below the transducers (gages) or LE used in the PDA, ft; and

J_c = Dimensionless Case damping factor presented in Table 2-7

The Case Method solution presented in the equations above is simple enough, computationally, so that on-site real-time predictions of pile capacity between hammer blows can be accomplished using the PDA. However, this estimated static resistance is a function of the dimensionless Case damping factor (J_c) selected by the operator, which can introduce subjectivity into the pile capacity determination. Therefore, a post-processing of the signal data is required and a signal matching technique is used for a more accurate result. To do that, the data from the PDA is used in tandem with signal matching program, such as CAPWAP, which is described in the following subsection.

Table 2-7 Summary of Case Damping Factors (J_c) for Static Soil Resistance (RSP) as Reported by Hannigan et al.(2006).

Soil Type at Pile Toe	**Original Case Damping Correlation Range** Goble et al. (1975)	**Updated Case Damping Ranges** Pile Dynamics (2004)
Clean Sand	0.05 to 0.20	0.10 to 0.15
Silty Sand, Sand Silt	0.15 to 0.30	0.15 to 0.25
Silt	0.20 to 0.45	0.25 to 0.40
Silty Clay, Clayey Silt	0.40 to 0.70	0.40 to 0.70
Clay	0.60 to 1.10	0.70 or higher

2.2.3.3 Case Pile Wave Analysis Program (CAPWAP)

Since the maximum stress in the pile may be greater than the stress determined at the gage location, the PDA data is coupled with a rigorous numerical modeling technique that performs wave equation analysis to evaluate the maximum stress in the pile. Computed stresses are based upon the superposition of the upward and downward traveling force waves derived from the PDA. This numerical technique was developed by Goble and his students in the 1970s (G. Likins, Rausche, & Goble, 2000) and implemented in a program known as the Case Pile Wave Analysis Program (CAPWAP). This process allows more accurate estimations of pile

capacity, soil resistance distribution, and dynamic soil properties. The program mimics the Smith (1962) soil-pile model, and performs a signal matching process to match measured and calculated force in the pile as a function of time, thus refining the PDA results.

The pile model is divided into a series of lumped masses (m) connected with linear elastic springs and linear viscous dampers. The pile lumped masses are linked to a series of soil models described with elastic-plastic springs and linear viscous dampers, as shown in Figure 2-18. The soil static resistances (Rs) and soil quakes (q) are used to define the soil elastic-plastic springs, while the linear damper of the soil models is characterized by the damping coefficient (Cs). The soil static resistance at each soil segment, soil quake, the Smith's damping factor (Js) and the Case damping factor (Jc) are adjusted until the best signal match is achieved between the measured and the computed signal. Figure 2-19 shows an example plot of the results of the signal matching process where the calculated wave is matched with measured wave by varying soil dynamic properties and pile capacity. CAPAWAP provides the soil shaft resistance as a summation of all adjusted soil resistances along the pile shaft; and the total pile capacity as a summation of the calculated shaft resistance and the soil resistance at the pile toe. Signal matching can be performed at the end of driving or at restrike. CAPWAP assumes a constant soil quake for all soil segments along the shaft, and a different quake value for the soil model at the pile toe. However, when dealing with very sensitive soils the values of shaft quake and shaft damping may not be constant during the blow in contrast to what the CAPWAP analysis assumes, which creates a source of error. Moreover, when a pile is driven into a weak sandstone, which crumbles into sand soil as the pile is advanced, the assumption of static-viscous toe resistance assumed in the CAPWAP analysis is no longer valid as this soil cannot not be described by a simple elastic-plastic model (Fellenius, 1988).

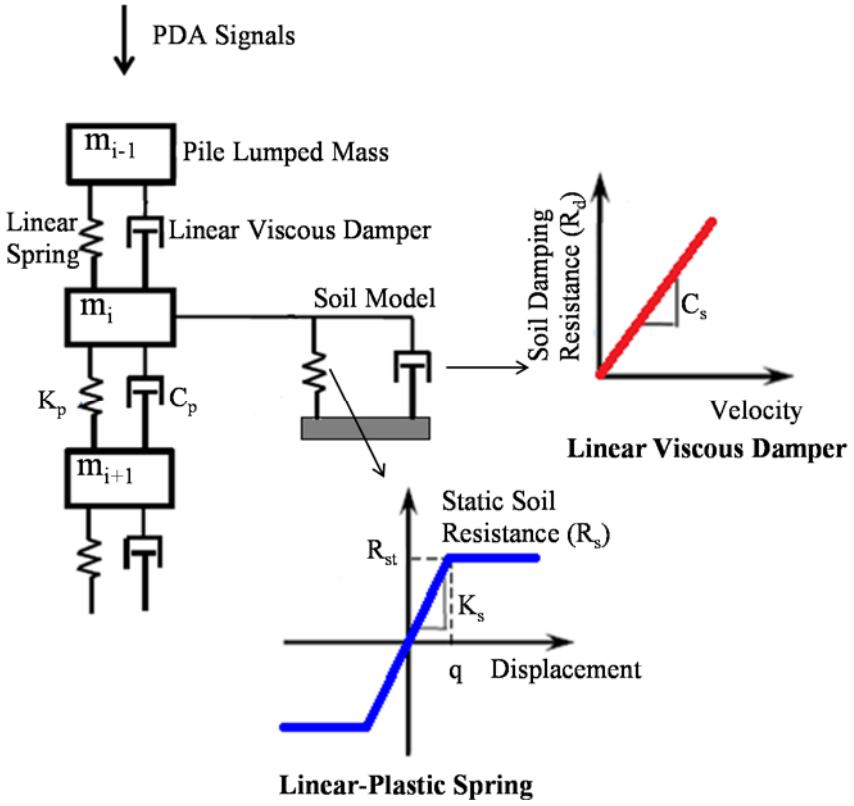

Figure 2-18 Illustration of CAPWAP Model Made of Pile Model as a Series of Lumped Masses Connected with Linear Elastic Springs and Linear Viscous Dampers, and Soil Models Described with Elastic-Plastic Springs and Linear Viscous Dampers.

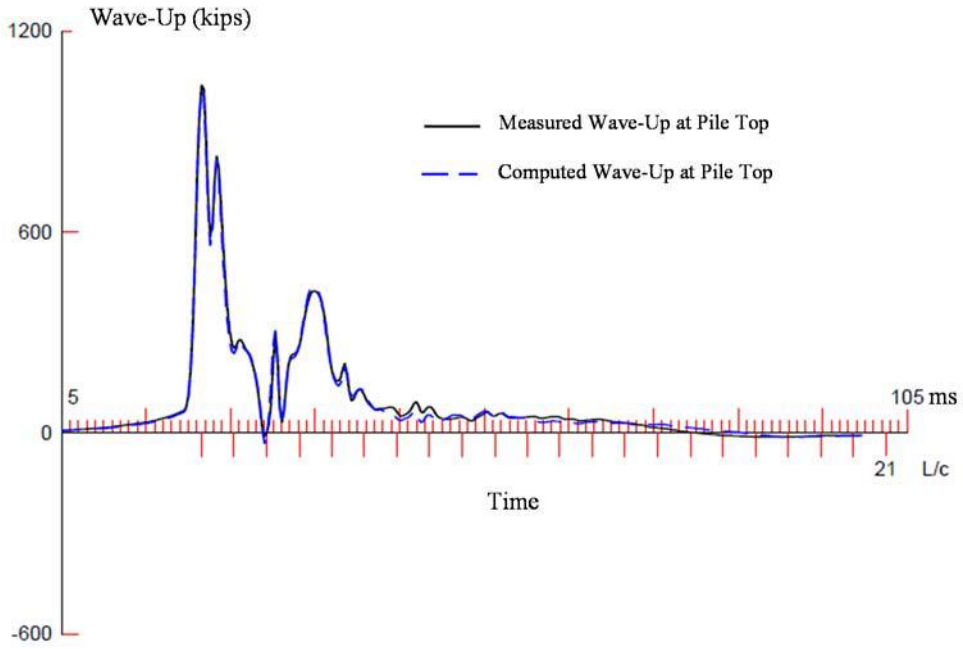

Figure 2-19 Example Plot of Results of CAPWAP Signal Matching by Varying Dynamic Soil Parameters and Pile Capacity.

2.2.3.4 Wave Equation Analysis Program (WEAP)

Wave equation analysis program (WEAP) computes the induced stress and displacement waves traveling along the pile after a single hammer blow. The program reports permanent set of the pile after elastic rebound (quake), and it can further assist in decisions about pile drivability by simulating the motion and force of a pile when driven by a hammer with specified characteristics. WEAP outputs a bearing graph that relates static bearing capacity to field blow count at the time of driving. Thus, the graph can be used to predict the static resistance corresponding to the field blow count at the time of driving.

The WEAP method was first developed by Smith (1962) based on a one-dimensional wave equation analysis. The method was later upgraded by Goble and Rausche into a commercial program, GRLWEAP (Hannigan et al., 2006). GRLWEAP models the pile and surrounding soil in a series of masses, springs and viscous dampers similar to the CAPWAP model to compute the hammer blow count, the axial driven pile stresses, hammer performance, and pile bearing capacity. This process is illustrated in Figure 2-20. Predicting pile capacity from GRLWEAP is neither an easy or straightforward task due to the large number of site-specific variables, modeling complexities, and the sensitivity of the output to all driving components, particularly the hammer efficiency. These site specific variables include the soil quake movement and the soil damping values for each soil supported pile element.

Typical application of GRLWEAP can often be at three stages: the first stage is during design, where the program is used to establish that the pile designed by static methods can be driven by available equipment. The second stage is after the final production hammer and driving accessories are selected. At this stage, the field bearing graph and hammer stroke to capacity plots, which control final penetration depths, are produced for confirmation of capacity

and acceptance of the pile. The third stage takes place during construction, where PDA and signal matching results are used to refine the GRLWEAP analysis for more accurate and optimized piling process. If the pile is restruck after a waiting period in order to consider set-up or relaxation, the BOR blow count is used to read the capacity from the bearing graph that has been established from the appropriate GRLWEAP model for restrike.

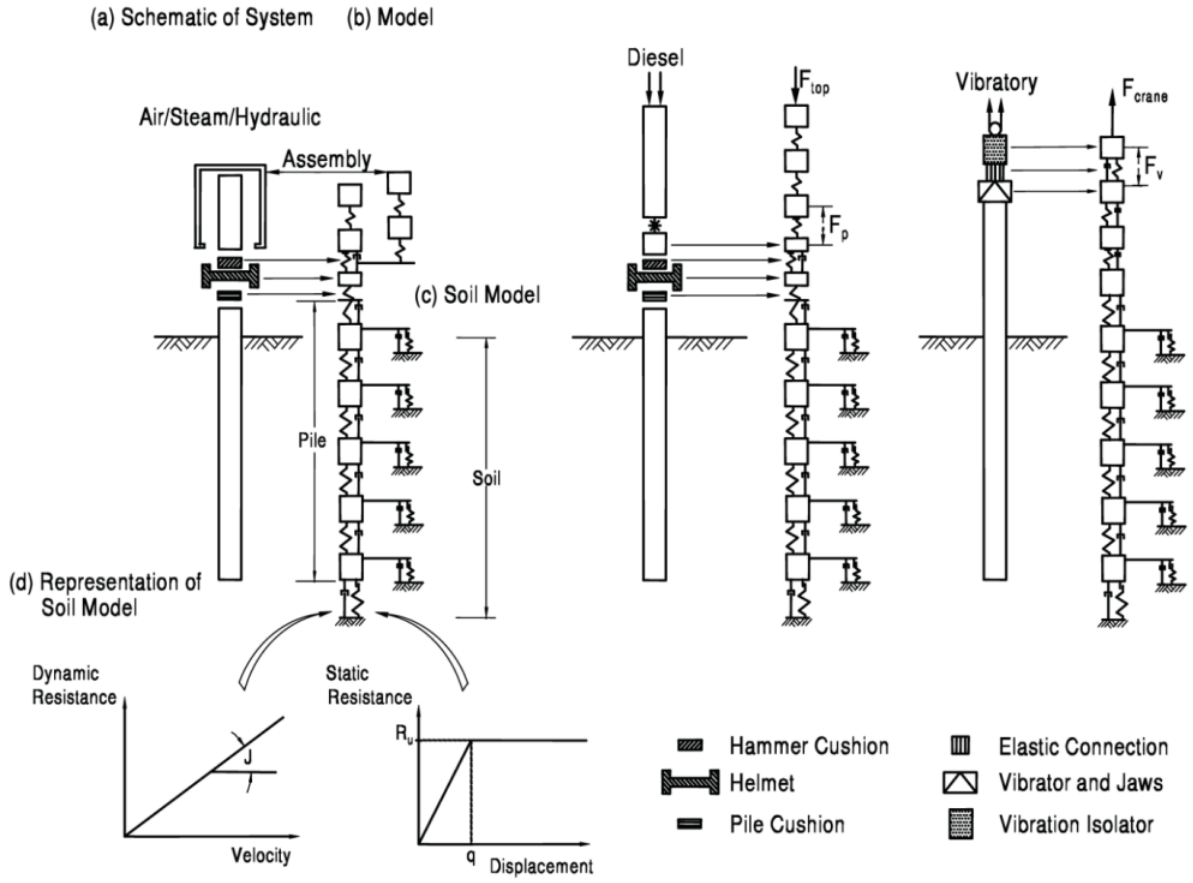

Figure 2-20 Illustration of GRLWEAP Models: a) Schematic of Hammer-Pile-Soil System, b) Hammer and Pile Model, c) Soil Model, and d) Representation of Soil Model (Rausche, Liang, Allin, & Rancman, 2004).

2.2.3.5 Pile Driving Monitor (PDM)

The Pile Driving Monitor (PDM) is a non-contact mobile device developed by Julian Seidel that is a supplemental method to the PDA which avoids the time required, installation problems and operational costs associated with the use of contact gauges on a pile. As reported by its manufacturer, the PDM is able to remotely, continuously, and accurately measure the pile set and temporary compression of pile at a safe distance of 5m to 25m from a pile. Presently, this device is fairly new in the US foundations industry. Case histories, such as the ones reported by Brown and Thompson (2011), indicate that PDA has become a popular and standard practice to monitor the piling process in field with its use on over 75 percent of the projects involving driven pile foundations. However, common practice is to test only 2 to 10 percent of all piles within projects using PDA like device and signal matching. The remaining 90 to 98 percent of piles on a project are either driven to specified design elevations, to practical refusal, or to a specified driving resistance/blow count based on pile driving formulas which have been shown to be fundamentally incorrect. The presence of site variability prohibits extending the results of a tested pile to untested piles, thus every pile in a project is equally important, and should be tested. The PDM has the ability to monitor and verify, in real-time, the capacity of every installed pile on a jobsite thanks to its quick and easy installation and interpretation of the results.

Component-wise, the PDM can be described as a basic mobile computer system for collecting measurement data on site. The system is composed of a tablet PC with PDM software installed and USB connection to a PDM device. The PDM makes use of Light Emitting Diode (LED) technology to collect measurements. There are four LED transmitters that transmit a very uniform light field with a dispersion angle of approximately 2.6 degrees (equivalent to a 450 mm active zone at a distance of 10 m). A LED light reflector (3M diamond grade reflective strip) is

placed on the pile within the active zone (Figure 2-21). The PDM measures reflector position at a peak digitization rate of 1050 Hz, which is a sufficient rate to measure the transient movements of the pile as a result of the impact, and most importantly, to capture the peak displacement of a pile during an impact event (John Pak, Danny Chung, Hammus Chui, Romeo Yiu, & Seidel, n.a). The combination of the offset-distance of the PDM to the pile, and the sufficient frequency for collecting data enables PDM to reduce the disturbance in measurements caused by the peak ground vibrations due to energy in ground surface produced by Rayleigh and shear waves. The PDM collects the transient movements and the peak displacements of the pile caused by hammer impact much earlier than the arrival time of the ground vibration waves at the PDM location. During the final set measurement for a series of 10 blows, the receiver continuously scans the active zone for the high intensity reflections from the strip, and detects the location of the strip. After completion of the 10 blows, a final position check is made, and the net movement of the pile (Final Set) for 10 blows is established.

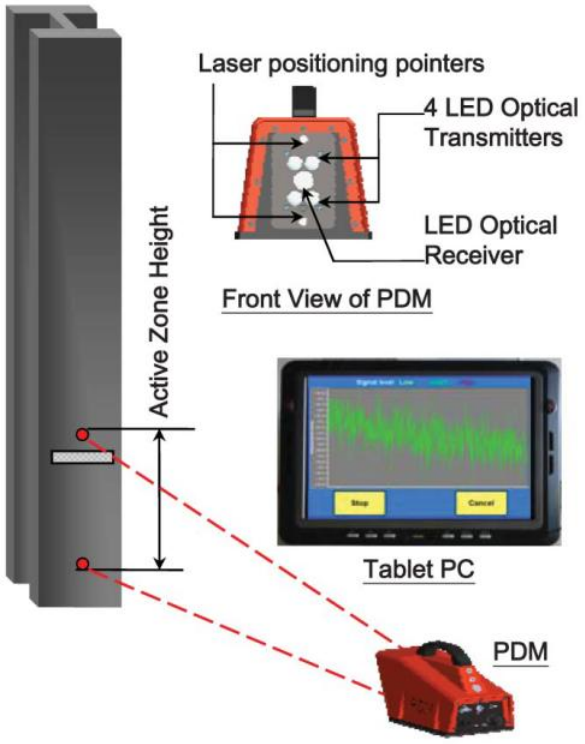

Figure 2-21 Illustration of Different Components, General Setup and Working Principles of Pile Driving Monitor-PDM (John Pak et al., n.a).

2.2.3.6 Comparison of Different Dynamic Methods

This subsection provides a summary in Table 2-8 that describes the approaches, assumptions, advantages, and limitations associated with each of the four dynamic analysis methods, namely PDA, CAPWAP, WEAP, and PDM.

Table 2-8 Comparison of Dynamic Analysis Methods revised from AbdelSalam et al.(2012).

Method	Approaches	Assumptions	Advantages	Limitations
PDA	• Measure pile top strain and acceleration • Case Method based on theory of wave propagation	• Uniform and linear elastic piles • Rigid plastic soils • Soil damping resistance at pile toe	• Quick and less expensive • Checks pile and hammer performances • Evaluates pile capacity over time • Non-destructive	• No account for soil damping along pile shaft • Less accurate in pile capacity estimation • Case damping is not well quantified
CAPWAP	• PDA records as input • Perform signal matching • Use wave equation algorithm • Smith's soil-pile model	• Linear elastic pile • Elastic-plastic soil • Lumped masses • Linear viscous pile and soil damping	• Accurate • Estimates soil resistance distribution • Evaluates pile capacity over time • Estimates dynamic soil properties	• Requires operational and interpretational skills • Non-unique results • Variable dynamic soil properties with time
WEAP	• One-dimensional wave equation analysis • Requires soil-pile-hammer information • Input soil profile • Smith's soil-pile model	• Linear elastic pile • Elastic-plastic soil • Lumped masses • Linear viscous pile and soil damping • Constant dynamic soil properties	• Less expensive • Driving analysis • Evaluates pile and hammer performance and ensures pile integrity before driving • Pile construction control	• Requires hammer information • Dynamic soil properties are not well quantified • Requires hammer blow count measurement for pile setup estimation
PDM	• Measure pile displacements and transient movements with Opto-electonics	• (Not available)	• Non-contact • Easy, quick and less expensive • Checks pile and hammer performances, and pile length • Non-destructive • All piles are testes • high resistance factor is used • operational health /safety	• Relatively new technology and fairly unfamiliar to the US foundations industry • Requires preliminary calibration for every jobsite • Poor number of PDM trained operators

2.2.4 Pile Static Load Test (SLT)

2.2.4.1 Different Static Load Test Methods

Static Load Testing (SLT) is the method that accurately measures the nominal capacity of a pile and determines the load-settlement relationship at the pile head. SLTs consist of applying static loads in increments and measuring the resulting pile displacements. Although SLTs are always technically desirable, they are not always performed because they are expensive. SLTs are recommended for design verification purposes, and they are used for calibrating resistance factors in RLFD design for bridge foundations making sure that these resistance factors provide safe and reliable results and eliminate excess conservatism. When SLTs are planned higher resistance factors can be used in the design.

The ASTM D1143/D1143M-07e1 (2007) standards describe several SLT methods, procedures, and equipment used for purposes of pile routine testing and proof testing. Among the different methods are the Quick Test (Procedure A) and Maintained Test (Procedure B). According to the U.S. Army Corps of Engineers (1997) the Maintained Test method is time consuming. Conversely, the Quick Test procedure is faster and more efficient when determining the pile capacity and is therefore more preferable than the procedure B. When performing the Quick load test, the load is applied in increments of 10 to 15 percent of the proposed design load with a constant time interval between load increments of 2 minutes or as specified. Load is added until continuous jacking is required to maintain the test load, i.e., plunging failure, or until the capacity of the loading apparatus is reached, whichever comes first.

Unfortunately, the definition of pile ultimate static capacity from load-displacement relations is not unique. Ideally, the measured load that corresponds to the load at plunging failure would represent the pile ultimate capacity. However, in practice many of loads tests are not

carried to complete plunging failure or the SLTs often do not yield a well-defined-load beyond which the pile plunges (Dennis, 1982). Several interpretation methods exist for determining pile capacity from SLT curves. When different interpretation methods, also known as Failure Criteria, are employed, they lead to significantly different pile capacities. Therefore, it is imperative that a single criterion be selected to interpret SLT results in a given study. The following sections briefly describe commonly used acceptance criteria.

2.2.4.2 Different Failure Criteria

Although the static load test is considered the most accurate test representing the actual response of the piles, determining the pile nominal capacity from the load-displacement curve can be challenging due to different definitions of failure criterion that exist. Perhaps the old definition of ultimate capacity was the load for which the total settlement of pile head is limited to a certain value, such as 10% of the pile diameter (Terzaghi, 1942), or a specified distance, such as 25.4 mm. According to Fellenius (2001) such definitions neglect the effect of elastic shortening of the pile, which can be substantial for long piles and negligible for short piles. Sometimes, the pile capacity is defined using shape of curvature criterion (Butler & Hoy, 1977), which defines pile capacity as the point of intersection between initial pseudo-elastic portion of the curve and the final pseudo-plastic portion. This criterion would also penalize long piles by underestimating their capacities because they have larger elastic movements. Better definitions exist which do consider the elastic shortening in determining pile capacity. Among those best interpretation methods for determining pile capacity, the most commonly used are briefly introduced; (1) Davisson's Criterion (Davisson, 1972), (2) the DeBeer log-log method (DeBeer, 1970), (3) the Hansen 80% criterion, (4) the Chin-Konder method, and (5) Decourt interpretation (Decourt, 1999).

2.2.4.2.1 The Davisson Criterion

The Davisson's criterion (Davisson, 1972) is one of the most popular methods used in the United States and seems to work best with data from Quick Load Tests (Fellenius, 2001). The Davisson offset limit load as presented in Equation 2-75 is defined as the load that corresponds to the movement that exceeds the elastic compression of the pile by an amount of 0.15 inch plus a factor equal to the pile diameter divided by 120. The later factor accounts for end bearing whereas 0.15 inch is the required displacement to mobilize side shear along the pile. Figure 2-22 shows that the Offset Limit Load does not necessary correspond to the plunging failure load.

$$S = \frac{Q \times L}{AE} + 0.15 + \frac{D}{120} \qquad \text{Equation 2-75}$$

where S is the pile settlement, Q is the defined pile capacity, L is the pile length, A is the pile cross-sectional area, E is modulus of elasticity of pile material, and D is the pile tip diameter in inches.

One of the main advantages of this method is that it is easier to apply than other methods that yield similar results. The fact that the offset line, parallel to the elastic compression line, (Davisson line) can be predicted even before starting the test, Davisson's method is considered to be an objective method and it is widely used as an acceptance criterion for static load test in North America. The method was found to perform best overall and was the only method used to calibrate resistance factors in the NCHRP report-507(Paikowsky et al., 2004).

2.2.4.2.2 De Beer Criterion

The De Beer Yield Load (DeBeer, 1970) is defined as the load at the intersection between the two straight portions of the graph of the load test data plotted on a log-log scale as

shown in Figure 2-23. Sufficient data points should be available before and after the ultimate load for the two linear trends to clearly develop.

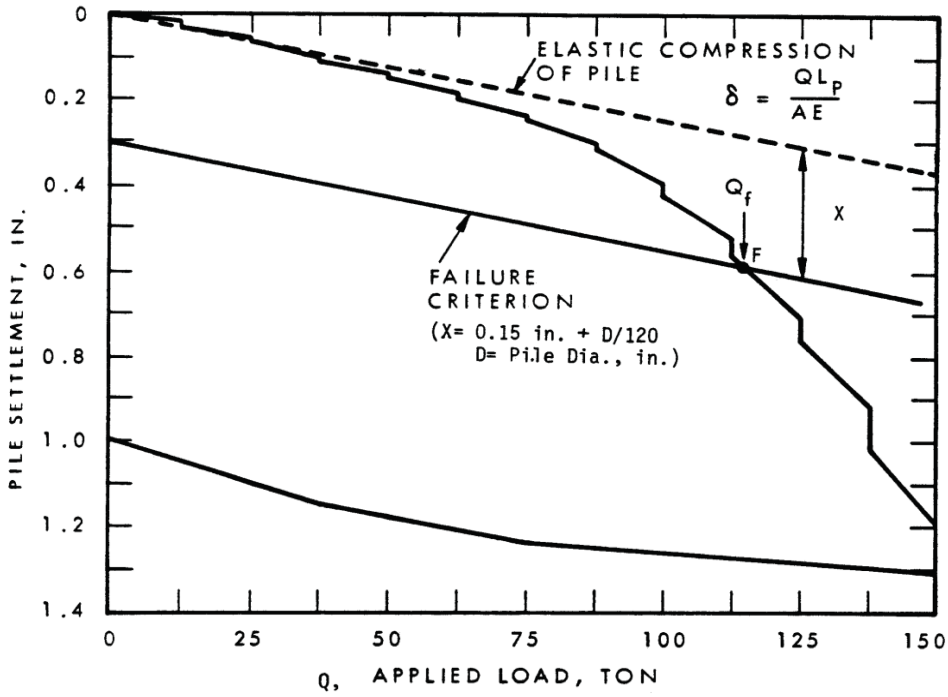

Figure 2-22 Example of Davisson's Interpretation Criterion from SLT Load-Displacement Curve (R. Cheney & Chassie, 2000).

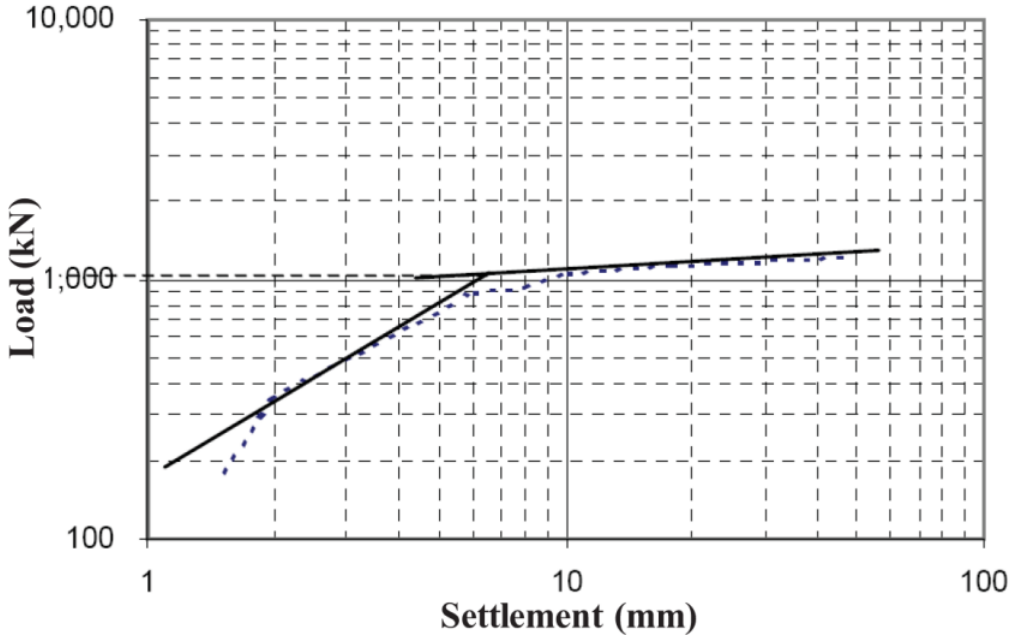

Figure 2-23 Example of De Beer's Interpretation Method from Static Load-Displacement Curve (AbdelSalam et al., 2012).

2.2.4.2.3 The Hansen 80%-Criterion

The Hansen 80%-Criterion defines pile capacity as the load that causes four times the movement of the pile head as obtained for 80% of that load. This interpretation was proposed by J. Brinch Hansen in 1963. The procedure is to make a graph of the square root of each movement value divided by its load value, $\sqrt{\rho}/Q$, and plotted against the movement, ρ, as shown in Figure 2-24. Then a straight line is fitted through data points, and its slope, a, and intercept, b, are determined. The pile capacity, Q_u is given by $Q_u = 1/\sqrt{ab}$.

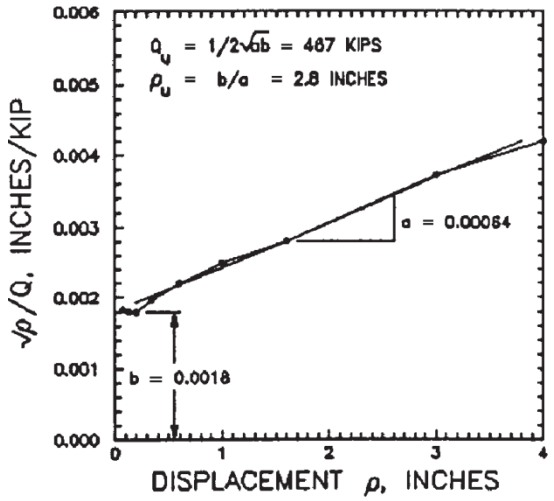

Figure 2-24 Hansen 80-percent Criterion from Transformed SLT Load-Displacement Curve (U.S. Army Corps of Engineers, 1997).

2.2.4.2.4 Chin-Kondner Criterion

Chin proposed a criterion similar to the Hansen method in 1970/1971. The method was based on pile load tests used in the general work done by Kondner in 1963. To find pile capacity by the Chi-Kondner criterion, each movement is divided by its corresponding load and plotted against the displacement. A straight line is then fitted to the data points after ignoring some initial variation. The ultimate load, Q_u, is then calculated as the inverse slope of the trend line as shown in Figure 2-25. According to Fellenius (2001) the Chin method can be applied to both quick and slow tests, but it requires that constant time increments be used when conducting the

SLT, which contradicts the procedures of the methods in the ASTM standard test. The method assumes a quasi-hyperbolic load-movement curve, and the transformed curve shows the correct straight line only when test load passes the Davisson's load.

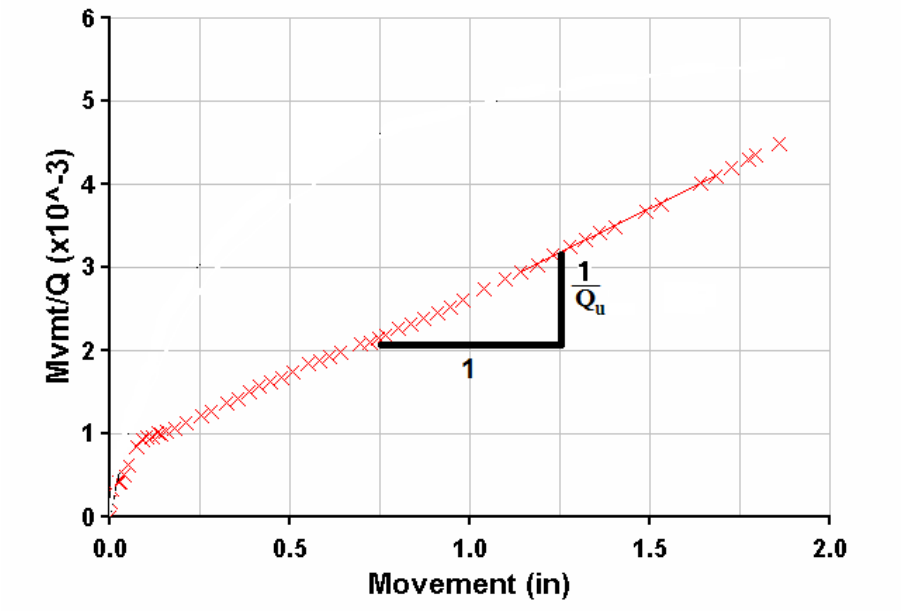

Figure 2-25 Chin-Kondner Interpretation Method from Transformed SLT Load-Displacement Curve (Fellenius, 2001).

2.2.4.2.5 Decourt Criterion

Decourt (1999) defined pile ultimate capacity from a transformed load-displacement curve. To apply the Decourt criterion, each load is divided by its corresponding movement and the result is plotted against the applied load. The intersection of the abscissa with the extended curve by linear extrapolation defines the pile capacity as illustrated in Figure 2-26.

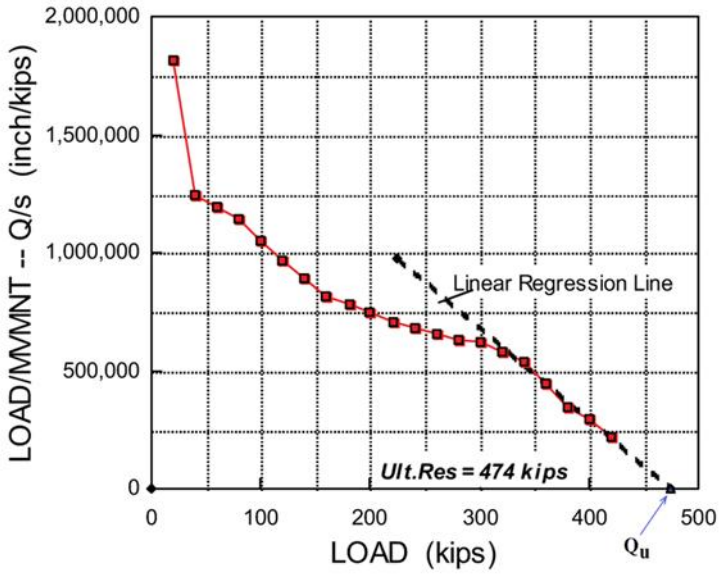

Figure 2-26 Decourt Interpretation Method from Transformed SLT Load-Displacement Curve (Fellenius, 2001).

2.2.4.3 Comparison of Different Failure Criteria

Table 2-9 provides a comparison between various criteria for determining ultimate pile capacity, and provides the appropriate pile types for each method, the recommended static load test type, advantages, limitations, and applicability.

Table 2-9 Comparison Between Various Criteria of Pile Ultimate Capacity Determination, modified from AbdelSalam et al.(2012).

Method	Year	Recommended pile types	SLT* type	Advantages	Limitations	Comments	Application
Shape of Curvature Method (Butler and Hoy)	1977	Bored, belled, and small diameter driven concrete piles as well as Franki piles	QM** test	Its yield failure loads are near to actual test failure loads	It is a subjective method, hence, results could greatly vary from one to other: conjecture and scale of the graph can change the interpreted capacity	It is a conservative method which is not suitable for long piles	Easy
Davisson's Method	1972	Driven piles as well as Franki piles	QM test	It is an objective method which can be used as a SLT acceptance criterion	For piles with cross-sectional area more than 24 inches, the method under predicts the pile capacity	It is a conservative method (recommended by specifications)	Easy
Chin and Kondner's Method	1970-1971	N/A	QM and SM*** tests	N/A	Constant time load increments required for accuracy. Also assumes hyperbolic load-settlement relation. Always it gives failure loads higher than that of actual test failure loads	Loads must be higher than that of Davisson's acceptance load	Easy
De Beer's Method	1967-1972	N/A	SM tests	N/A	Subjective method	Drawn on log scale	Moderate
Hansen's 90	1963	Small diameter driven concrete piles	CRP**** tests	N/A	Trial and error	N/A	Moderate
Hansen's 80	1963	N/A	QM and SM tests	Criteria agrees well with plunging failure	Not suitable for tests that include unloading cycles or unachieved plunging	Assumes that the load-displacement curve is parabolic	Moderate
Limited Total Settlement Method	N/A	N/A	N/A	Objective method	Not suitable for long piles, as elastic settlement exceeds limit without inducing plastic deformations	Pile may fail before reaching the settlement limit of the method	Easy
Decourt	1999	N/A	QM and SM tests	N/A	When straight-line starts to develop during test the capacity can be projected directly	Construction is similar to Chin-Kondner and Hansen methods	Easy
Vander Veen's Method	1953	Small diameter concrete driven piles	N/A	N/A	Time consuming	N/A	Difficult

*Static Load Test ; **QM: Quick Maintained Test; ***SM: Slow Maintained Test; ****CRP: Constant Rate of Penetration Test

Chapter 3 Preliminary Calibration of Resistance Factors

3.1 Methodology for Reliability based LRFD Calibration of Resistance Factors

This chapter covers the reliability procedures employed to calibrate resistance factors for driven piles based on design methods and construction experiences available for the state of Arkansas. For the purpose of this LRFD calibration a well-organized database was developed. The database contains 102 pile load tests collected from various sources together with their corresponding boring logs.

3.1.1 Calibration Framework for Developing the LRFD Resistance Factors

The AASHATO LRFD Bridge Design Specifications (2012) recommends that local LRFD calibration be performed following the calibration framework used to establish the specifications. In this regards, this study conducted the preliminary calibration of the LRFD resistance factors in Arkansas following the general process used in NCHRP report 507 by Paikowsky et al.(2004). However, to increase the accuracy of the calibration results, advanced statistical analyses were performed to better fit data distribution to smooth theoretical distributions. Additional steps were added to the typical calibration framework to enhance agreement between design and construction results. The calibration framework is presented in the form of flow chart in Figure 3-1, and explained in the following 8 steps:

Step1. Gathering data required for statistical analysis: a database containing driven pile data was developed. The database consists of soil parameters and profiles, pile properties and geometry, pile driving information such as hammer properties, time to restrikes, PDA/CAPWAP information, and static load test with its interpreted nominal pile capacity based on Davisson failure criterion.

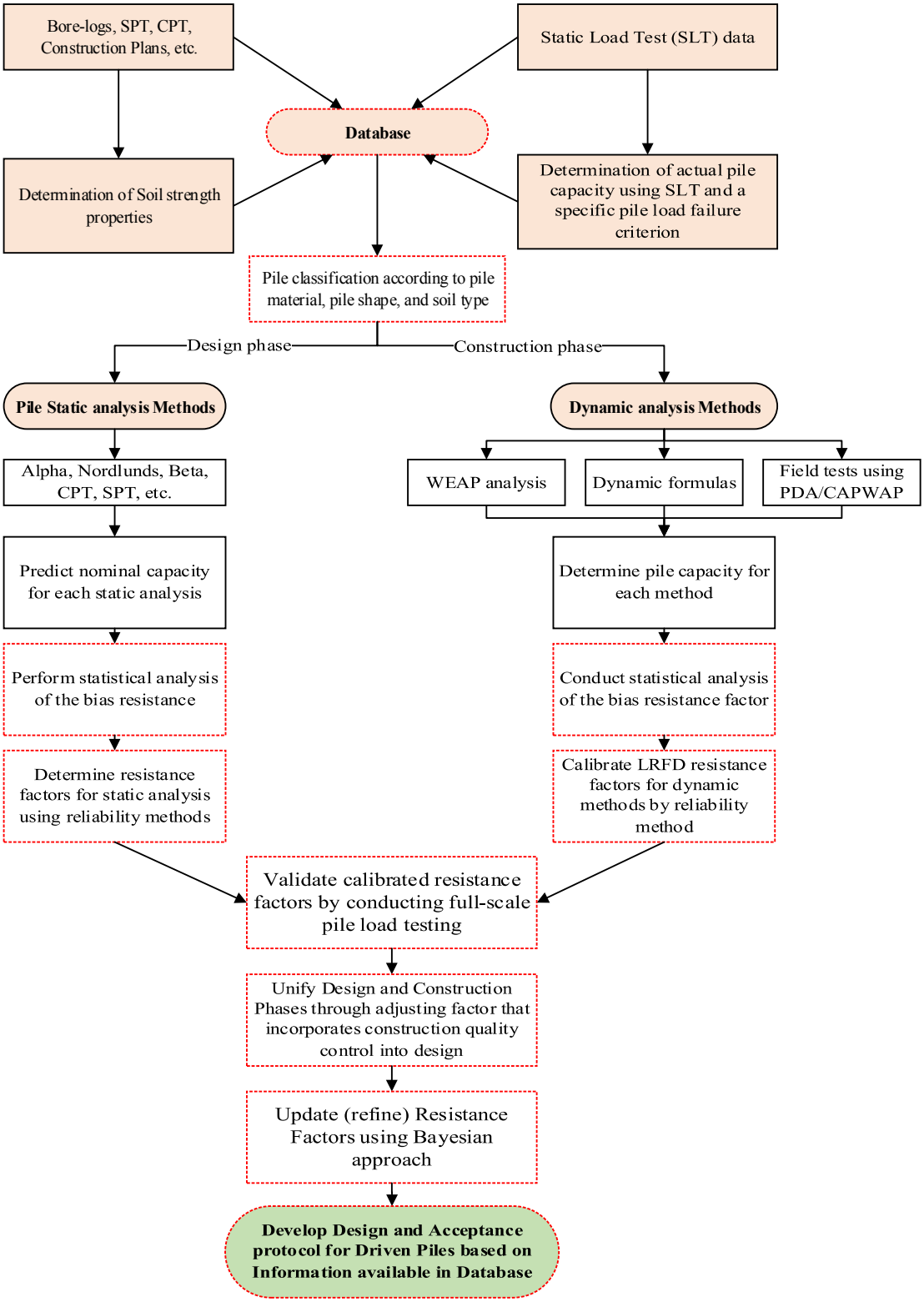

Figure 3-1 Process for Calibrating the LRFD Resistance Factors and for Developing Design /Acceptance Protocols of Driven Piles using Reliability Approach.

Step2. Determining capacity or resistance ratios for further study of the bias of the resistance. This step involves 4 tasks:

Task 1: The database is sorted into different groups, where each group represents a specific soil type (cohesive, sand, mixed) and pile type (concrete, pipe pile, H-piles, etc.). Grouping similar pile load tests enhances the precision and efficiency of the expected resistance factors. Thus, pile regrouping is one of the ways to reduce uncertainties from various sources, if the number of data within each group is sufficient for the analysis.

Task 2: The actual capacity of piles is determined using the load-displacement relationship obtained from the SLT. Although many distinct failure criteria exist for interpreting load-displacement behavior of a pile, Davisson's criterion is selected for this study as the standard method for determining actual pile capacity.

Task 3: Prediction of the nominal capacity of each pile is performed using any desired static, dynamic analyses methods, or dynamic formulas.

Task 4: For every pile within each pile group, the bias factor of the methods used is determined by calculating the ratios of actual to nominal pile capacity.

Step3. Determining statistical parameters such as the mean, standard deviation, and coefficient of variation (COV) for load and resistance probability density functions (PDFs). Within each pile group in the database the PDF of the bias is studied and the type of PDF and its statistical characteristic parameters are determined. Testing the goodness of fit of the PDF to the data is required to insure that the reliability of the calibration results are within acceptable range. Goodness of fit tests for each dataset is are performed using available statistical distribution identification tests (such as Anderson-Darling, Lilliefors composite, Kolmogorov-Smirnov, and Chi-Square tests). A standalone compiler (ReliaPile) that contains these Goodness-of-fit tests is

deployed using MATLAB program. Depending upon the results of the best-fit tests, the mean and COV of the dataset are to be adjusted accordingly.

Step4. Selecting appropriate reliability methods for calibration: the FOSM, improved FOSM, FORM, and Monte Carlo Simulation (MCS) are selected as the appropriate reliability approaches for the LRFD calibrating process. These reliability approaches are detailed in Section 2.1.2.3.3 of the literature review and their comparative study is presented herein (See Section 3.2).

Step5. Selecting the target reliability index, β_T, is reached based on the margin of safety required in the design specifications, and by considering the recommended levels of reliability used in geotechnical designs. The NCHRP report 507 (Paikowsky et al., 2004) recommends a β_T of 2.33 corresponding to a 1% probability of failure for driven piles when used in groups of 5 or more piles. A reliability index of 3.0 is recommended for single piles and groups containing 4 or less piles corresponding to a 0.1% probability of failure. In this step, the dead to live load ratio (DL/LL) is taken as 2.5. This value of DL/LL was also used in NCHRP 507, which is the basis of the current AASHTO LRFD bridge design specifications. Figure 2-4 shows that the results of the LRFD calibration are not significantly affected when the DL/LL is greater than 2. The ASSHTO LRFD recommended load parameters are: dead load factor of 1.25, live load factor of 1.75, dead load bias of 1.05, live load bias of 1.15, COV of dead load bias of 0.1, and COV of live load bias of 0.2.

Step6. Locally calibrated resistance factors are determined using FOSM, FORM, and MCS. To check the correctness and accuracy of the results, different reliability approaches with different degrees of sophistication are employed. The results of calibration are then compared against the resistance factors given in the AASHTO LRFD bridge design specifications.

Step7. Unifying design and construction phases and checking for reliability and consistency of the calibrated resistance factors. Even though static and dynamic prediction methods are calibrated against the same actual (SLT) capacity, there is always non-agreement between design and in-situ capacity values. This non-agreement is due to the differences in prediction approaches for both static and dynamic analyses. The disparity in results can be reduced by introducing a multiplier in the design phase which would adjust for construction quality control practices. Use of a multiplication factor was also proposed in NCHRP report 507, but there was no appropriate methodology established to derive it. The adjusting factor would be multiplied by the calibrated static resistance factor for obtaining factored resistance. Its derivation is discussed in more depth in Section 5.1.

Step8. Validation of calibrated resistance factors. To validate the calibrated resistance factors, a full-scale pile load testing program needs to be carried out in different soil types within the state of Arkansas. The factored measured resistances resulting from full-scale pile load testing should then be compared to factored static pile resistances. The results of the pile load testing are also utilized to update the calibrated resistance factors. Based on available information in the database and the additional information contributed by field testing, appropriate recommendations for the LRFD-based design and acceptance for driven pile foundations are developed.

3.1.2 Development of Driven Pile Database

3.1.2.1 Motivation

In Arkansas, despite many years of using driven piles for transportation related foundations, no database has been developed containing pile load tests that could be used for calibration purposes. In addition, it is practically impossible to find static load test records for driven piles in the State of Arkansas. Information that is available through the Arkansas

State Highway and Transportation Department (AHTD) on driven piles is in the form of a construction report, making its direct usage for the LRFD calibration process burdensome. The development of resistance factors and establishment of a pile acceptance protocol based on a reliability approach requires a high quality structured and stable pile database that contains essential pile information about the site location, subsurface conditions, pile properties, hammer characteristics, EOD/BOR blow count, and static load test results. As part of the calibration process, a well-structured pile database was developed using various features of the Microsoft Office Access™. To enhance the outlook and the efficiency of the developed database two existing pile databases namely the FHWA's Deep Foundation Load Test Database (Kalavar & Ealy, 2000) and the Electronic Database for Pile Load Tests (Roling, Sritharan, & Suleiman, 2010) were referenced. This newly created database aims to ease referencing, storing, and retrieving pile information for efficient performance of the calibration analyses and future updating of resistance factors. The potential benefit of this electronic database is that the foundation design and construction practices will improve as the database is updated with newly collected pile load test data, which in turn will result in high quality assurance provisions as the resistance factor converges towards its highest stagnation level.

3.1.2.2 Key Features of the Database

The goal of developing this pile database was to help establish a specific LRFD design and acceptance protocol for the region through the use of static and dynamic methods. Thus, it was decided that the database should be organized so that data are amassed in a hierarchical order. This hierarchical classification is based on the methods of pile analysis. For static analysis methods, the database allows the grouping of piles based on a detailed site investigation and evaluation of the soil parameters. For dynamic methods, driving record information and reported pile driving equipment characteristics may be used as criteria for

grouping piles together. Table 3-1 presents the different hierarchical classifications of different data fields in the database.

The database contains one main datasheet (Figure 3-2) that stores all input information. The user can apply filters and various queries to the data when performing analyses. For quick and easy data input, the database contains a pop-up form (Figure 3-3) that allows the user to feed data into the database in an organized fashion. This data-entry form contains tabs which give access to a multitude of self-explanatory database fields. This form serves as a template for navigating through recorded pile load information.

Table 3-1 Database Fields in Different Hierarchical Classifications.

Project Information	Pile Information	Average Soil Profile
Pile ID	Pile Material	Average Soil Profile Data
Project Number	Pile Shape	Soil layer ID
Job Number	Pile Size	Material Description
Bridge Number	Toe Treatment	Layer Thickness
State	Construction Method	Material Unit Weight
County	Elastic Modulus	SPT value
Route	Specific Weight	Undrained Cohesion Value
Bent Number	Section Area	Internal Friction Angle
Contractor	Toe Area	Strength Measurement Method
Date Driven	Pile Perimeter	Comments
Test Number	Cut off Length	Total Soil Layer Thickness
Date Tested	Driven Length	Pile Bearing Classification
Tested by	Ground Water Depth	Factor of Safety
Date Reported	Embedded Depth	Test Site Soil Classification
Data Folder Location	Pre-boring Depth	
Pile Nomenclature (Project Related)	Pile Tip Elevation	
Pile Additional Information		

Borehole/SPT Information	Advanced In-Situ Tests	Static Pile Capacity Results
Borehole/SPT Information Table	CPT Performed?	Pile Capacity by CPT Method
Borehole Number	Number of CPTs	by Schmertmann
Soil Layer ID	Other Tests?	by de Ruiter&Beringen
Layer Description		by LCPC
Layer Thickness		Pile Capacity by Nordlund Method
Average SPT Value		Pile Capacity by Alpha-Tomlinson
Number of Boreholes		Pile Static Capacity (Reported)
Number of Boreholes with SPT Data		Pile Static Capacity by DRIVEN*
Boreholes near Pile Location?		DRIVEN Toe Resistance
SPT Data Available near Pile Location		DRIVEN Shaft Resistance
Usable Static Test?		DRIVEN Cohesionless Resistance
		DRIVEN Cohesive Resistance
		DRIVEN Analysis File Attachment
		Pile Capacity by Beta Method

*Soil profiles were interpreted by me and capacity calculations were done using FHWA-DRIVEN

Static Load Test Results	Dynamic Formula Results
Static Load Test Results	Capacity by ENR
Load	Capacity by Modified ENR
Gauge Reading (Displacement)	Capacity by Gates
Pile Capacity by Static Load Test	Capacity by FHWA - Gates
Davisson Criterion	Capacity by Janbu
DeeBeer Criterion	
The Hansen 80%-Criterion	
Chin-Kondner Criterion	
Decourt Criterion	
Static Load Test Graph	
Usable Static Load Test?	
Static Load Test Remarks	

Table 3-1 Database Fields in Different Hierarchical Classifications (Cont.).

Dynamic Analysis Parameters

- Hammer
  - Hammer ID
  - Manufacturer
  - Model
  - Type
  - Rated Energy
  - Ram Weight
  - Modifications
- Anvil/Base Weight
- Striker Plate
  - Material
  - Thickness
  - Area
  - Module of Elasticity
  - Coefficient of Restitution (COR)
- CapBlock/Hammer Cushion
  - Material
  - Thickness
  - Area
  - Modulus of Elasticity
  - Coefficient of Restitution (COR)
- Pile Cap/Helmet
  - Weight
  - Bonnet Material
  - Anvil Bock Remarks
  - Drivehead
  - Accessories
- Pile Cushion
  - Cushion Material
  - Thickness
  - Module of Elasticity
  - Cushion COR
- Driving Condition (EOD/BOR)
- Number of Blows/ft @the last 6"
- Hammer Stroke
- Average Energy Transfer
- Usable Dynamic Test?
- Comments on Stroke and Blows

Dynamic Analysis Results (EOD)

- Pile Capacity by WEAP
  - WEAP File Attachment
  - Shaft Quake used in WEAP
  - Toe Quake used in WEAP
  - Shaft Damping Factor-WEAP
  - Toe Damping Factor-WEAP
- Pile Capacity by PDA
  - PDA Case Damping Factor
- Pile Capacity by CAPWAP
  - CAPWAP Shaft Resistance
  - CAPWAP Toe Resistance
  - Maximum Compressive Stress
  - Maximum Tensile Stress
  - Smith Shaft Damping Factor
  - Smith Toe Damping Factor
  - Shaft Quake
  - Toe Quake
  - Case Shaft Damping Factor
  - Case Toe Damping Factor

Dynamic Load Test Results (BOR)

- PDA for Monitoring Pile Driving/Restrike?
  - EOD Date/Time
  - EOD Capacity
  - First Restrike Date/Time
  - Capacity After First Restrike
  - Second Restrike Date/Time
  - Capacity After Second Restrike
  - Third Restrike Date/Time
  - Capacity After Third Restrike
  - Fourth Restrike Date/Time
  - Capacity After Fourth Restrike
  - Fifth Restrike Date/Time
  - Capacity After Fifth Restrike
  - Sixth Restrike Date/Time
  - Capacity After Sixth Restrike

Overall

- Comments and Attachments

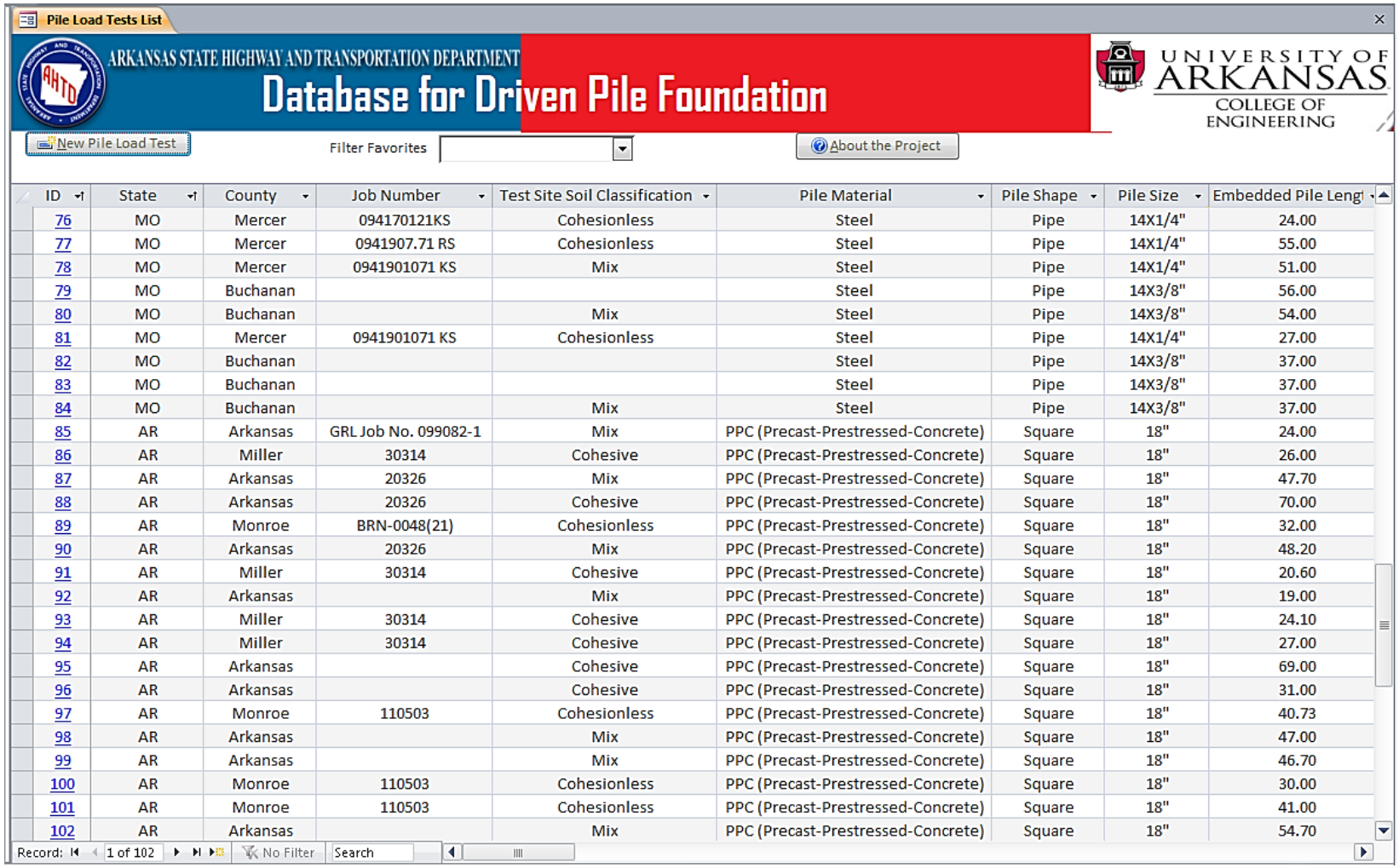

ID	State	County	Job Number	Test Site Soil Classification	Pile Material	Pile Shape	Pile Size	Embedded Pile Leng
76	MO	Mercer	094170121KS	Cohesionless	Steel	Pipe	14X1/4"	24.00
77	MO	Mercer	0941907.71 RS	Cohesionless	Steel	Pipe	14X1/4"	55.00
78	MO	Mercer	0941901071 KS	Mix	Steel	Pipe	14X1/4"	51.00
79	MO	Buchanan			Steel	Pipe	14X3/8"	56.00
80	MO	Buchanan		Mix	Steel	Pipe	14X3/8"	54.00
81	MO	Mercer	0941901071 KS	Cohesionless	Steel	Pipe	14X1/4"	27.00
82	MO	Buchanan			Steel	Pipe	14X3/8"	37.00
83	MO	Buchanan			Steel	Pipe	14X3/8"	37.00
84	MO	Buchanan		Mix	Steel	Pipe	14X3/8"	37.00
85	AR	Arkansas	GRL Job No. 099082-1	Mix	PPC (Precast-Prestressed-Concrete)	Square	18"	24.00
86	AR	Miller	30314	Cohesive	PPC (Precast-Prestressed-Concrete)	Square	18"	26.00
87	AR	Arkansas	20326	Mix	PPC (Precast-Prestressed-Concrete)	Square	18"	47.70
88	AR	Arkansas	20326	Cohesive	PPC (Precast-Prestressed-Concrete)	Square	18"	70.00
89	AR	Monroe	BRN-0048(21)	Cohesionless	PPC (Precast-Prestressed-Concrete)	Square	18"	32.00
90	AR	Arkansas	20326	Mix	PPC (Precast-Prestressed-Concrete)	Square	18"	48.20
91	AR	Miller	30314	Cohesive	PPC (Precast-Prestressed-Concrete)	Square	18"	20.60
92	AR	Arkansas		Mix	PPC (Precast-Prestressed-Concrete)	Square	18"	19.00
93	AR	Miller	30314	Cohesive	PPC (Precast-Prestressed-Concrete)	Square	18"	24.10
94	AR	Miller	30314	Cohesive	PPC (Precast-Prestressed-Concrete)	Square	18"	27.00
95	AR	Arkansas		Cohesive	PPC (Precast-Prestressed-Concrete)	Square	18"	69.00
96	AR	Arkansas		Cohesive	PPC (Precast-Prestressed-Concrete)	Square	18"	31.00
97	AR	Monroe	110503	Cohesionless	PPC (Precast-Prestressed-Concrete)	Square	18"	40.73
98	AR	Arkansas		Mix	PPC (Precast-Prestressed-Concrete)	Square	18"	47.00
99	AR	Arkansas		Mix	PPC (Precast-Prestressed-Concrete)	Square	18"	46.70
100	AR	Monroe	110503	Cohesionless	PPC (Precast-Prestressed-Concrete)	Square	18"	30.00
101	AR	Monroe	110503	Cohesionless	PPC (Precast-Prestressed-Concrete)	Square	18"	41.00
102	AR	Arkansas		Mix	PPC (Precast-Prestressed-Concrete)	Square	18"	54.70

Record: 1 of 102 No Filter Search

Figure 3-2 Database Main Display Form Developed in the Microsoft Office Access™ 2013.

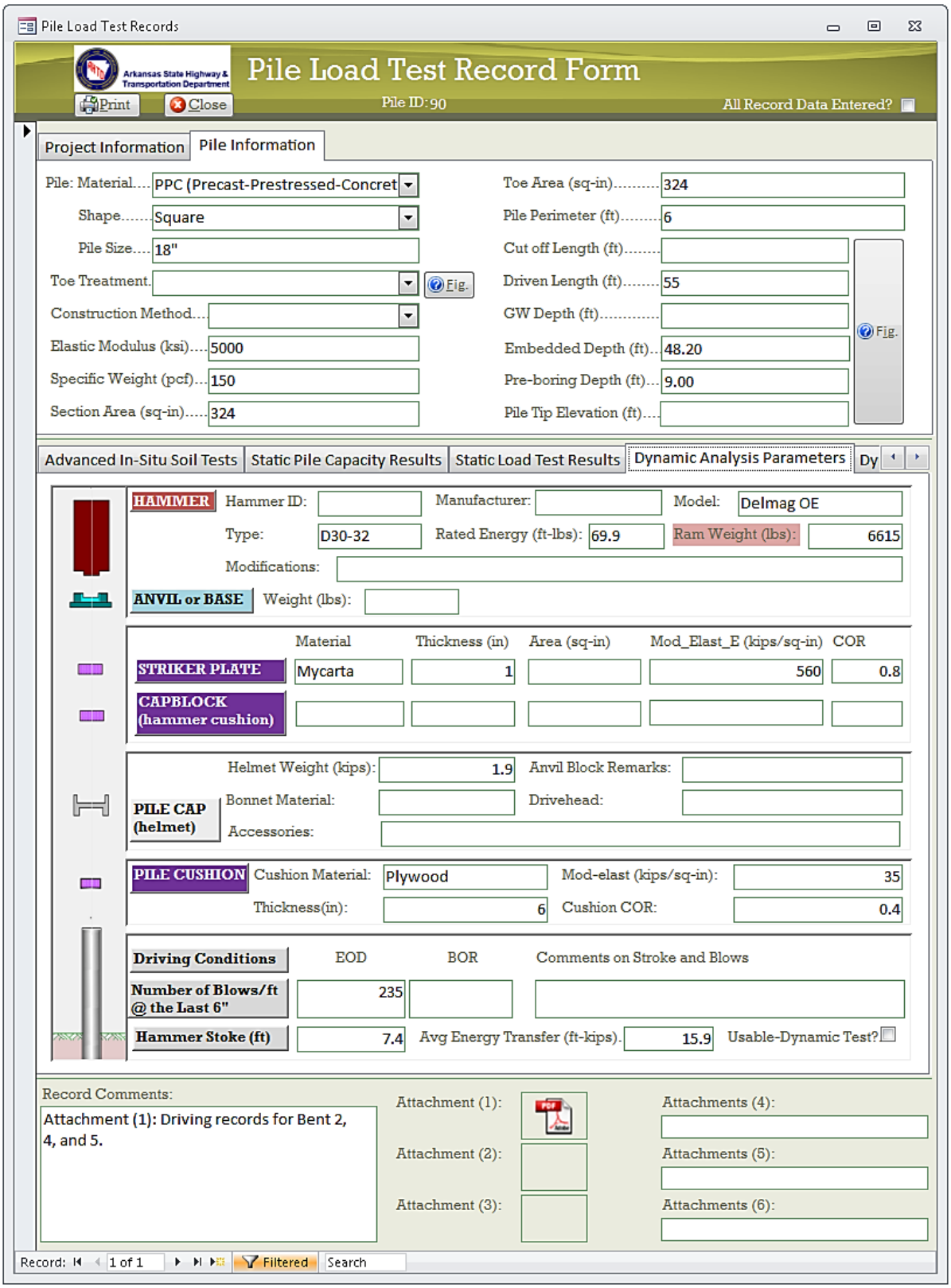

Figure 3-3 Data Entry Form for the Developed Electronic Database.

3.1.3 Description of the Amassed Information in Database

3.1.3.1 Generality

The AHTD practice for pile acceptance is mainly the dynamic load test to validate and verify the pile capacity estimates based on a selected design procedure. If a dynamically tested pile fails to provide the required support for the design load, the pile will be built-up and driven until the required ultimate capacity is obtained, thus increasing the length of the driven pile (AHTD, 2003, 2014). Due to the current AHTD practice, Static Load Test (SLT) records are unavailable with in the State of Arkansas for LRFD calibration purposes. In order to establish a preliminary LRFD calibration of resistance factors for Arkansas, sites that have similar soil settings as Arkansas were located in neighboring states. The selected sites where static and dynamic load test have been conducted are located in Louisiana, and Missouri. The available pile load test records for Louisiana were collected from the published report of the Louisiana Department of Transportation and Development, LADOTD, and all selected piles that possess adequate soil data and had been load tested to failure are PPC piles (Abu-Farsakh, Yoon, & Tsai, 2009). For all 53 cases of driven piles reported from Louisiana, none possessed driving information such as; type of hammer used during driving, transmitted energy during piling, or blow count resistance. However, they do have SLT derived capacities based on Davisson's failure criterion, despite missing load-displacement data. Like Arkansas, most of the other collected pile data from Missouri has detailed soil and driving information, except that SLT derived capacities were not reported.

Piling cases from unpublished pile design and construction reports (AHTD, n.a.; MoDOT, n.a.) were carefully reviewed and evaluated for potential inclusion in the database. Overall, the criterion for inclusion in the database is based on the accessibility of proper

documentation in pile records such as site location, sufficient subsurface exploration and soil testing from borings (SPT results, shear strength data) to characterize the soil, pile data during design, installation and testing. When a pile possessed an adequate load test (either static or dynamic), that pile was considered and recorded in the database.

At the time of the preliminary calibration of the LRFD resistance factors, the pile database contained 102 pile case histories: Arkansas accounts for 18 PPC pile cases, Louisiana accounts 53 cases of PPC piles, and Missouri has 31 cases, which include 4 PPC piles, 5 steel H-shaped piles, and 22 closed ended steel pipes. In all cases, piles were driven in varying soil profiles including cohesive, non-cohesive, and mixed soils.

3.1.3.2 Pile Classification based on Soil Type

The database contains two methods of soil classification. One is determined based on soil borings and the results of laboratory testing. This type of classification is simply a classic soil classification method involving soil composition, where each soil layer is classified as either clay, silt, or sand based on Unified Soil Classification System (USCS). The second soil classification is based on the contribution of each soil type to the overall pile bearing capacity. In this regard the pile is said to be driven into cohesive (fine-grained or clay) soils when over 70% of the pile capacity is due to cohesive soil layers. The pile is said to be in cohesionless soils (coarse-grained soils or Sand) when over 70% of the pile capacity is due to non-cohesive materials. Otherwise, the pile is said to be in mixed soils. Based on the second classification, the available piles in the database were separated into three different categories:

- Piles driven into primarily cohesive soils,
- Piles driven into primarily cohesionless soils, and
- Piles driven into primarily mixed soils.

When each major category possesses different pile types such as H-pile, Pipe pile, or PPC pile, then corresponding subgroups are created. The database also contains another type of pile classification, which is based on percentage of contribution of the side and tip resistance to the overall capacity of pile. When the majority of pile capacity is mobilized through shaft resistance, the pile is classified as friction or skin pile, otherwise the pile is classified as end bearing pile.

The majority of piles in the database are classified as friction piles as 97 percent of all piles had an end bearing capacity less than 20 percent of the total pile capacity. Pile lengths ranged between 30 and 125 feet, whereas embedded lengths into the soil ranged from 19 to 124 feet. Figure 3-4 gives more details about the pile distribution according to the embedded lengths of the piles within specific soil type. The database contains three (3) types of driven piles based on material type that pile is made from. Figure 3-5 shows the composition of the database based on pile material. There are 75 PPC piles, 22 pipe piles, and 5 H-shaped piles. Figure 3-6 shows a detailed breakdown of the available piles according to their material types, shapes, and size. All PPC piles are square in shape, and their size ranges from 14 inches to 30 inches. All pipe piles are 14 inches in diameter with varying thickness from 1/4 to 3/8 inches. All H-shaped piles are HP12x53. A more complex chart that shows various categories of piles based on soil type, pile material, and pile shape is presented in Figure 3-7. In total there are 36 piles driven into soils that are predominantly cohesive, 39 cases driven into predominantly non-cohesive soils, 17 pile cases driven into mixed soils, and 10 piles with limited information about soil type as shown in Table 3-2.

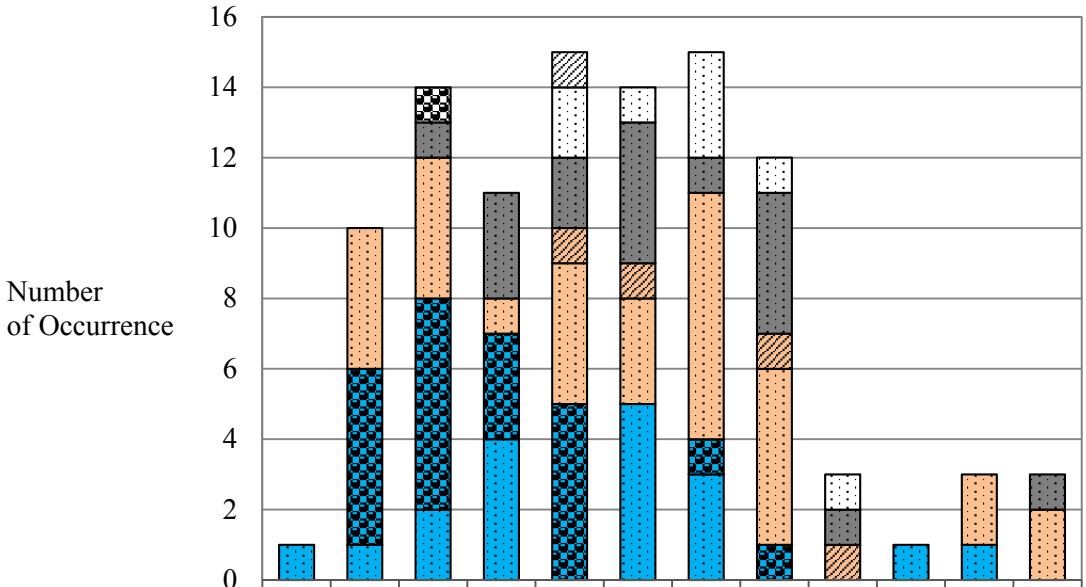

Embedded Pile Lengths →	10-20	20-30	30-40	40-50	50-60	60-70	70-80	80-90	90-100	100-110	110-120	120-130
n.a - Steel-Pipe			1									
n.a - Steel H-Shaped					1							
n.a - PPC					2	1	3	1	1			
Mix - PPC			1	3	2	4	1	4	1			1
Cohesive - Steel H-Shaped					1	1		1	1			
Cohesive - PPC		4	4	1	4	3	7	5			2	2
Cohesionless - Steel-Pipe		5	6	3	5		1	1				
Cohesionless - PPC	1	1	2	4		5	3			1	1	

Figure 3-4 Pile Distribution According to Embedded Pile Lengths for Different Types of Pile and Soil within Database.

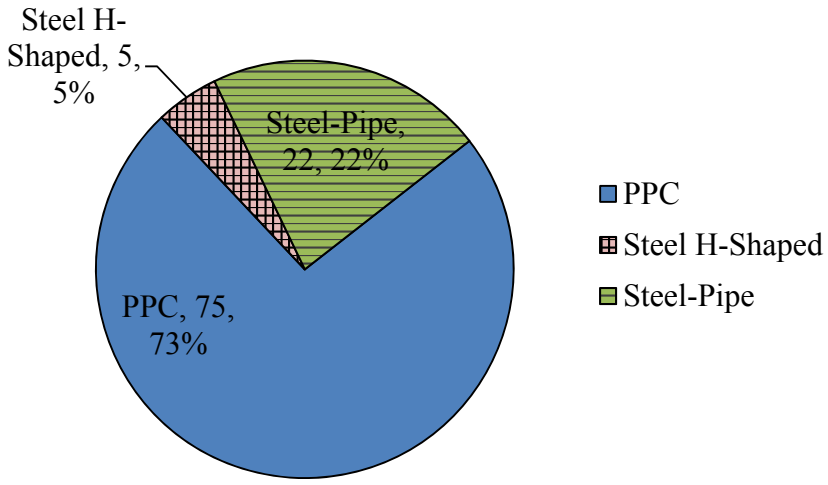

Figure 3-5 Database Composition by Pile Material, and Pile Shape.

.

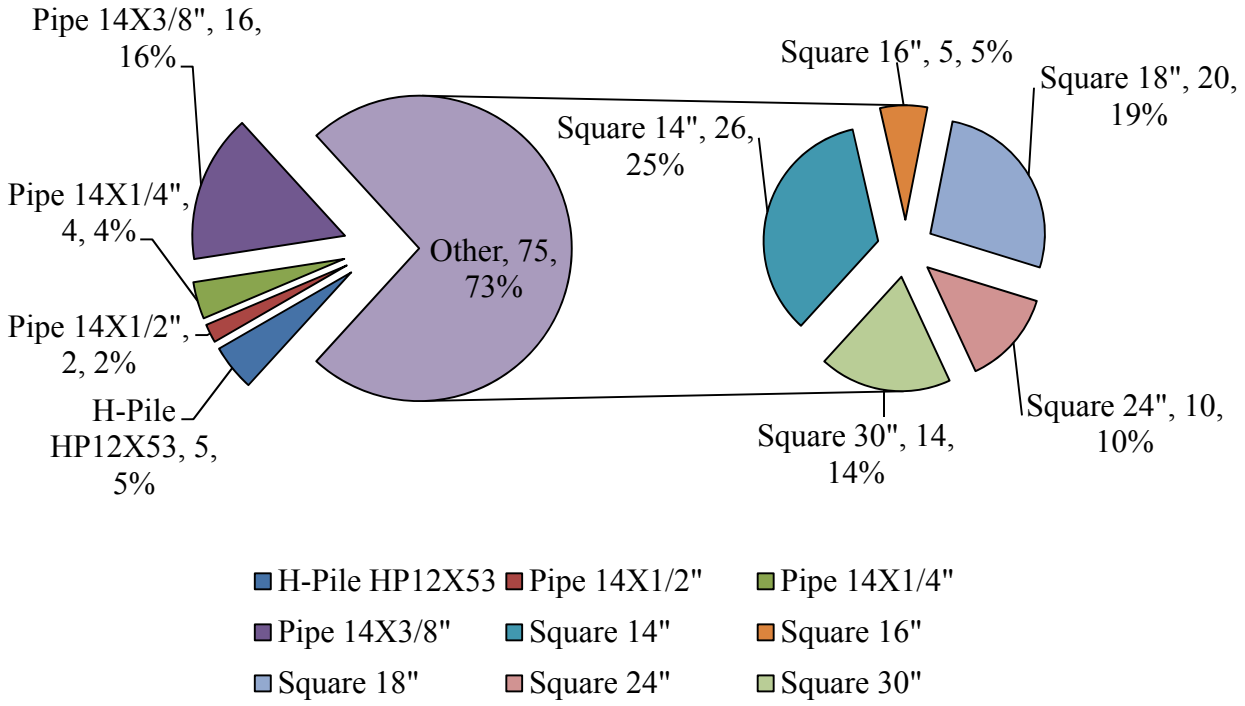

Figure 3-6 Database Composition by Pile Type and Size.

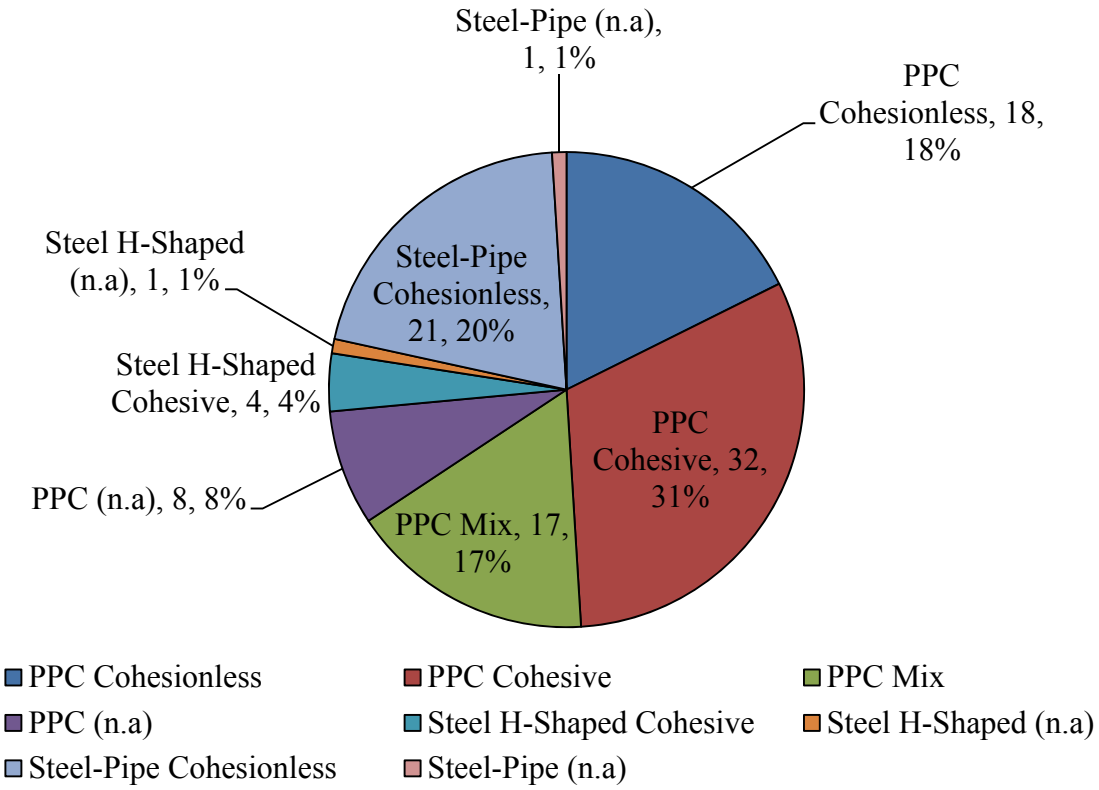

Figure 3-7 Database Composition by Soil Type and Pile Type.

Table 3-2 Pile Distribution According to their Construction Material and Shapes in Different Soil Types in which Piles were Driven.

Pile/Soil Type	Number of Cases
PPC	**75**
Cohesionless	18
Cohesive	32
Mix	17
(n.a)	8
Steel H-Shaped	**5**
Cohesive	4
(n.a)	1
Steel-Pipe	**22**
Cohesionless	21
(n.a)	1
Grand Total	**102**

Apparently, based on the available information in the database, the current practice for driven piles in the region is to drive PPC piles. H-shaped piles were difficult to find as they only constitute five percent of the entire database. However, if H-shaped piles are used, they are mainly driven to a great depth (Figure 3-4) through soils that are predominantly cohesive (Figure 3-7). Likewise, closed ended pipe piles are mostly driven into predominantly cohesionless soils as indicated in Table 3-2. A detailed description of the available pile cases is presented in an electronic copy of the Database for Driven Pile Foundation in Arkansas (Jabo, 2014a)

3.1.4 Different Pile Analysis Procedures Used to Predict Pile Capacity

3.1.4.1 Introduction and Assumptions

Three different pile capacity prediction approaches were used to analyze each pile in the database. The three approaches are static pile analysis methods, based on stratigraphy and soil properties, dynamic pile analysis methods, based on wave equation theory, and pile driving formulas based on penetration resistance. The basic working principles of all these methods are detailed in the literature review. For a given pile, where site and soil information were limited, assumptions were made.

When calculating static pile capacity, the elevation of the ground surface was extracted from pile driving records. If the ground elevation was not mentioned in the driving records, it was assumed to be the bottom of the footing taken from construction plans of the bridge. If construction plan was not available, the elevation of the ground surface for static pile analysis was assumed to be the same elevation as that of the boring log closest to the pile under consideration. If the elevation of the ground surface at the pile was lower than the elevation of the soil boring, it was assumed that pre-boring was performed before the piling process. If the elevation of the ground surface at the pile was higher than the elevation of the soil borehole, it

was assumed that fill was placed before the pile was driven, and the description of the fill material was read from construction plans. Where available, the location of groundwater table was taken as the free water surface reported on the boring log closest to the pile location. If there no water table was reported, then it was assumed to be coinciding with the ground surface.

Predicting pile capacity using driving formulas was done by collecting blow count information at the EOD and its corresponding hammer transferred energy at that stage of pile driving. This important information was gathered from pile driving records. However, there were few cases where some piles exhibited a significant increase in blow count resistance at the EOD. In this case, to compute the pile capacity using driving formula only the last blow count before this significant increase in blow count resistance was considered, and its corresponding transferred energy or hammer stroke was found.

3.1.4.2 Prediction of Static Pile Capacity by Static Analysis Methods

The static analysis methods employed for predicting pile capacity include the α-Tomlinson method in cohesive soils and Nordlund's method in cohesionless soils. Static capacity by CPT method was also considered in this study as some pile load test cases collected from Louisiana had only CPT test results along with their corresponding predicted capacities by CPT method.

The α-Tomlinson, and Nordlund's methods were implemented using the program DRIVEN, which is a geotechnical program developed by the FHWA in 1998 for calculating static capacity of piles. The program calculates the pile capacity versus depth and uses Nordlund method for cohesionless layers and the α-method for cohesive layers. Most of the time, available soil parameters related to soil strength for input into DRIVEN were standard penetration test blow count, SPT-N data. For cohesionless soils, N values are input directly into DRIVEN to

calculate an effective friction angle for the layer using Meyerhof's method. For clays and silts the N values were first correlated to undrained shear strength using Table 2-5 originally presented by Terzaghi and Peck (1961). In some instances shear strength values based on Pocket Penetrometer were provided together with SPT-N values. These shear strength values were compared to the undrained shear strength derived from N values and in most cases there was no match between them. Thus experience and engineering judgment are required when determining shear strength values of cohesive soils based on N values.

During static analysis of pipe piles no check for the FHWA plugged condition was required as piles were all close ended. To arrive at the static pile capacity for H-Piles two approaches were used. The first approach, which assumes unplugged condition, was to calculate the capacity by using H-perimeter for side friction and the metal area for tip bearing resistance. The second approach was to calculate the capacity by using Box perimeter/area, which is related to plugged-box dimensions. Only the least value of the two capacities was recorded. All concrete piles available for this study are square shaped piles, therefore they were all supported in DRIVEN for analysis.

3.1.4.3 Dynamic Analysis Methods

Three dynamic analysis methods based on wave equation theory were employed. These methods were peak resistance using the Pile Driving Analyzer (PDA) method, Case Pile Wave Analysis Program (CAPWAP), and Wave Equation Analysis Program (WEAP).

3.1.4.3.1 Pile Driving Analyzer (PDA) coupled with Signal Matching (CAPWAP)

From bridge design and construction reports PDA/CAPWAP measurement records were collected. In some cases pile capacities from the PDA analysis were based on a single dimensionless Case damping factor and the capacity issued from signal matching were directly

reported. The information entered into database included hammer type, rated and delivered hammer energy, pile capacity from PDA interpretation, toe and shaft capacity by CAPWAP signal matching using PDA results as input, and soil quake and damping parameters used for the pile tip and side. In the database 61 out of 102 driven piles had capacity derived from signal matching, and 15 of these were reported to have capacities that correspond to restrike conditions. Table 3-3 shows a summary of pile case histories by pile location and capacity prediction methods.

3.1.4.3.2 Wave Equation Analysis Program (WEAP)

To predict capacity using wave equation analysis program, WEAP, the soil profile for each pile was imported into GRLWEAP from the FHWA-DRIVEN program. In addition to the soil profile the program requires the type of driving hammer, which was extracted from the piling records. To compare the results of signal matching and WEAP, the pile driveability option in WEAP was selected. This option analyzes the driving process as the pile penetrates into the ground. The results of this process include pile-set for each hammer blow, hammer transferred energy, induced driving stresses (compressive or tensile) within pile. At the end of pile driving a bearing graph is produced. This bearing graph relates pile capacity to blow count resistance at the EOD or at the BOR. The analysis required that some assumptions be made. As the soil profile was imported from DRIVEN, the assumption made for water table remained the same and kept constant at EOD as well as at BOR. In case pre-boring took place before piling, the soil within this zone was considered as an overburden pressure and the effective embedded depth was adjusted accordingly.

The program also requires the assumption of the shaft resistance percentage to be used in earing graph analysis. This percentage of shaft resistance was derived from the results of signal

matching. Should signal matching results be missing the percentage of shaft resistance was calculated based on shaft and total pile capacity determined using DRIVEN. However, when the soil was considered to be very soft, end bearing resistance was assumed constant. Soil quakes and damping coefficients for the pile tip and side were extracted from signal matching results. If these soil dynamic parameters were not available the recommended default parameters from WEAP were used.

Pile capacity at EOD/BOR was interpreted from the bearing graph using the measured hammer blow that was read from manually recorded data at different stage of pile driving. If this pile resistance was not recorded, the pile set at EOD/BOR derived from signal matching was transformed into blow count resistance. A capacity corresponding to that blow count on the bearing graph was recorded as the ultimate capacity of the pile. Should hammer stroke have been given instead of pile set, the bearing graph relating the hammer stroke and blow counts was developed and connected to pile capacity versus blow counts. In total 49 pile cases from Arkansas and Missouri which had detailed soil profiles, driving records, soil dynamic parameters, and blow count at the EOD were analyzed. Case histories from Louisiana did not have pile driving records and could not be analyzed.

3.1.4.4 Prediction of Pile Capacity by Dynamic Formulas

Two pile driving formulae were employed in the prediction of capacity for 49 pile cases from Arkansas and Missouri as indicated in Table 3-3. Since pile driving records are lacking for Louisiana, the prediction of pile capacity by dynamic formula was not performed. The Engineering News Record (ENR) and the FHWA-Gates were the two selected Formulas for the analysis. Both formulas involve blow count at the EOD and hammer transferred energy in the form of hammer weight and drop height. The ENR formula is selected because it constitutes one

of the standard practices of establishing termination criteria for piling process in the state of Arkansas, and the FHWA modified Gates formula is selected because of its well-known performance over all other available formulas and because it is recommended in the 2007 through 2012 editions of the AASHTO-LRFD Bridge Design Specifications over other dynamic prediction methods for construction control of driven piles (AASHTO, 2007, 2012).

3.1.4.5 Pile Capacity Interpretation from Pile Static Load Test

The data set is composed of 53 pile case histories with Static Load Test (SLT) from Louisiana. The actual SLT capacities for the remaining 49 pile case histories of the database are still unknown. The collected values of SLT capacities were interpreted using Davisson failure criterion (Abu-Farsakh et al., 2009). These SLTs served as basis or reference values for the calibration of LRFD resistance factors.

Table 3-3 Number of Pile Case Histories According to Pile Location and Capacity Prediction Methods.

Location		**Static capacity prediction methods**				**Signal matching**		**Drivability**	**Driving formulas**
Location	Total cases	SLT	CPT	Reported static pile capacity*	Calculated static pile capacity**	EOD	BOR	Wave equation	ENR and FHWA-Gates
AR	18	0	0	0	18	18	0	18	18
LA	53	53	42	34	45	12	9	7	0
MO	31	0	0	0	31	31	4+(2)	31	31
Total	102	53	42	34	94	61	15	56	49

* α-Method by Tomlinson for Cohesive soil layers and Nordlund method for cohesionless soil layers: soil interpretation and capacity prediction done by Louisiana.

** Tomlinson/Nordlund methods using the FHWA-DRIVEN program with soil profile interpretation done by me.

( ) Cases with second restrikes

3.2 Selection of Reliability Analysis Methods for LRFD Calibration

The choice of reliability analysis method during LRFD calibration may affect the results of calibration. The most commonly used reliability method is the FOSM method. Two other reliability methods with higher degrees of sophistication were reported in the literature review. First Order Reliability Method (FORM), and Monte Carlo Simulations (MCS) were the more sophisticated methods used in this study. The FOSM uses a closed form solution represented by the Equation 2-16 and its accuracy depends on the range of the COV values. Although FOSM is easy to use, it may only be valid for preliminary analyses. This is because the closed form solution uses a direct but erroneous approximation of the COV of the combined live and dead load presented in Equation 2-15. Nevertheless, the accuracy of the FOSM can be improved by using the relationship presented in the Equation 2-14, the solution would then require an iterative process and one has to assume the values of nominal forces in action, which do not really affect the final answer. The resulting improved procedure is more accurate than the simplified closed form solution, and it gives same results as the more sophisticated methods. For comparison purposes, the simplified closed form solution is denoted as FOSM1 and the improved solution that incorporates both Equation 2-14 and Equation 2-16 is denoted as FOSM2. For quick convergence of the solution for FOSM2, the approximate solution from FOSM1 is utilized as a starting point in FOSM2. An explicit but more complex form of this improved method FOSM2 was found by solving the two expressions using a MATLAB based code provided as an Appendix to the ReliaPile user's manual (Jabo, 2014b).

From the assumed set of resistance factors, a corresponding set of reliability levels is calculated. From the calculated set of reliability indices, a desired resistance factor that corresponds to target reliability index (β_T) is found. Both methods, FOSM1 and FOSM2, require

the limit state function, g, to be linear. If the latter performance function is a non-linear failure criterion, FOSM exhibits an invariant problem, and more robust and advanced reliability methods would be needed for accurate results. Hasofer and Lind (1974) presented an iterative procedure for a modified reliability index, which did not exhibit the invariance problem. The procedure requires finding a design point located on the failure surface represented by g = 0, and at the shortest distance (reliability index) from the origin of the reduced variable space. Thus, the problem becomes one of constrained optimization. This constrained optimization can be performed using either the Taylor series approach or the Lagrangian multiplier approach. More details about these two approaches are described by Baecher and Christian (2003). To implement the Hasofer—Lind procedure, Rackwitz and Flessler (1978) developed a solution algorithm that was later employed by Low and Tang (1997; 2004) using the Solver add-in for nonlinear optimization in EXCEL. The same approach was attempted in the current study, but the solution was not stable. The result depended on the initial guess of the design point, and the solution would be the localized infimum point close to the initial assumed values of the variables instead of global minimization. The same observations were reported by Phoon (2004, 2008). Moreover, when the COV of the variables becomes large, the convergence of the solution becomes slower. In order to overcome these computational issues, the FORM was performed following the algorithm presented in Figure 3-8 that executed the analysis steps elaborated in Section 2.1.2.3.3.2.2. The optimization is achieved using the built-in minimization function of MATLAB based on Sequential Quadratic Programming (SQP). To check for the validity and convergence of the solution, the Lagrangian multiplier approach was chosen. The approach suggests that the Lagrangian multiplier (λ) becomes null at the design point z*, which is the solution to the Equation 3-1.

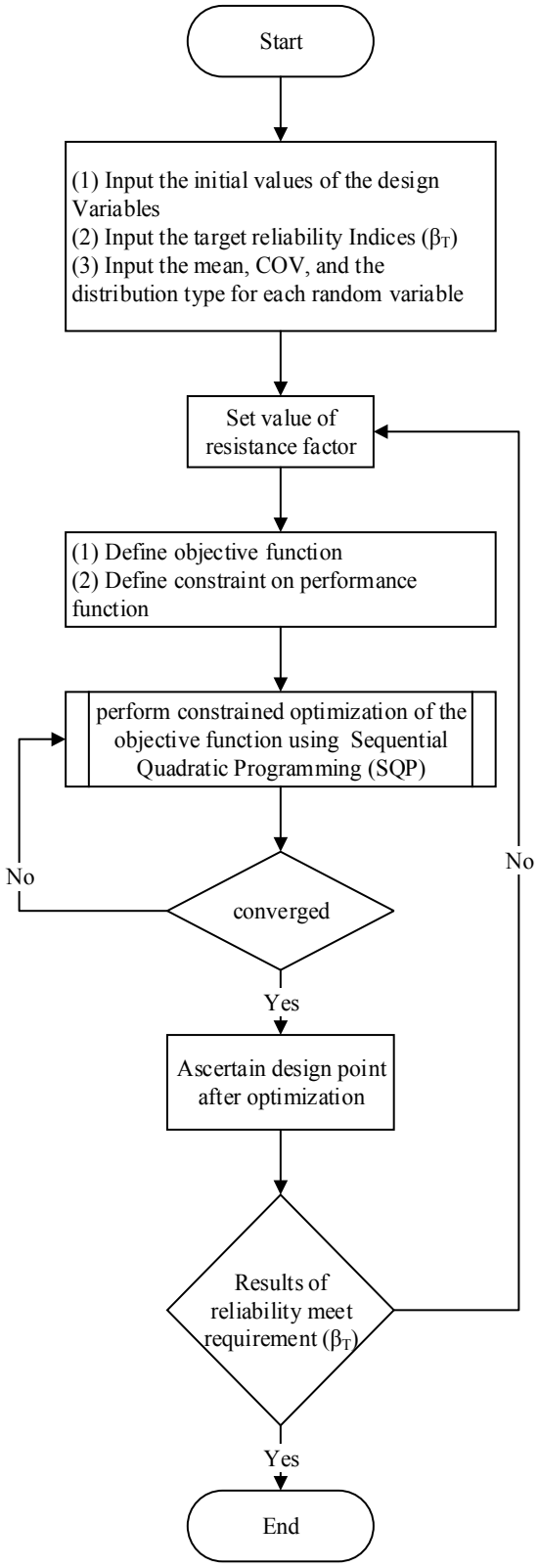

Figure 3-8 Algorithm used for First Order Reliability Method (FORM) during Calibration of Resistance Factors.

$$L = d + \lambda g(z^*) = \sqrt{(z^*)^t (z^*)} + \lambda g(z^*)$$ Equation 3-1

where d is the distance from the origin to the failure criterion as defined in Equation 2-23. With this Lagrangian multiplier approach the accuracy of the solution is controlled during computation process as minimum of (L) and (d) have to be the same and equal to the reliability index β.

Due to scarce pile information in database, some data subsets may not have enough quantity of data for significant statistical analysis. Having limited quantity of data would restrict the reliability of the analysis. In this regard the Monte Carlo Simulation (MCS) technique is required to supplement and analyze the data. In MCS, a random number generator is used to extend the values of the CDFs of random variables. To test the stability of the result given by the MCS method in the MATLAB program, the simulation was run using a set of random numbers generated by a different generator from MATCAD program, and the results were similar. This allowed the built-in MATLAB generator of random numbers to be trusted for subsequent analyses. MCS approach was implemented following the algorithm shown in Figure 3-9 that execute the analysis steps elaborated in Section 2.1.2.3.3.2.1.

To compare the four reliability methods (FOSM1, FOSM2, MCS, and FORM) the statistics for SLT were used. By definition the mean bias is 1.0 for SLT. The value of COV would depend on site variability. For comparison purposes three categories of site classification based on site variability are employed. These categories comprise low site variability with a COV of 0.15, medium site variability with a COV of 0.25, and high site variability with a COV of 0.35 as reported by Kulhawy and Trautmann (1996) and elsewhere (Paikowsky et al., 2004). Figure 3-10 presents the relationship between SLT resistance factor and reliability index for different reliability methods. In all cases the improved FOSM2, FORM, and MCS give similar results.

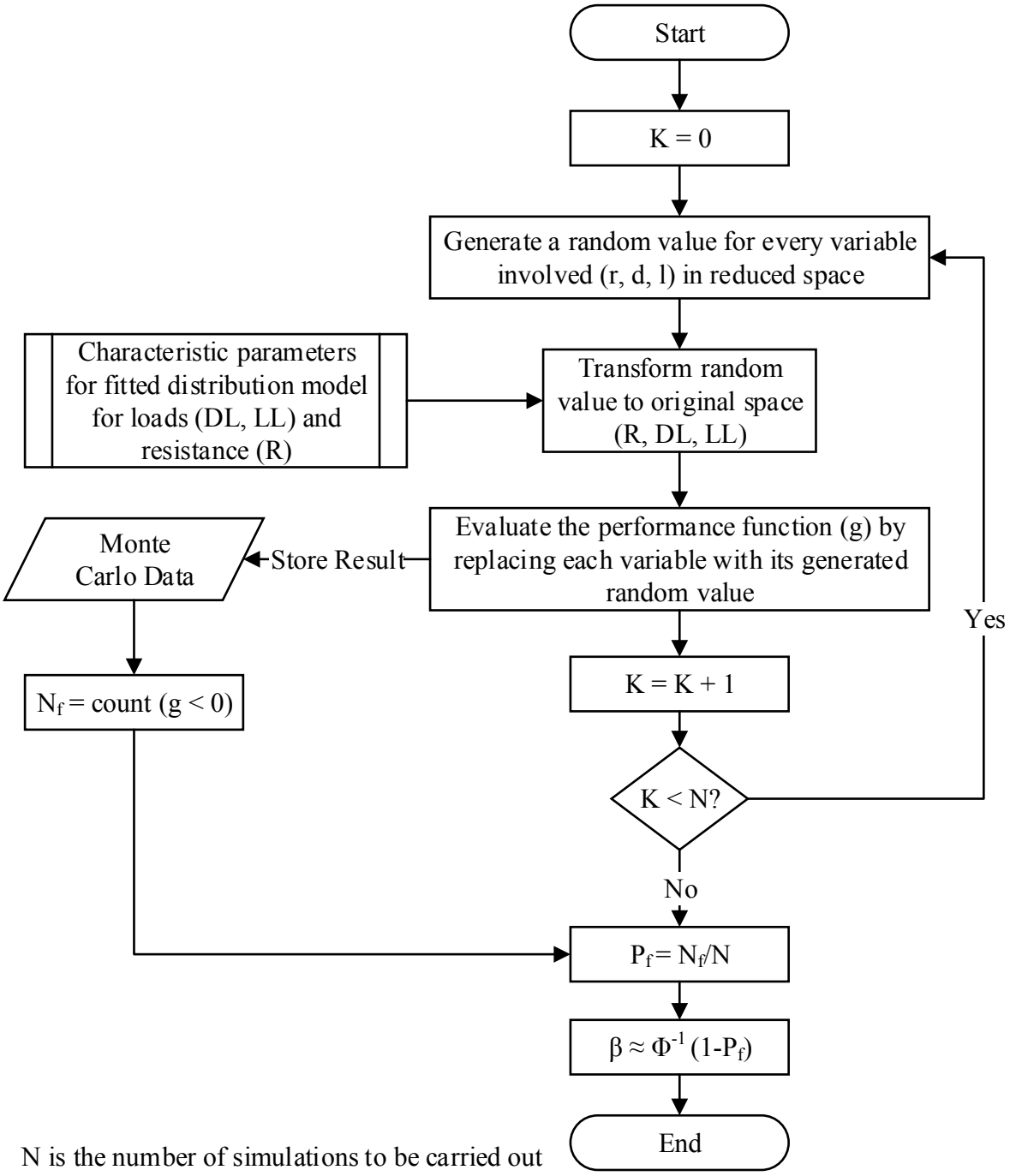

Figure 3-9 Algorithm for performing Monte Carlo Simulation (MCS) for Reliability Analysis during Calibration Process.

While the simplified closed form solution, FOSM1, is a straight forward approach and easy to use, it underestimates the resistance factor by near 20%, 15%, and 12% for low, medium, and high site variability respectively (Table 3-4 and Figure 3-10). Likewise, FOSM1, which was the basis of establishing current AASHTO specifications, gives very conservative values of resistance factors for low COVs in the resistance bias factor. Consequently, any effort put forward in collecting good quality pile data would be inhibited by the use of this reliability approach (FOSM1) during the calibration process, unless the method is improved to the FOSM2. The other two methods, FORM and MCS, produce accurate results for desired reliability levels during calibration processes. According to Rackwitz (2001) FORM delivers a numerical accuracy that is usually more than sufficient for 90% of all applications. Thus any amount of effort one would spend in developing a higher order reliability method would not be justified by the improvement of the accuracy brought by the method.

Table 3-4 Comparison of Reliability Analysis Methods based on Resistance Factors established using a Static Load Test with Bias Factor of Resistance of 1.0 and Coefficients of Variation for low, medium, and high site variability.

Reliability Index	**2.33**			**3.00**		
Site Classification	Low	Medium	High	Low	Medium	High
COV	0.15	0.25	0.35	0.15	0.25	0.35
FOSM1	0.703	0.594	0.485	0.588	0.476	0.370
FOSM2/FORM/MCS	0.853	0.683	0.540	0.759	0.576	0.426
Difference	18%	13%	10%	23%	17%	14%

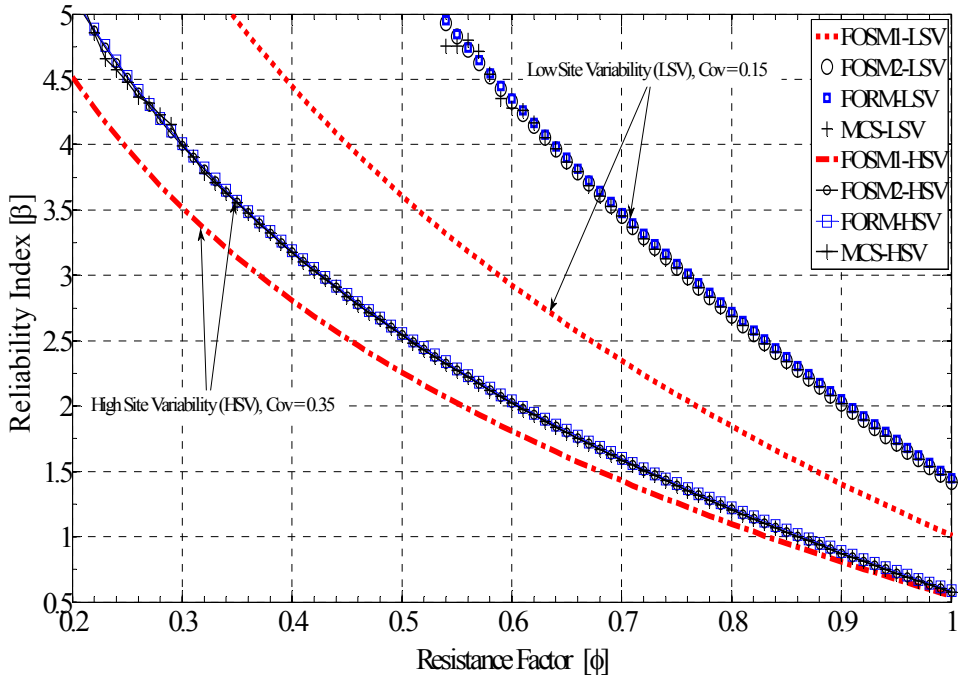

(a)

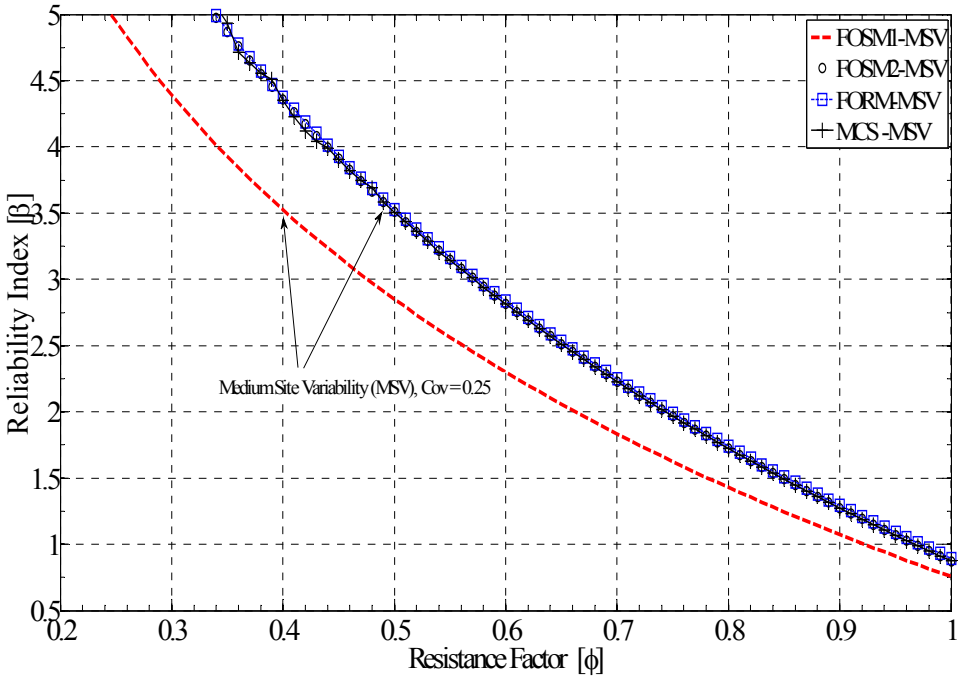

(b)

Figure 3-10 Comparison between FOSM1, FOSM2, FORM, and MCS for (a) Low and High Site Variability and (b) Medium Site Variability.

3.3 Comparative Study of the Pile Analysis Methods by Robust Regression Analysis

The prediction methods for pile capacity that were employed in this study are static methods, dynamic formulas, wave equation, and dynamic testing in tandem with signal matching. To evaluate the performance of these prediction methods, the predicted capacities are compared to measured capacities. First, the predicted capacity is compared to measured SLT capacity. This SLT serves as benchmark of performance because it is the sole known method up to now that accurately measures the nominal capacity of a pile. Second, the predicted capacities are compared against measured capacities by means of dynamic measurements, i.e., PDA coupled with signal matching. This comparison is necessary because the current practice of the AHTD does not include SLT in piled foundation due to high cost associated with it. The AHTD practice is to use static prediction methods to determine the design length of driven pile and use signal matching to verify the pile capacity in the field.

To quantify the accuracy and performance of the different pile capacity estimation methods, the ratio of predicted to measured capacity (Q_P/Q_M) can be employed. The average trend, μ, of the method to over-predict or under-estimate the capacity is given by Equation 2-1:

$$\mu = \frac{1}{n}\sum_{i=1}^{n}\left(\frac{Q_P}{Q_M}\right)_i \qquad \text{Equation 3-2}$$

where μ is the average trend of the method that measures its accuracy, Q_P is the predicted capacity, Q_M is the measured capacity, and n is the number of piles in evaluation. The precision of the method can be judged from standard deviation, σ, of the method as defined in Equation 3-3. However, a good measure of scatter in data is to define the coefficient of variation (COV) of the method determined as the inverse of the signal (μ) to noise (σ) ratio expressed in Equation 3-4.

$$\sigma = \sqrt{\frac{1}{n-1}\sum_{i=1}^{n}\left[\left(\frac{Q_P}{Q_M}\right)_i - \mu\right]^2} \qquad \text{Equation 3-3}$$

$$COV = \frac{\sigma}{\mu} \qquad \text{Equation 3-4}$$

This approach of evaluating the performance of the prediction methods is easy to apply and straightforward for comparing the results of several methods. However, the reliability of the resulting statistics depends upon the size of the sample, n. Furthermore, the average trend, μ, of the method is prone to the presence of outliers and extreme values. Consequently, this approach was used only as a guideline, but the in-depth comparison of the performance of different prediction methods was achieved through robust regression analysis.

The prediction methods for pile capacity are either empirically or semi-empirically based, and were derived based on the actual SLT capacity. Subsequently, it is expected that a linear correlation model would exist between predicted and measured capacity values. Equation 3-5 indicates a general form of the linear regression model, which relates measured to predicted quantities.

$$Q_P = a + b \,.\, Q_M \qquad \text{Equation 3-5}$$

where Q_P = predicted quantity, Q_M = measured quantity, b = coefficient of regression, and a = initial offset of the regression, which is constrained to zero in this study.

The linear regression analysis served as a tool to compare calculated to measured capacity. Scatter in data is studied and data points that require further attention are identified using Cook's distance (Cook, 1977). To check the status of data point using Cook's distance, a new regression that ignores that data point is performed. The distance by which the new regression curve moves from the previous is determined. If that distance (Cook's distance) is too

large, that data point has a great influence on the regression model and special attention (data verification) is required. The predicted linear model is further studied through analysis of variance (ANOVA), in which F-test (Fisher test) and t-test (Student's t- test) are employed. To reduce the effects of potential outliers and extreme values in the dataset, robust regression is used. This robust regression is an iterative process, where a lower weight is assigned to the data points far away from the predicted model. A bisquare weight function (Beaton & Tukey, 1974) is used. The bisquare uses a tuning value of 4.865 times the standard deviation of the errors, thus producing 95 percent efficiency in protecting the regression model against outliers. Through regression analysis, the following section compares different pile analysis methods.

3.3.1 Predicted Capacity versus Measured SLT Ultimate Pile Resistance

The performance of both static and dynamic analysis methods is investigated through regression analysis by establishing a linear relationship between predicted capacity and derived capacity from statically loaded test piles. In the database, only piles collected from the state of Louisiana possess SLT capacity. Since all these piles are only PPC piles, the results refer to such type of piles.

3.3.1.1 Predicted Capacity by DRIVEN versus SLT (Davisson Criterion)

To determine pile capacity, Nordlund's method and Tomlinson's alpha method are used for non-cohesive and cohesive layers respectively. In the process of calculating the capacity, shear strength parameters are interpreted from boring logs and SPT data. To speed up the process of computation of resistance the program DRIVEN, developed by FHWA, is employed. The analysis included 45 case histories. Figure 3-11 plots linear regression model between static analysis method and SLT capacity. The general trend of the results is that static analysis method tends to over-predict capacity by about 40 percent as the regression coefficient, b, is 1.4.

Although the analysis combined all pile cases and all soil types, it is clear that the regression line is significantly influenced by piles driven in to cohesive and mixed soils. The ANOVA results established in Table 3-5 confirm the predicted regression model as the best fit at desired confidence level of 95 percent using the F-test. Likewise t-test confirms the value of 1.4 as the best coefficient of regression with a significance level of 5 percent. A coefficient of determination, R^2, of 0.5 is obtained. This low value of R^2 suggests that the regression model explains only half of the variation, which reinforces the fact that the author of the alpha method (Tomlinson, 1971) recommended a minimum safety factor of 2.5. Despite the low value of R^2, diagnostic plots in Figure 3-12(a) through (d) show that the patterns of the residuals are randomly distributed. This randomness in distribution of the residuals indicates that the proposed regression model was successful in capturing the real trend in the dataset.

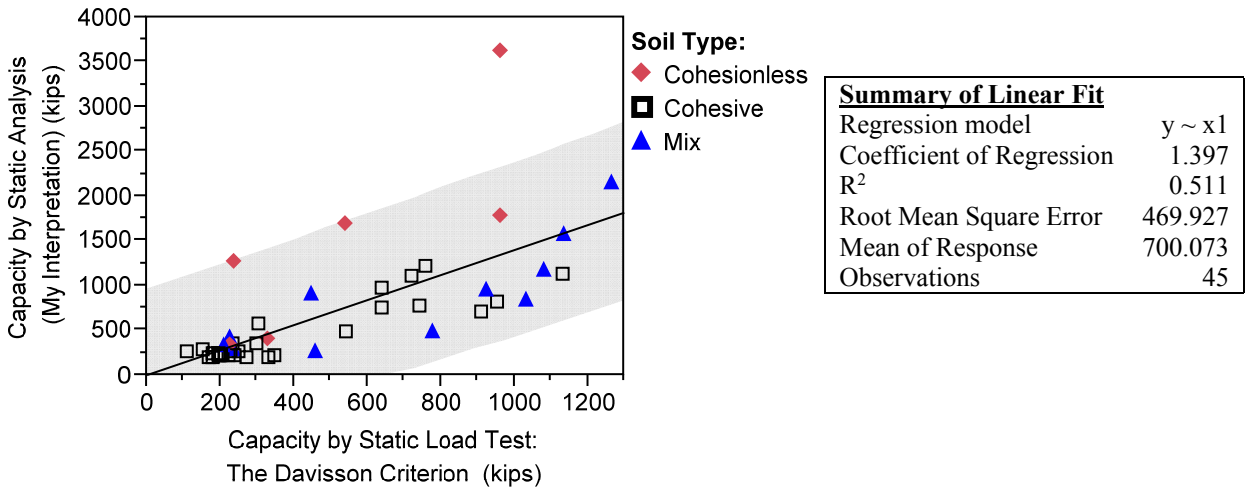

Figure 3-11 Linear Fit of Static Capacity for PPC-Piles using DRIVEN versus SLT Davisson Capacity.

Table 3-5 Analysis of Variance (ANOVA) and Parameter Estimates for Regression Analysis of Static Capacity versus SLT Capacity

Testing against reduced model					
Source	**D.F.**	**Sum of Squares**	**Mean Square**	**F Ratio**	**Prob(> F)**
Model	1	31997413	31997413	144.8950	<0.0001*
Error	44	9716599	220831.79		
Corrected Total	45	41714012			
Parameter Estimates					
Term		**Estimate**	**Std. Error**	**t Ratio**	**Prob(>|t|)**
Intercept (constrained)		0	0	-	-
Regression coefficient		1.3973281	0.116084	12.04	<0.0001*

*Tested against reduced model: p value < the desired significance level of 0.05.

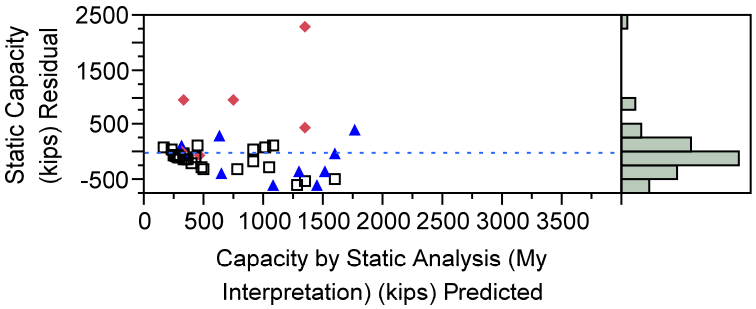

(a)

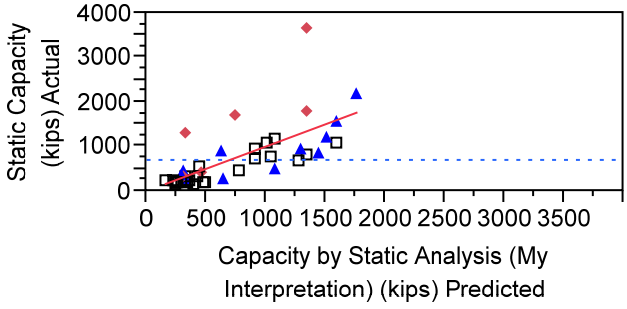

(b)

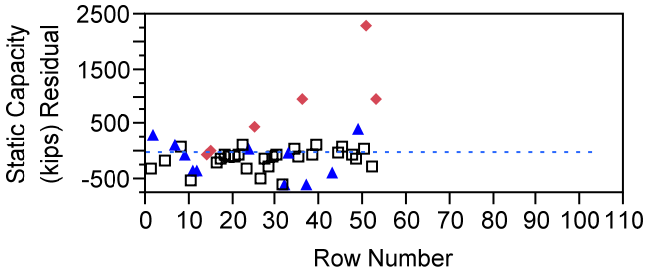

(c)

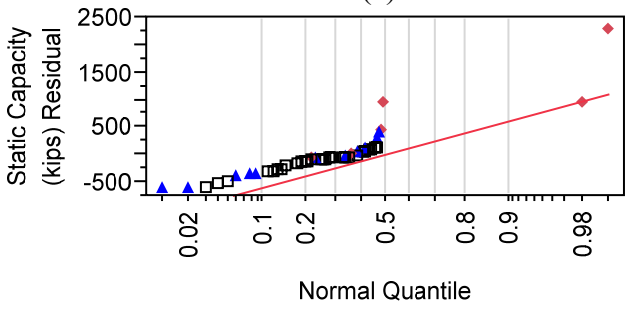

(d)

Figure 3-12 Diagnostics Plots of (a) Residual versus Predicted, (b) Actual versus Predicted, (c) Residual versus Row Order, and (d) Residual Normal Quantile for the Regression Analysis of Static Pile Capacity versus SLT capacity presented in Figure 3-11.

When the regression analysis is performed with respect to the soil type that the piles were driven into, the static method better predicts the capacity in cohesive and mixed soils, with a coefficient of regression of 1.1 and 1.2 respectively. This relatively good accuracy in capacity prediction is not astonishing because Tomlinson (1957, 1971) adjusted soil strength biases through adhesion factor. Figure 3-13 shows regression models in different soil types. The static analysis in cohesionless soils over-predicts the actual pile capacity by a factor of about 2.8. The reason for this over-prediction could be due to the interpretation of shear parameters of the soil derived from SPT-N values, but the size of the analyzed dataset for non-cohesive soils is too small, statistically, to draw final conclusions about the accuracy and precision of the prediction method. The ANOVA presented in Table 3-6 summarizes the statistics of the regression with respect to soil types. Despite the tendency of over-predicting the capacity by the static method the ANOVA analysis still confirms a strong relationship between actual and predicted capacities.

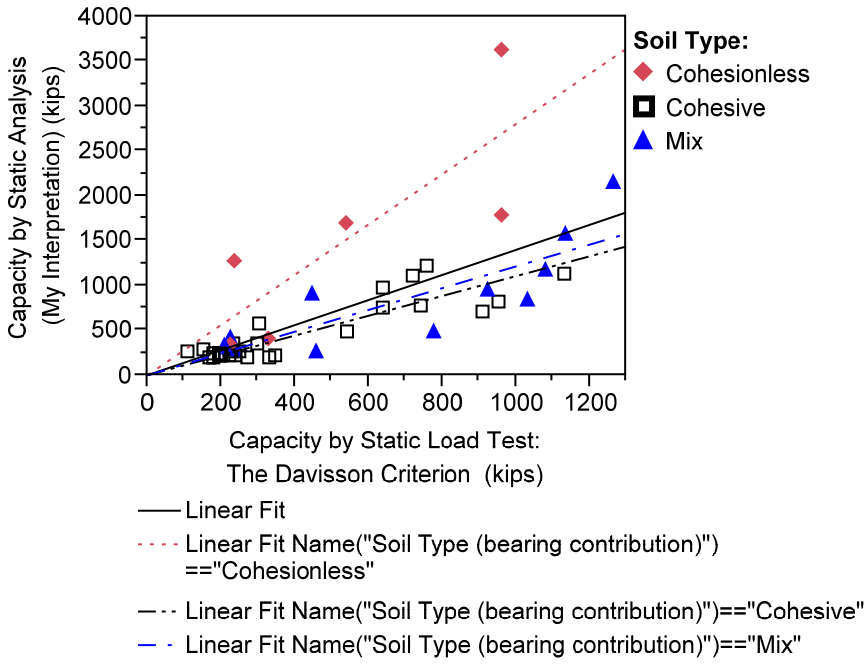

Figure 3-13 Linear Fit of Static Pile Capacity using DRIVEN by SLT Davisson Capacity in Different Soil Types.

Table 3-6 Comparison of Regression Results of the Static Capacity Prediction versus SLT Capacity in Non-cohesive, Cohesive, and Mixed Soils using ANOVA.

Soil Type	Cases	b^+	R^2	F-value*	Prob(> F)	t-value**	Prob(>|t|)
Cohesionless	6	2.800	0.858	37.5246	<0.0017	6.13	<0.0017
Cohesive	28	1.104	0.924	339.7455	<0.0001	18.43	<0.0001
Mixed	11	1.213	0.897	97.1681	<0.0001	9.86	<0.0001
All cases	45	1.397	0.511	144.8950	<0.0001	12.04	<0.0001

b^+= coefficient of regression; * for testing against reduced model; ** for parameter estimates

Based upon the predicted static capacities provided by the Louisiana DOT, the analysis of regression for all soil types gives a coefficient of regression close to unity with an R^2 value equal to 0.9 as shown in Figure 3-14. Although it is indicated that the static analysis in predicting pile capacity followed Tomlinson and Nordlund's methods, it is unclear how soil strength parameters were interpreted. The frequency histogram of the residuals presented in Appendix A.1 shows that the error is randomly distributed but different from a Gaussian distribution.

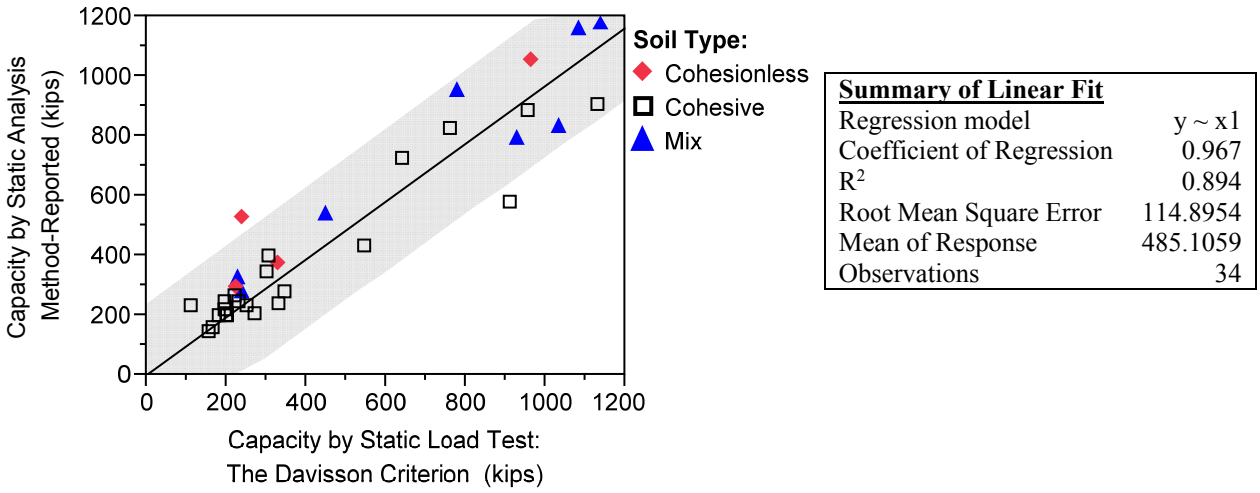

Figure 3-14 Linear Fit of Static Pile Capacity (Reported Capacity Values by Louisiana DOT) by SLT Davisson Capacity.

3.3.1.2 Dynamic Testing with Signal Matching versus Static Load Test

The study of the performance of this dynamic analysis method is achieved by performing a regression analysis between derived capacity from signal matching and measured capacity through static load testing. In the database, a total of 12 PPC piles possess STL and

PDA/CAPWAP (EOD) capacities. From the results of the regression model, on average the signal matching predicts about 34 percent of the measured SLT capacity at end of driving (Figure 3-15 & Appendix A.2). It is inconclusive if the method under- or over-predicts the capacity because the measured capacity at EOD reflects short term pile resistance. Whereas SLT capacity corresponds to the long term pile resistance that includes a setup effect. Nevertheless, the prediction of 34% of the capacity at EOD indicates a set up factor of about 3. Long et al. (1999) reported a setup factor varying between 4 and 5 corresponding to a period of 100 days after installation of various types of driven piles into various types of soils. A value R^2 of 0.73 indicates a consistent prediction of this dynamic analysis method. The accuracy of the PDA/CAPWAP is improved from 34 to about 92 percent when measurements are performed at 14 day restrike (Figure 3-16). The results of this analysis suggest that more than half of the long term capacity is developed through setup effect within 14 days after piling process is completed. The signal matching at BOR still slightly under-predicts the pile capacity about 8% less. The diagnostic plots at EOD and BOR presented in Appendix A.3 and A.4 show that the distributions of residuals are random in nature, which is a good measure of the regressed model. Overall, the method tends to under-predict long-term resistance of piles due to the fact that soil is disturbed during the piling process and CAPWAP assumes a constant soil quake for all soil segments along the shaft during the signal matching process.

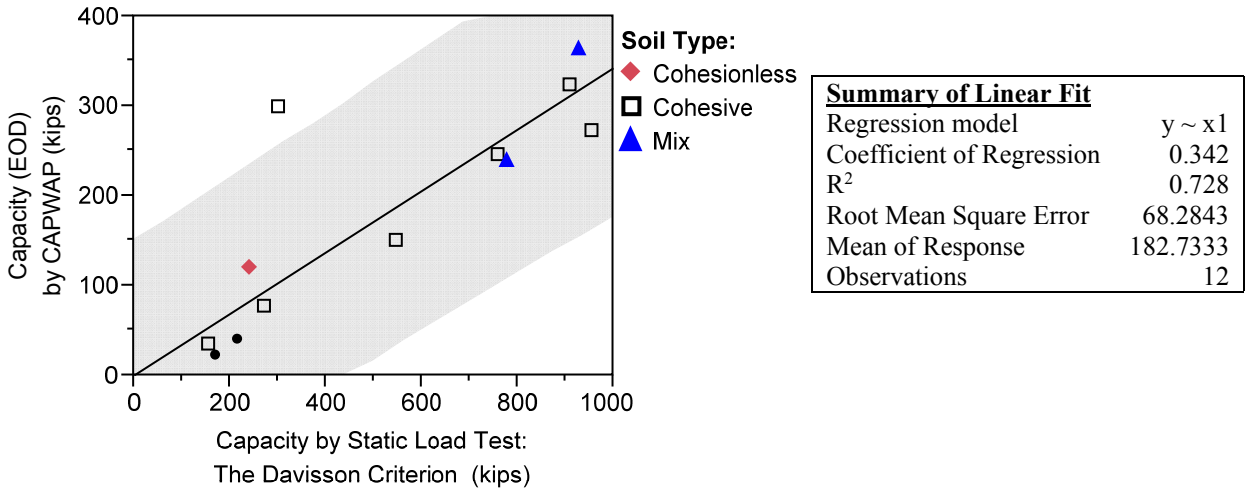

Figure 3-15 Linear Fit between CAPWAP Capacity at EOD and SLT-Davisson Capacity.

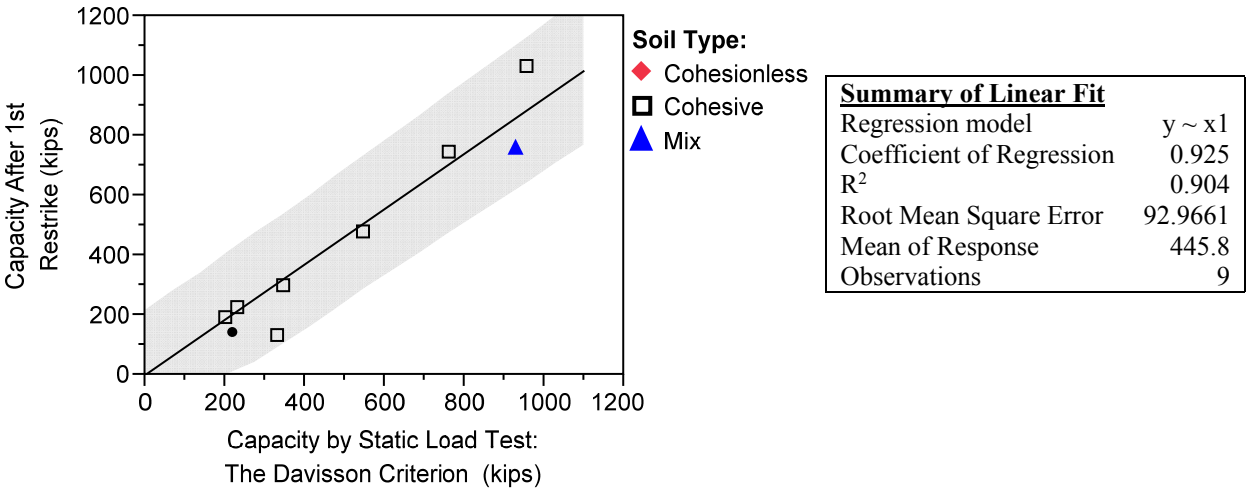

Figure 3-16 Linear Fit between CAPWAP Capacity at BOR versus SLT-Davisson Capacity.

3.3.2 Pile Capacity Prediction Method versus Measured PDA/CAPWAP Resistance

As stated earlier, due to its high cost the SLT is seldom performed on job site. The common practice is to determine contract pile length based on static analysis methods, select piling equipment with help of a wave equation analysis, terminate driving based on a WEAP bearing graph or dynamic formula, and verify capacity using the signal matching process. Thus, there is a need to evaluate the agreement between various pile analysis methods and PDA/CAPWAP method.

3.3.2.1 Static Analysis versus Measured PDA/CAPWAP Capacity at EOD

For the purpose of establishing a relationship between static analysis and signal matching at EOD, regression analysis is performed. Figure 3-17 shows a regression analysis between static capacity calculated using DRIVEN and capacity determined by signal matching. In total there are 59 cases combining H-piles, close-ended pipe piles, and PPC piles embedded into various types of soil. The statistics show that the static analysis predicts greater capacity than CAPWAP-EOD by an average factor of about 1.3. Appendix A.5 shows Diagnostics plots of the distribution of residuals. The distribution is heavily skewed towards the negative side of the residuals.

The fact that static analysis over-predicts the capacity puts the structure in a risky situation because the predicted pile length would be shorter than required. However, this shortcoming of the static analysis would be in part compensated by the fact that pile capacity verification is mostly performed using CAPWAP analyses at EOD, which under-predicts long term pile capacity. Although this compensation could balance safety, this unexplained overestimation of about 30 percent could involve additional cost associated with unpredicted pile built-up to reach required ultimate capacity. The statistics of agreement between static analysis and signal matching at end of driving in various soil types are presented in Table 3-7. The static

method agrees fairly well with signal matching at EOD in non-cohesive soils because pile capacity in such soils is not expected to change significantly over time. Regression coefficients of about 1.6 and 1.4 in cohesive and mixed soils respectively indicate the need to perform restrikes to account for the potential increase in capacity due to setup.

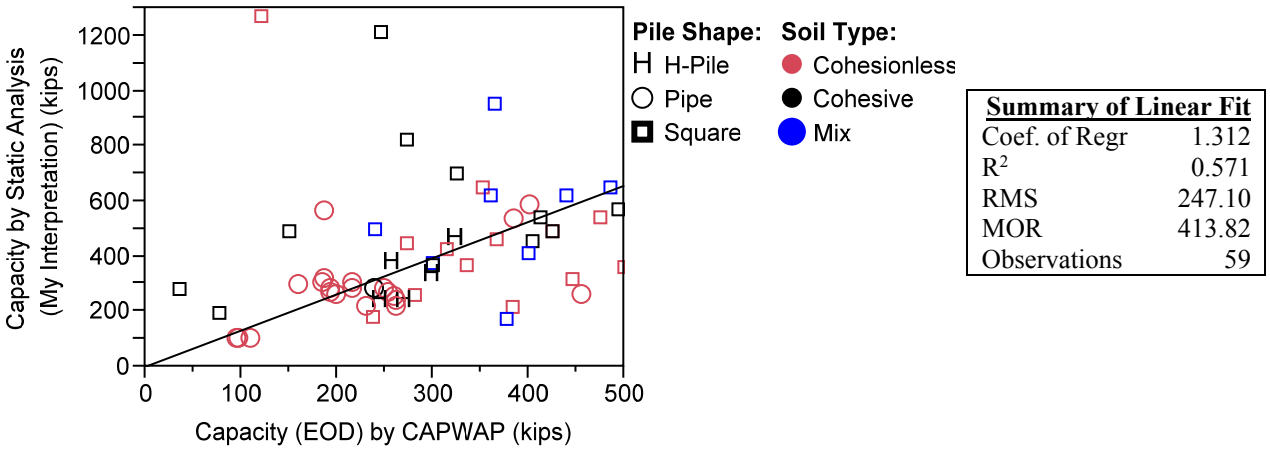

Figure 3-17 Linear Fit of Static Analysis by CAPWAP-EOD.

Table 3-7 Regression Results by ANOVA of the Static Capacity Prediction versus PDA/CAPWAP (EOD) Capacity in Non-cohesive, Cohesive, and Mixed Soils.

Soil Type	Cases	b^+	R^2	F-value*	Prob(> F)	t-value**	Prob(>|t|)
Cohesionless	34	1.156	0.680	73.26	6.84E-10	8.56	6.84E-10
Cohesive	15	1.581	0.736	42.97	1.28E-05	6.56	1.28E-05
Mixed	8	1.417	0.837	42.03	0.0003	6.48	0.0003
All cases	59	1.312	0.571	160.33	<0.0001	12.66	<0.0001

b^+= coefficient of regression; * for testing against reduced model; ** for parameter estimates

3.3.2.2 Measured PDA/CAPWAP (BOR, 14 days) versus PDA/CAPWAP (EOD)

The interpreted pile capacity by signal matching at 14 day restrike shows an average increase in capacity of 100 percent over the capacity predicted at EOD. Figure 3-18 shows scatter plot for CAPWAP capacities at EOD and BOR and different linear regression lines for piles driven into different soil types. On average, diagnostic plots in Appendix A.6 show that the

regression model failed to capture a real trend in the dataset because the residuals still have a clear non-random pattern for each soil type. As one would expect, when soil type is taken into consideration, square PPC piles a presented higher capacity gain factor (about 3.4) in cohesive soils than in mixed soils (about 2). A setup factor of 1.3 is obtained in non-cohesive soils. The increase in pile carrying capacity with time in cohesionless soils could be attributed to two factors: the threshold used for soil classification and arching action. For soil classification, although soil profile is classified as cohesionless, pile resistance generated by the cohesive layers could be nearly 30 percent of the total pile capacity. Hence these cohesive layers could have gained strength by the time of restrike. The second factor is the arching mechanisms described by Robinsky and Morison (1964) and revisited by Chow et al. (1998). The arching mechanism takes place when load is shared by shear transfer along the pile skin and by compression near the pile tip (Loukidis & Salgado, 2008).

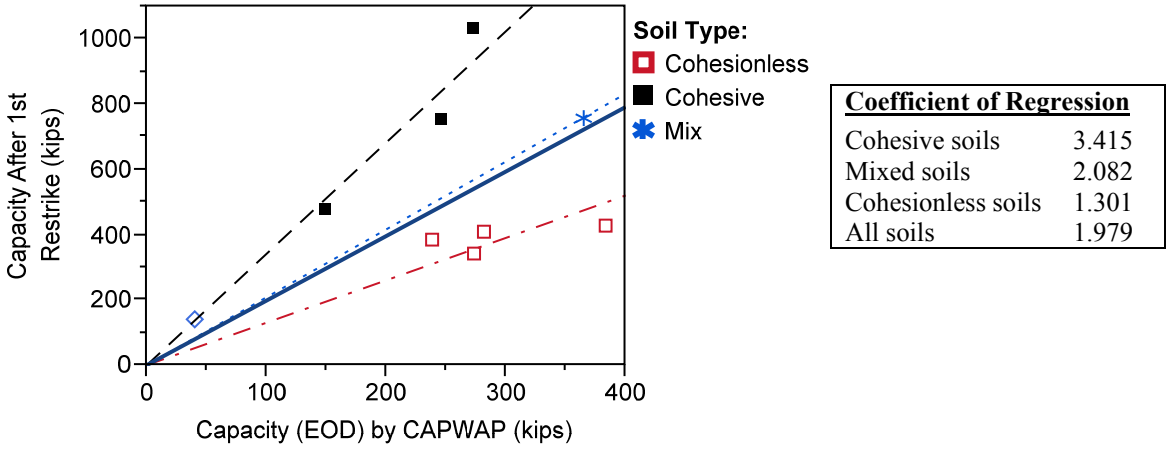

Figure 3-18 Linear Fit of CAPWAP Capacity-BOR by CAPWAP-EOD Capacity for PPC Piles.

3.3.2.3 Predicted Capacity by WEAP versus Measured PDA/CAPWAP Capacity (EOD)

Using the Wave Equation Analysis Program (WEAP) drivability, internally induced driving stresses, and eventually capacity at the end of driving or at the time of restrikes can be

analyzed. To study the performance of the wave equation analysis method, linear regression was performed between WEAP and CAPWAP at EOD condition. Prediction of capacity by WEAP used soil dynamic properties issued from signal matching at EOD. The regression statistics are reported in Figure 3-19. There is a close agreement between these two methods verified by a regression coefficient of 0.91. This value, close to unity, was expected because the WEAP and the signal matching methods are both based on the same principles of wave equation theory and use a similar pile-soil model. The diagnostic test plots in Figure 3-20 show that the distribution of the residuals is quasi symmetric about the regression line model, and the scatter in data increases as the magnitude of predicted capacity increases. This increase in amount of scatter is probably caused by the fact that signal matching is non-unique solution technique that has more unknowns than equations requiring engineering judgment to make assumptions for a final solution. The error in results could become more pronounced as the predicted capacity increases, i.e.; an increasing bias in capacity estimation with increase in actual capacity.

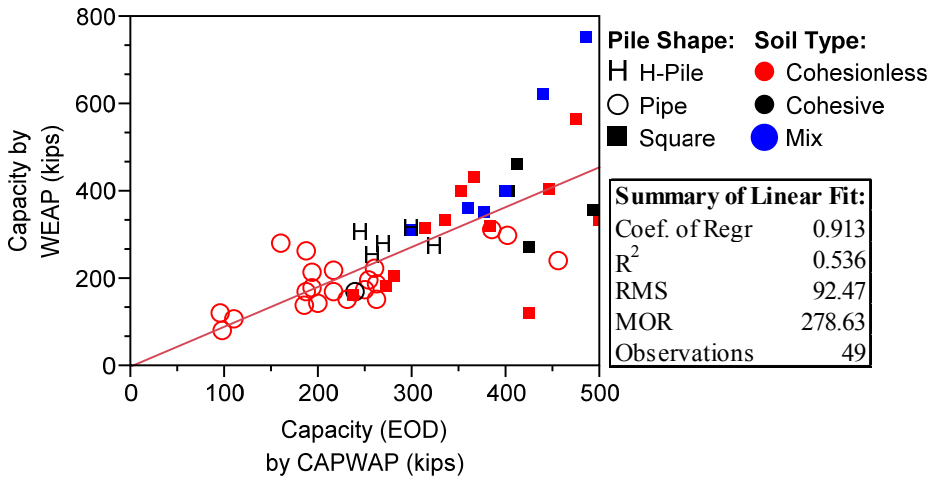

Figure 3-19 Linear Fit between WEAP and CAPWAP at EOD Condition.

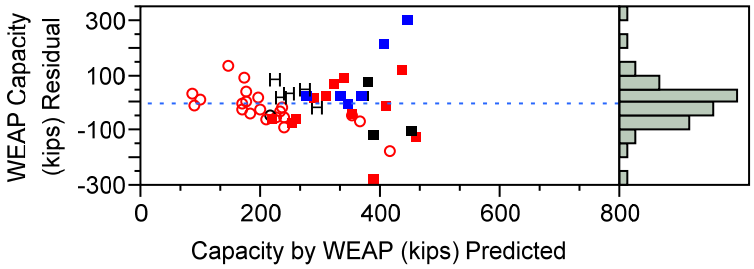

(a)

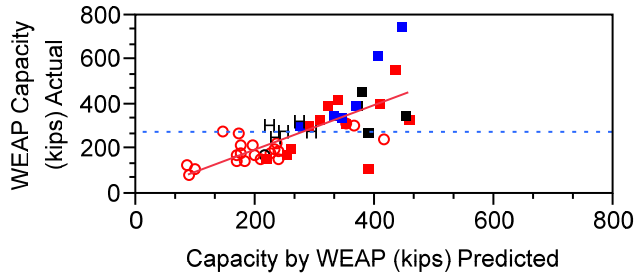

(b)

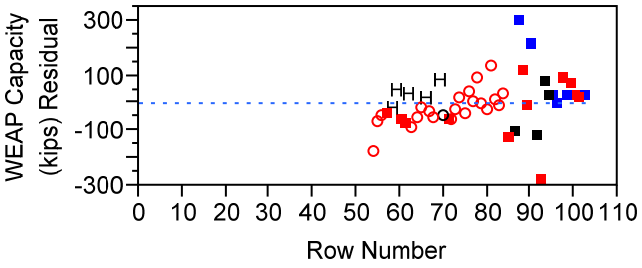

(c)

Figure 3-20 Diagnostics Plots of (a) Residual versus Predicted, (b) Actual versus Predicted, and (c) Residual versus Row Order for the Regression Analysis between WEAP and CAPWAP-EOD presented in Figure 3-19.

3.3.2.4 Capacity by Dynamic Formulas versus Measured Capacity by CAPWAP at EOD

Dynamic formulas can be employed to check pile capacity or terminate pile driving based upon hammer stroke and blow count resistance. Most of the time, when dynamic formula is employed to establish piling stopping criterion, signal matching would be used to check the pile capacity. Thus, the study of agreement between the two methods is indeed needed. Two formulas, ENR and FHWA-Modified Gates, were compared to the measured CAPWAP capacity at EOD condition. By regression analysis, the ENR formula predicts about 3 times more capacity than CAPWAP (EOD) does. Figure 3-21 plots the relationship between CAPWAP (EOD) and ENR, in which all available pile types driven into various soil profiles are presented. As depicted on Figure 3-22 the FHWA-Gates predicts only about half of the capacity predicted by the ENR with a coefficient of regression of about 1.6. The FHWA-Gates has a small amount of data scatter when compared to the scatter in the ENR formula. The level of precision of a method is measured by the value of R^2, which is about 0.45 for ENR and about 0.72 for the FHWA-modified Gates formula. Diagnostic plots of the two methods are presented in Appendices A.7 and A.8 respectively. The distributions of the residuals for both formulas are quasi symmetric about the trend line. The fact that driving formulas over-predict EOD capacity is not surprising because they were developed to estimate long term capacity of driven piles, thus incorporating a factor that adjusts for soil setup.

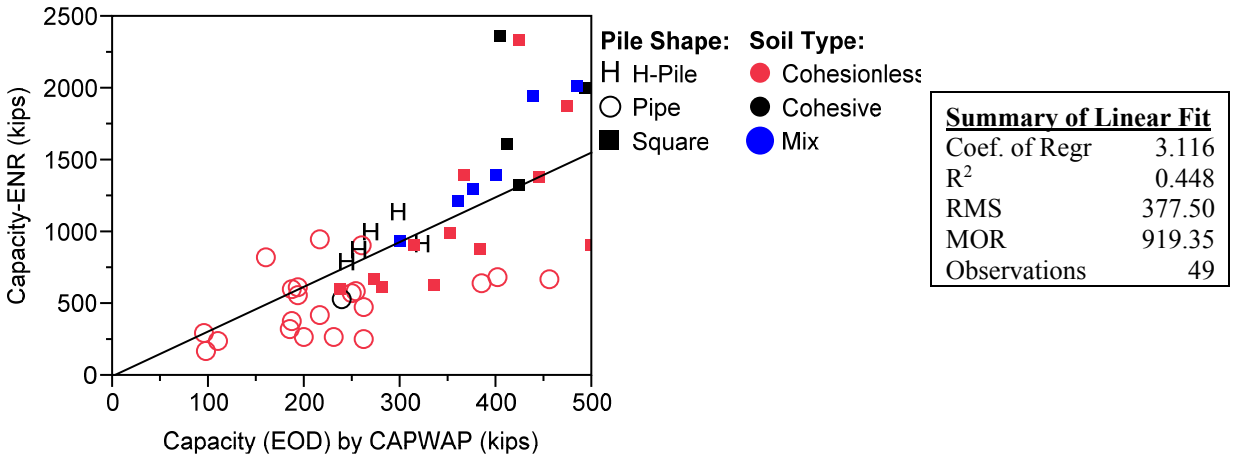

Figure 3-21 Linear Fit of ENR Capacity by CAPWAP-EOD Capacity.

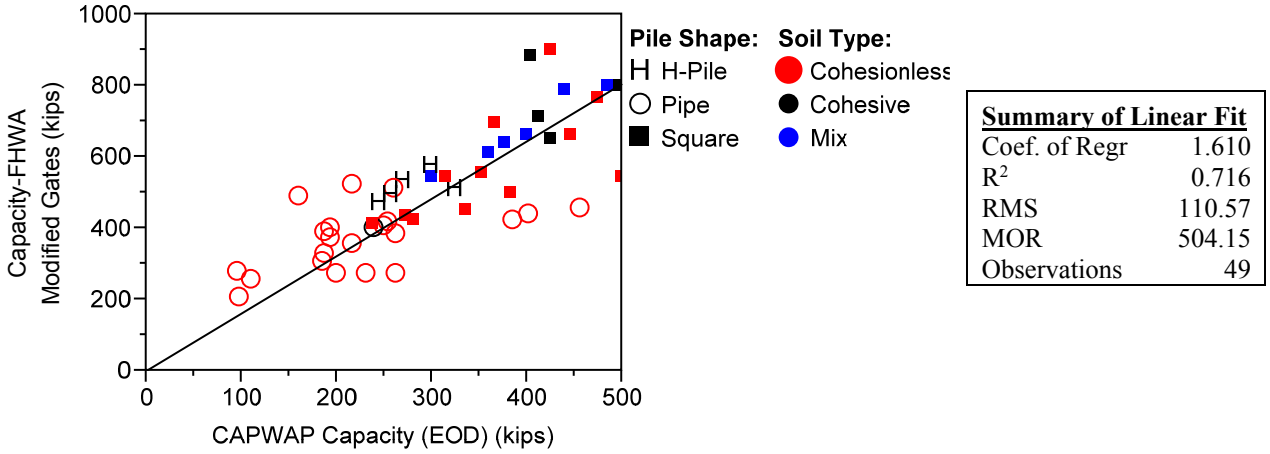

Figure 3-22 Linear Fit between the FHWA-Gates Capacity and CAPWAP-EOD Capacity.

3.3.3 Pile Analysis Methods versus Signal Matching at the Time of Restrike

Because pile capacity measurements at restrike are expected to yield better results (see Section 3.3.1.2), PDA/CAPWAP at BOR has become standard means of pile acceptance. For that reason signal matching at restrike is compared to other prediction methods, namely the static analysis using DRIVEN, WEAP, the ENR and the FHWA-modified Gates formulas. The comparison is performed though linear regression analysis and the statistics are summarized in Table 3-8. Based upon those results, the static analysis method using DRIVEN agrees fairly well with signal matching at 14 day restrike with a coefficient of regression of about a unity. However, the amount of precision in data (Figure 3-23) between the two methods as measured

by R^2 is equal to about 0.66, which indicates the persistence of significant data scatter that could cause disagreement between designed and driven lengths. To have a better agreement between predicted and driven pile lengths, a conversion factor between static analysis and signal matching at BOR is required. Based upon updated empirical cumulative distribution of the capacity ratio such conversion factor is established in Section 5.1.2.

While the FHWA-Gates formula agreed fairly well with signal matching at 14 day restrike (with an average excess of about 12 percent) the ENR formula overestimated that capacity by a factor of about 1.8, whereas WEAP estimated about half of the CAPWAP (BOR) capacity. However, these results are based on only 4 PPC pile cases as presented in Appendix A.9.

Table 3-8 Regression Results of various Prediction Methods versus PDA/CAPWAP (BOR) Capacity in all Types of Soils.

Reference Method	Prediction Methods	Cases	Regression Coefficient	R^2	Model		Parameter estimates	
					F-value	Prob(> F)	t-value	Prob(>|t|)
Measured Capacity by Signal Matching at BOR	Static Capacity	12	1.027	0.657	420.6	<0.0001	20.51	<0.0001
	WEAP-EOD	4	0.557	0.119	59.3	0.0045	7.700	0.0045
	ENR	4	1.755	0.252	151.1	0.0012	12.29	0.0012
	FHWA-Gates	4	1.126	0.532	508.7	0.0002	22.56	0.0002

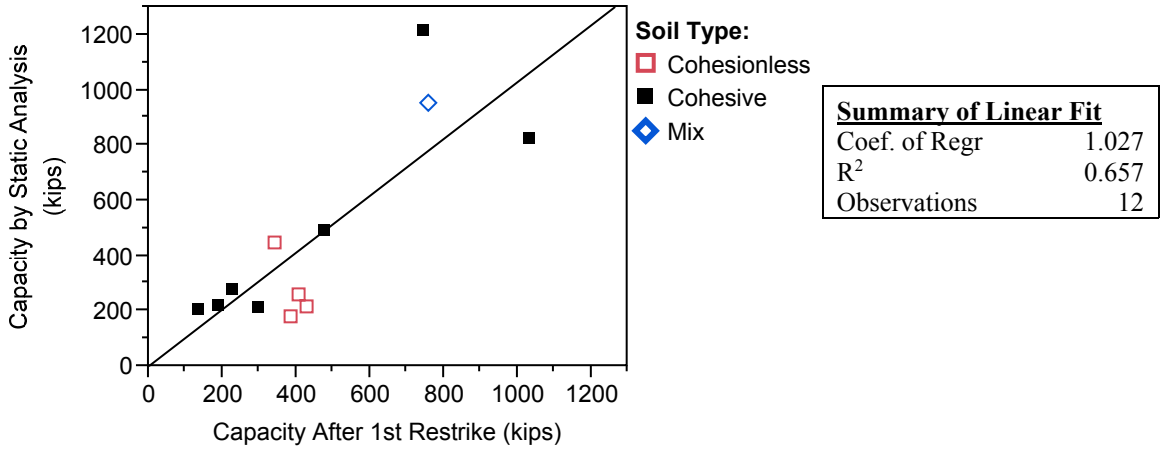

Figure 3-23 Linear Fit between Static Analysis and Signal Matching at BOR (PPC Piles).

3.3.4 Conclusions on Performance of Pile Analysis Methods

Based upon available pile load tests in the database, the performance of various pile capacity prediction methods were studied and the related results are presented in Table 3-9, which summarizes the statistics of the agreement between various pile analysis methods that were discussed in this chapter. The following observations were made:

Signal matching at 14 day restrike stands out in yielding the best agreement with SLT measurements. Therefore, the use of dynamic measurements coupled with signal matching at restrikes would constitute the best option for QA/QC on a job site. In most cases, it would be too conservative to directly compare the results of PDA/CAPWAP at EOD to the required ultimate capacity, because CAPWAP (EOD) does not incorporate soil setup effect into capacity. If the EOD results have to be used in verifying pile bearing capacity, a time dependent soil-setup relationship should be established for the region and should be coupled with the EOD capacity. Nevertheless, PDA/CAPWAP at EOD better serves to the monitor of the piling process than dynamic formulae and also helps in preventing potential pile damage. If the construction project is subjected to busy schedule and the capacity predicted by signal matching at EOD does not fulfill acceptance criterion after the pile has reached the contracted length, a 24 hour restrike could be planned to assess any possible setup development before pile is driven further or is spliced.

Overall, driving formulas tend to over-predict ultimate carrying capacity of piles. Although this fact of over-predicting the capacity may prevent imminent damage of the pile from potential high induced driving stresses, there is a great risk that embedded pile length determined from dynamic formula may be insufficient in providing the required ultimate bearing. Even though the AHTD specifications solely recommends the ENR among all available driving

formulas, the FHWA-modified Gates formula has performed better than the ENR. The AASHTO LRFD Bridge Design Specifications (2012) has also designated the FHWA-modified Gates as the most accurate of the dynamic formulas and has recommended its use over any other dynamic formulas.

Static pile analysis using DRIVEN tends to over-predict long term carrying capacity of piles. This is due in part to correlations embedded into the program to acquire soil strength parameters from field test results, and other external transformations that the user of the program has to perform before analysis. The fact that this method over-predicts pile capacity could cause non-agreement between contract (design) pile length and the driven length on jobsite. To enhance agreement between static analysis and dynamic monitoring by maintaining the safety of the structure within an acceptable reliability level, calibration of resistance factors and the use of correction factors are required to bring the capacity ratio of the two methods close to unity.

The study of the performance of pile analysis methods shows that the accuracy of the prediction method can be enhanced through robust regression studies which bring the overall coefficient of regression closer to unity. However, scatter/precision in data is inherent to the prediction methods. The LRFD calibration of resistance factors based on reliability theory handles this problem of precision in data to an acceptable level of risk.

Table 3-9 Performance Statistics through Robust Regression for Various Methods of Pile Capacity Analyzes.

Reference Method	Prediction Method	Number of Cases	Regression Coefficient	R^2	Model		Parameter estimates	
					F-value	Prob(> F)	t-value	Prob(>|t|)
Static Load Test Capacity (Davisson Interpretation)	Static capacity[1]	45	1.397	0.511	144.9	<0.0001	12.04	<0.0001
	Static capacity[2]	34	0.967	0.894	828.1	<0.0001	28.78	<0.0001
	CAPWAP (EOD)	12	0.342	0.728	110.7	<0.0001	10.52	<0.0001
	CAPWAP (BOR)	9	0.925	0.904	298.7	<0.0001	17.28	<0.0001
Measured Capacity by Signal Matching at the End of Driving	SLT-Davisson	12	2.657	0.749	110.7	<0.0001	10.52	<0.0001
	Static Capacity[1]	59	1.312	0.571	160.3	<0.0001	12.66	<0.0001
	CAPWAP (BOR)	9	1.980	0.399	38.6	0.0003	6.21	0.0003
	WEAP	49	0.913	0.536	499.1	<0.0001	22.34	<0.0001
	ENR	49	3.116	0.448	348.7	<0.0001	18.67	<0.0001
	FHWA-Gates	49	1.610	0.716	1084.7	<0.0001	32.94	<0.0001
Measured Capacity by Signal Matching at BOR	Static Capacity[1]	12	1.027	0.657	420.6	<0.0001	20.51	<0.0001
	WEAP (EOD)	4	0.557	0.119	59.3	0.0045	7.70	0.0045
	ENR	4	1.755	0.252	151.1	0.0012	12.29	0.0012
	FHWA-Gates	4	1.126	0.532	508.7	0.0002	22.56	0.0002

[1] α-method for cohesive soils and Nordlund for non-cohesive soils using FHWA-Driven 1.2 version program.
[2] Static pile capacity as reported within the source document.
EOD = at the end of driving condition.
BOR = at the beginning of restrike condition.

3.4 Preliminary Calibration of Resistance Factors

Although a correction factor based upon robust regression analysis can enhance the accuracy of pile analysis method, it is statistically difficult to deal with the method's precision. It is necessary to look at more than the coefficient of regression and coefficient of determination to establish a reliable pile analysis method. The reliability approach uses the bias of measured to predicted capacity ratios (bias resistance factors) and its coefficient of variation (COV) to determine a resistance factor that fulfills the required geotechnical safety level. Preliminary calibration of resistance factors calls upon the statistics of the prediction method by fitting probability distribution models to the bias factors of resistance derived from datasets. The capacity ratio for each pile case can be determined using Equation 2-17. Table 3-9 presents the number of different case histories available in the database used to define the required statistics for calibration purposes.

3.4.1 Distribution Model for Measured to Predicted Capacity Ratio

3.4.1.1 Identifying Best Fit Distributions

Previous studies for distribution of loads and resistances have shown that resistance and load biases nearly follow a lognormal distribution (Barker et al., 1991; Briaud & Tucker, 1988; Cornell, 1969; Dennis, 1982; Isenhower & Long, 1997; Long & Shimel, 1989; Paikowsky et al., 2004). Subsequently, for the purpose of establishing resistance factors, the values of resistance bias were fitted to log-normal distribution within the expected zone of the design point, even if a particular set of data suggested a different type of distribution. Assuming that the bias (λ) of loads and resistances follow a log-normal distribution, they can be described as Gaussian with a natural logarithm transform having a mean μ_{ln} and a standard deviation σ_{ln} using Equation 3-6.

$$ln(\lambda) \equiv Gaussian(\mu_{ln}, \sigma_{ln})$$ Equation 3-6

3.4.1.2 Determination of Parameters of Best Fit Distribution by Least-Squares Estimator

To find the solution (μ_{ln} , σ_{ln}) to the Equation 3-6, the assumed distribution models were fitted to the non-parametric empirical cumulative distribution function (ECDF) of the datasets. This ECDF was estimated based on the relationship presented in Equation 3-7 as recommended by various authors, such as Martinez (2001). For a random sample of size, n, with ordered statistics X_1, X_2, …, X_n, the quantile of X_j is estimated as follows:

$$ECDF\left(X_j\right) = \frac{(j-0.5)}{n} \qquad with\ \ j = 1, 2, \ldots, n \qquad \text{Equation 3-7}$$

The calibration of resistance factors for deep foundations calls for small allowable probabilities of failure, 0.1 and 1.0 percent for non-redundant and redundant pile foundations respectively. Thus, the design point for the reliability approach is expected to be located in the lower tail of the cumulative distribution of the resistance bias values. The weighted least-squares estimator was used in approximating the distribution in lower tail of resistance , because many statistical computer programs fit a distribution to data in the area of the mean, and that may produce unsuitable results in the area of the tails,. Model parameter estimations were performed using MATLAB's nonlinear least-squares regression method using a Gauss–Newton algorithm. Figure 3-24 plots a flow chart illustrating different steps in defining the theoretical probability distribution that best fits the dataset. At the end of distribution fitting, the reported parameter errors were estimated by taking the square root of the diagonal of the covariance matrix (inverse of the Fisher's information matrix which represents the asymptotic standard errors. To enhance the stability of the nonlinear regression process and the speed of computation, which depends on the initial guess for values of the parameters, the maximum likelihood estimations (MLE) of the dataset were used as starting values of the iterative computation process.

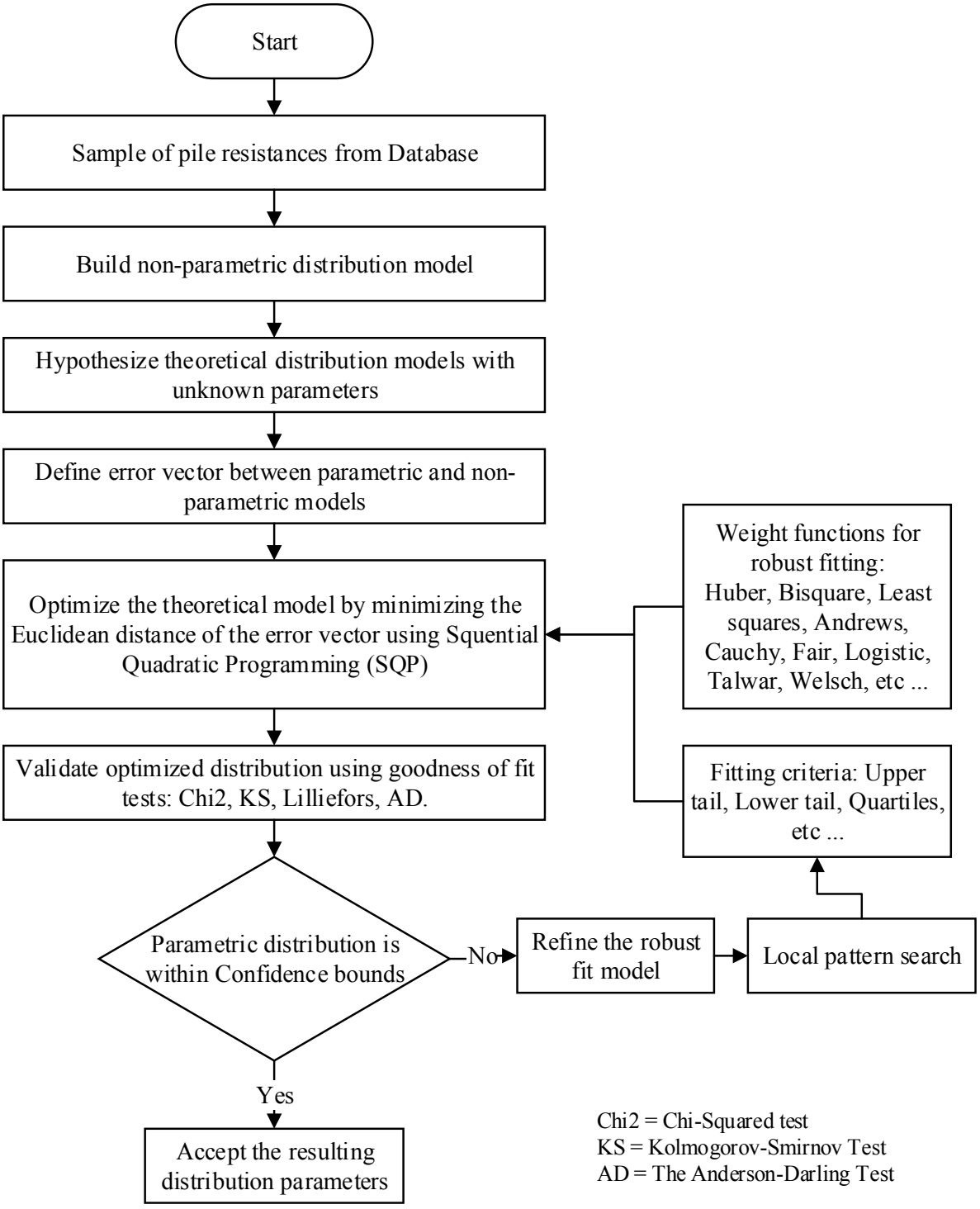

Figure 3-24 Flow Chart for Determining Unknown Parameters of the Theoretical Probability Distribution that best fit the Measured to Predicted Pile Capacity Ratios.

The accuracy of the calibration depends on how well the data points fit the lower tail of the theoretical distribution. The lower tail fitting process progressed from the left of the data points, which is a more conservative region for reliability analyses. To insure that the predicted models were in good agreement with available observations, the estimated CDF models were tested under several statistical tests described in Section 2.1.2.4. Confidence bounds at the five percent level of significance were calculated and visualized together with CDF and dataset. This approach of replacing the empirical CDF by a smooth fitted theoretical CDF is a robust way of effectively performing reliability analysis. It was observed that this kind of regression on the amassed datasets yields reliable parameters for calibration process.

Figure 3-25 shows a histogram of the resistance bias factors, and it graphically compares two distribution models, normal and lognormal, fitted to the tail of the ECDF for the ratios of SLT to predicted static capacity. By visual observations of the distributions a general trend of the resistance bias can be traced from histogram. However, this judgment could be effected by the width of the bins. Subsequently, cumulative distribution functions (Figure 3-26) were used to qualitatively assess the fitted probability models. It was observed that the lognormal distribution better fitted the ECDF than normal distribution. This also holds true in the lower tail where resistance bias factors are lesser than unity, i.e., where failure is most likely to occur due to the fact that predicted capacity overestimates the actual capacity. One of the 4 performed tests for goodness of fit (Table 3-10) rejected the hypothesis of log-normality due to 2 data points located outside the 95 confidence bounds established in Figure 3-27. For this particular case, although 95% confidence bounds for normal distribution seem to cover most of the data points (Figure 3-28), there is a strong reason to believe that lognormal is the best model over a normal probability distribution because the resistance bias factor could theoretically vary from zero to

infinity with an expected optimum value of unity (Abu-Farsakh et al., 2009). The summary of the statistics for fitting probability distribution models to ECDF of the static analysis bias values is presented in Table 3-10. In that table, the regressed mean and COV values of the bias of resistance for both normal and lognormal models are comparable to each other. The mean square error (MSE) for lognormal model is only half of the MSE for predicted normal distribution; thus verifying that the lognormal distribution is the best continuous probability distribution for the ECDF of the resistance bias. The distributions of the resistance bias for other capacity prediction methods were analyzed in the same way and graphical presentations are reported herein.

Figure 3-29 presents a histogram and both the predicted normal and lognormal PDFs of the bias of the resistance for the static analysis method using the DRIVEN program. The five percent confidence bounds of the fitted lognormal distribution cover all data points in its lower tail (Figure 3-30). For predicting probability distribution of the ratio SLT/Signal Matching at EOD for PPC piles Figure 3-31 is plotted. The plot presents histogram and Predicted Normal and Log-Normal PDFs of Resistance Bias Factors. Due to small number of available data points (only 12) the histogram plot seems not to help much in deciding which distribution that best models the empirical data. The fitted lognormal CDF of the SLT/CAPWAP-EOD ratio as presented in Figure 3-32 offers 5% confidence bounds that cover all available data points, which is not surprising because all values of the bias are greater than unit. However, when the estimation of the distribution is performed at the BOR, the robust fitting ignores 2 extreme values (Figure 3-33) in the upper tail and fits all the lower tail data points within a five percent confidence bounds of the estimated lognormal CDF (Figure 3-34).

To study the probability distribution of various analysis methods the pile capacity derived from signal matching at BOR was used as reference value in place of SLT capacity because not

all pile load cases in the database possess an SLT capacity.. Figure 3-35(a) through Figure 3-35(f) illustrate the fitted normal and lognormal CDFs for the various static analysis methods; WEAP, signal matching, ENR, and FHWA-Gates formulas. The estimated parameters for the best fit lognormal distribution are tabulated in Table 3-11 through Table 3-16 for different pile analysis methods referenced to either measured capacity by SLT or signal matching.

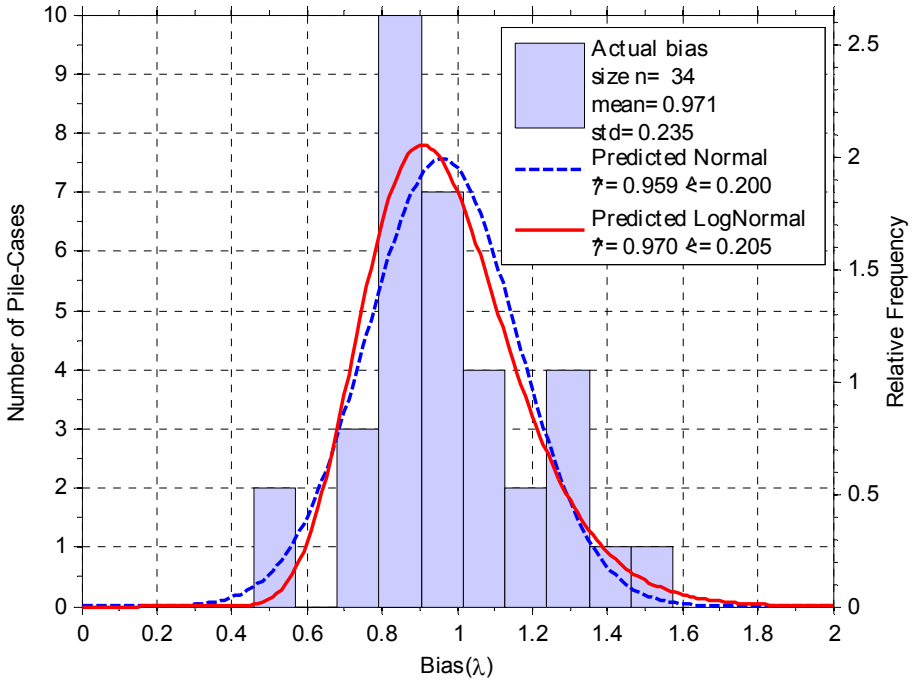

Figure 3-25 Histogram and Predicted Normal and Log-Normal PDFs of Resistance Bias Factors (SLT/Static Analysis-Reported) for PPC Piles.

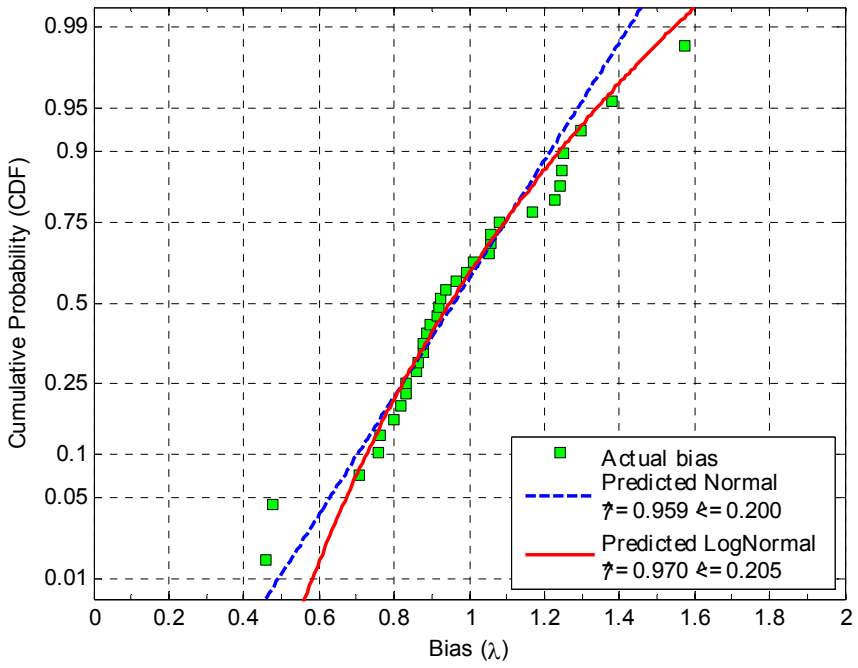

Figure 3-26 Fitted Normal and Log-Normal Cumulative Distribution Functions (CDFs) of Resistance Bias Factors (SLT/Static Analysis-Reported) for PPC Piles.

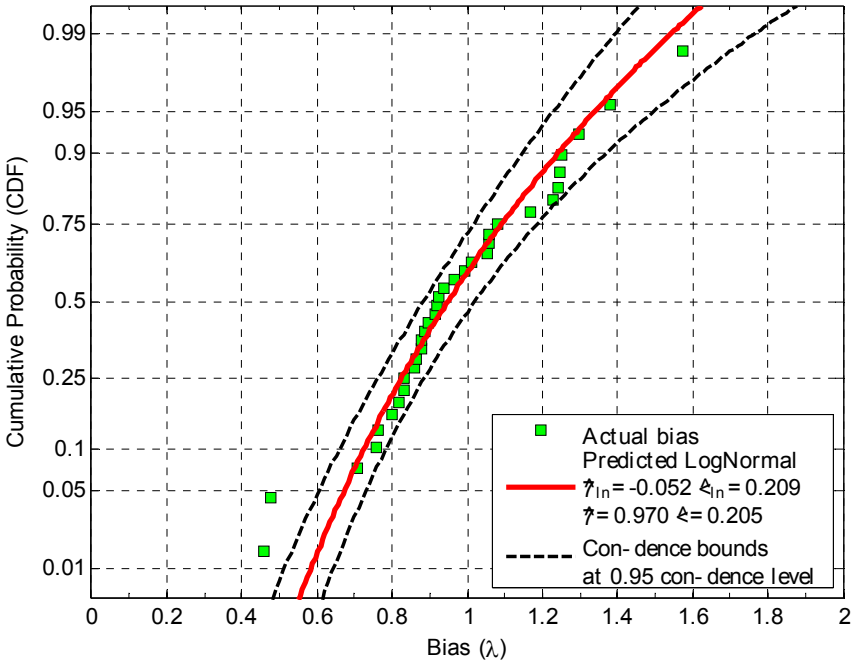

Figure 3-27 Confidence Bounds at 5 percent Significance Level for Fitted Log-Normal CDF of Resistance Bias Factors (SLT/Static Analysis-Reported) for PPC Piles.

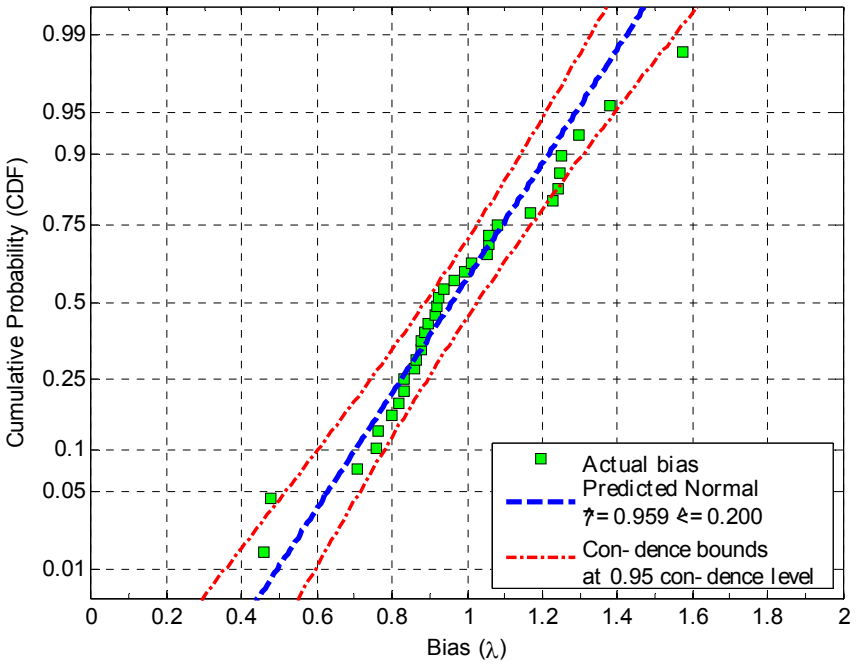

Figure 3-28 Confidence Bounds at 5 percent Significance Level for Fitted Normal CDF of Resistance Bias Factors (SLT/Static Analysis-Reported) for PPC Piles.

Table 3-10 Summary Statistics for Predicted Probability Distributions of the Resistance Bias (SLT/Reported Static*), and Goodness of fit test Results.

Prediction	Mean λ	COV	Mean Square Error	Covariance Matrix**
Normal	0.958952	0.208879	0.002042	$10^{-05}.\begin{pmatrix}2.46 & 1.67\\ 1.67 & 2.32\end{pmatrix}$
LogNormal	0.969902	0.211589	0.001016	$10^{-05}.\begin{pmatrix}1.25 & 7.46\\ 7.46 & 1.64\end{pmatrix}$

Summary of Goodness of Fit at 95.0 Percent Confidence Level					
Prediction	**Measure**	**Chi-square test**	**Kolmogorov-Smirnov test**	**Lilliefors test**	**Anderson-Darling test**
Normal	H	0	0	0	0
	P	0.16237	0.713583	0.282365	0.062913
	Statistic value	3.635759	0.115319	0.115945	0.712760
	Critical value	0.05	0.227455	0.149674	0.05
LogNormal	H	0	1	0	0
	P	0.351728	6E-31	0.2472	0.058534
	Statistic value	2.089794	0.992538	0.119074	0.725458
	Critical value	0.05	0.227455	0.149628	0.05

*Static pile capacity based on Alpha and Nordlund's methods as reported by the Louisiana DOT.

** Inverse of the Fisher's information matrix.

H: Hypothesis of the test, H_0: the null hypothesis for accepting the hypothesized distribution, and H_1: the alternate to reject the hypothesized distribution

P-value: Probability that corresponds to the event of observing a test statistic as the one actually observed.

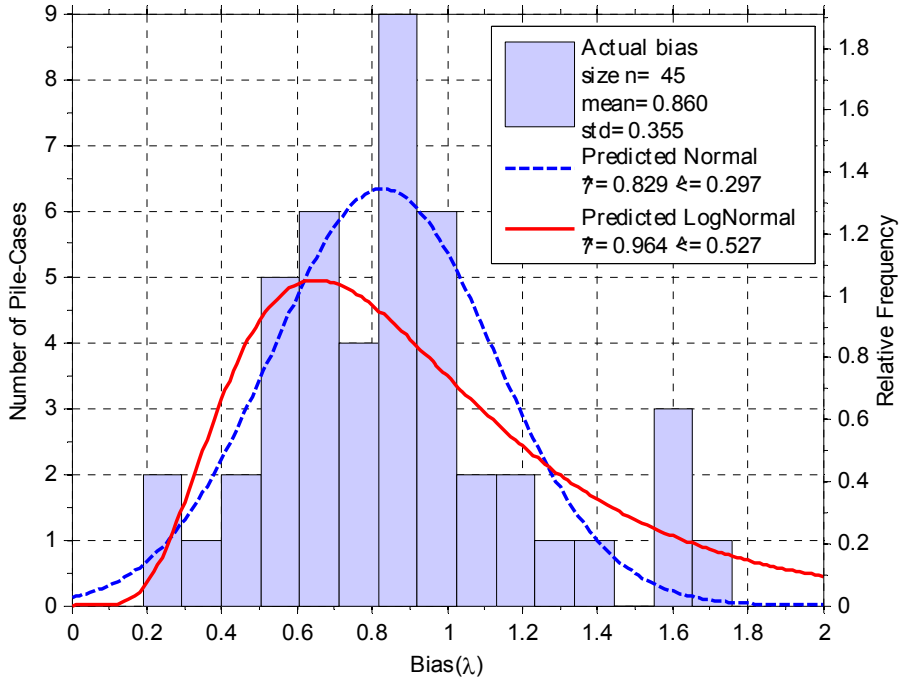

Figure 3-29 Histogram and Predicted Normal and Log-Normal PDFs of Resistance Bias Factors (SLT/Static Analysis-DRIVEN) for PPC Piles.

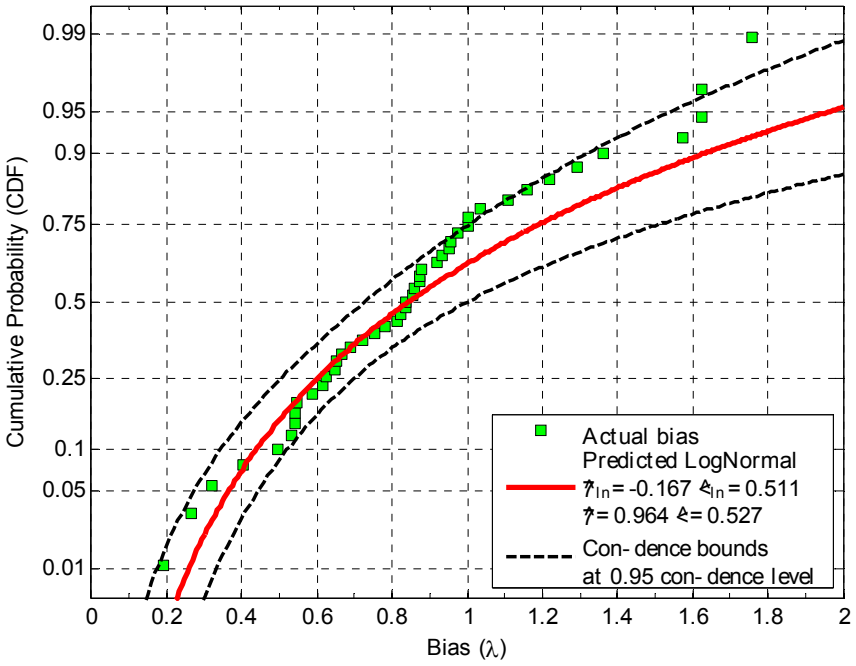

Figure 3-30 Confidence Bounds at 5 percent Significance Level for Fitted Log-Normal CDF of Resistance Bias Factors (SLT/Static Analysis-DRIVEN) for PPC Piles.

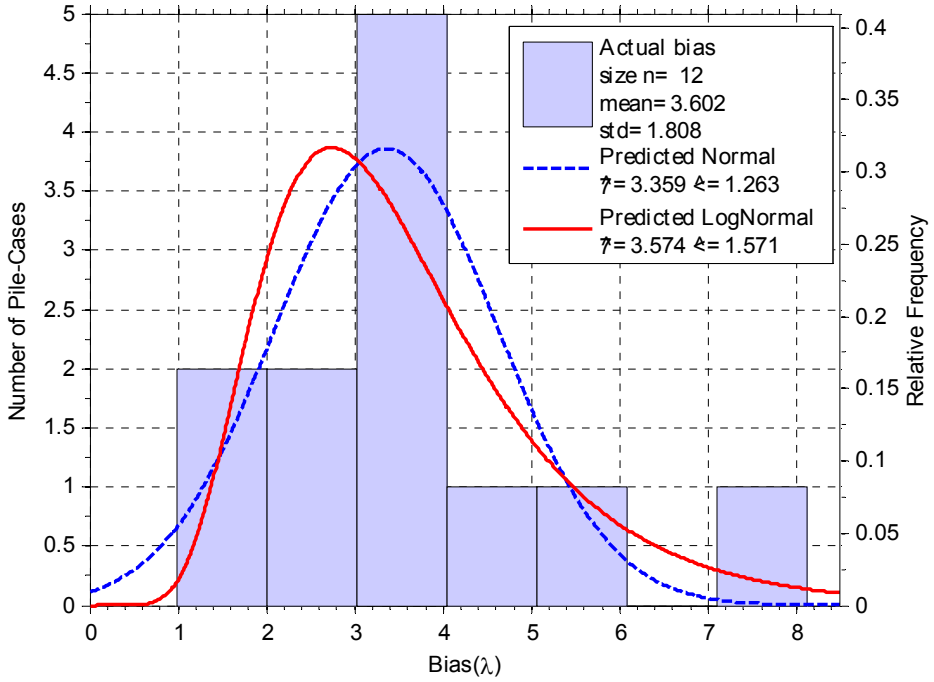

Figure 3-31 Histogram and Predicted Normal and Log-Normal PDFs of Resistance Bias Factors (SLT/Signal Matching at EOD) for PPC Piles.

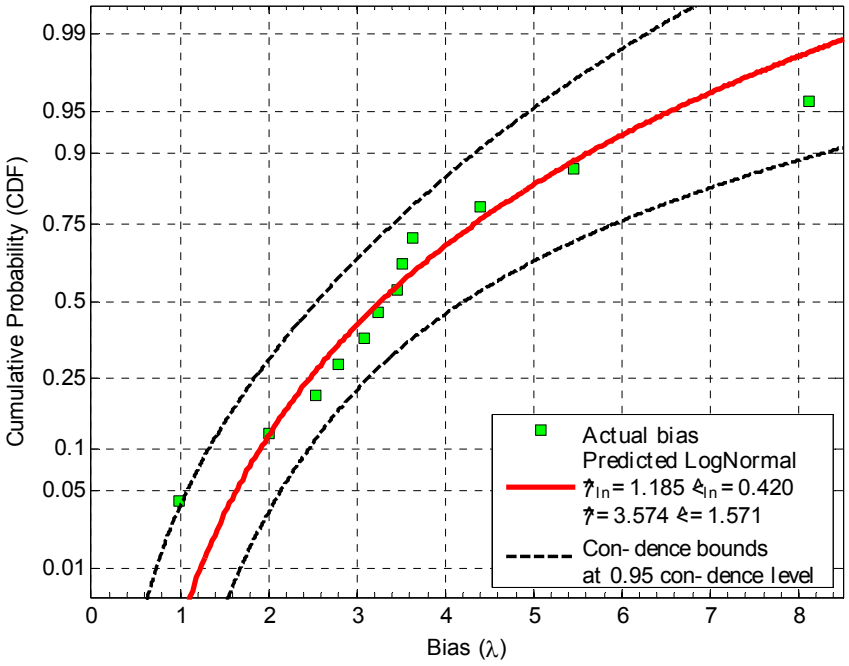

Figure 3-32 Confidence Bounds at 5 percent Significance Level for Fitted Log-Normal CDF of Resistance Bias Factors (SLT/Signal Matching at EOD) for PPC Piles.

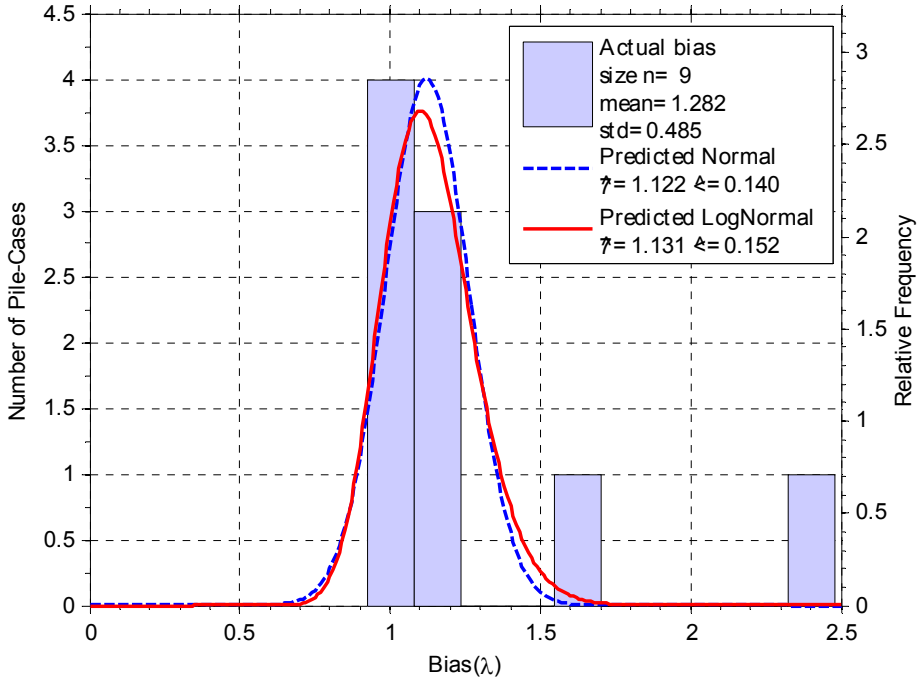

Figure 3-33 Histogram and Predicted Normal and Log-Normal PDFs of Resistance Bias Factors (SLT/Signal Matching at BOR) for PPC Piles.

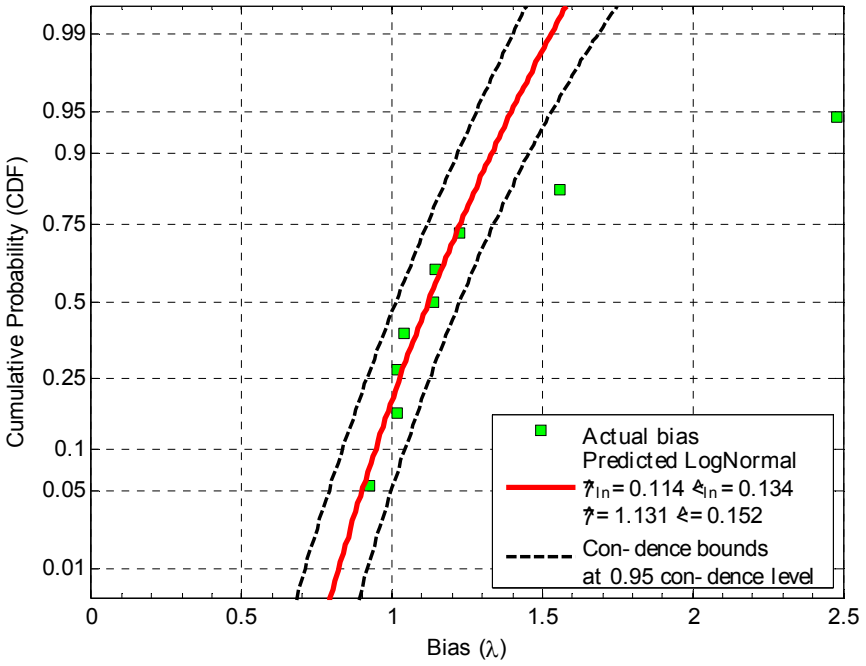

Figure 3-34 Confidence Bounds at 5 percent Significance Level for Fitted Log-Normal CDF of Resistance Bias Factors (SLT/Signal Matching at BOR) for PPC Piles.

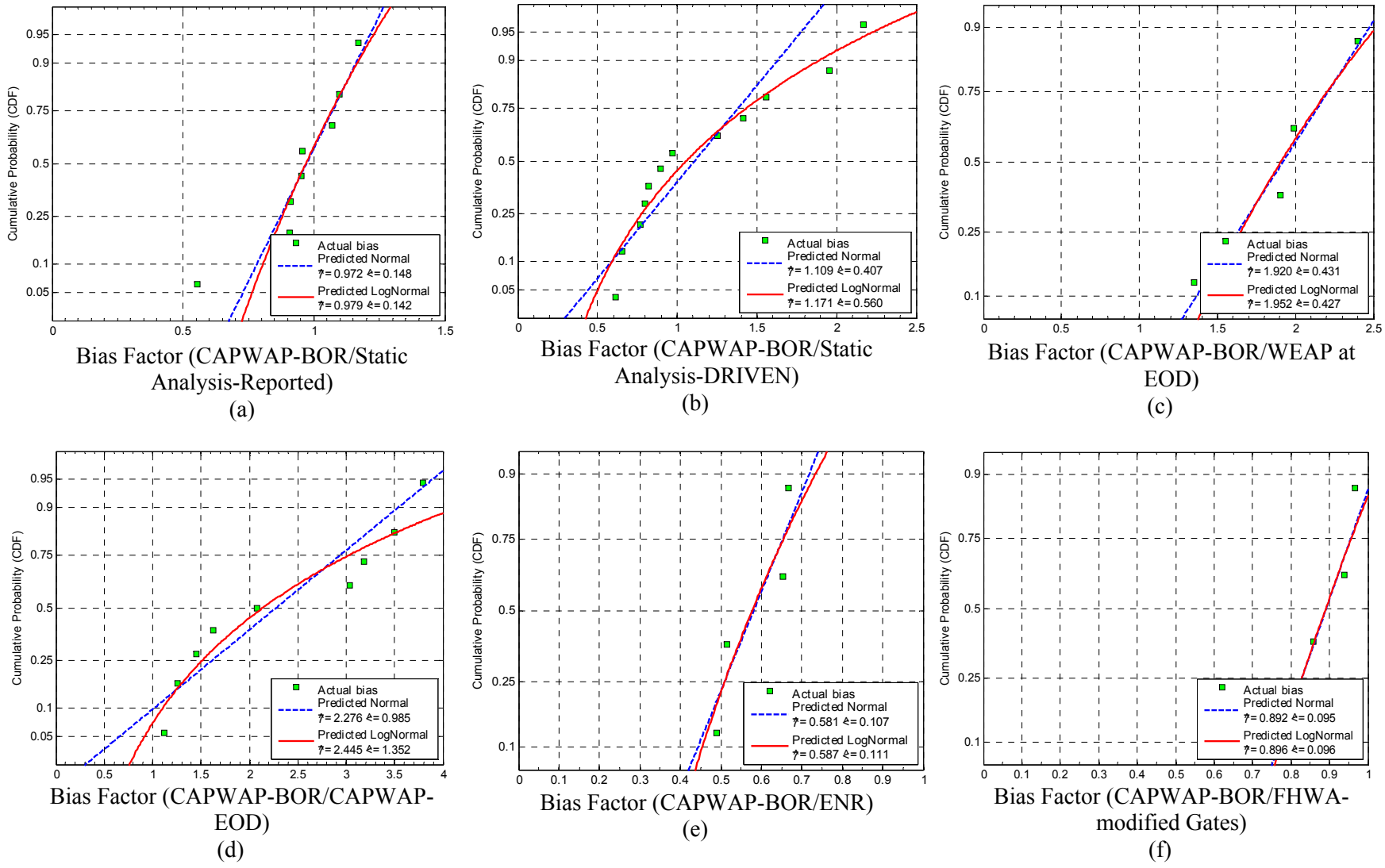

Figure 3-35 Fitted Normal and Log-Normal Cumulative Distribution Functions (CDFs) of Resistance Bias Factors (a) CAPWAP-BOR/Static Analysis-Reported, (b) CAPWAP-BOR/Static Analysis-DRIVEN, (c) CAPWAP-BOR/WEAP at EOD, (d) CAPWAP-BOR/CAPWAP-EOD, (e) CAPWAP-BOR/ENR, (f) CAPWAP-BOR/FHWA-modified Gates.

3.4.2 Computation of the LRFD Resistance Factors

3.4.2.1 Function Tolerance and Constraints

The calibration process of the LRFD resistance factor makes use of the predetermined distribution parameters, namely mean bias and its coefficient of variation. The relationship between the reliability index and resistance factor is plotted for reliability analysis of several methods of pile capacity prediction. The reliability analysis used four different approaches, the FOSM, improved FOSM, MCS, and FORM. A minimum number of 100,000 simulations were used for MCS. The FORM used constrained optimization, with a sequential quadratic programing (SQP) that used a Quasi-Newton line search of the solution. Exit flag for the optimization process was set to a maximum of 10^{-06} for both objective and performance functions.

3.4.2.2 Reliability based Efficiency Factor for Pile Analysis Method

A higher resistance factor can be achieved by reducing the coefficient of variation (COV) of a given pile analysis method. Reducing COV value can be accomplished by either decreasing the standard deviation (σ) or by increasing the mean bias (λ_R) of the method. While reducing the σ value would always improve the precision of the prediction method, increasing the λ_R could make prediction method underestimate the capacity of pile, thus compromising the economy of the structure. Having a higher resistance factor does not necessary imply an efficient pile analysis method. In order to effectively compare the reliability performance of different pile analysis methods an efficiency factor is introduced.

The design equation for an axial driven pile can be rewritten from Equation 2-1 by replacing factored loads with design capacity (P_{Design}) as follows:

$$P_{Design} = \phi R_n \qquad \text{Equation 3-8}$$

where ϕ is the resistance factor, and R_n is the nominal resistance of the pile. By defining the resistance bias factor (λ_R) as the ratio of measured (R_m) to predicted nominal resistance, Equation 3-8 can be re-written as:

$$P_{Design} = \left(\frac{\phi}{\lambda_R}\right) R_m \qquad \text{Equation 3-9}$$

The relationship presented in Equation 3-9 indicates that only a portion of the measured capacity is allowed for design to meet the required reliability level. The efficiency factor, ϕ/λ_R, can be obtained through the LRFD calibration process and can efficiently quantify the performance of the pile analysis method. A better pile analysis method would possess a higher efficiency factor, thus reducing the number of piles required to support the design load (Michael C McVay, Alvarez, Zhang, Perez, & Gibsen, 2002).

3.4.2.3 Preliminary Results of the Local LRFD Calibration

Calibration of resistance factors used the fitted lognormal CDF that was estimated based on the lower tail of the ECDF of the resistance bias. During the calibration process extreme values were searched for, identified, and reassessed before being included in the analysis to produce the required statistics. As a result of this process no outlier search was performed.

The calibration first considered the entire database without making any distinction between pile type and soil type. Using the statistics established in Section 3.4.1.2 for various pile analysis methods, resistance factors were determined using FOSM, Improved FOSM, FORM, and MCS methods. Figure 3-36 plots the relationship between resistance factor and reliability index for static analysis, and signal matching at EOD as well as at BOR. The advanced reliability methods (FORM, MCS) and the Improved FOSM produced virtually identical plots in Figure 3-36(b) through (d). The FOSM plot presented in Figure 3-36(a) underestimated the resistance factors by about 7 to 25 percent. For a complete understanding of the calibration results by soil

type to the reader is referred to the Appendix B, which contains additional plots that relate calibrated resistance factors to reliability indices. Specific values of the resistance factors that correspond to reliability indices of 2.33 and 3.00 were extracted from these graphs and are summarized in Table 3-11 through Table 3-16. To verify the assumption of the location of the design point, FORM was employed and the details of the optimization process were recorded. For all cases of the calibration, the design points were located in lower tail of the fitted distribution as suggested previously. Table 3-13 gives some of the examples of the design points that were computed using the FORM approach for a probability of failure of 1.0 percent. In the same Table 3-13 the number of performed iterations to arrive to the solution, stopping criteria of the optimization process, as well as the type of algorithm are reported. On average nine iterations are required for the optimization process to converge to the solution. This is because the first guess of the most probable point was set to the origin point in the reduced space, which corresponds to the mean in the original space.

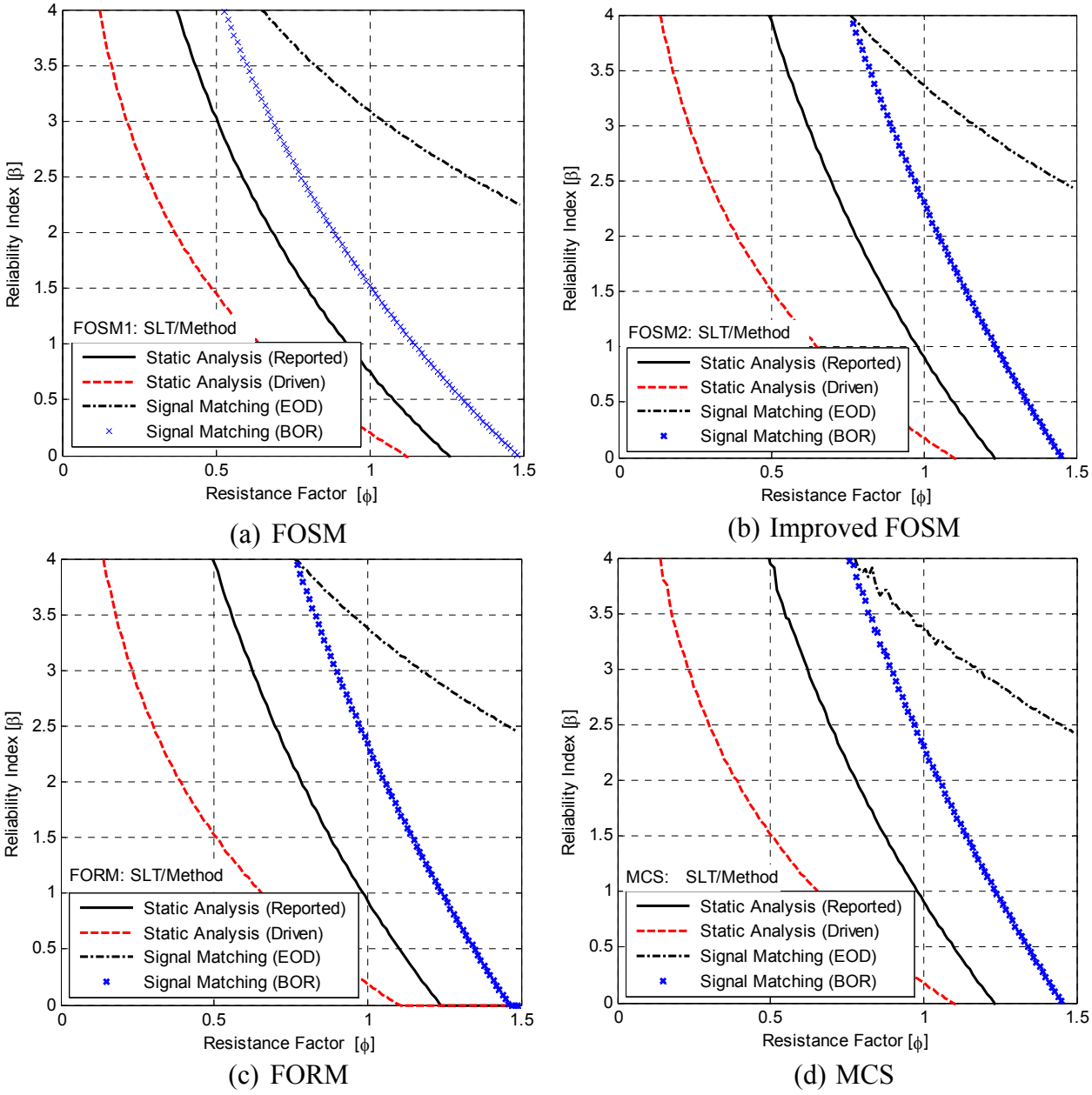

Figure 3-36 Resistance Factor versus Reliability Index for different Pile Analysis Methods based on (a) First Order Second Moment (FOSM), (b) Improved FOSM, (c) First Order Reliability Method (FORM), and (d) Monte Carlo Simulations (MCS) with Statistics presented in Table 3-11.

Table 3-11 Statistics for Calibration of Resistance Factors based on Reliability Theory with reference to Measured Capacity by Static Load Test.

Best fit lognormal distribution					Resistance Factors (ϕ)								Efficiency
Bias Factors (λ) = SLT/Analysis Method					β = 2.33				β = 3.00				Factor
	Method	N	Mean λ_R	COV	FOSM_1	FOSM_2	FORM	MCS	FOSM_1	FOSM_2	FORM	MCS	ϕ/λ_R
Static Load Test/	Static Analysis (Reported)	34	0.970	0.211	0.619	0.723	0.727	0.722	0.505	0.621	0.624	0.621	0.749
	Static Analysis (Driven)	45	0.964	0.546	0.306	0.327	0.329	0.327	0.211	0.231	0.233	0.230	0.383
	Signal Matching (EOD)	12	3.574	0.439	1.434	1.559	1.567	1.558	1.043	1.169	1.175	1.174	0.435
	Signal Matching (BOR)	9	1.131	0.134	0.813	0.996	1.001	0.996	0.684	0.894	0.898	0.894	0.781

Table 3-12 Statistics for Calibration of Resistance Factors based on Reliability Theory with reference to Measured Capacity by Signal Matching at the Beginning of Restrike.

Best fit lognormal distribution					Resistance Factors (ϕ)								Efficiency
Bias Factors (λ) = Signal Matching at BOR/ Method					β = 2.33				β = 3.00				Factor
	Method	N	Mean λ_R	COV	FOSM_1	FOSM_2	FORM	MCS	FOSM_1	FOSM_2	FORM	MCS	ϕ/λ_R
Signal Matching at BOR/	Static Analysis (Reported)	8	0.979	0.145	0.693	0.843	0.848	0.843	0.581	0.752	0.756	0.749	0.872
	Static Analysis (Driven)	12	1.171	0.178	0.789	0.940	0.945	0.939	0.653	0.822	0.827	0.819	0.817
	Signal Matching (EOD)	9	2.445	0.553	0.765	0.817	0.821	0.820	0.525	0.575	0.578	0.575	0.342
	WEAP- EOD	4	1.952	0.219	1.228	1.429	1.437	1.428	0.998	1.221	1.227	1.222	0.752
	ENR	4	0.587	0.188	0.389	0.461	0.463	0.461	0.321	0.401	0.403	0.401	0.798
	FHWA-Gates	4	0.896	0.107	0.666	0.832	0.836	0.831	0.565	0.757	0.760	0.755	0.941

Table 3-13 Design Points Identified by FORM for a Reliability Index of 2.33 Corresponding to a Probability of Failure of 1.0 Percent (All Pile Cases Combined).

SLT/ Prediction Method	λ^*_R	Number of Iterations	Predicted Change in the Objective Function	Maximum Constraint Violation	Δβ with Closest calculated point	Algorithm used
Static Analysis (Reported)	0.610	9	1.727e-11	-2.5536e-12	1.771e-02	medium-scale: SQP, Quasi-Newton, line-search
Static Analysis (Driven)	0.263	8	2.098e-07	-4.599e-08	5.576e-03	
Signal Matching (EOD)	1.261	8	1.684e-07	-7.237e-08	4.103e-03	
Signal Matching (BOR)	0.873	9	5.899e-10	1.455e-12	-8.324e-03	
CAPWAP at BOR/ Prediction Method						
Static Analysis (Reported)	0.732	9	2.018e-10	-5.646e-12	1.738e-02	
Static Analysis (Driven)	0.804	9	1.579e-10	-5.239e-12	-2.522e-02	
Signal Matching (EOD)	0.755	8	2.969e-07	-4.577e-08	-3.124e-03	
WEAP- EOD	1.127	9	1.415e-11	-2.013e-12	9.280e-03	
ENR	0.395	9	1.069e-10	-4.704e-13	-3.345e-02	
FHWA-Gates	0.741	9	8.583e-10	-4.686e-13	3.445e-02	

λ^*_R = design point, solution to the performance function;
SQP = Sequential Quadratic Programming

Table 3-14 Statistics for Calibration of Resistance Factors based on Reliability Theory for Driven Piles in Mixed Soils.

	Best fit lognormal distribution				Resistance Factors (ϕ)								Efficiency
	Bias Factors (λ) = Static Load Test/ Method				β = 2.33				β = 3.00				Factor
	Method	N	Mean λ_R	COV	FOSM_1	FOSM_2	FORM	MCS	FOSM_1	FOSM_2	FORM	MCS	ϕ/λ_R
Mixed Soils	Static Analysis (Reported)	8	0.943	0.195	0.618	0.729	0.733	0.729	0.508	0.631	0.635	0.631	0.778
	Static Analysis (Driven)	11	0.943	0.491	0.338	0.364	0.366	0.364	0.240	0.265	0.267	0.265	0.392
	Signal Matching (EOD)	2	2.943	0.557	0.913	0.975	0.980	0.974	0.625	0.684	0.688	0.683	0.338

Table 3-15 Statistics for Calibration of Resistance Factors based on Reliability Theory for Driven Piles in Cohesive Soils.

Best fit lognormal distribution					Resistance Factors (ϕ)								Efficiency
Bias Factors (λ) = Static Load Test/ Method					β = 2.33				β = 3.00				Factor
	Method	N	Mean λ_R	COV	FOSM_1	FOSM_2	FORM	MCS	FOSM_1	FOSM_2	FORM	MCS	ϕ/λ_R
Cohesive Soils	Static Analysis (Reported)	22	1.028	0.221	0.644	0.750	0.754	0.749	0.523	0.640	0.643	0.639	0.738
	Static Analysis (Driven)	28	0.918	0.326	0.469	0.524	0.527	0.524	0.362	0.420	0.422	0.420	0.576
	Signal Matching (EOD)	7	3.313	0.228	2.050	2.377	2.389	2.374	1.660	2.019	2.030	2.010	0.765
	Signal Matching (BOR)	7	1.106	0.147	0.782	0.950	0.955	0.949	0.655	0.846	0.850	0.846	0.763
Bias Factors (λ) = Signal Matching at BOR/ Method					β = 2.33				β = 3.00				Efficiency
	Method	N	Mean λ_R	COV	FOSM_1	FOSM_2	FORM	MCS	FOSM_1	FOSM_2	FORM	MCS	ϕ/λ_R
Cohesive Soils	Static Analysis (Reported)	7	0.983	0.167	0.674	0.808	0.812	0.808	0.560	0.711	0.715	0.710	0.853
	Static Analysis (Driven)	7	0.960	0.353	0.463	0.514	0.516	0.514	0.353	0.405	0.407	0.405	0.545
	Signal Matching (EOD)	3	3.318	0.414	1.405	1.536	1.544	1.535	1.036	1.168	1.174	1.168	0.462

Table 3-16 Statistics for Calibration of Resistance Factors based on Reliability Theory for Driven Piles in Cohesionless Soils.

Best fit lognormal distribution					Resistance Factors (ϕ)								Efficiency
Bias Factors (λ) = Signal Matching at BOR/ Method					β = 2.33				β = 3.00				Factor
	Method	N	Mean λ_R	COV	FOSM_1	FOSM_2	FORM	MCS	FOSM_1	FOSM_2	FORM	MCS	ϕ/λ_R
Sands	Static Analysis (Driven)	4	1.758	0.445	0.696	0.756	0.760	0.756	0.505	0.564	0.568	0.564	0.471
	WEAP- EOD	4	1.952	0.219	1.227	1.429	1.437	1.428	0.998	1.221	1.227	1.221	0.752
	Signal Matching (EOD)	4	1.375	0.184	0.918	1.089	1.094	1.088	0.757	0.949	0.954	0.951	0.803
	ENR	4	0.587	0.188	0.389	0.461	0.463	0.461	0.321	0.401	0.403	0.400	0.798
	FHWA-Gates	4	0.896	0.108	0.665	0.831	0.835	0.830	0.564	0.756	0.759	0.755	0.940
Bias Factors (λ) = Static Load Test/ Method					β = 2.33				β = 3.00				Efficiency
	Method	N	Mean λ_R	COV	FOSM_1	FOSM_2	FORM	MCS	FOSM_1	FOSM_2	FORM	MCS	ϕ/λ_R
Sands	Static Analysis (Reported)	4	0.799	0.295	0.435	0.490	0.493	0.490	0.341	0.400	0.402	0.400	0.652
	Static Analysis (Driven)	6	0.518	0.718	0.114	0.120	0.120	0.120	0.072	0.078	0.078	0.078	0.254

3.4.2.4 Comparison among Various Pile Analysis Methods based on Calibration Results

Based on efficiency factors and other calibration statistics presented in Table 3-11, signal matching at 14 day restrike (BOR) performed better than all other methods with an efficiency factor of about 78 percent. This relatively good efficiency factor is attributed to the good accuracy of the method that is explained by an average resistance bias factor of 1.282 and a good precision corresponding to a coefficient of variation of 0.134. This average mean bias of the resistance indicates that at the end of a 14 day period after driving about 78 percent of the long term capacity is obtained. The exactness of the signal matching at the beginning of restrike is also verified by a resistance factor very close to unity (1.001 for $\beta = 2.33$, FORM) for a probability of failure equal to 1.0 percent.

At the second position in the ranking comes the static analysis method (as interpreted by the state of Louisiana) with an efficiency factor of 0.749, average mean bias of the resistance equal to about 0.971, and a COV of the bias equal to 0.211. This static analysis method with its corresponding soil interpretation allows only about 75 percent of long term pile capacity to be used for design to meet a reliability index of 2.33.

Signal matching at EOD comes in third rank with an efficiency factor of 0.435 and a resistance factor of $\phi = 1.567$ ($\beta=2.33$, FORM). This very high resistance factor accompanied by a low efficiency factor. The high resistance factor is the result of the method significantly under predicting long term pile capacity. Resistance factors greater than unity take into consideration soil disturbance caused by pile driving and the soil setup effect that were otherwise ignored by the measurements at EOD. The factor greater than unity for EOD condition suggests that a pile could be accepted even if its measured capacity at EOD is less than the required ultimate bearing. Although this high resistance factor associated with PDA/CAPWAP at EOD sets the

acceptance value to about 64 percent of the required ultimate capacity for redundant pile foundation, the signal matching at EOD allows only about 44 percent of the long term pile capacity to be utilized for design purpose as indicated by the efficiency factor. The average bias of the resistance indicates that a setup factor of about 3.6 is expected and only about 28 percent of the capacity is mobilized at the EOD. In such context, dynamic resistance factor for dynamic testing at the EOD becomes similar to the effective setup factor, and its obtained value of ϕ= 1.567 is consistent with the values of recommended setup factors established by Likins et al. (1996), reported by Rausche et al. (2004), and adopted by Table 9-20 of the FHWA manual on design and construction of driven pile foundations (Hannigan et al., 2006),. The values are reproduced in Table 3-17 below.

Table 3-17 Recommended Soil Setup Factors as Reported by Hannigan et al. (2006).

Predominant Soil Type along Pile Shaft	Range in Soil Setup Factor	Recommended Soil Setup Factor	Number of Sites and (% of Database)	
Clay	1.2 – 5.5	2.0	7	(15%)
Silt-Clay	1.0 – 2.0	1.0	10	(22%)
Silt	1.5 – 5.0	1.5	2	(4%)
Sand-Clay	1.0 – 6.0	1.5	13	(28%)
Sand-Silt	1.2 – 2.0	1.2	8	(18%)
Fine Sand	1.2 – 2.0	1.2	2	(4%)
Sand	0.8 – 2.0	1.0	3	(7%)
Sand-Gravel	1.2 – 2.0	1.0	1	(2%)

Based on available data, static analysis using the program DRIVEN shows a poor performance, with an efficiency factor of 0.383 and a resistance factor of ϕ= 0.329 when it is referenced to static load test. Note that the performance of the static analysis method using the program Driven is greatly affected by the type of correlations used to interpret the soil properties.

The presumption is that poor correlations used to generate soil strength properties will produce poor and erratic predictions of pile capacity.

When calibration of resistance factors are referenced to CAPWAP at BOR (Table 3-12 and Appendix B.1), the FHWA-Gates formula performs best among driving formulas. WEAP at EOD conditions produces acceptable results for drivability analysis, and its resistance factor accounts for soil setup. For static analysis method, the performance of the analysis depends on the quality of the utilized correlations to estimate the soil strength form the measured soil properties.

3.4.2.5 Preliminary Resistance Factors versus Bridge Specifications

The resistance factors established in Table 3-15 through Table 3-16 were calibrated using reliability theory. For driven piles in cohesive soils, the resistance factor (ϕ_{stat}) associated with static analysis method, using α-Method (Tomlinson, 1971) in the program Driven, is equal to 0.527 (β=2.33, FORM). This resistance factor is greater than ϕ_{stat} of 0.35 presented by AASHTO LRFD specifications (2012). These specifications also recommended a maximum resistance factor (ϕ_{dyn}) of 0.75 for signal matching regardless of soil type. However, based on available information in database, the current analysis shows that ϕ_{dyn} of 0.955 (β=2.33, FORM, Table 3-15) can be utilized on piles driven in cohesive soils if a 14 day restrike is performed.

For piles in Mixed Soils (Table 3-14), the calibration shows that a resistance factor ϕ_{stat} of 0.366 would be required to design a pile group using static analysis method. For signal matching method at EOD, ϕ_{dyn}=0.980 is required for piles in mixed soils at a probability of failure of 1.0%.

The calibration of resistance factor in cohesionless soils (Table 3-16) was performed for various pile analysis methods. For the static analysis method in sands the Nordlund/Thurman method was employed to predict pile capacity. The calibration yielded a resistance factor of

0.493 (FORM) for reported static capacity and 0.120 with the DRIVEN program at a reliability index of 2.33. The resistance factor of 0.120 is significantly lower than the value of 0.45 recommended by the AASHTO LRFD specifications. Note that only six pile case studies were available in current database, which may not be good representation of the probability distribution for the method. Moreover, the results of the calibrations depend upon the correlations used for determining soil strength parameters.

For driving formulas in sands, due to lack of sufficient SLT results in the database, pile capacity interpreted from signal matching at BOR was used for defining the bias factor of the resistance. Only 4 pile cases were available. Based on calibration statistics the FHWA-modified Gates performed better than ENR formula with a resistance factor of 0.835 (β=2.33, FORM). Although the reference capacity for calibration could have been underestimated, the resulting resistance factor gives a better idea on how local calibration can improve the resistance factor, of only 0.40 recommended by AASHTO LRFD specifications. Likewise the resistance factor corresponding to signal matching at EOD was found to be 1.094 (β=2.33, FORM), which was better than the overall value of 0.75 recommended by the LRFD specifications. For this signal matching analysis at EOD in sands, about 80% of the 14 day restrike capacity is allowed for design, and on average about 73 percent of the long term capacity is mobilized at the EOD.

Based on the load tests available in the database, the difference between resistance factors for redundant and non-redundant piles ranges between 7 and 35 percent. This which is right in line with the AASHTO LRFD recommendation to reduce the resistance factor for redundant foundation by 20 percent to obtain the resistance factor for a non-redundant pile foundation. Moreover, if static load test is used to design piles driven into a well characterized site, a

resistance factor could be increased to 0.853 (Table 3-4). This is in line with AASHTO LRFD Bridge Design specifications, which provide the maximum value of 0.80.

The preliminary calibrated resistance factors were also compared to the results obtained in NCHRP report 507 as summarized in Table 3-18, For α-Tomlinson method (Tomlinson, 1971) on piles driven into clay soils, local calibration allowed a reduction of the level of uncertainties in data. The recorded gain of about 40% in efficiency factor is accompanied by a significant increase in resistance factor by about 45%. For sands and mixed soils, the size of data is not large enough to arrive at a final conclusion for the general performance of the static analysis method. When all soil types and pile types are considered, signal matching, WEAP, and FHWA modified Gates show similar trends in results that show an increase in efficiency factor accompanied by an increase in resistance factor.

Table 3-18 Comparison of Statistics from current Study and NCHRP report 507 for Calibration of Resistance Factors (based on FORM).

		Bias Factors (λ) = SLT/Analysis Method			Resistance Factors		Efficiency
					β = 2.33	β = 3.00	Factor
Method	**Source**	**N**	**Mean λ_R**	**COV**	**FORM**	**FORM**	**ϕ/λ_R**
α-Tomlinson (Clay) Concrete Piles	Reported	22	1.028	0.221	0.754	0.643	0.738
	DRIVEN	28	0.918	0.326	0.527	0.422	0.576
	NCHRP507	18	0.870	0.480	0.360	0.260	0.410
Nordlund (Sand) Concrete Piles	Reported	4	0.799	0.295	0.493	0.402	0.652
	DRIVEN	6	0.518	0.718	0.120	0.078	0.254
	NCHRP507	36	1.020	0.480	0.420	0.310	0.420
α-Tomlinson / Nordlund (Mixed Soils) Concrete Piles	Reported	8	0.943	0.195	0.733	0.635	0.778
	DRIVEN	11	0.943	0.491	0.366	0.267	0.392
	NCHRP507	33	0.960	0.490	0.390	0.290	0.410
CAPWAP-EOD	Study	12	3.574	0.439	1.567	1.175	0.435
	NCHRP507	125	1.626	0.490	0.640	0.460	0.400
CAPWAP-BOR	Study	9	1.131	0.134	1.001	0.898	0.781
	NCHRP507	162	1.158	0.339	0.650	0.510	0.560
WEAP-EOD	Study*	4	1.952	0.219	1.437	1.227	0.751
	NCHRP507	99	1.656	0.724	0.390	0.250	0.240
ENR	Study*	4	0.587	0.188	0.463	0.403	0.843
	NCHRP507	384	1.602	0.910	0.260	0.150	0.160
FHWA modified Gates	Study*	4	0.896	0.107	0.836	0.760	0.941
	NCHRP507	384	0.940	0.502	0.360	0.260	0.380

* Bias Factors (λ) = Signal Matching at BOR/Analysis Method from **Table 3-12**

The benefits of local calibration are more explicit when compared to the current AHTD specifications. For instance, if termination criteria is determined based on ENR formula, as recommended by AHTD, it would require the pile to be driven until it reaches about2.2 the required safe bearing value (ϕ=0.463, β=2.33, Table 3-12). This requirement offers enormous saving as opposed to value of ϕ=0.1 proposed by AASHTO LRFD, or ϕ=0.228 as suggested by NCHRP report 507. As a result of this local calibration, the FHWA modified Gates formula is recommended for it only requires about 20% more than the required safe bearing to terminate piling process.

For the WEAP approach, AHTD specifications require a design bearing capacity to be at most equal to 0.364 times the calculated ultimate bearing capacity. This multiplication factor is close to the resistance factor of 0.390 (NCHRP Report 507) and the 0.40 recommended by the 4th

Edition of the AASHTO LRFD (2007) at EOD only, but different from ϕ=0.50 provided by the 6th Edition of the AASHTO LRFD (2012) when the performance of hammer is confirmed in field. Current results of calibration show that a pile at EOD could be designed or accepted with a resistance factor of about 1.437 (Table 3-12). This resistance factor already incorporates soil setup because it was calibrated based upon pile capacity at BOR. This resistance factor, greater than unit, suggests that a pile could be designed or accepted for EOD capacity lesser than targeted bearing within acceptable reliability limits.

For dynamic testing with signal matching, AHTD specifications require a design bearing capacity to be at most equal to 0.40 times the ultimate bearing capacity as determined by dynamic testing. This multiplication factor is too conservative when it is compared to the values of ϕ=0.65 and 0.75 recommended by AASHTO LRFD. Preliminary calibration indicates that a resistance factor equal to about a unity could be used when dynamic testing is used to establish driving criteria and to perform quality control at BOR conditions. At EOD conditions a resistance factor of 1.567 could be used to account for soil setup. Although the EOD resistance factor is 57 percent more than the BOR, the BOR allocates about 88 percent of the long term capacity to design while EOD resistance factor allows only about 44 percent. This means that if dynamic testing at restrike conditions is properly planned, savings could be assured by optimizing pile design. However, the anticipated savings should be compared with construction schedule. If schedule is too tight to wait for soil-setup confirmation at restrike, dynamic testing at EOD could be used to verify the capacity despite its under-prediction behavior.

3.5 Preliminary Conclusions and Recommendations

1. In general, when local calibration of resistance factors is performed according to soil type, the level of uncertainties decreases while resistance factors and their corresponding efficiency factors increase.

2. The calibrated resistance factor for dynamic testing with signal matching at EOD considers soil setup.
3. The dynamic testing at 14 day restrike performs the best because it reflects long term capacity of the pile, and it can help detect soil setup/relaxation at the time of restrike.
4. The values provided by AASHTO LRFD specifications and NCHRP 507 for WEAP are based upon default input values of the hammer and dynamic parameters of the soil. A more accurate, reliable, and cost effective design could be achieved by establishing dynamic properties of the soil based on the results from signal matching at EOD and BOR.
5. The performance study of the driving formulas indicated that they significantly overestimate the EOD capacity, and they better correlate with BOR capacity. Because they are only employed at EOD conditions to predict long term capacity, a supplementary verification of the pile capacity by dynamic testing at BOR is recommended.
6. Resistance factors established for static analysis in non-cohesive soils correspond only to the Nordlund/Thurman (Nordlund, 1963; Thurman, 1964) approach using the program DRIVEN. Likewise, the calibrated resistance factors for static analysis in cohesive soils correspond only to α-Tomlinson's method, where undrained cohesion was derived from SPT values using the correlations from Terzaghi and Peck (1961). Therefore, any change in static analysis method or soil interpretation procedure would require a new calibration.
7. Resistance factors calibrated against SLT are all for PPC piles mostly driven in clays found in south Louisiana. The majority of sites encountered in the state of Missouri and Arkansas have stiff cohesive soils and sandy soils; and pile load test data in these sites do not contain any SLT results. Therefore, a validation of calibration results is highly recommended by conducting full scale pile load testing program.

Chapter 4 Updating Resistance Factors Based on Bayesian Theory

4.1 Prior, Likelihood, and Posterior Distributions

The prior distribution of the mean bias of pile resistance for a specific capacity prediction method is estimated from the established pile load test database. Such a distribution is assumed to be lognormal and it is empirically established by fitting a lognormal density function to the ratio of the measured and predicted resistances. When new pile load test data arrives sequentially, the likelihood distribution is constructed. That new piece of information is used to update the prior information to its posterior distribution. Subsequently, if there is a new incoming observation, the current knowledge becomes prior and the updating process becomes recursive. This process of coupling new and existing information uses Bayesian updating because any incoming information has more value than just feeding a new entry in to the database.

As explained in Section 2.1.2.5, a Bayesian update requires that the newly collected set of data come from a population with a known variance. Frequently, this variance is not known and one has to infer its value from newly observed information. Zhang and Tang (2002) suggested that the best estimate is to assume the standard deviation to be proportional to the mean pile capacity, which would mean to assume a constant mean value of the coefficient of variation (COV) equal to the mean value of COV of the within-site variability.

4.2 Effects of the within-site Variability on the Updated Results using Simulations

The problem of finding the updated resistance factor involves determining the posterior distribution of the pile capacity based on both prior and additional data. The results of applying the Bayesian updating technique to this problem are shown in Figure 4-1 through Figure 4-4.

To study the effects of the assumed variance of the likelihood on the updated resistance factors, the existing statistics of the static analysis method ($\lambda_R = 0.964$, COV = 0.546 in Table

3-11) are taken as prior statistics. New pile dataset for the likelihood is simulated by generating 60 log-normally distributed random resistances whose average mean bias is equal to 1.00 and COV of 0.35, 0.25, and 0.15 for high, medium and low site variability, respectively. By applying Bayes' rule to each data point of the simulated dataset, the updated statistics are determined. The updating process is continued by considering the posterior as the prior for the next sample value. The results of the updating process are presented in Figure 4-1.

As illustrated in Figure 4-1, when the standard deviation of the simulated test sample is utilized in lieu of the assumed value for the likelihood function, the updated resistance factor becomes steady beyond 30 tests. The same effect is observed for the efficiency factor defined as ϕ/λ. The effect of the first prior mean on the updated mean of the capacity ratio diminishes significantly after about 15 load tests. The calculations of updated statistics show that the final posterior distribution remains the same, regardless of the order or grouping of the data values. Nonetheless, based on the results from several simulations that were run in a similar fashion, the updated resistance factor has a random pattern when the number of simulated load tests is less than 10 (Figure 4-1). Thus, if the dataset comes from a population with unknown variance, the first collected data will likely have different posteriors. But as more data are collected and combined with the existing data, their posteriors will tend to converge.

It is believed that the correct characteristics of the pile population could be determined if a large sample of load tests is collected. However, in most cases, a very limited number of load tests is usually specified on the job site to accept the entire population of production pile. In practice, as rule of thumb, if there is not enough load test data available, the COV value of the test outcome can be set equal to the COV of the within-site variability where the load tests were conducted. As expected, the increase in the within-site variability causes both the updated mean

and the COV value of the bias of the capacity to increase, while the updated resistance factor decreases with an increase in within-site variability.

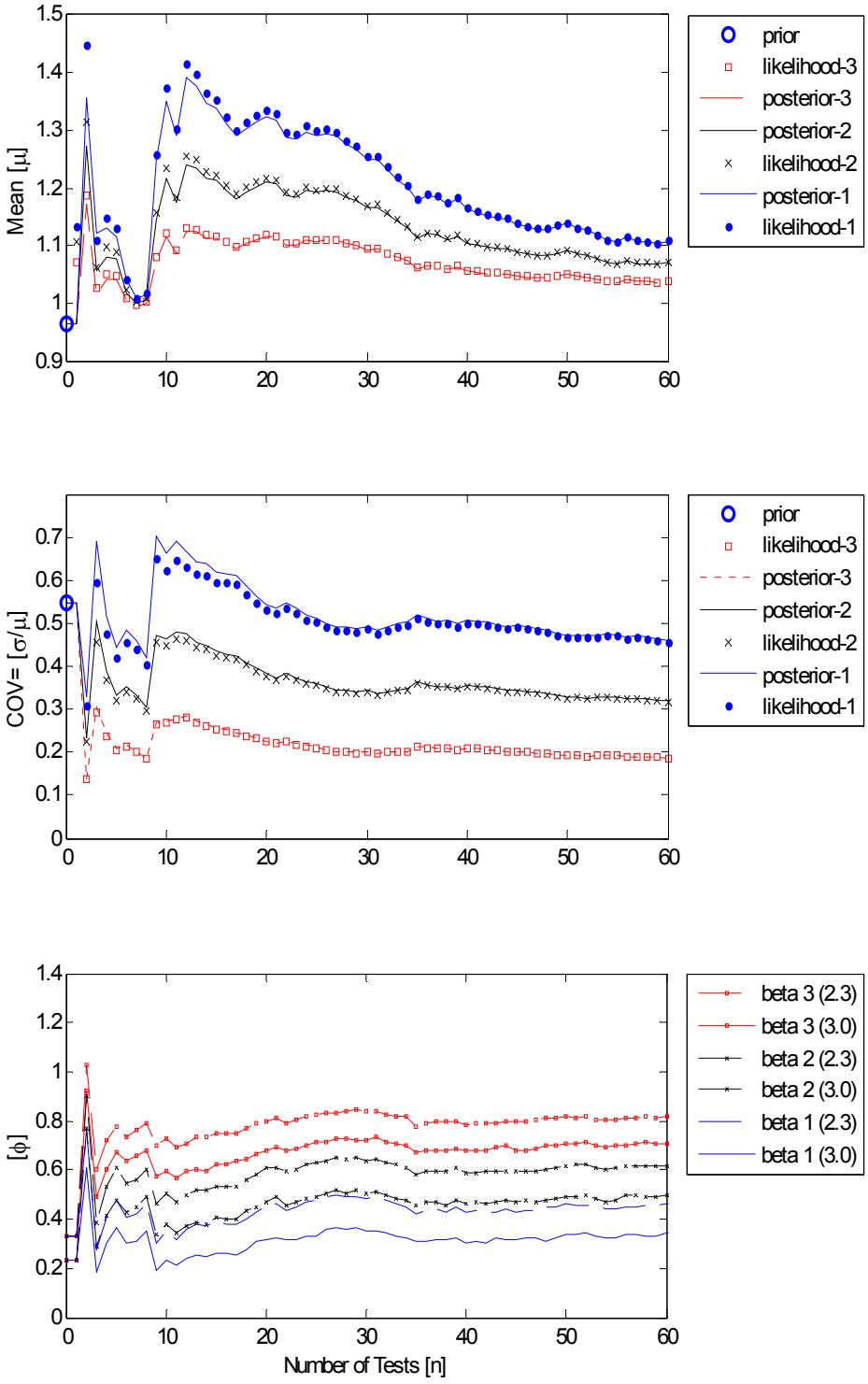

Figure 4-1 Mean Bias, Coefficient of Variation of the Bias, and Resistance Factors as function of Number of Load Tests. Variance of the likelihood is estimated from new load test dataset simulated from lognormal random numbers with mean of 1.00 and COV corresponding to high (1), medium (2), and low (3) site variability. Resistance Factors are calculated using Monte Carlo Simulations.

To further investigate the effects of the Bayesian updating on the posterior mean and updated resistance factors, it is assumed that early load test data is produced sequentially with a mean ratio of the resistance of 1.00 and a coefficient of variation of 0.25 corresponding to the average within-site variability. To show the effect of a greater amount of data, 10 incoming load tests are considered. Figure 4-2 shows the effects of ten (10) additional load tests on the updated probability density distribution (PDF). The plotted PDF of the posterior has shifted away from the prior and closer to the data.

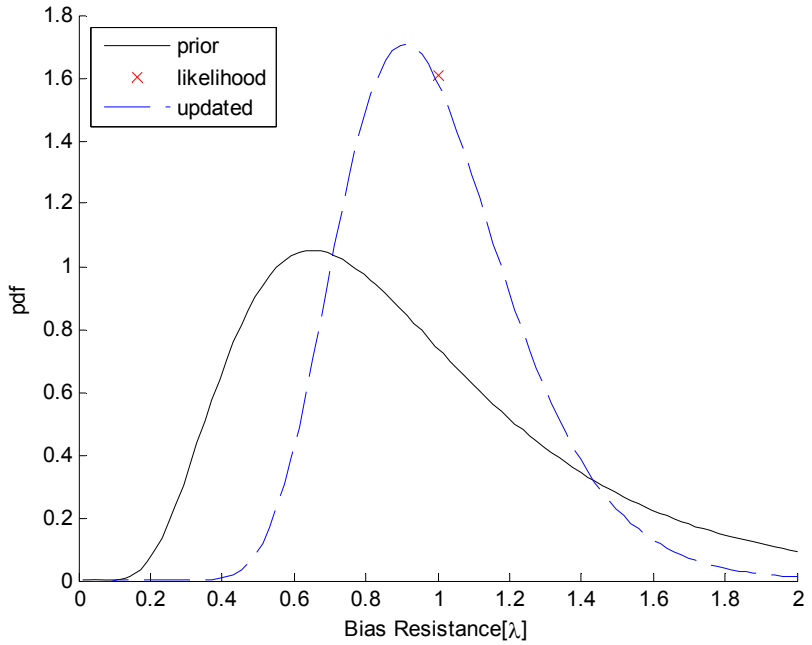

Figure 4-2 Prior and Updated Probability Density Functions associated with the Static Analysis by Driven when ten load tests are performed.

Table 4-1 lists the prior statistics for zeroth updating and the values characterizing the posterior at the end of 10th load test. Figure 4-3 plots the curves for the prior and updated resistance factor with respect to the reliability index, where each curve corresponds to one of the posterior distributions. Curves that are based on more data are rendered in dotted lines from left to right. Figure 4-4 presents the updated mean and COV of the capacity ratio with respect to the number of load test collected, when the COV of the load test sample is assumed constant.

Table 4-1 Statistics of the Prior and Posterior for the Pile Resistance and their corresponding Resistance Factors.

	Best fit lognormal distribution Bias Factors (λ) = SLT/Analysis Method				Resistance Factors (ϕ)		Efficiency Factor
					β = 2.33	β = 3.00	
	Method	N	Mean λ_R	COV	MCS	MCS	ϕ/λ_R
Static Load Test/	Static Analysis (Driven)	45	0.964	0.546	0.327	0.230	0.383
	Update with 10 tests	10	0.998	0.253	0.679	0.558	0.680

The study of sequential events in Figure 4-3 and Figure 4-4 shows that only the very first three load tests are the most relevant to the process of updating resistance factors using Bayesian approach. This is because the COV of the likelihood remains the same during the updating process. Figure 4-3 shows that such observation is independent of the values of the reliability index because all successive posteriors are typically close to the very first ones. For target reliability indices of 2.33 and 3.00 the updated mean resistance, COV, and resistance factor (ϕ) keep improving as more data keep coming in. Before considering any additional load test, the values of ϕ were 0.33 (for $\beta_T = 2.33$) and 0.23 (for $\beta_T = 3.00$). After three (3) load tests, ϕ values increased substantially to about 0.68 and 0.56 and remain almost constant afterwards. This corresponds to an increase of about 30% in efficiency factor for this specific static pile analysis, i.e.; after the update, a pile can be designed to carry 68% instead of 38% of the measured static resistance at reliability index of 2.33.

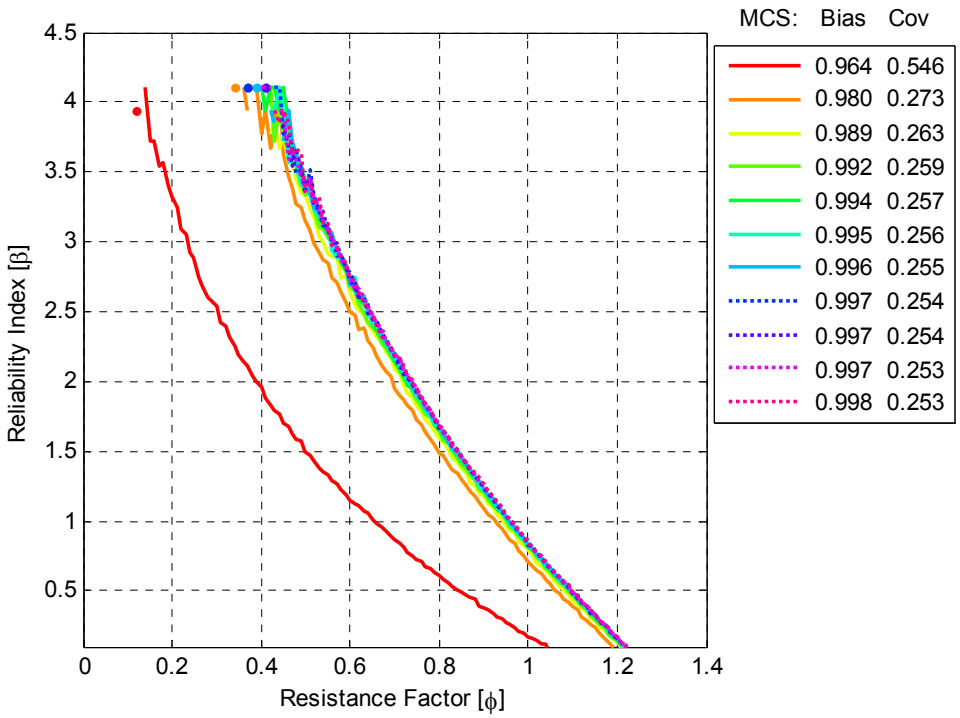

Figure 4-3 Resistance Factors by Monte Carlo Simulations versus Reliability Index as Collection of New Load Test Data Progresses.

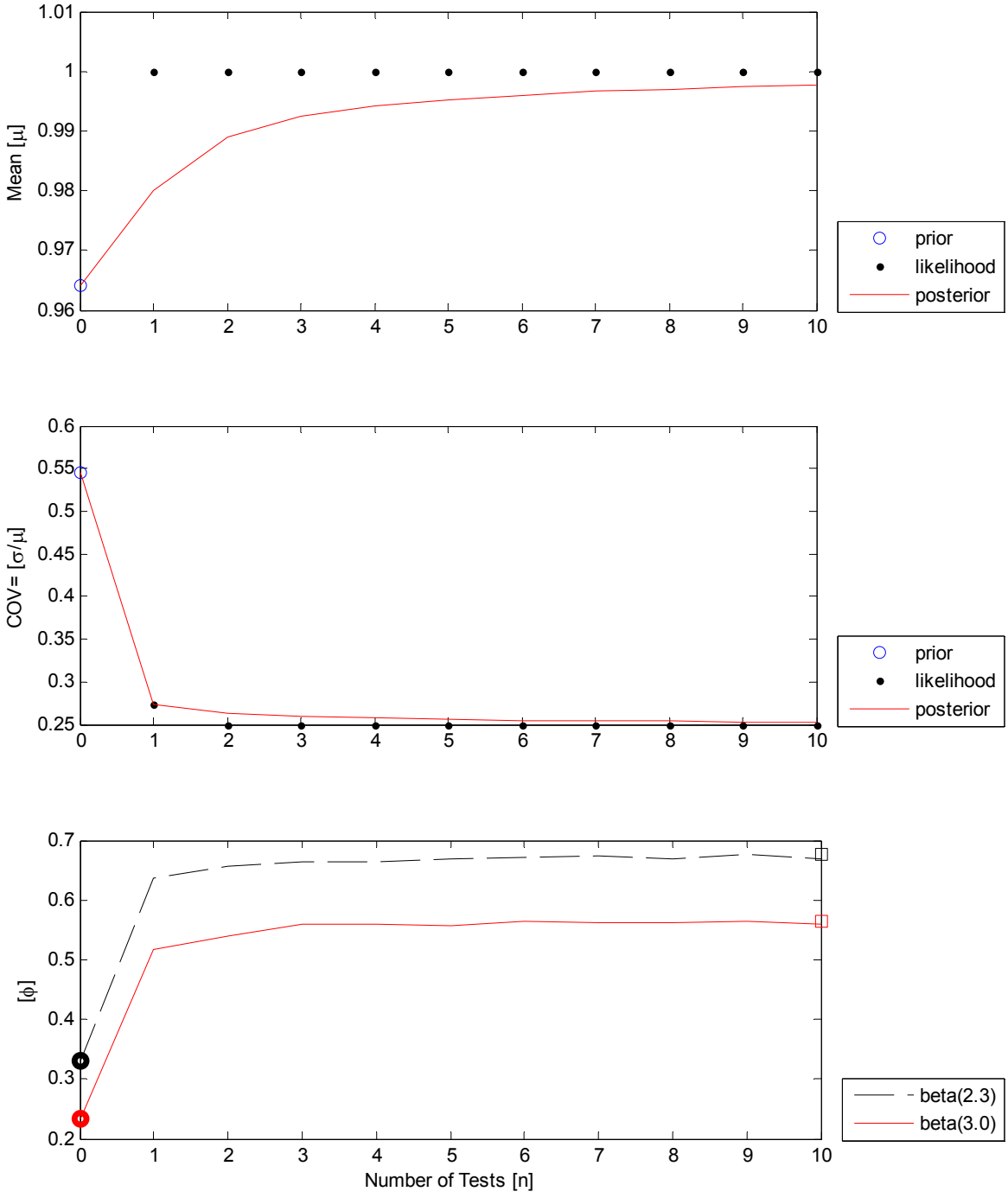

Figure 4-4 Mean, Cov, and Resulting Values of the Resistance Factors as Function of Number of Tested Piles: (Cov of the likelihood is assume to be constant and equal to the average within-site variability cov = 0.25)

4.3 Observations and Conclusion on Updating Process

Although the current study of Bayesian updating utilized simulated data in lieu of the measured load test data, it is clear that the Bayesian posterior (updated) would incorporate the newly collected (observed) test data through the likelihood. Because the value of the standard deviation of the likelihood can be set before the updating process begins, the size of the sample is not required to be known in advance; and the resistance factor updates continually as measurement data accumulates. The updating process can be stopped at any time when the pile load test data is in short supply and may be continued later. Whether the results of the updating process are in the expected direction, the process is worthwhile because it supports the accumulation of knowledge. As more pile load test data is collected, the result of the updating process will converge to the truth. Thus, as more evidence accumulates in the future, this process of Bayesian updating could be employed to achieve more reliable pile designs in deep foundations.

Chapter 5 Recommended Design and Acceptance Protocol

5.1 Incorporating Construction Control Methods into Design Process

5.1.1 Introduction of the Approach

Due to the disparity in results between pile design and construction phases (see problem statement in Section 1.2), there is a need to unify the two phases in order to have a more reliable and cost effective pile foundation. Incorporating the effects of construction control method into the design would reduce unnecessary cost due to driving more pile length than planned or due to unnecessary pile splicing. The first attempt to unify the design with the construction phases was proposed by Barker, et al. (1991) in the NCHRP Report 343. In their report a parameter, λ_v, is employed to modify the recommended resistance factors of various static analysis methods for driven piles in order to account for the effect of quality control procedure during pile driving. Similarly, Paikowsky et al. (2004) proposed in the NCHPR report 507 the possibility of using a modification factor, ξ, as shown in Equation 5-1, but failed to delineate a methodology for finding such a factor.

$$\xi\phi R_n > \gamma Q \qquad \text{Equation 5-1}$$

where ϕR_n is the factored resistance, γQ is the factored load, and ξ is the factor incorporating construction control methods into the design.

This study utilized a similar approach of a modification factor to incorporate the effect of construction control into the design process. The methodology of establishing this knowledge-based factor consisted of evaluating capacity estimation methods used in design and in the construction. During the design phase, if static analysis is employed to determine the contract length of the pile and dynamic measurements are planned to monitor the piling process, then Equation 5-1 at the limit state equilibrium should be:

$$\xi_{sd}\phi_{st}R_{st} = P_{Design}$$ Equation 5-2

where ξ_{sd} is the factor incorporating dynamic testing into static design, $\phi_{st}R_{st}$ is the factored static resistance, and P_{Design} is the design load.

The introduced correction factor, ξ_{sd} in Equation 5-2 would change the reliability level for static design. To maintain the same level of reliability, the factor $\xi_{sd}$is affected to the mean bias of static analysis method by keeping constant the coefficient of variation of the method. Correcting for the bias of static analysis method enables an estimated dynamic capacity to be calculated from that static method. Thus, the construction control factor ξ_{sd} can be determined from the following expression:

$$\xi = \frac{\lambda_{dyn}}{\lambda_{st}}$$ Equation 5-3

where ξ is the ratio of the bias of the dynamically measured capacity (λ_{dyn}) to the bias of the static predicted capacity (λ_{st}). Due to a scarcity of data for static load tests in the database for defining the biases of the analysis methods, the quantity ξ is defined using the following expression:

$$\xi = \frac{R_{st}}{R_{dyn}}$$ Equation 5-4

where R_{dyn} is the measured nominal resistance by dynamic method during the construction control phase, and R_{st} is the nominal pile resistance estimated by the static analysis method during the design phase.

5.1.2 Determination of Correction Factor ξ_{sd} to Account for Control Method into Design

5.1.2.1 Target Level of Significance and Testing Data Distribution

Since the ratio of predicted to measured pile resistance follows lognormal distribution (Barker et al., 1991; Briaud & Tucker, 1988; Cornell, 1969; Dennis, 1982; Isenhower & Long,

1997; Long & Shimel, 1989; Paikowsky et al., 2004), the quantity ξ defined in Equation 5-4 also follows similar distribution. The correction factor ξ_{sd} is found by minimizing the average discrepancy in nominal pile capacities of static and dynamic methods. Because lognormal is a skewed distribution, the median is a better descriptor and more resistant to extreme values than the mean. Therefore, the adjusting factor ξ_{sd} is calculated using the Equation 5-5 which corresponds to 50% of the cumulative distribution of the quantity ξ.

$$\xi_{sd} = \xi_{50} = \frac{\mu_\xi}{\sqrt{1 + COV_\xi^2}} \qquad \text{Equation 5-5}$$

where μ_ξ is the mean value of the capacity ratio ξ, and COV_ξ is the coefficient of variation of the variable ξ. Various tests for goodness of fit at 95% confidence interval were employed to verify the lognormality against normality of the variable ξ. The median value ξ_{50} insures a 50 percent chance of having agreement between predicted and measured capacities, which in turn makes the actual and predicted pile lengths congruent.

5.1.2.2 Evaluation of Predicted (static) to Measured Capacity Ratio

Construction control factor ξ_{sd} was calculated using Equation 5-5 by extracting the mean value μ_ξ and the coefficient of variation COV_ξ from the fitted lognormal CDF of the capacity ratio ξ defined in Equation 5-4. Figure 5-1 shows the fitted cumulative probability distribution (CDF) curves and their corresponding 95 percent confidence bounds (CB) for the ratios of the predicted static capacity to that determined by:

(a) Signal matching at EOD,

(b) Signal matching at BOR,

(c) WEAP at EOD,

(d) Static Load Test with Davisson interpretation,

(e) Engineering news-Record Formula (ENR), and

(f) FHWA modified Gates Formula

The CDF curves combined cases of all soil types. Similarly, correction factors ξ_{sd} for the static analysis method were determined in each individual soil type. The corresponding statistics are shown in Table 5-1. The resulting resistance factors of static analysis combine both the calibrated resistance factors ϕ_{st} and the adjusting factors ξ_{sd}. For instance, if α-method is implemented using the program DRIVEN to predict the pile resistance in clay, a resistance factor of 0.527 (Table 3-15) is recommended. If signal matching is planned to verify the pile capacity at the time of restrike, a ξ_{sd} factor of 1.110 is recommended. Thus, the resulting resistance factor to be used in design for that particular situation is 0.585 (0.527×1.110).

The lower bound of the correction factor is taken to be unit (1.000). In most cases when the correction factor is much less than unit, the construction control method is not better than the static analysis method. For example, in the case of the driving formulas, the corresponding construction control factors are below unit, therefore, the resistance factor for the static analysis should not be corrected. For piles embedded in predominantly cohesive profile, a correction factor of 1.822 is obtained when signal matching is scheduled at EOD. This high correction factor is not surprising because it tries to improve the design by putting soil setup into play. However, since capacity verification at EOD does not verify possible soil setup, the use of this correction factor would compromise the safety of the design. Therefore, scheduled PDA measurements with subsequent signal matching at EOD should not affect pile design process in cohesive soils if there is not an intended plan for soil setup verification.

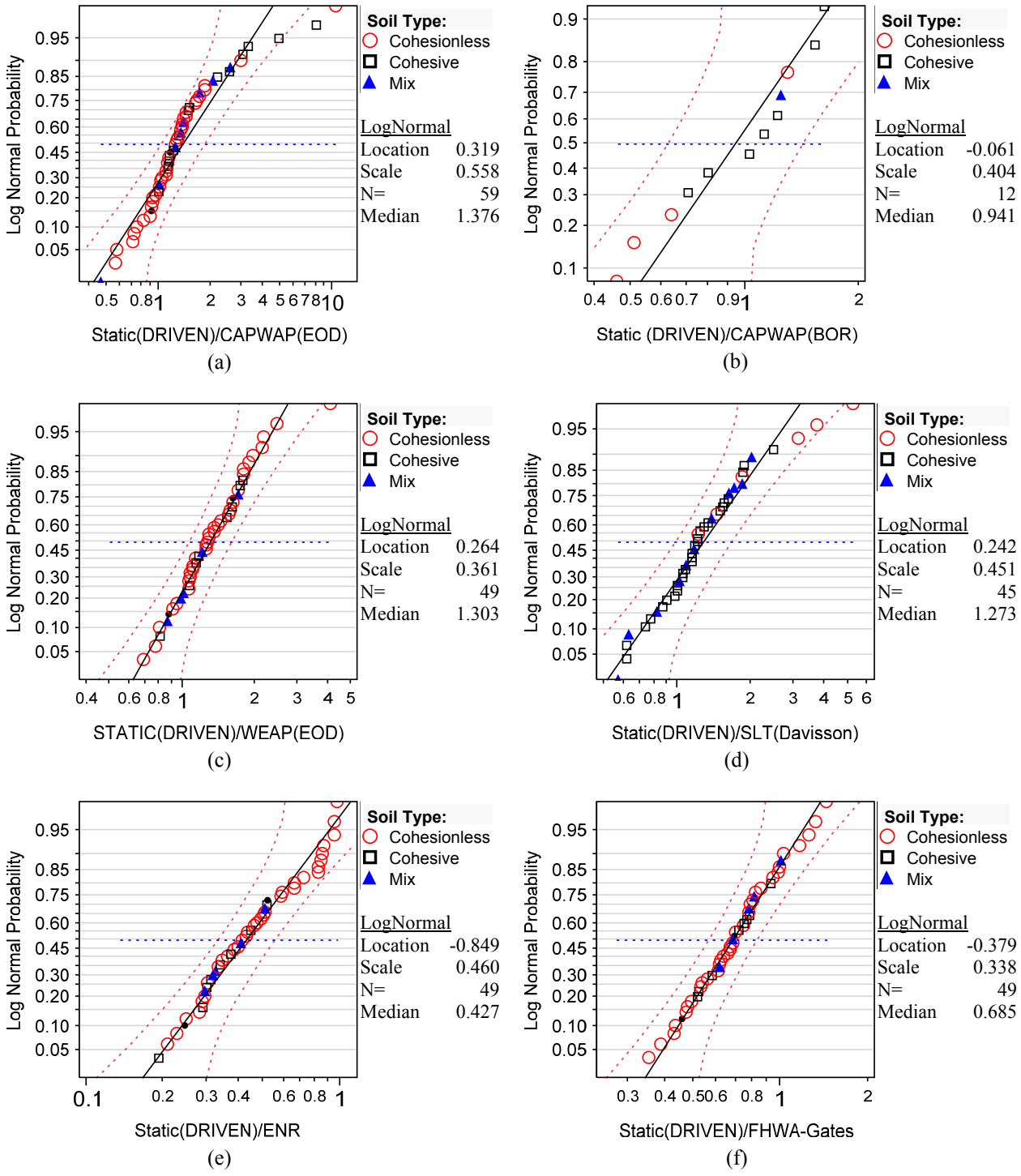

Figure 5-1 CDFs and 95% CBs for Predicted Log-Normal Distribution of Capacity Ratio, ξ, of Static Method-DRIVEN to (a)Signal Matching at EOD and (b)Signal Matching at BOR, (c)WEAP at EOD condition, (d)Static Load Test with Davisson Criteria, (e)ENR, and (f)FHWA-modified Gates.

Table 5-1 Calculated Construction Control Factors and their corresponding Resistance Factors Recommended for Static Design.

Static Analysis Method by FHWA-DRIVEN			β = 2.33		β = 3.00	
Capacity Verification Method	**Type of Soil**	ξ_{SD}	Initial ϕ_{st}	Corrected ϕ_{st}	Initial ϕ_{st}	Corrected ϕ_{st}
Signal Matching – EOD (PDA/CAPWAP)	Clay	1.822	0.527	0.960	0.422	0.769
	Sand	1.169	0.120*	0.140	0.078*	0.091
	Mixed	1.413	0.366	0.517	0.267	0.377
	All	1.376	0.329	0.453	0.233	0.321
Signal Matching – BOR (PDA/CAPWAP)	Clay	1.110	0.527	0.585	0.422	0.468
	Sand	0.644	0.120*	0.120	0.078*	0.078
	Mixed	*	0.366	*	0.267	*
	All	0.941	0.329	0.329	0.233	0.233
Wave Equation Analysis – EOD (WEAP)	Clay	1.332	0.527	0.702	0.422	0.562
	Sand	1.358	0.120*	0.163	0.078*	0.106
	Mixed	1.008	0.366	0.369	0.267	0.269
	All	1.303	0.329	0.429	0.233	0.304
Engineering News-Record Driving Formula (ENR)	Clay	0.335	0.527	0.527	0.422	0.422
	Sand	0.489	0.120*	0.120	0.078*	0.078
	Mixed	0.326	0.366	0.366	0.267	0.267
	All	0.427	0.329	0.329	0.233	0.233
FHWA-Modified Gates Driving Formula	Clay	0.682	0.527	0.527	0.422	0.422
	Sand	0.685	0.120*	0.120	0.078*	0.078
	Mixed	0.703	0.366	0.366	0.267	0.267
	All	0.685	0.329	0.329	0.233	0.233
Static Load Test (Davisson)	Clay	1.147	0.527	0.604	0.422	0.484
	Sand	2.418	0.120*	0.290	0.078*	0.189
	Mixed	1.185	0.366	0.434	0.267	0.316
	All	1.273	0.329	0.419	0.233	0.297

*The number of data points is insufficient to support calculations that are statistically significant.

5.1.3 Evaluation of the Performance of the Calibrated Resistance Factors

In order to examine the performance of the calibrated resistance factors, the actual pile capacities derived from SLT (using Davisson's criteria) were compared to the factored capacities that were estimated using several pile analysis methods. For a specific pile analysis method, the factored pile capacity is a product of the resistance factor of the method and the estimated capacity by the same method.

Figure 5-2 compares three quantities: SLT results using Davisson's criterion, the predicted nominal capacity, and the factored capacity using static analysis method (by DRIVEN). The graph plots all available cases of PPC piles regardless of their size, classification, and soil types. Likewise, Figure 5-3 compares similar quantities to the previous case. However, the factored static capacity uses the corrected resistance factor which incorporates signal matching as a means of pile capacity verification at the EOD. Before applying the resistance factors to the nominal static capacities, more than 50% of all cases were above the line of equality (Rst = SLT). As shown in Figure 5-2 and Figure 5-3, the static analysis method overestimates the capacity in nature, but use of either the preliminary or the corrected resistance factor results in acceptable factored resistance, with the exception of only 3 pile cases. These 3 cases were further documented in the database and were identified to be piles that were classified as end bearing piles driven mainly into cohesionless soils. The correction factor established in the previous section does a good job of optimizing a design by bringing the design capacities closer to the line of equality, while preserving the desired reliability level of the design. The anomaly presented by the reported 3 cases shows that the calibrated resistance factors are better designated for piles classified as skin friction piles.

Appendices C.1 through C.6 present individual plots of the SLT derived capacity versus the nominal and the factored design capacities which were estimated using static analysis method by DRIVEN (for cohesive, mixed, and cohesionless soils). In every individual case, the calibrated resistance factor performed satisfactorily. Signal matching at EOD produced factored capacities that were greater than the nominal capacities measured at EOD (Appendix C.7). Since 10 of 12 analyzed cases were in cohesive and mixed soils, use of the resulting resistance factor includes the soil setup in the design. The obtained resistance factor of 1.567 suggests that a pile

could be designed to mobilize about 64 percent of its long term capacity at EOD, then the pile will develop the remaining 36 percent afterwards. The resistance factor corresponding to the BOR condition performs very well, and all nominal and factored capacities are well below the SLT Davisson's capacities (Appendix C.8).

In general, there is a large variation in the pile nominal capacities predicted by either static method or signal matching at EOD. Fortunately, this large variation is considerably reduced after applying the locally calibrated resistance factors. Overall, as expected, the factored capacity did not exceed the actual SLT capacity. It has also been observed that a preliminary selection of the pile capacity verification method during design process could allow the use of a higher LRFD resistance factor within allowable limits.

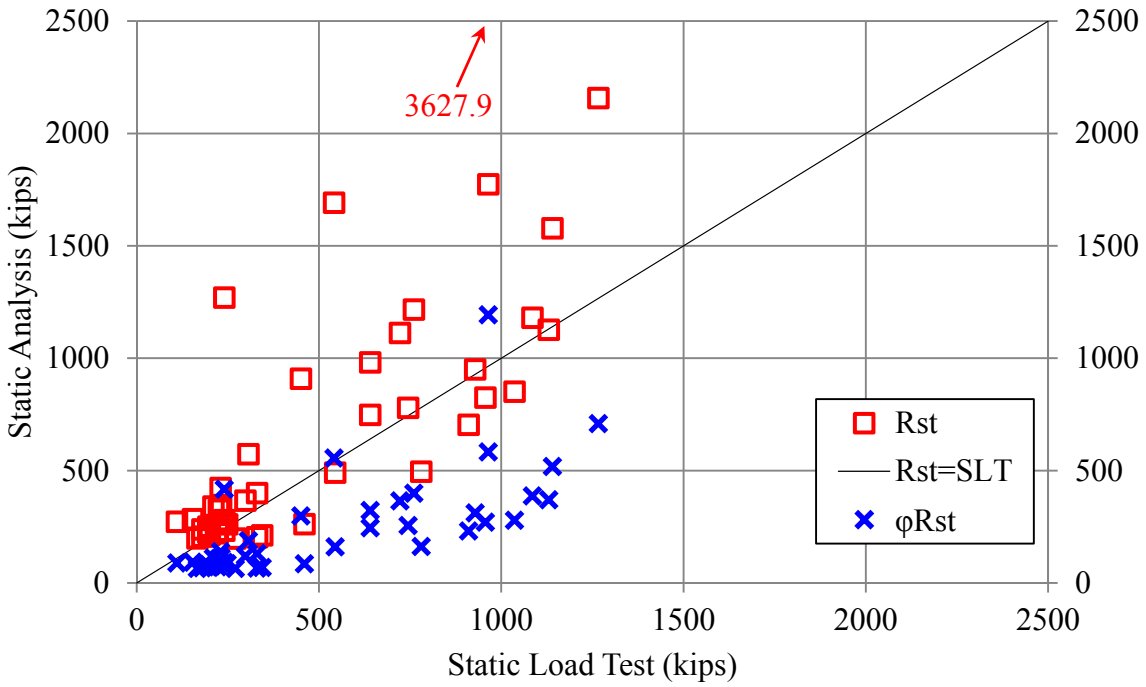

Figure 5-2 Davisson's Criterion versus Static Analysis Method: Nominal and Factored Capacities ($\beta = 2.33$, $\phi = 0.329$, All Soil Types).

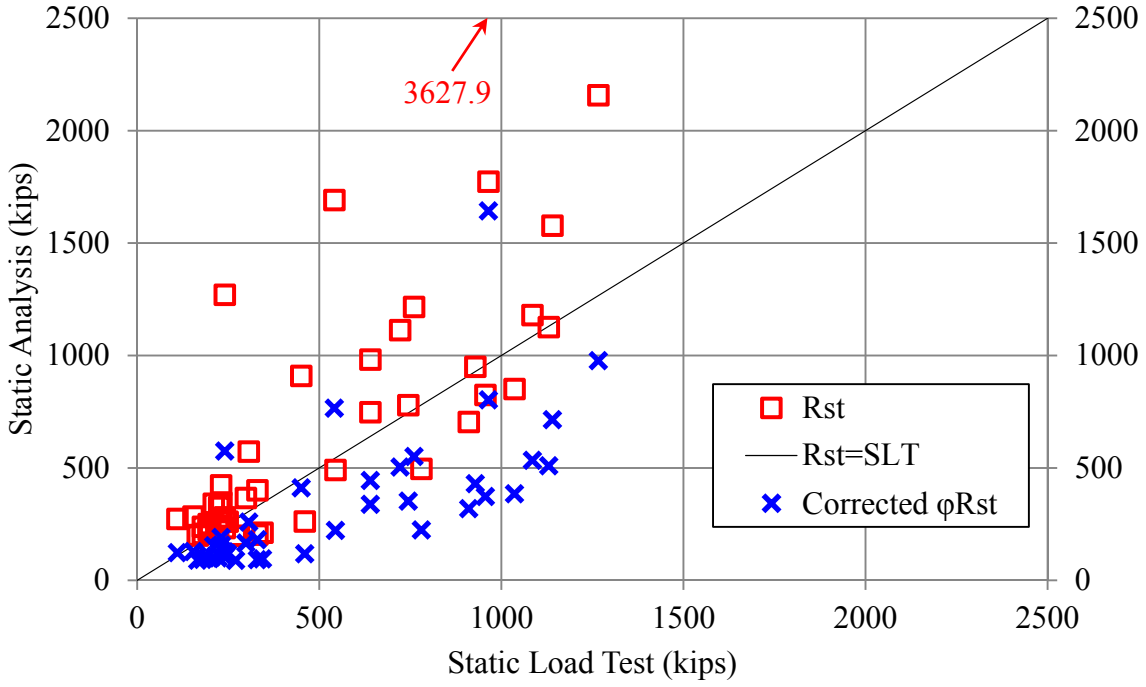

Figure 5-3 Davisson's Criterion versus Static Analysis Method by Incorporating Construction Control Method ($\beta = 2.33$, $\phi = 0.453$, All Soil Types)

5.2 Quality Control and Acceptance Criteria for a Set of Production Piles

5.2.1 Sampling without Replacement within a Set of Production Piles

Dynamic load testing is widely employed for monitoring and accepting driven piles on a construction site. However, due to the high cost of testing, only a small portion of production piles is tested to ensure that the construction is satisfactory. For acceptance purposes, dynamic test results at EOD or BOR can be compared with factored design loads. For instance, if the quantity (t) symbolizes the ratio of dynamically measured resistance (R_{dyn}) to factored design load (P_{Design}) as it is in Equation 5-6, the ratio (y) of actual pile capacity (from SLT) to factored design load can be expressed by Equation 5-7.

$$t = \frac{R_{dyn}}{P_{Design}} \qquad \text{Equation 5-6}$$

$$y = \frac{SLT}{P_{Design}} = \frac{SLT}{R_{dyn}} \cdot \frac{R_{dyn}}{P_{Design}} = \lambda_{dyn} \cdot t \qquad \text{Equation 5-7}$$

where SLT is the actual pile capacity derived from static load test, and λ_{dyn} is the ratio (bias) of the measured static capacity to that measured by dynamic method. The quantities y, λ, and t follow lognormal distribution. Yang (2006) delineated acceptance criteria for accepting entire population of production piles based on few tested piles, and demonstrated that the lower one-sided confidence interval on the population mean, μ_{lnY} could be expressed as follows:

$$\overline{ln\ y} - Z_{\alpha}\left(\frac{\sigma_{lnY}}{\sqrt{n}}\right) \leq \mu_{lnY} \qquad \text{Equation 5-8}$$

where $\overline{\ln\ y} =$ mean of $\ln y$, $Z_{\alpha} = \beta_T = \Phi^{-1}(1-\alpha) =$ Reliability index corresponding to the value of random variables having the standard distribution and cutting off α percent in the tail of the distribution (α = level of significance) with $\alpha = 1 - \gamma$ ($\gamma =$ level of confidence), Φ^{-1} is the

inverse of the cumulative distribution function of the standard normal, μ_{lnY} and σ_{lnY} are the lognormal parameters of the variable Y, and n = Sample size.

Equation 5-8 is based on central limit theorem. However, to accept piling work, the sampling process is done without replacement on a population of production piles of a finite size N. When a sampling fraction n/N is not small (>5-10%), a correction factor for finite population is employed to reduce the standard error of the mean (Ayyub & McCuen, 2002). By applying this concept, Equation 5-8 becomes:

$$\overline{ln\ y} - Z_\alpha \sqrt{\frac{N-n}{N-1}} \cdot \frac{\sigma_{lnY}}{\sqrt{n}} \leq \mu_{lnY} \qquad \text{Equation 5-9}$$

By ignoring the uncertainties associated with load components (they are much smaller than those associated with resistance components) and by using Equation 2-8 and Equation 2-9 to transform lognormal to normal parameters for mean and standard deviation of the variables, the following expression is obtained:

$$ln\,\bar{t} + ln\,\mu_\lambda - \beta_T \sqrt{\frac{N-n}{N-1}} \cdot \sqrt{\frac{ln(1+cov_\lambda^2+cov_t^2)}{n}} \leq ln\,\mu_Y \qquad \text{Equation 5-10}$$

where $\bar{t} = \sqrt[n]{\prod_{k=1}^{n} t_k}$ = the geometric mean of the sample, μ_λ and μ_Y are the mean values of the variables λ and Y respectively. In order to assure safety at a target reliability index, β_T, the population mean should not be less than the factored design load, i.e., $\mu_Y \geq 1$, or the lower side of $\ln \mu_Y$ should not be less than zero. When this condition is met the following expression is obtained:

$$\bar{t}_{min} = \frac{e_f}{\phi_{dyn}} exp\left(\beta_T \sqrt{\frac{N-n}{N-1}} \cdot \sqrt{\frac{ln(1+cov_\lambda^2+cov_t^2)}{n}}\right) \qquad \text{Equation 5-11}$$

where the measured $\bar{t}$ should be greater than $\bar{t}_{min}$ for a whole set of N driven piles to be accepted. ϕ_{dyn} is the resistance factor of the utilized dynamic method, and e_f is the efficiency factor of the same method (defined in Equation 3-9). For a predetermined acceptance value of $\bar{t}_{min}$, the number of piles (n) that should be dynamically load tested on a project depends upon the project size (expressed by N), variability of the subsurface conditions (expressed by the cov_t of the site variability), the type of utilized dynamic method (expressed by ϕ_{dyn}, e_f, and cov_λ), and the reasons for performing the dynamic tests (expressed by β_T).

5.2.2 Determination of Number of Load Tests and Criterion for Accepting a Set of Piles

Equation 5-11 and the statistics of the construction control methods (Table 5-2) were utilized to calculate the required number, n, of driven piles to be tested on construction site; which makes part of the quality assurance testing plan. Figure 5-4 and Figure 5-5 present the relationship between number of piles to be tested on a job site and its corresponding acceptance ratio. This ratio is defined by the measured nominal capacity divided by the factored design load, when measurements are performed using signal matching at BOR (for a β_T of 2.33). It is clear that, for a given reliability level, the required number of tests increases with increase in within-site variability. Subsequently, if a site is well characterized, the effort spent to do so could be compensated in the construction control plan. The required value of $\bar{t}$ ratio for accepting a set of driven piles could be reduced if the construction site is well characterized during site exploration or if the level of sampling effort is increased during construction phase. However, it has been observed that only the very first few tests are critical to reducing the acceptance criterion, since the number of tested piles beyond 10 has been found to have very limited effect in reducing the required value of $\bar{t}$. For that reason, only optimum values of n and $\bar{t}$ are presented in Table 5-3. This Table describes the ratio $\bar{t}$ as a function of the site variability, population size on

construction site, number of piles tested, and target reliability for several construction control methods.

For CAPWAP at BOR, the average capacity is set to a minimum of 83% of the nominal ultimate capacity as an acceptance criterion when entire population of production piles is load tested (Figure 5-5). This minimum value is close to the minimum value of 85% proposed by Paikowsky et al (2004). For acceptance ratios of 1.2, 1.3, and 1.4 for low, medium and high site variability, respectively, a minimum number of 3 dynamic load tests is required at BOR. This minimum number of tests agrees with Hannigan et al. (2006) who suggested a minimum of two dynamic pile tests for small projects.

For CAPWAP at EOD, the available database suggests that a set of driven piles could be accepted based on a sole pile test result that generates at least 85% of the nominal ultimate capacity. Such a result should only be employed when the context is similar to this study, where driven pile is purely frictional and high soil set up is anticipated and verifiable. However, in the process of verifying gain in capacity, a great number of pile tests may be tested may be required if significant time dependent soil setup is anticipated.

For the ENR formula, at the reliability index of 2.33, the required optimum capacity is about 2.5 times the nominal ultimate load. An optimum value of about 1.5 is set for the FHWA modified Gates formula. In both cases, 6 pile test results are sufficiently enough to either accept or reject an entire set of production piles. If the acceptance ratio needs to be lowered, higher pile resistances (in terms of blow counts at EOD) are required for a great number of production piles.

Table 5-2 Statistical Parameters for Various Test Methods available in Pile Database.

Load test method	Number of cases	Average bias, λ	Coefficient of variation, COV
CAPWAP-EOD	12	3.632	0.467
CAPAWAP-BOR	4	1.199	0.218
WEAP-EOD	4	1.951*	0.219
ENR	4	0.587*	0.188
FHWA-Gates	4	0.895*	0.107

*Average bias is referenced to the CAPWAP capacity at the BOR condition.

Table 5-3 Recommended Number of Load Tests, n, to be Conducted for Quality Control of Driven Piles and their corresponding $\bar{t}$ Value for β_T of 2.33.

	Test methods		SLT	CAPWAP		WEAP	ENR	FHWA Gates
		Condition	14days	EOD*	BOR	EOD	EOD	EOD
Low site variability		Required $\bar{t}$	1.45	0.85	1.20	0.95	2.35	1.45
	N value	≤10	1	1	3	1	3	3
		11-20	1	1	3	1	3	3
		21-50	1	1	3	1	3	3
		51-100	1	1	3	1	3	3
		≥100	1	1	3	1	3	3
Medium variability		Required $\bar{t}$	1.80	0.90	1.30	1.10	2.30	1.60
	N value	≤10	1	1	3	1	4	3
		11-20	1	1	3	1	5	3
		21-50	1	1	3	1	6	3
		51-100	1	1	3	1	6	3
		≥100	1	1	3	1	6	3
High site variability		Required $\bar{t}$	1.75	1.00	1.40	1.00	2.45	1.60
	N value	≤10	2	1	3	2	4	4
		11-20	2	1	3	2	5	5
		21-50	2	1	3	2	6	5
		51-100	2	1	3	2	6	5
		≥100	2	1	3	2	6	5

*Great number of piles to be tested may be required for soil setup verification after installation.

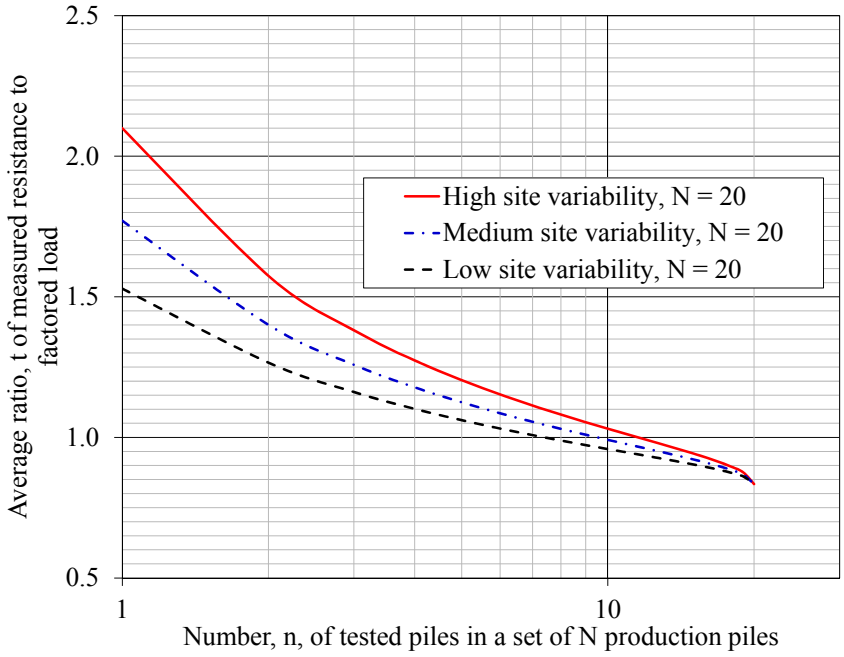

Figure 5-4 Effects of within-site Variability on Required Number of dynamically Tested Piles, and Required Average Ratio $\bar{t}$ of Measured Capacity by Signal Matching at BOR to Factored Load for 20 Production Piles, at Reliability Index of 2.33.

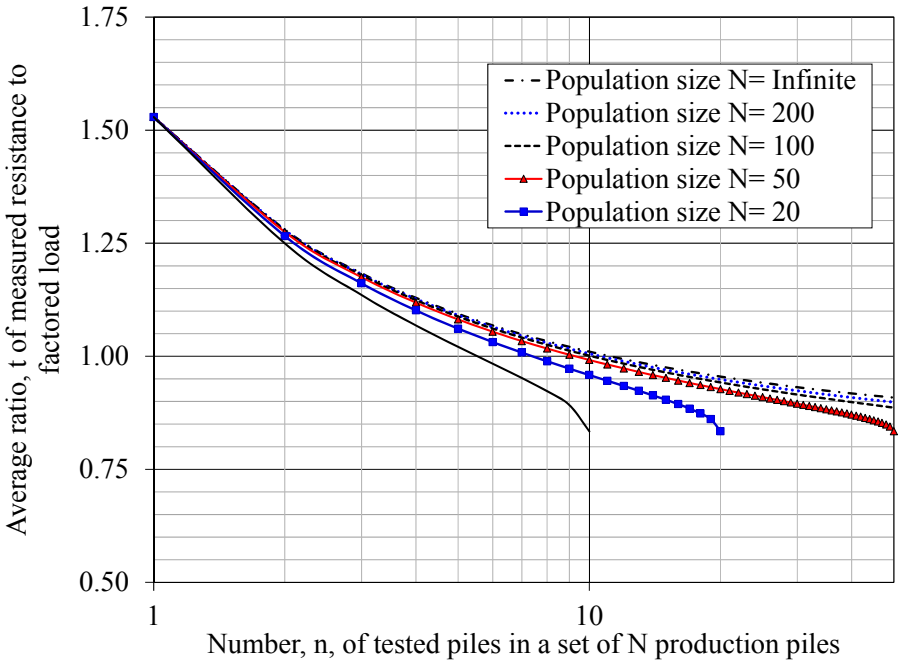

Figure 5-5 Changes in Requirements of the Average Measured Nominal Resistance with respect to the Number of Tested Piles within N number of Production Piles (Case of Signal Matching Measurements, and Low level of within-site Variability at Reliability Index of 2.33).

5.3 Recommended Pile Design and Acceptance Protocol

During design phase, piles are designed using static analysis methods with their corresponding resistance factors. The α-Tomlinson's method in cohesive soil layers and the Nordlund's method in non-cohesive soil layers are common practice for driven piles. Driving criteria are established based upon acceptable construction control methods, such as: (1) use of a bearing graph developed from WEAP approach or from FHWA-modified Gates formula, (2) Pile Driving Analyzer (PDA) with subsequent pile signal matching analysis using the CAPWAP performed on test piles or on a few production piles, (3) a combination of WEAP and PDA with subsequent signal matching, and (4) use of Pile Driving Monitor (PDM) or a combination of PDM, PDA and signal matching.

5.3.1 Overview of Pile Design and Construction Steps

The general overview of the herein recommended procedure for designing driven piles is an adaptation of the current research observations, and the design and construction procedures described in AASHTO LRFD (2012) and FHWA (Hannigan et al., 2006) manuals. Contrary to typical procedure, the herein recommended design and acceptance procedure uses an overall classification of soil profile based on the percentage of bearing capacity contributions from different soil layers. Choosing the resistance factor for the design involves prior knowledge of the anticipated construction control method. The acceptance criteria of the construction work vary depending upon the tested pile percentage of production piles. The general overview of the design and construction procedures is presented in the following 10 steps:

5.3.1.1 Design Phase

1 Develop the bridge situation plan including bridge type, size, and location

2 Develop the soils package including soil borings and foundation recommendations

3 Determine the pile arrangement, pile loads, and other design requirements

4 Estimate the nominal geotechnical resistance along the pile embedment

5 Select the design resistance factor based on the soil profile and construction control

6 Calculate the required nominal pile resistance, Rn

7 Estimate the contract pile length, L

8 Estimate the target nominal pile driving resistance, Rnd

5.3.1.2 Construction Phase

9 Prepare the bearing graph to determine driving criteria

10 Observe the construction, record driven resistance, and resolve any piling issues

Basic information for geotechnical pile design is determined in Steps 1 through 3 and they can vary based upon the size of the bridge project and local practice. Steps 4 through 8 are specific to this study and involve the use of the locally calibrated resistance factors in predicting contract length. Steps 9 and 10 involve monitoring piling process and accepting construction work on the job site. Figure 5-6 shows the design and construction control flow chart. The chart describes the process to be followed during the design and construction phases in order to achieve the required nominal bearing resistance at the acceptable level of reliability.

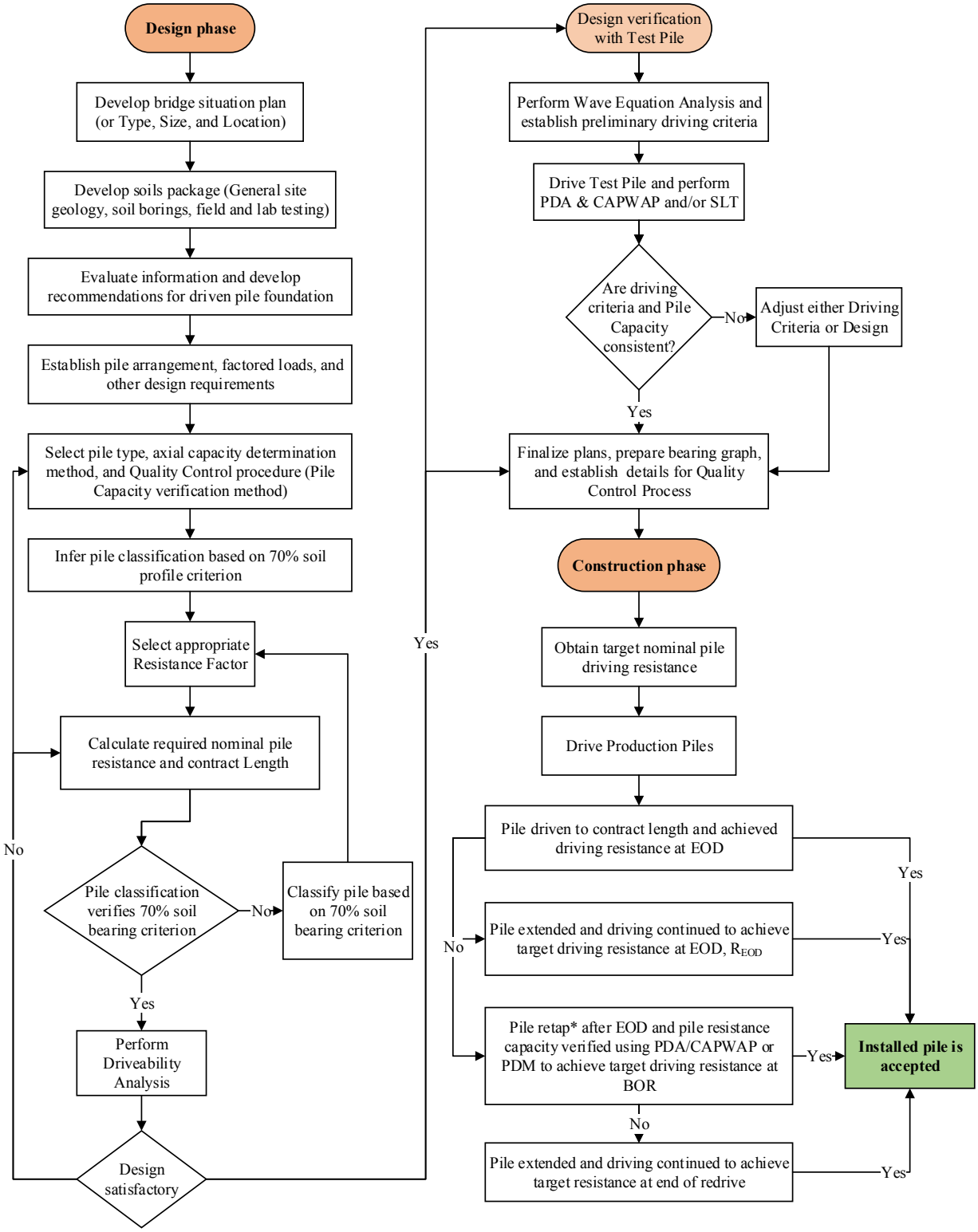

Figure 5-6 Flow Chart for the Proposed Design and Construction Control Procedures for Driven Piles.

5.3.2 Description of the Pile Design and Construction Steps

Step 1. Develop the bridge situation plan.

The initial phase of the design deals with collecting important design information, such as topographical plots, the location of the bridge, general type of superstructure, location of the substructure units, elevations of foundations, hydraulic information, and other basic information that characterize the bridge. Plan and longitudinal section of the bridge are developed from these preliminary plots, which in turn provide information needed for the pile design. That information may include span length of the bridge, type of beams of the superstructure, bridge skew, location of piles, bottom of abutment footing elevation, and so on.

Step 2. Develop soils package, including soil borings and foundation recommendations.

Based on potential locations of the pile, corresponding soil borings are plotted on a longitudinal section, and special geotechnical conditions are checked on the site. Recommendation for foundation type along with any applicable special design considerations is made.

Step 3. Determine the pile arrangement, pile loads, and other design requirements.

Based on the situation plan from Step 1 and the soils data from Step 2, the following information is determined to obtain the required pile length: (1) number of piles under each substructure unit of the bridge; (2) required ultimate vertical load per pile; (3) special conditions such as uplift, scour or downdrag, accelerated or delayed construction, and lateral load; (4) type of construction control such as WEAP analysis, PDA/CAPWAP at restrike, PDM, or Driving Formula.

Step 4. Estimate the nominal geotechnical resistance along the pile embedment.

Based on the selected static analysis method and the soil boring information that is specific to the location of the pile being designed, estimate the nominal pile resistances along the soil profile and plot a bearing graph of the estimated nominal resistance per pile versus depth. Figure 5-7 presents an example of a bearing graph that plots the predicted static capacity versus depth.

Step 5. Select a resistance factor based on soil profile and construction control.

The site must first be characterized (as cohesive, mixed, or non-cohesive) based on the overall classification of the soil profile. Assuming that the predominant soil type is the one that most likely represents ≥ 70% of the pile embedment, use the chart in Figure 5-8 to select the recommended resistance factor φ_{sd} for estimating contract length according to scheduled construction control method.

Step 6. Calculate the required nominal pile resistance, Rn.

The required nominal pile resistance, Rn, is calculated as follows:

$$R_n = \frac{\sum \eta\gamma Q}{\varphi_{sd}} \qquad \text{Equation 5-12}$$

where η is the load modifier and is equal to 1.0 in most cases (AASHTO LRFD), and φ_{sd} is carefully chosen from Figure 5-8 at the reliability index of 2.33, or from Table 5-1 for a reliability index of 3.

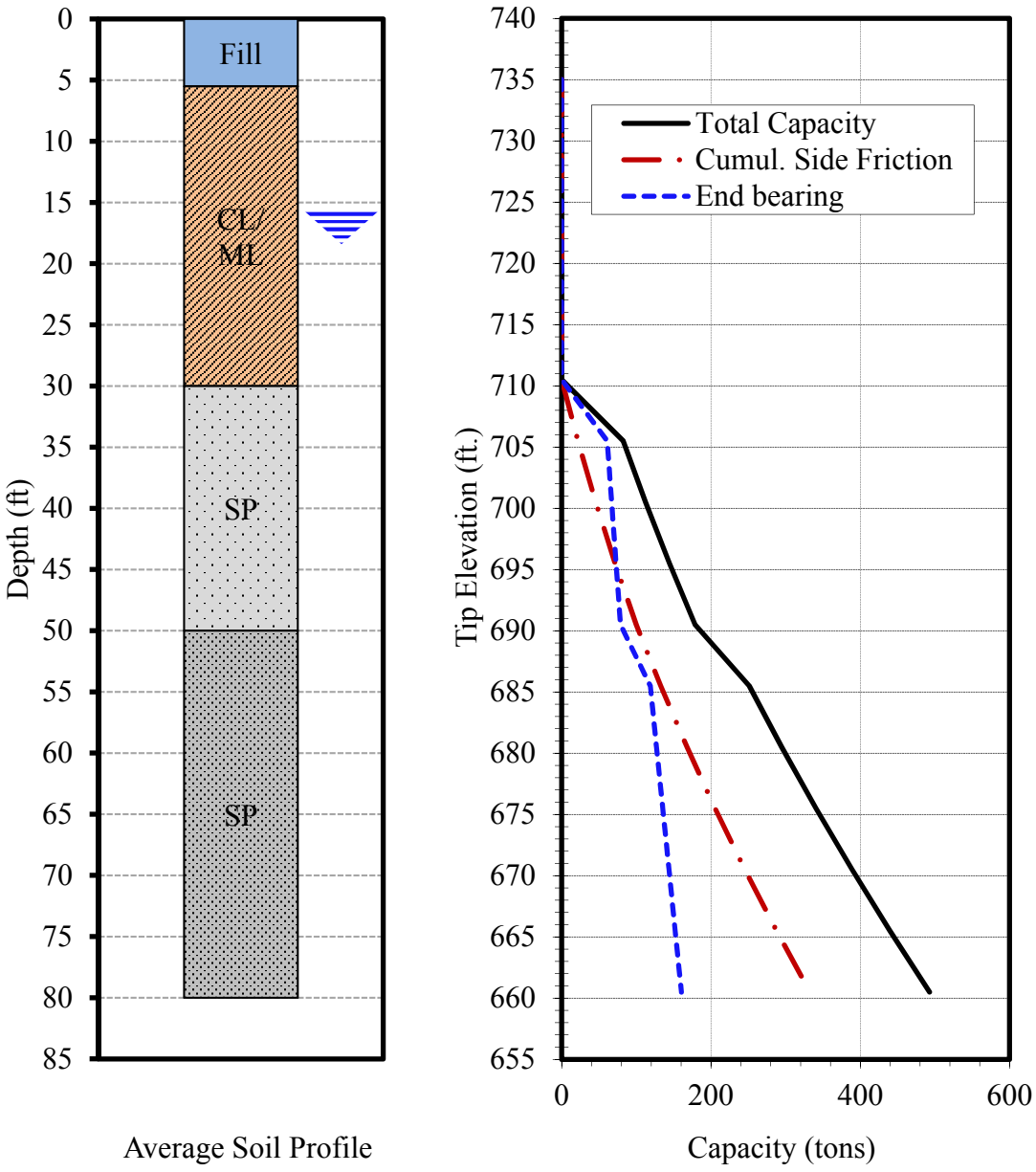

Figure 5-7 Example of a Plot of Nominal Pile Resistance along Pile Depth for Determining Required Pile Length.

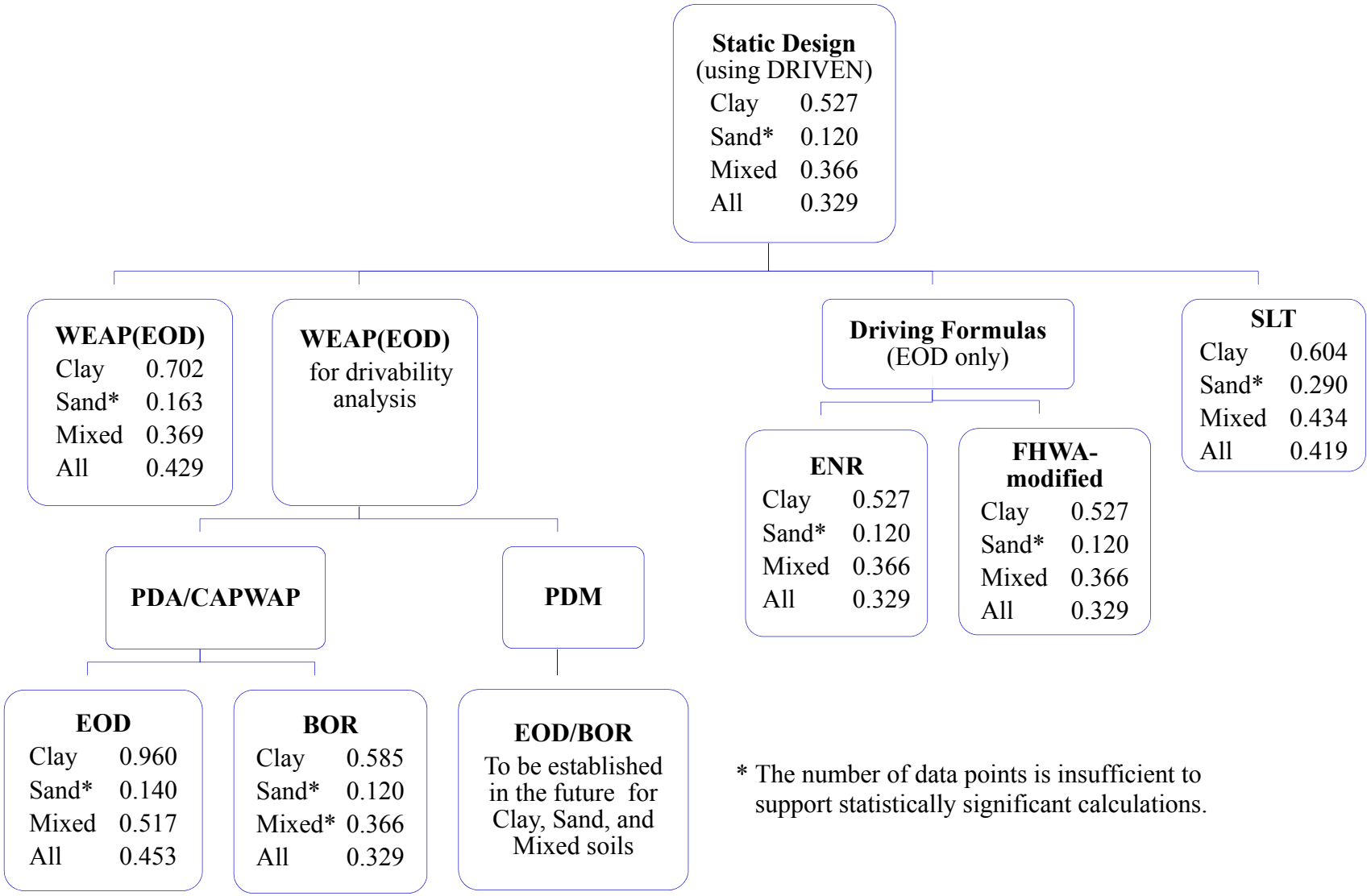

Figure 5-8 Resistance Factors (φ_{sd}) for Static Design of a Pile in Axial Compression at a Reliability Index of 2.33 for a given Type of Construction Control Method: These values only correspond to the static design using the program DRIVEN.

Step 7. Estimate contract pile length, L.

From the graph of nominal resistance along the pile length established in Step 4, extract the depth, L, below the footing necessary to achieve the required nominal resistance R_n (calculated in Step 6). At this point, the embedded pile length is known and it is necessary to check the selected resistance factor according to soil type. This is accomplished by calculating the resistance contributed by each soil layer to the total pile capacity in terms of percentage, and by classifying the overall soil profile (as cohesive, non-cohesive, or mixed) based on 70% rule of the bearing contribution. Check whether the soil profile classification matches with the previous assumption in Step 5. If the selected resistance factor were incorrect, Step 6 and Step 7 must be repeated based on this newly determined soil classification. Check for any additional length requirements (cutoff due to driving damage, footing embedment, etc.).

Step 8. Estimate target nominal pile driving resistance, Rnd.

The general expression for pile driving resistance can be presented as follows:

$$R_{nd} \geq \frac{\sum \gamma Q}{\varphi_d} \qquad \text{Equation 5-13}$$

where φ_d corresponds to the resistance factor from Table 3-11 through Table 3-16 for the chosen control method for piling process. Step 8 ends the design and the construction phase starts.

Step 9. Prepare a bearing graph for the piling process.

To establish a bearing graph for the piling process, the contractor must provide a list of proposed hammer types, including all pertinent information about the driving equipment, such as the cap or helmet number, hammer identification, hammer cushion, and pile cushion as well as pile size, pile length, and estimated pile driving resistance. The wave equation approach is preferred over driving formulas for preparing a bearing graph for the piling process.

In the event that WEAP is employed to set up the driving criteria, the provided hammer records together with R_{nd} are used to complete the WEAP analysis. Results from the WEAP analysis are then utilized to prepare the driving graph. This driving graph includes curves of nominal driving resistance versus blows per foot and identifies specific driving conditions, where driving stress is a concern. Figure 5-9 presents a typical driving graph derived from WEAP analysis.

Among driving formulas, the FHWA-modified Gates formula is preferred. When this formula is chosen to determine the driving criteria, the provided hammer information together with R_{nd} are employed to complete a bearing graph plotting pile resistance (blows/in) versus stroke or energy. Figure 5-10 shows an example of typical lines of the bearing graph and a minimum pile energy line that corresponds to refusal of 20 blows per inch (as set by the AHTD construction specifications for piling).

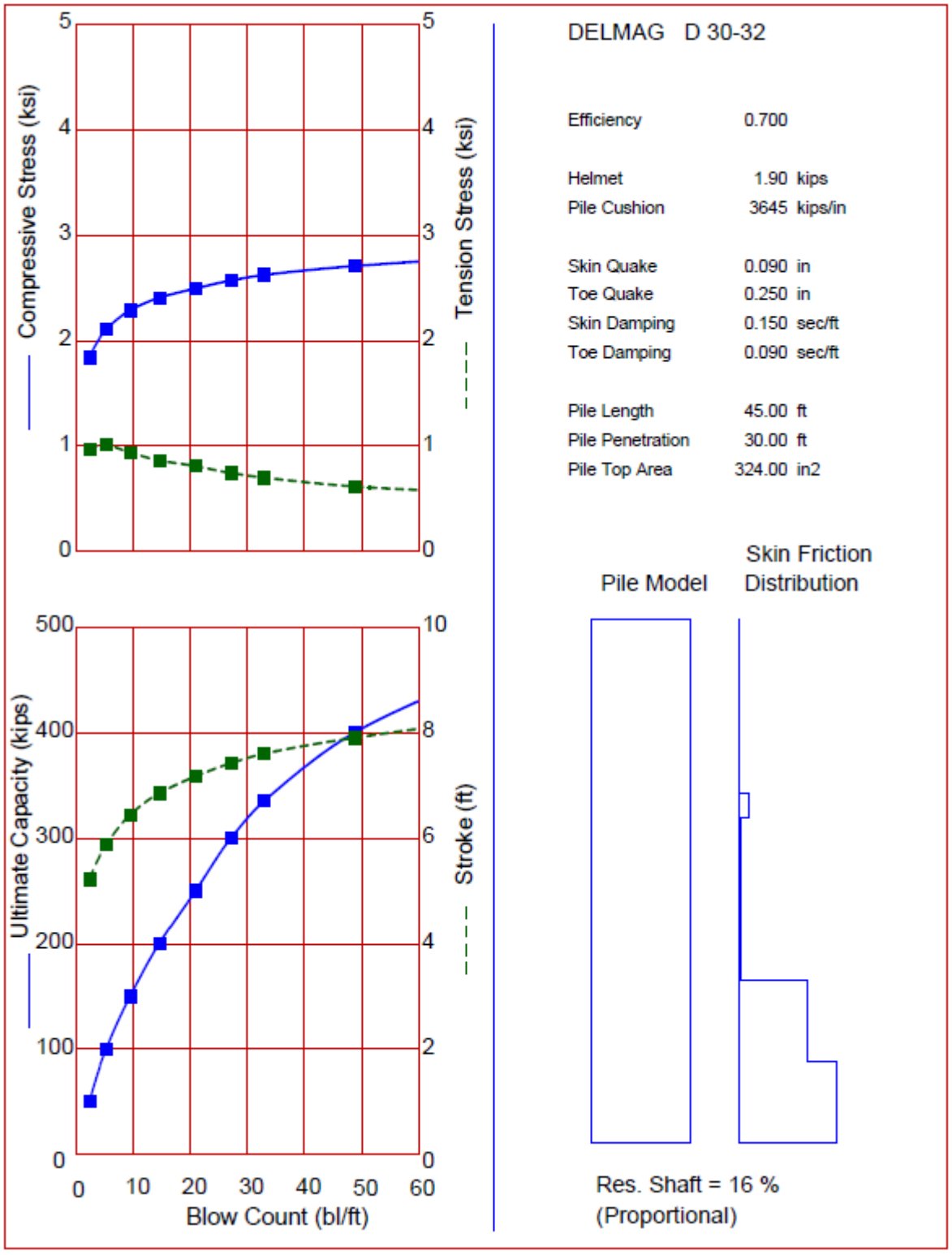

Figure 5-9 Typical WEAP Bearing Graph used to derive Driving Criteria.

Pile Driving Resistance Calculation (FHWA-Modified Gates)

INPUT --> Input in yellow cells only.

Notes:

- This spreadsheet calculates the "Blows"per x inch of pile penetration required for a given pile capacity according to the Dynamic FHWA Gates Formula.

- A minimum pile energy is also shown on the chart. This value is calculated from a recommended practical refusal limit of 20 blows per 1.0 inch as specified by Arkansas 2003 Standard Specifications for Highway Construction, or described in the publication "Design and Construction of Driven Pile Foundations Reference Manual-Volume II" (FHWA-NHI-05-043). Any data below this line on the chart is typically ignored.

Input Required Pile Capacity As Shown On Plans				
Design Bearing =	**150**	kips	Resistance Factor for Design =	**0.45**
Nominal Axial Compressive Resistance =		kips		
Input Hammer Properties				
Ram Weight =	**4149**	lbs.	Typical Range (3300-6600 lbs.)	
Hammer Efficiency =	**80**	%	See AHTD 2003 Spec (Sec 805 Piling): 67/50/72	

Units for Set:	**in./1 blows**
Practical refusal:	**20 blows/in.**
Units for Resistance:	**Blows/ 1 in.**
dR_u =	**50 kips.**

FHWA Gates Equation

$$R_u = 1.75 \times \sqrt{W_R \cdot h} \log_{10}(10 \times N_b) - 100$$

R_u = 333 kips

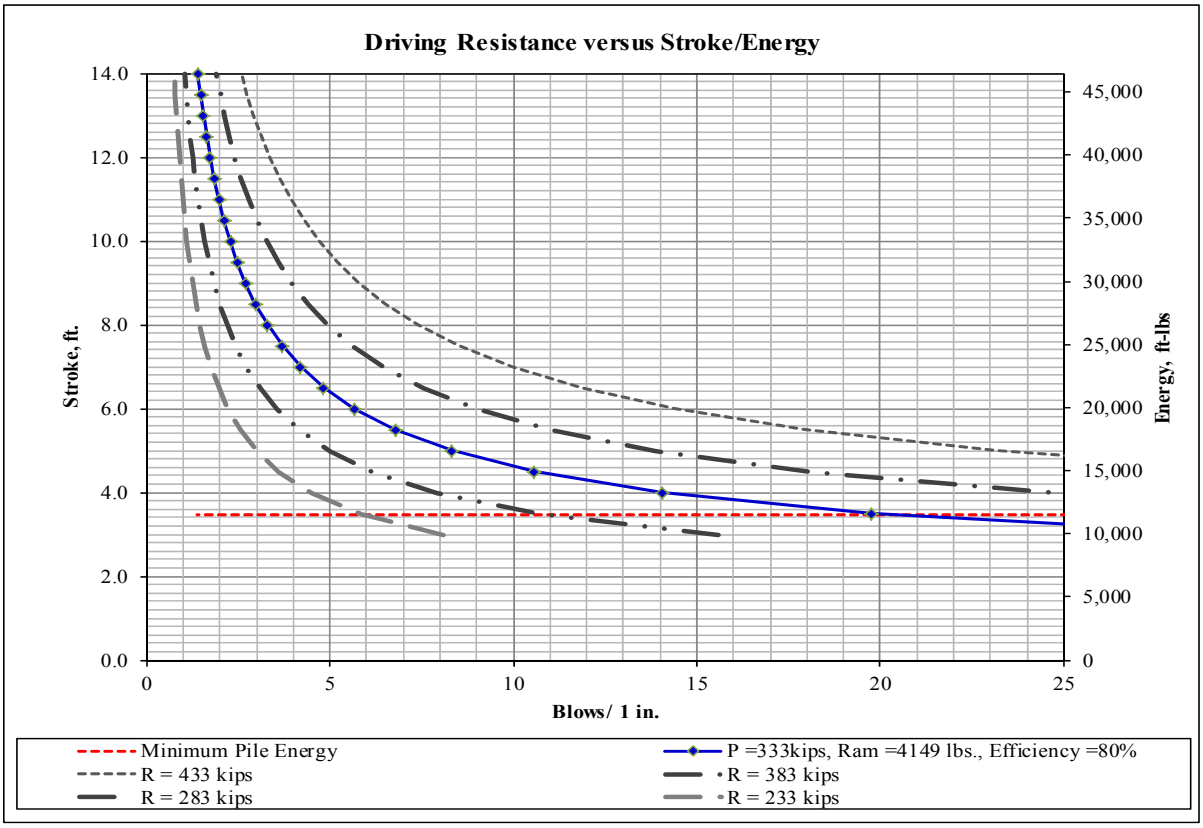

Figure 5-10 Driving Resistance (Blows/inch) versus Stroke and Energy for a specified Hammer Type and Nominal Pile Driving Resistance.

Step 10. Observe construction, record driving resistances, and resolve any construction issues.

As part of the piling process, hammer stroke and number of blows to advance the pile an equivalent penetration of 1 ft are recorded in the form of a pile driving log which is illustrated in Figure 5-11. The recorded information is converted using a driving graph similar to either Figure 5-9 or Figure 5-10 to record the driven resistance per pile at EOD.

In Section 5.1.2 an adjusting factor was introduced to make the actual and the predicted pile lengths agree. However, if the pile is driven to its estimated contract length and the recorded driving resistance at EOD is less than the target pile nominal driving resistance (R_{nd}), different steps that were described in Figure 5-6 could be followed to handle such pile capacity issues during the construction phase.

If the recorded pile driving resistance at EOD is less than the target pile nominal driving resistance (R_{nd}), the pile could be restuck about 24 hours after EOD. If the 24 hour retap does not indicate sufficient driven resistance, an extension to the pile could be added. Since extensions are expensive, the benefit of the soil setup could be considered, but it should not be overestimated. If construction is not on a busy schedule, an alternative solution is to allow more time (up to 14 days) for the capacity to develop when the soil setup is expected. However, if construction is on a tight schedule, pile extension can be approved. In that situation the production pile can be spliced with an extension, and redriving can be continued in order to avoid construction delay. Due to redriving, the setup resistance initially developed is ignored and the pile is extended until the new measured driving resistance reaches the target nominal driving resistance at EOD.

Single piles are accepted or rejected based on Equation 5-13. However, if it is too expensive or practically impossible to test the entire population of production piles, the untested piles could be accepted or rejected based on a sampling of a few tested piles on the same job site, using Equation 5-11 or Table 5-3. To use Table 5-3, the geometric mean of the results of the tested piles is determined. All tested piles should be included regardless of their performance. If the mean capacity of the tested piles is greater than the recommended percentage of the nominal ultimate capacity, then that set of piles is accepted. If this requirement is not met, then the piles could be driven deeper or the required nominal capacity could be reduced by adding more piles. The recommended values in Table 5-3 relate to similar pile types driven at similar site conditions.

PILE DYNAMIC TEST REPORT

Project No. _____ Project Name: _____ Date Pile Driven: _____

Pile ID: _____ County: _____ Location/Bent: _____

Pile Type: _____ Battered/Vertical: _____ Pile size (Butt/Tip): _____

Ground Elevation: _____ Cut off Elevation: _____ Pile Tip: _____

Pile Length: _____ Time Start: _____ Time Finish: _____

Hammer Type/Size: _____ Inspector: _____

Pile Driving Log						Ultimate Bearing-Starting Depth				
Depth(ft.)	Blows/Ft	Remarks	Depth(ft.)	Blows/Ft	Remarks	Depth (ft.)	3" Intervals	Blows/Inch	Stroke (ft)	Remarks
1			31				0" — 3"			
2			32				3" — 6"			
3			33				6" — 9"			
4			34				9" — 1 ft.			
5			35				0" — 3"			
6			36				3" — 6"			
7			37				6" — 9"			
8			38				9" — 1 ft.			
9			39				0" — 3"			
10			40				3" — 6"			
11			41				6" — 9"			
12			42				9" — 2 ft.			
13			43				0" — 3"			
14			44				3" — 6"			
15			45				6" — 9"			
16			46				9" — 3 ft.			
17			47				0" — 3"			
18			48				3" — 6"			
19			49				6" — 9"			
20			50				9" — 4 ft.			
21			51				0" — 3"			
22			52				3" — 6"			
23			53				6" — 9"			
24			54				9" — 5 ft.			
25			55				0" — 3"			
26			56				3" — 6"			
27			57				6" — 9"			
28			58				9" — 6 ft.			
29			59							
30			60							

Remarks:

Interruptions and any other irregularities during driving:	Depth Occurred:	Time:

Figure 5-11 Example of a Pile driving log.

Chapter 6 Summaries, Conclusions, and Recommendations

6.1 Summaries and Conclusions Based on Available Data

6.1.1 Overall Summary of the LRFD Calibration Work

To overhaul the gaps that exist in the AHTD standard specifications for piling processes, a study of the LRFD calibration process for driven piles was initiated. The outcomes of this research led to creation of an LRFD design and acceptance protocol for driven piles in the State of Arkansas. The new protocol incorporates locally calibrated resistance factors for available pile analysis methods, local construction experiences, and local practices.

Piles that had been tested either with dynamic or static load tests were collected from different project archives at the Arkansas State Highway and Transportation Department, the Missouri Department of Transportation, and the Louisiana Department of Transportation. The developed database is composed of 102 pile cases and represents typical subsurface soil conditions along with design and construction practice encountered in the region. Pile capacities were estimated using three different approaches: static pile analysis, dynamic methods based on wave equation theory, and empirical dynamic formulas. Statistical analyses were performed to compare the predicted and the measured axial resistances. In general, the static analysis method using the program DRIVEN and the dynamic formulas (ENR and FHWA modified Gates) overestimated pile capacity. However, dynamic analysis methods utilizing the stress wave procedures underestimated pile capacity. A standalone program "ReliaPile" was written in MATLAB® to speed up the reliability analysis of the information contained in the database. The program uses the First Order Second Moment (FOSM) Method, the First Order Reliability Method, and Monte Carlo simulations to compute resistance factors. An improved FOSM method was developed, which is explicit in form and requires less computational capability

requirements. All reported resistance factors were determined based on the strength limit state at the target reliability indices of 2.33 and 3.00.

The process of developing the LRFD protocol led to a much better understanding of factors that contribute to the performance of deep foundations. This study also addressed a Bayesian technique to update resistance factors when new load tests are added to the database. This study delivered the following benefits:

1. A well-structured and easy to navigate electronic database that contains pile load test data and relevant soils information.
2. A calibrated and cost effective LRFD protocol that seeks to unify the level of reliability for deep foundations through both the design and construction phases.
3. A clear, concise, and reliable LRFD framework that can be utilized to refine resistance factors for a local pile design.
4. A monitoring program which increases the accuracy of estimates of the actual in-situ capacity during pile driving.
5. A methodology to properly compare predicted static pile capacity to driving resistance through a correction factor.

As a result of the above listed deliverables, piles could be designed for much higher loads or could be driven to a lower blow count for the required design loads.

6.1.2 Ranking Pile Analysis Methods

6.1.2.1 Signal Matching at BOR and Wave Equation Analysis

Based on the efficiencies of different pile analysis methods, signal matching by CAPWAP at 14 day restrike performs best and is recommended for the construction control of

driven piles. CAPWAP capacities at BOR are close to the capacities measured by static load tests; and they can help detect soil setup or relaxation at the time of restike.

The use of the bearing graph derived from WEAP is less efficient when compared to signal matching. However, WEAP becomes more effective when it is utilized in tandem with signal matching. It was documented that the calibration results provided by the AASHTO LRFD specifications for WEAP are based on default input of dynamic parameters for both the hammer and the soils. The performance of the WEAP method could be improved if the dynamic characteristics describing the interaction of the hammer-pile-soil system are derived from signal matching.

6.1.2.2 Signal Matching at EOD

Dynamic measurement with subsequent signal matching at EOD does not account for the time dependent soil-setup. Consequently, it would be too conservative to directly compare the EOD results to the required ultimate capacity. However, during the piling process, dynamic measurements and quasi-real time signal matching can help prevent pile damage resulting from over driving by measuring internally induced driving stresses.

The calibrated resistance factor for dynamic testing with subsequent signal matching at EOD did consider soil setup because the calibration was referenced to the long term SLT capacity. To reap the benefits of the soil-setup effect, a resistance factor greater than unity and equivalent to the effective soil-setup factor is employed at the EOD. In that context, the PDA/CAPWAP results at EOD could be employed to accept the pile construction work in cohesive soils, but soil-setup must be verified afterwards. The alternative option is to establish a time dependent soil-setup relationship for the region which would be coupled with the EOD capacity to predict long term capacity.

When capacity by signal matching at EOD does not fulfill the acceptance criterion after the pile has reached the contract length, a 24 hour restrike can be planned to assess the possibility of soil-setup before the pile is driven further or is spliced. This could save time for a busy construction scheduled or help avoid price overruns associated with waiting time to restrike.

In general, the PDA combined with CAPWAP at EOD works best when it is employed to measure capacities of end bearing piles on rock or piles driven into soils where soil-setup is not anticipated.

6.1.2.3 Driving Formulas

Overall, driving formulas have the tendency to over-predict the ultimate capacity of the piles. Over-predicting the capacity could lead to a greater risk that the driven pile length would become too short to provide adequate bearing. But the tendency to over-predict the capacity could also prevent imminent damage of the pile from potential high induced driving stresses

The ENR formula performed poorly, and its use should be avoided. This is in contrast to current AHTD specifications. The FHWA-modified Gates formula performed better than the ENR and this finding agrees with AASHTO LRFD Bridge Design Specifications (2012). In general, the use of driving formulas is not recommended. However, if it is deemed necessary to use them, the FHWA-modified Gates formula would be the best choice.

The comparison between driving formulas and signal matching (EOD and BOR) revealed that although they are utilized at EOD, they are designated to predict long term capacity. Therefore, if a driving formula is used to establish stopping criteria, a supplementary verification of the pile capacity by dynamic testing at BOR is strongly recommended.

6.1.2.4 Static Pile Analysis Method

Static pile analysis using the program DRIVEN tends to over-predict long term capacity of piles. This is due in part to correlations utilized in transforming field test results to soil strength parameters. Over-predicting the ultimate pile resistance could cause non-agreement between contract and driven pile lengths on the jobsite. A correction factor was introduced to promote agreement between static analysis and dynamic monitoring, and to enable a direct comparison between the predicted static capacity and the dynamically measured capacity.

Resistance factors that were established for static analysis in non-cohesive soils only correspond to the Nordlund/Thurman method (Nordlund, 1963; Thurman, 1964) imbedded in the program DRIVEN. Likewise, the calibrated resistance factors for static analysis in cohesive soils only correspond to the α-Tomlinson's method (1957, 1971). In this study, where undrained cohesion of the soil was not available, it was derived from SPT N-values using Terzaghi and Peck (1961) correlations.

6.1.3 Reliability Methods and the Use of the Calibrated Resistance Factors

During the calibration process, the simplified closed form solution using FOSM underestimated resistance factors by about 20%, 15%, and 12% in low, medium, and high site variability respectively. Therefore, this FOSM reliability method should only be restricted to preliminary analyses. On the other hand, the Improved-FOSM is recommended because it has lower computing requirements and yields similar results as the FORM and Monte Carlo Simulations.

Regardless of the reliability method utilized, the resistance factors are reduced by about 20% for non-redundant pile groups (with β_T of 3.00) when compared to those of redundant piles (with β_T of 2.33). Despite this difference in resistance factors and pile redundancy, the overall

resulting foundation has an equivalent target reliability of 3.00, which corresponds to a 0.1% probability of failure.

The accuracy of pile analysis method can be increased through robust regression analysis by bringing the overall coefficient of regression close to unity. However, it is practically impossible to improve the precision (scatter) in actual data with the same regression approach because the precision is inherent to the prediction method. Through the LRFD calibration based on reliability theory, the calculated resistance factors solved those precision issues to an acceptable level of risk.

When more soils and load test data was available, the more likely the calibrated resistance factors were closer to or greater than those recommended by the AASHTO LRFD Bridge Specifications. The use of those calibrated resistance factors significantly reduced the large variation that was apparent in the predicted and measured nominal pile resistances. Knowing in advance the field capacity verification method allows the use of a higher resistance factor during the design phase.

Locally calibrated resistance factors are bound to the procedures used during calibration process, and this remains true for every step of the calibration. A new LRFD calibration is required whenever any (minor or major) alteration is made in the design or construction procedure. For instance, when SPT-N values are the only available soil data for cohesive layers and are utilized to estimate undrained shear strength using new or existing transformations, then each transformation should have its own calibrated resistance factor.

6.1.4 Bayesian Updating and Adjusting Factor

To incorporate future pile load data in the calibration process, an updating technique was introduced based on the Bayesian approach. It was observed that, at the end of a simulated

process of updating, it did not matter whether pile load data arrived sequentially or in groups. This finding makes the updating process easy and continuous. In general, as more pile load test data is collected, the uncertainties will continue to diminish and the updated resistance factors will continue to become more definitive. Subsequently, the updated design and acceptance protocol will continue to yield more and more reliable pile foundations.

A correction factor was introduced to reduce the disparity between the results of the design and construction phases, and it resulted from the statistical analysis between static pile design method and pile capacity verification method. This correction factor was also needed to promote agreement between predicted and measured pile capacities, and between contract and driven pile lengths. As more pile data continue to accumulate, the correction factor will continue to adjust and the level of agreement is expected to rise.

Bayesian simulations revealed that the resistance factor updates continually as the measurement pile load data accumulate. As more load test data is produced in the future, this process of Bayesian updating can be employed to achieve more economical pile designs in deep foundations.

6.1.5 Acceptance Criteria

A set of acceptance criteria was developed as part of the quality assurance testing plan to accept untested piles based on a set of randomly and successfully tested production piles. Those criteria were established based on the confidence interval approach. The determined series of acceptance criteria satisfies the acceptable owner's risk, and allows the contractor to minimize the risk for incorrectly rejecting a set of production piles.

According to the acceptance criteria, the number of piles that should be load tested on a jobsite depends on the variability of the subsurface conditions, the size of the project, the type of

construction control method, and the reasons for performing the tests. To check the correctness of the developed acceptance criteria, back analyses using a Bayesian approach were successfully performed. It was observed that the first few pile load tests are the most compelling factors in reducing acceptance criteria, and that the testing many piles reduces that criteria by only a small amount.

When a construction site is well characterized, the acceptance ratio and the number of load tests required to accept a set of driven piles could be reduced, thus reducing the cost of the quality assurance testing plan.

Based on the available information in the database, the general findings of this work are better applied to piles classified as friction piles. Although a full scale pile load testing program is still required to verify and refine the proposed LRFD design and acceptance protocol, it is believed that this protocol closes the gaps that exists in the AHTD piling specifications.

6.2 Recommendations and Future Work

6.2.1 Full Scale Pile Load Testing Program and Need for More Data

As in any newly developed approach, a validation phase is recommended to verify the applicability of the design and acceptance protocol beyond the actual available database. For the effectiveness of this validation phase, it was determined that a full-scale pile load testing program is required to verify both the reliability and the consistency of the calibrated resistance factors. This program would be composed of at least 15 driven piles that had been dynamically and statically load tested. Those load tests should be closely monitored to increase the accuracy of the soil property and the driving data. The outcomes of these load tests would be used to statistically refine both the calibrated resistance factor by means of a Bayesian technique and the correction factor that incorporate the method of construction control into the design. By way of

conducting full scale field verification, a more reliable and cost effective piled foundation would be achieved.

In general, categorizing soils and piles would reduce uncertainties in the data, and would result in increased resistance factors and efficiency factors. However, due to insufficient data in some of the cases in this study, categorization actually resulted in higher coefficients of variation and lower resistance factors rather than improving them. To adequately address more definitive results and achieve an optimized design and acceptance protocol for each and every soil and pile category, more data for soils and pile load tests is required. It is therefore not if but when such high quality soils and load test data is going to be collected within the State of Arkansas. Much larger resistance factors can be locally adopted in design after a large-scale and high quality data is collected and fed to the existing database.

6.2.2 LRFD Calibration Based on Serviceability Limit State

The strength limit state has been the only equilibrium state used for a typical calibration of resistance factors in deep foundations. However, if settlement is an issue to the superstructure, the design of its foundation should be based on serviceability. It is imperative that future work also consider calibrating resistance factors based on the serviceability limit state. The outcome of such calibration would provide a great opportunity to interactively compare the resulting foundations based on those two limit states.

6.2.3 Refining LRFD Design Protocol by Dynamic Testing

Due to high cost associated with static load testing (SLT) and inaccuracy in using driving formulas, dynamic testing coupled with signal matching has become the sole preferred method of monitoring in pile driving industry. For a dynamically load tested pile, static capacity is found by subtracting dynamic resistance from total resistance at EOD or at BOR conditions. The obtained

static capacity is used to either accept or reject the pile. Based on the existing studies of the bias of the pile resistance measured by dynamic method, future measurements of the pile capacity using dynamic methods could be employed to improve the resistance factor for the static analysis methods. This approach of updating existing resistance factors using dynamic testing (without requiring SLT) would result in optimized design and construction of piled foundation through testing, and would cut the cost otherwise required by the SLT.

6.2.4 Using SLT Proof Tests in the LRFD calibration Process

The LRFD calibration process for pile foundations requires that piles be statically load tested until failure so that the ultimate capacity can be known. However, for many cases histories in the past pile capacity verification was based on proof load tests that were not carried to failure, and that practice has persisted even today. For instance, the AHTD specifications manual only requires the maximum test load for an SLT to be twice the design load. Any pile that fulfills this acceptance criterion would have its ultimate capacity (although unknown) greater than the maximum load. It is recommended for future work to look into possibility of incorporating proof load test results into LRFD calibration process because, in reliability analysis of deep foundations, any existing or new information related to the foundation in question could be utilized to improve the design. This could be done by using censored data analysis techniques to handle proof load test results.

6.2.5 The PDM for More Reliable Foundations and Inexpensive QA Program

It was observed that the greater the number of tested production piles, the more reliable the measured ultimate capacity becomes, and the smaller the acceptance ratio could become. However, the increase in sampling effort would increase the cost associated with testing and slow the construction effort. In an effort to beat the high cost and increased time associated with

an increased sampling effort, a new Pile Driving Monitoring (PDM) device is recommended. This non-contact device would facilitate the acceptance testing of every pile on the jobsite. The capability of the PDM to quickly measure capacity in real time for each and every element of the entire population of production piles would result in more reliable foundation and in a much reduced acceptance capacity. The use of the PDM could provide mobility and ease in performing dynamic measurements, but most importantly it could provide valuable data correlations that can be utilized to update the existing pile load test database. This enormous quantity data would help in reducing some of the unknown parameters that are inherent to current pile design practices.

6.2.6 Combining Indirect or Direct Pile Verification Tests to Minimize the QA Cost

The application of the Bayesian technique showed that the exercise of updating the LRFD design and acceptance protocol can be repeated if more indirect or direct verification tests are conducted. Bayesian technique could be employed to combine several pile testing techniques on large projects. Inference made from the results of previous chapters indicates that a high resistance factor could be obtained without compromising the safety of the foundation if several testing methods are combined on the same construction site. For example, the following scenario could be studied: The AHTD could first set preliminary pile length based on a static pile analysis and this would constitute the prior knowledge. The pile performance would then be verified by PDA tests using either preliminary test piles or a portion of production piles. The combination of the static analysis (prior) and the PDA tests will result in a posterior distribution. Considering the posterior distribution after the PDA tests as a prior, the pile performance is further updated based on the outcome of the signal matching using CAPWAP analyses, and the final stage can be updated based on the outcome of the static load tests on piles tested to failure or proof load tests. The outcome of that study could be formulated in a structured statement such as: After

estimating the design length, a specified percentage of the production piles is required to verify the design parameters and to test the workmanship. In addition, up to a specified percentage of the production piles may be monitored using PDA, and a specified portion of these PDA tests may be analyzed by CAPWAP. At the end of construction, a specified small percentage of production piles may be proof-tested using static loading tests.

References

AASHTO. (1997). Standard Specifications for Highway Bridges: 16th Edition (1996 with 1997 interims). Washington, D.C.: American Association of State Highway and Transportation Officials.

AASHTO. (2004). LRFD Bridge Design Specifications (3rd ed.). Washington, D.C.: American Association of State Highway and Transportation Officials.

AASHTO. (2007). LRFD Bridge Design Specifications (4th ed.). Washington, D.C.: American Association of State Highway and Transportation Officials.

AASHTO. (2012). LRFD Bridge Design Specifications (6th ed.). Washington, D.C.: American Association of State Highway and Transportation Officials.

AbdelSalam, S. S., Ng, K. W., Sritharan, S., Suleiman, M. T., & Roling, M. (2012). Development of LRFD Procedures for Bridge Pile Foundations in Iowa-Volume III: Recommended Resistance Factors with Consideration of Construction Control and Setup.

Abu-Farsakh, M. Y., Yoon, S., & Tsai, C. (2009). Calibration of Resistance Factors Needed in the LRFD Design of Driven Piles.

AHTD. (2003). Standard Specifications for Highway Construction *Piling* (Vol. 2003, pp. 731-758). Little Rock, Arkansas: Arkansas State Highway and Transportation Department.

AHTD. (2014). Standard Specifications for Highway Construction *Piling*. Little Rock, Arkansas: Arkansas State Highway and Transportation Department.

AHTD. (n.a.). *The AHTD Construction Reports*. Piling reports. Arkansas Highway and Transportation Department.

Allen, T. M. (2005). Development of the WSDOT Pile Driving Formula and Its Calibration for Load and Resistance Factor Design (LRFD).

Allen, T. M., Laboratory, W. D. o. T. M., & Institute, N. H. (2005). *Development of Geotechnical Resistance Factors and Downdrag Load Factors for LRFD Foundation Strength Limit State Design: Reference Manual*: US Department of Transportation, Federal Highway Administration, National Highway Institute.

Anderson, T. W., & Darling, D. A. (1954). A test of goodness of fit. *Journal of the American Statistical Association, 49*(268), 765-769.

Ang, A. H. S., & Tang, W. H. (1975). *Probability concepts in engineering planning and design* (Vol. 1): John Wiley & Sons, New York.

Ang, A. H. S., & Tang, W. H. (2007). Probability Concepts in Engineering-Emphasis on Applications to Civil and Environmental Engineering, : John Wiley & Sons, New York.

API. (2000). Recommended Practice for Planning, Designing, and Constructing Fixed Offshore Platforms-Working Stress Design *American Petroleum Institute Recommended Practice 2A-WSD (RP 2A-WSD)* (21 ed.). Washington, D.C.

ASTM Standard D1143/D1143M-07e1. (2007). Standard Test Methods for Deep Foundations under Static Axial Compressive Load. West Conshohocken, PA: ASTM International.

ASTM Standard D4945-12. (2012). Standard Test Method for High-Strain Dynamic Testing of Deep Foundations. West Conshohocken, PA: ASTM International.

Ayyub, B. M., & McCuen, R. H. (2002). *Probability, statistics, and reliability for engineers and scientists*: Chapman & Hall/CRC.

Baecher, G. B., & Christian, J. T. (2003). *Reliability and statistics in geotechnical engineering*: John Wiley & Sons Inc.

Barker, R., Duncan, J., Rojiani, K., Ooi, P., Tan, C., & Kim, S. (1991). NCHRP report 343: manuals for the design of bridge foundations. *Transportation Research Board, National Research Council, Washington, DC*.

Beaton, A. E., & Tukey, J. W. (1974). The Fitting of Power Series, Meaning Polynomials, Illustrated on Band-Spectroscopic Data. *Technometrics*, 147-185.

Becker, D. E., & Devata, M. (2005). *Implementation and Application Issues of Load and Resistance Factor Design (LRFD) for Deep Foundations.* Paper presented at the Contemporary Issues in Foundation Engineering (GSP 131).

Bowles, J. E. (1996). *Foundation Analysis and Design*: McGraw-Hill, New York.

Briaud, J.-L., & Tucker, L. M. (1988). Measured and predicted axial response of 98 piles. *Journal of Geotechnical Engineering, 114*(9), 984-1001.

Brown, D. A., & Thompson, W. R. (2011). *Developing Production Pile Driving Criteria from Test Pile Data* (Vol. 418): Transportation Research Board.

Butler, H. D., & Hoy, H. B. (1977). *Users manual for the Texas quick-load method for foundation load testing*. Washington, D.C.: FHWA-IP- 77-8. FHWA, Offices of Research and Development, Implementation Division.

Chellis, R. D. (1949). The Relationship between Pile Formulas and Load Tests. *Transactions of the American Society of Civil Engineers, 114*(1), 290-309.

Chellis, R. D. (1951). *Pile Foundations: Theory, Design, Practice*. New York: McGraw-Hill Book Co.

Cheney, R., & Chassie, R. (2000). *Soils and Foundations Workshop Reference Manual*. Washington, DC: National Highway Institute, Federal Highway Administration, U.S. Department of Transportation

Cheney, R. S., & Chassie, R. G. (1982). *Soils and Foundations Workshop Manual*: Department of Transportation, Federal Highway Administration.

Chow, F., Jardine, R., Brucy, F., & Nauroy, J. (1998). Effects of time on capacity of pipe piles in dense marine sand. *Journal of Geotechnical and Geoenvironmental Engineering, 124*(3), 254-264.

Conover, W. J. (1999). Statistics of the Kolmogorov-Smirnov type. *Practical nonparametric statistics*, 428-473.

Cook, R. D. (1977). Detection of influential observation in linear regression. *Technometrics*, 15-18.

Cornell, C. A. (1969). *A probability-based structural code.* Paper presented at the American Concrete Institute Journal Proceedings.

D'Agostino, R. B. (1986). *Goodness-of-fit-techniques* (Vol. 68): CRC.

D'Andrea, A. W., & Tsai, C. (2009). Louisiana Department of Transportation and Development's Experience with LRFD. *Transportation Research E-Circular*(E-C136).

Davisson, M. T. (1972). *High capacity piles.* Paper presented at the Proceedings Lecture Series on Innovations in Foundation Construction, Chicago, IL.

DeBeer, E. E. (1970). Experimental determination of the shape factors and the bearing capacity factors of sand. *Geotechnique, 20*(4), 387-411.

Decourt, L. (1999). *Behavior of foundations under working load conditions.* Paper presented at the Proceedings of the 11th Pan-American Conference on Soil Mechanics and Geotechnical Engineering, Foz DoIguassu, Brazil.

Dennis, N. D. (1982). *Development of correlations to improve the prediction of axial pile capacity.* University of Texas at Austin.

Dennis, N. D. (2012). [Personal communication on driven piles that were driven in geological settings similar to Arkansas].

Devroye, L. (1986). *Non-uniform random variate generation* (Vol. 4): Springer-Verlag New York.

Ebeling, C. E. (1997). An introduction to reliability and maintainability engineering: The Mcgraw-Hill Companies, Inc., New York.

Esrig, M. I., & Kirby, R. C. (1979). Soil Capacity for Supporting Deep Foundation Members in Clay. *ASTM STP. No. 670*, 27-63.

Fellenius, B. H. (1988). *Variation of CAPWAP results as a function of the operator.* Paper presented at the Proc. of the 3rd Int. Conf. on the Application of Stress Wave Theory to Piles, Ottawa, Canada.

Fellenius, B. H. (1991). Summary of pile capacity predictions and comparison with observed behavior. *American Society of Civil Engineers, ASCE, Journal of Geotechnical Engineering, 117*(1), 192−195.

Fellenius, B. H. (2001). *What capacity value to choose from results of a static loading test*. Paper presented at the Fulcrum, Deep Foundation Institute New Jersey.

Fragaszy, R. J., Argo, D., & Higgins, J. D. (1989). Comparison of formula predictions with pile load tests. *Transportation Research Record*(1219).

Fragaszy, R. J., Higgins, J. D., & Lawton, E. C. (1985). Development of Guidelines for Construction Control of Pile Driving and Estimation of Pile Capacity-Phase I-Final Report

Gates, M. (1957). Empirical formula for predicting pile bearing capacity. *Civil Engineering, 27*(3), 65-66.

Gibbons, J. D., & Chakraborti, S. (2003). *Nonparametric statistical inference* (Vol. 168): CRC press.

Glanville, W. H., Grime, G., Fox, E. N., Davies, W. W., & Institution of Civil, E. (1938). *An investigation of the stresses in reinforced concrete piles during driving*: HM Stationery Office.

Goble, G. G., Likins, G., & Rausche, F. (1975). Bearing Capacity of Piles from Dynamic Measurements–Final Report. *Dept. of Civil Engineering, Case Western Reserve University, Cleveland, Ohio*.

Goble, G. G., & Rausche, F. (1980). The analysis of pile driving A state-of-the-art. *Int. Seminar on the Application of Stress-Wave Theory on Pile/Stockholm*, 131-161.

Hammersley, J. M., & Handscomb, D. C. (1964). Monte Carlo Methods, Methuen's Monographs on Applied Probability and Statistics. *Methuen & Co., London*.

Hannigan, P. J., Goble, G. G., Likins, G. E., & Rausche, F. (2006). Design and Construction of Driven Pile Foundations (Volume I and II). *Report No. FHWA-NHI-05, National Highway Institute, Washington, DC*.

Hannigan, P. J., Goble, G. G., Thendean, G., Likins, G. E., & Rausche, F. (1998). Design and Construction of Driven Pile Foundations-Volume I.

Hara, A., Ohta, T., Niwa, M., Tanaka, S., & Banno, T. (1974). Shear modulus and shear strength of cohesive soils. *Soils and Foundations, 14*(3), 1-12.

Hasofer, A. M., & Lind, N. C. (1974). Exact and invariant second-moment code format. *Journal of the Engineering Mechanics Division, 100*(1), 111-121.

Isenhower, W. M., & Long, J. H. (1997). Reliability evaluation of AASHTO design equations for drilled shafts. *Transportation Research Record: Journal of the Transportation Research Board, 1582*(1), 60-67.

Jabo, J. (2014a). Database for Driven Pile Foundation in Arkansas.

Jabo, J. (2014b). ReliaPile 1.0: A MATLAB® Based Program for Analyzing Pile Capacity Distribution and LRFD Calibration for Driven Piles. User's Manual.

Janbu, N. (1953). Une analyse energetique du battage des pieux a l'aide de parametres sans dimension. *Norwegian Geotech. Inst*, 63-64.

John Pak, C. H., Danny Chung, K. C., Hammus Chui, W. M., Romeo Yiu, F. H., & Seidel, J. P. (n.a). Innovative Method for Remote Measurement of Pile Set and Temporary Compression of Driven H-piles in Hong Kong Retrieved 29 Jan., 2013, from http://piling.ir/images/stories/HKIE%20Paper%20-%20Pioneering%20Use%20of%20PDM.pdf

Jones, A. L., Kramer, S. L., & Arduino, P. (2002). *Estimation of uncertainty in geotechnical properties for performance-based earthquake engineering*: Pacific Earthquake Engineering Research Center, College of Engineering, University of California.

Kalavar, S., & Ealy, C. (2000). *FHWA Deep Foundation Load Test Database.* Paper presented at the New Technological and Design Developments in Deep Foundations (GSP100)-Proceedings of Sessions of Geo-Denver 2000, Denver.

Kay, J. N. (1976). Safety factor evaluation for single piles in sand. *Journal of the Geotechnical Engineering Division, 102*(10), 1093-1108.

Kraft, L. M., Amerasinghe, S. F., & Focht, J. A. (1981). Friction capacity of piles driven into clay. *Journal of the Geotechnical Engineering Division, 107*(11), 1521-1541.

Kulhawy, F. H., & Phoon, K. K. (2002). *Observations on geotechnical reliability-based design development in North America.* Paper presented at the Proc. Int. Workshop on Foundation Design Codes and Soil Investigation in view of International Harmonization and Performance Based Design.

Kulhawy, F. H., & Trautmann, C. H. (1996). *Estimation of in-situ test uncertainty.* Paper presented at the Uncertainty in the Geologic Environment:from Theory to Practice (GSP 58).

Lacasse, S., Guttormsen, T. R., & Goulois, A. (1990). *Bayesian updating of axial capacity of single pile.* Paper presented at the Structural Safety and Reliability.

Lacasse, S., Tan, A. H., Keaveny, J., Goulois, A., & Boisard, P. (1992). Expert assistant for updating axial pile capacity from pile driving observations. *Publikasjon-Norges Geotekniske Institutt, 186*.

Lazarte, C. A. (2011). *Proposed Specifications for LRFD Soil-Nailing Design and Construction* (Vol. 701): Transportation Research Board.

Likins, G., Rausche, F., & Goble, G. G. (2000). *High strain dynamic pile testing, equipment and practice.* Paper presented at the Proceedings of the Sixth International Conference on the Application of Stress-wave Theory to Piles.

Likins, G. E., Rausche, F., Thendean, G., & Svinkin, M. (1996). *CAPWAP correlation studies.* Paper presented at the STRESSWAY'96 Conference, Orlando, FL.

Lilliefors, H. W. (1967). On the Kolmogorov-Smirnov test for normality with mean and variance unknown. *Journal of the American Statistical Association, 62*(318), 399-402.

Long, J. H., Kerrigan, J. A., & Wysockey, M. H. (1999). Measured time effects for axial capacity of driven piling. *Transportation Research Record: Journal of the Transportation Research Board, 1663*(1), 8-15.

Long, J. H., & Shimel, S. (1989). *Drilled Shafts—A Database Approach.* Paper presented at the Foundation Engineering: Current Principles and Practices.

Loukidis, D., & Salgado, R. (2008). Analysis of the shaft resistance of non-displacement piles in sand. *Géotechnique, 58*(4), 283-296.

Low, B. K., & Tang, W. H. (1997). Efficient reliability evaluation using spreadsheet. *Journal of engineering mechanics, 123*(7), 749-752.

Low, B. K., & Tang, W. H. (2004). Reliability analysis using object-oriented constrained optimization. *Structural safety, 26*(1), 69-89.

Martinez, W. L., & Martinez, A. R. (2001). *Computational statistics handbook with MATLAB*: CRC press.

Mathias, D., & Cribbs, M. (1998). DRIVEN 1.0: A Microsoft Windows (Trademark) Based Program for Determining Ultimate Vertical Static Pile Capacity. User's Manual.

McVay, M. C., Alvarez, V., Zhang, L., Perez, A., & Gibsen, A. (2002). Estimating driven pile capacities during construction.

McVay, M. C., Birgisson, B., Zhang, L., Perez, A., & Putcha, S. (2000). Load and resistance factor design (LRFD) for driven piles using dynamic methods: A Florida perspective. *ASTM geotechnical testing journal, 23*(1), 55-66.

Meyerhof, G. (1956). Penetration tests and bearing capacity of cohesionless soils. *Journal of the Soil Mechanics and Foundations Division, ASCE, 82*(SM1), 1-19.

Meyerhof, G. (1976). Bearing Capacity and Settlement of Pile Foundations. *Journal of the Geotechnical Engineering Division, ASCE, 102*(3), 195-228.

MoDOT. (n.a.). *The MoDOT construction reports*. Driven Piles. Missouri Department of Transportation.

Nordlund, R. L. (1963). Bearing capacity of piles in cohesionless soils. *ASCE, SM&F Journal SM-3, 89*, 36.

Nottingham, L., & Schmertmann, J. H. (1975). An Investigation of Pile Capacity Design Procedures. *Final Report D629 to Florida Department of Transportation, Department of Civil Engineering, University of Florida*.

Nowak, A. S. (1999). NCHRP report 368: Calibration of LRFD bridge design code. Washington, DC.: Transportation Research Board.

Olson, R. E., & Flaate, K. S. (1967). Pile-Driving Formulas for Friction Piles in Sand. *Journal of Soil Mechanics and Foundation Division*(ASCE, No. SM 6), 279−296.

Paikowsky, S. G., Birgisson, B., McVay, M., Nguyen, T., Kuo, C., Baecher, G. B., . . . Chernauskas, L. (2004). *Load and resistance factor design (LRFD) for deep foundations. NCHRP Report 507*. Washington DC: Transportation Research Board of the National Academies.

Paikowsky, S. G., Canniff, M. C., Lesny, K., Kisse, A., Amatya, S., & Muganga, R. (2010). LRFD design and construction of shallow foundations for highway bridge structures. NCHRP Report 651. *Transportation Research Board, Washington, DC*.

Peck, R. B., Hanson, W. E., & Thornburn, T. H. (1974). *Foundation engineering*: Wiley New York.

Phoon, K. K. (2004). General non-Gaussian probability models for first order reliability method (FORM): A state-of-the art report. *ICG Rep*(2004-2), 4.

Phoon, K. K. (2008). *Reliability-based design in geotechnical engineering: computations and applications*. New York: Taylor & Francis.

Phoon, K. K., & Kulhawy, F. H. (2005). Characterization of model uncertainties for laterally loaded rigid drilled shafts. *Géotechnique, 55(1)*, 45–54.

Rackwitz, R. (2001). Reliability analysis—a review and some perspectives. *Structural Safety, 23*(4), 365-395.

Rackwitz, R., & Flessler, B. (1978). Structural reliability under combined random load sequences. *Computers & Structures, 9*(5), 489-494.

Rahman, M. S. (2002). *Load and Resistance Factor Design (LRFD) for Analysis/Design of Piles Axial Capacity.* North Carolina State University.

Rausche, F., Liang, L., Allin, R. C., & Rancman, D. (2004). *Applications and correlations of the wave equation analysis program GRLWEAP.* Paper presented at the Proceedings, VII Conference on the Application of Stress Wave Theory to Piles.

Rausche, F., Nagy, M., Webster, S., & Liang, L. (2009). CAPWAP and Refined Wave Equation Analyses for Driveability Predictions and Capacity Assessment of Offshore Pile Installations. Retrieved February 11, 2014, from http://www.piledrivers.org/files/uploads/6BD01A99-679C-4D5F-92A9-D8920952ED61.ppt

Razali, N. M., & Wah, Y. B. (2011). Power comparisons of shapiro-wilk, kolmogorov-smirnov, lilliefors and anderson-darling tests. *Journal of Statistical Modeling and Analytics, 2*(1), 21-33.

Robinsky, E., & Morrison, C. (1964). Sand displacement and compaction around model friction piles. *Canadian Geotechnical Journal, 1*(2), 81-93.

Roling, M. J., Sritharan, S., & Suleiman, M. T. (2010). Development of LRFD Procedures for Bridge Pile Foundations in Iowa Volume I: An Electronic Database for PIle LOad Tests (PILOT).

Schmertmann, J. H. (1975). *Measurement of in situ shear strength, state-of-the-art report.* Paper presented at the Proceedings of the American Society of Civil Engineers Conference on In Situ Measurements of Soil Properties, Raleigh, NC.

Schmertmann, J. H. (1978). Guidelines for Cone Penetration Test.(Performance And Design).

Sidi, I. D., & Tang, W. H. (1985). *Updating friction pile capacity in clay.* Paper presented at the Proceedings of the 5 th International Conference on Application of Statistics and Probability in Soil and Structural Engineering.

Smith, E. A. (1962). Pile driving analysis by the wave equation. *American Society of Civil Engineers Transactions*.

Smith, T., Banas, A., Gummer, M., & Jin, J. (2011). Recalibration of the GRLWEAP LRFD Resistance Factor for Oregon DOT.

Smith, T., & Dusicka, P. (2009). Application of LRFD Geotechnical Principles for Pile Supported Bridges in Oregon: Phase 1.

Terzaghi, K. (1942). *Discussion of the progress report of the committee on the bearing value of pile foundations.* Paper presented at the Proceedings, ASCE.

Terzaghi, K., & Peck, R. B. (1961). *Die Bodenmechanik in der Baupraxis*: Springer.

Thurman, A. G. (1964). *Computed load capacity and movement of friction and end-bearing piles embedded in uniform and stratified soils.* Carnegie Institute of Technology.

Tomlinson, M. J. (1957). *The adhesion of piles driven in clay soils*.

Tomlinson, M. J. (1971). *Some effects of pile driving on skin friction*.

Tomlinson, M. J. (1987). Foundation Design and Construction. *Scientific and Technical, Essex, England*.

U.S. Army Corps of Engineers. (1997). *Design of Deep Foundations, Technical Instructions*. Washington, DC.

Vijayvergiya, V. N., & Focht Jr., J. A. (1972). A New Way to Predict Capacity of Piles in Clay. *Proceedings of the 4th Annual Offshore Technology Conference, Texas, 2*, 856-874.

Wainaina, N., Kim, K. J., & Chen, C. (2009). North Carolina Department of Transportation's Experience with LRFD. *Transportation Research E-Circular*(E-C136).

Wellington, A. M. (1888). Formulae for Safe Loads of Bearing Piles. *Engineering News 20*, 509-512.

Withiam, J. L., Voytko, E. P., Barker, R. M., Duncan, J. M., Kelly, B. C., Musser, S. C., & Elias, V. (1998). Load and resistance factor design (LRFD) for highway bridge substructures. *Report FHWA HI-98-032. Federal Highway Administration, Washington, DC*.

Yang, L. (2006). *Reliability-Based Design and Quality Control of Driven Piles.* The University of Akron. Retrieved from http://etd.ohiolink.edu/send-pdf.cgi/Yang%20Luo.pdf?akron1153755606

Zhang, L. (2004). Reliability verification using proof pile load tests. *Journal of geotechnical and geoenvironmental engineering, 130*(11), 1203-1213.

Zhang, L., & Tang, W. H. (2002). *Use of load tests for reducing pile length*.

Appendix A Results of the Regression Analysis

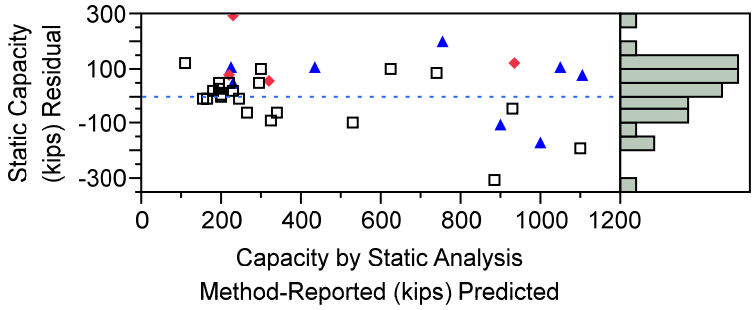

(a)

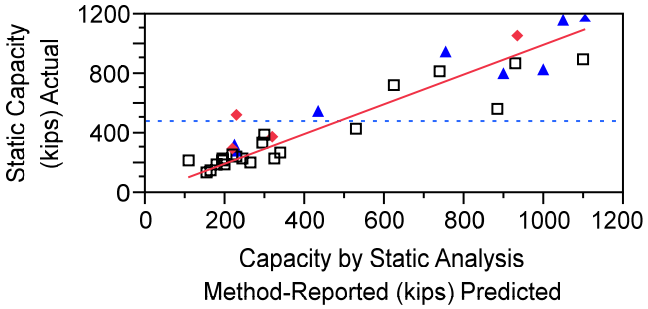

(b)

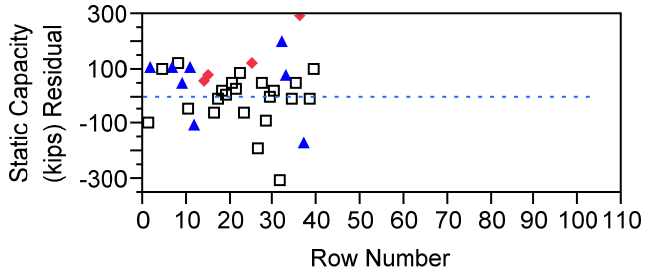

(c)

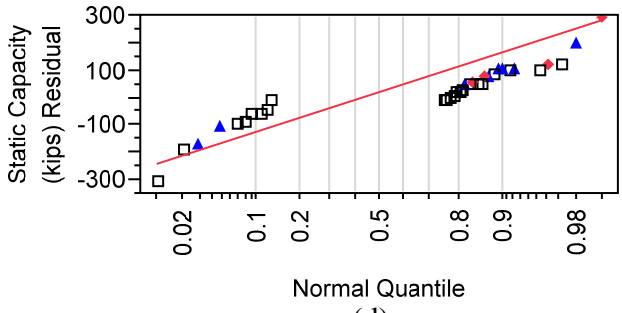

(d)

A.1 Diagnostics Plots of (a) Residual versus Predicted, (b) Actual versus Predicted, (c) Residual versus Row Order, and (d) Residual Normal Quantile for the Regression Analysis of Static Pile Capacity (Reported Capacity Values by Louisiana DOT) versus SLT capacity presented in Figure 3-14.

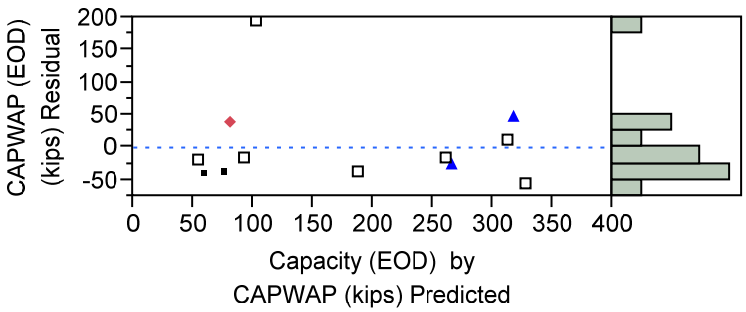

(a)

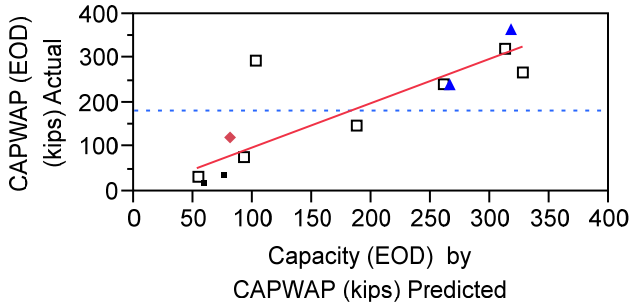

(b)

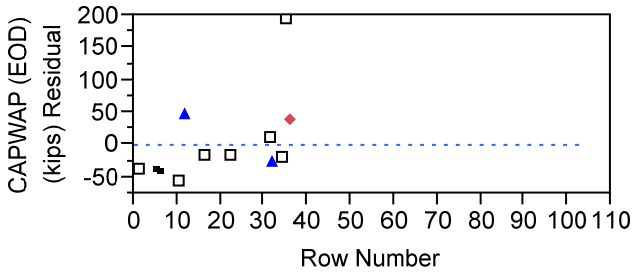

(c)

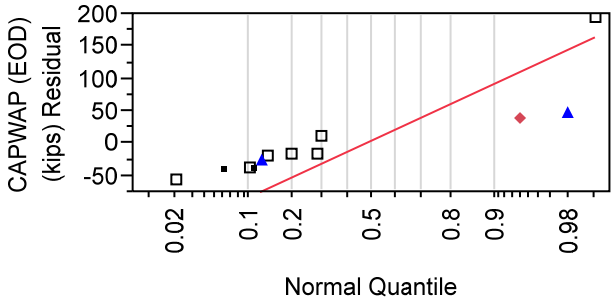

(d)

A.2 Diagnostics Plots of (a) Residual versus Predicted, (b) Actual versus Predicted, (c) Residual versus Row Order, and (d) Residual Normal Quantile for the Regression Analysis of CAPWAP Capacity versus SLT capacity presented in Figure 3-15.

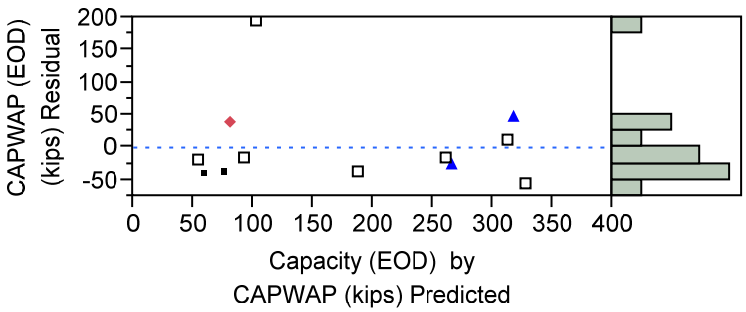

(a)

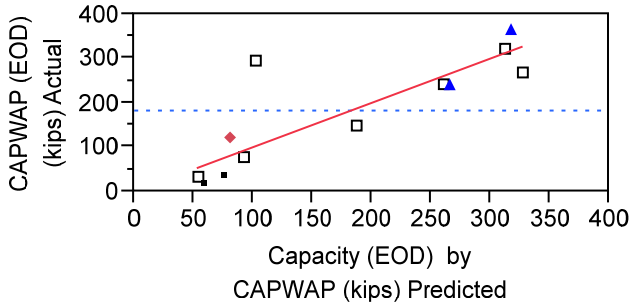

(b)

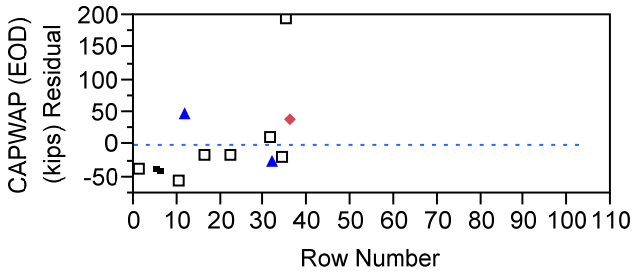

(c)

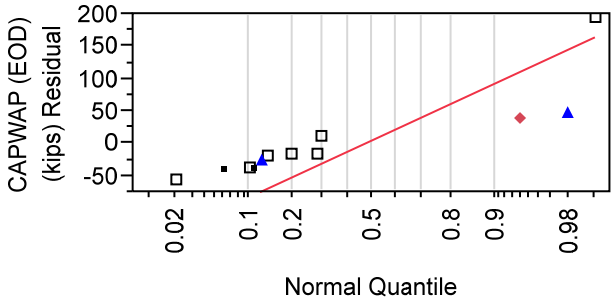

(d)

A.3 Diagnostics Plots of (a) Residual versus Predicted, (b) Actual versus Predicted, (c) Residual versus Row Order, and (d) Residual Normal Quantile for the Regression Analysis of CAPWAP Capacity versus SLT capacity presented in Figure 3-15.

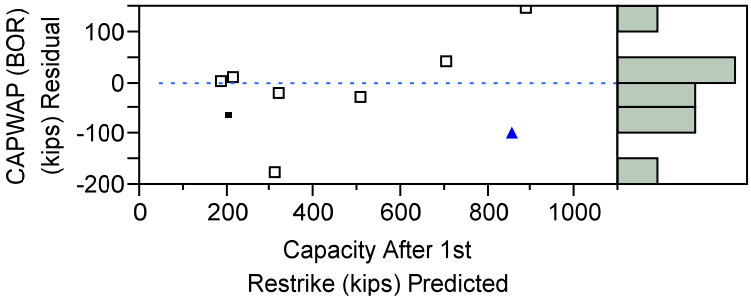

(a)

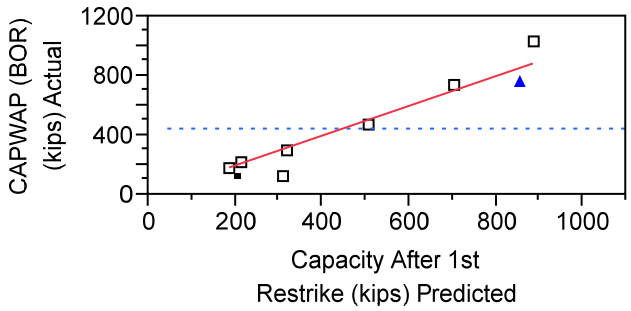

(b)

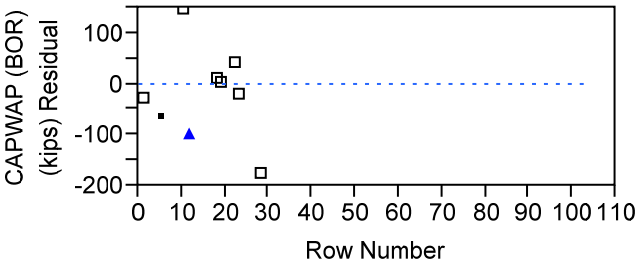

(c)

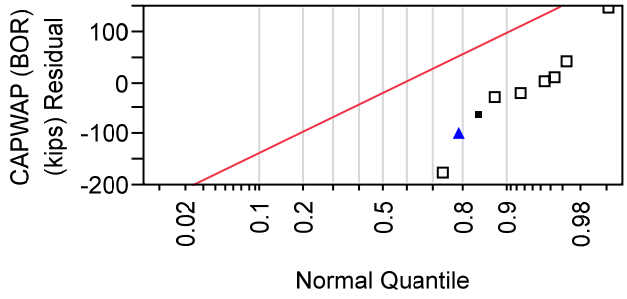

(d)

A.4 Diagnostics Plots of (a) Residual versus Predicted, (b) Actual versus Predicted, (c) Residual versus Row Order, and (d) Residual Normal Quantile for the Regression Analysis of CAPWAP (BOR-14 days) Capacity versus SLT Capacity presented in Figure 3-16.

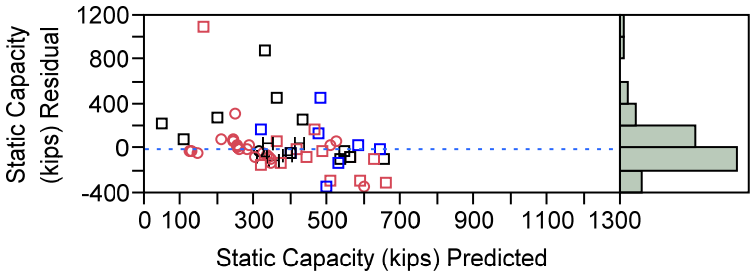

(a)

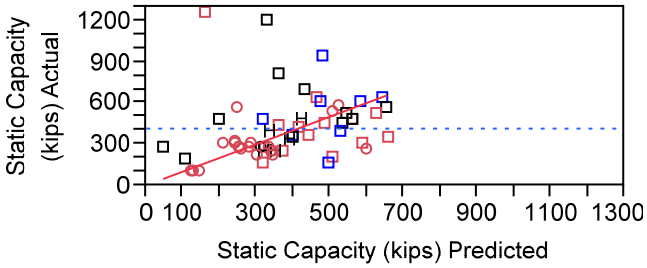

(b)

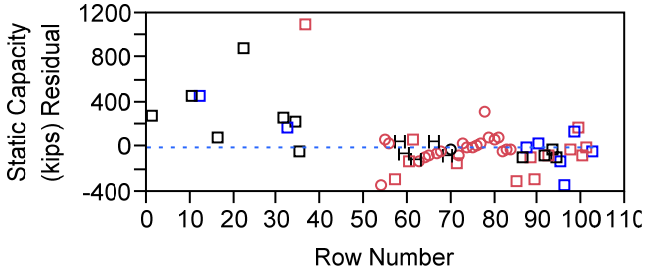

(c)

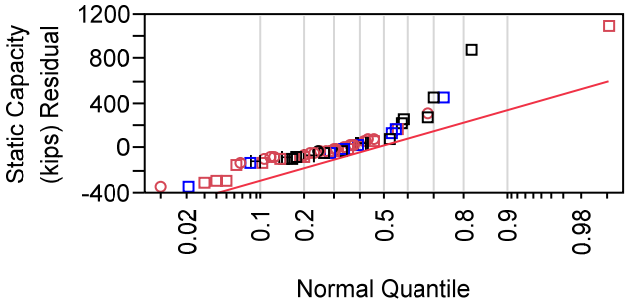

(d)

A.5 Diagnostics Plots of (a) Residual versus Predicted, (b) Actual versus Predicted, (c) Residual versus Row Order, and (d) Residual Normal Quantile for the Regression Analysis of Static Analysis (DRIVEN) versus CAPWAP (EOD) presented in Figure 3-17.

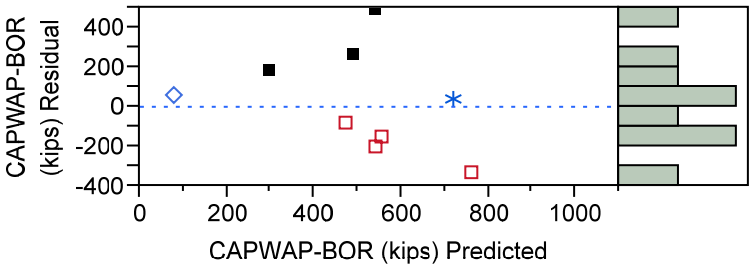

(a)

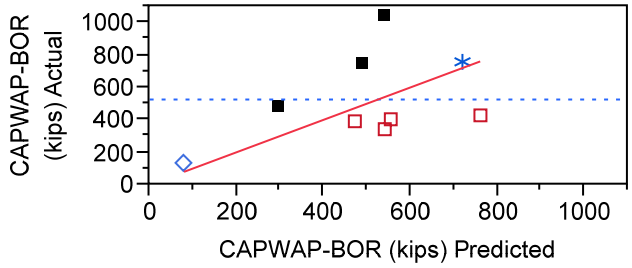

(b)

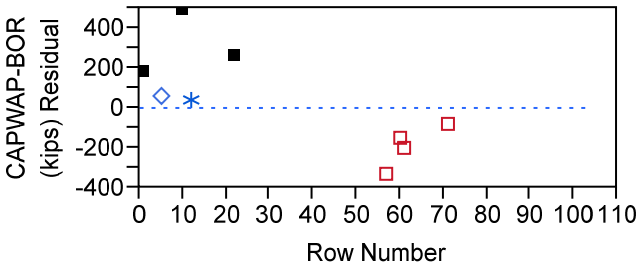

(c)

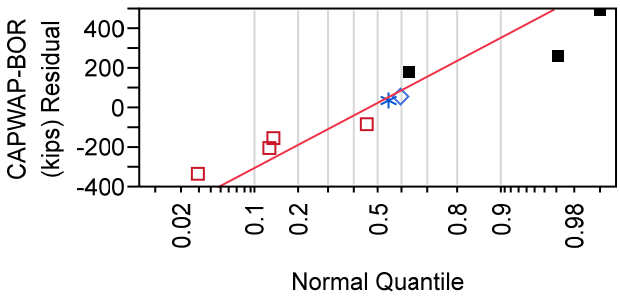

(d)

A.6 Diagnostics Plots of (a) Residual versus Predicted, (b) Actual versus Predicted, (c) Residual versus Row Order, and (d) Residual Normal Quantile for the Regression Analysis between CAPWAP-BOR and EOD presented in Figure 3-18

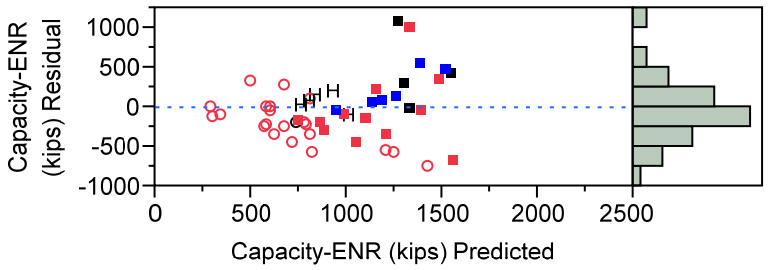

(a)

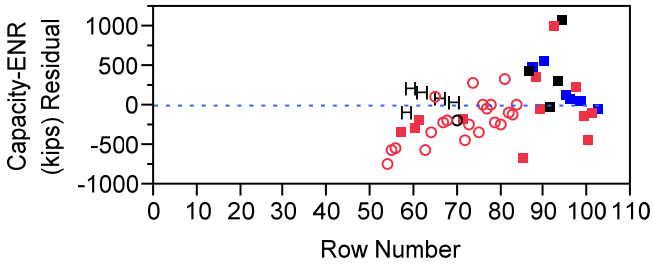

(b)

A.7 Diagnostics Plots of (a) Residual versus Predicted, and (b) Residual versus Row Order for the Regression Analysis of ENR Capacity versus CAPWAP-EOD Capacity presented in Figure 3-21.

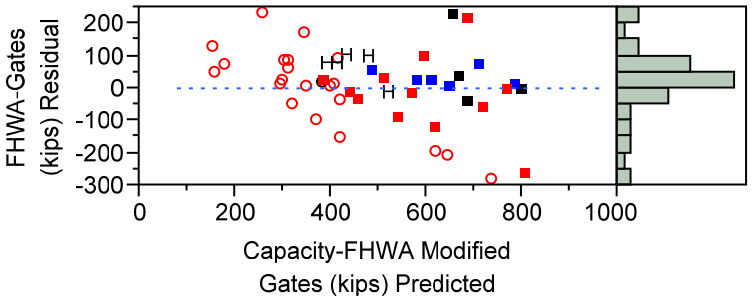

(a)

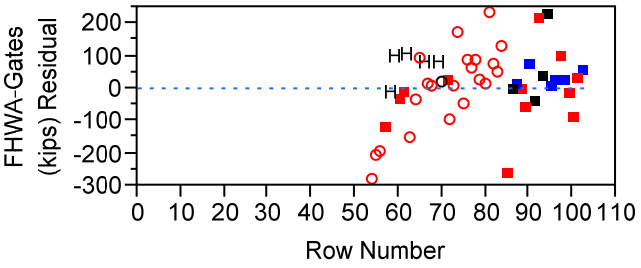

(b)

A.8 Diagnostics Plots of (a) Residual versus Predicted, and (b) Residual versus Row Order for the Regression Analysis of FHWA-Gates Capacity versus CAPWAP-EOD Capacity presented in Figure 3-22.

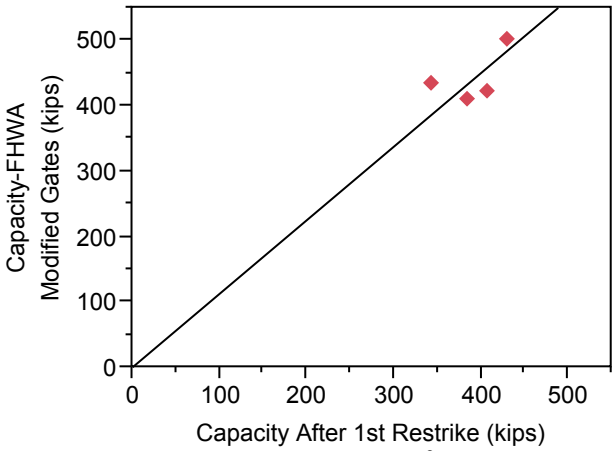

(a) b = 1.126, R^2= 0.532

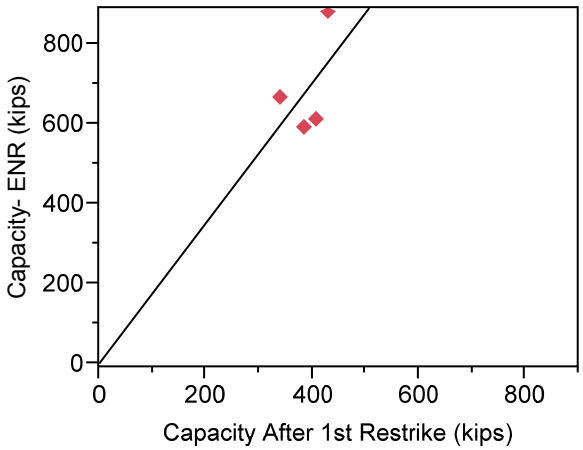

(b) b = 1.755, R^2= 0.252

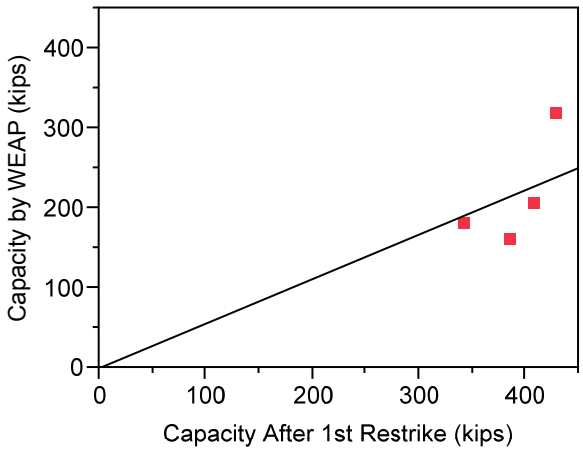

(c) b = 0.557, R^2= 0.119

A.9 Linear Fit between Capacity by CAPWAP-BOR and (a) FHWA-Gates Capacity, (b) ENR Capacity, and (c) WEAP Capacity as Discussed in Section 3.3.3.

Appendix B Resistance Factor versus Reliability Index

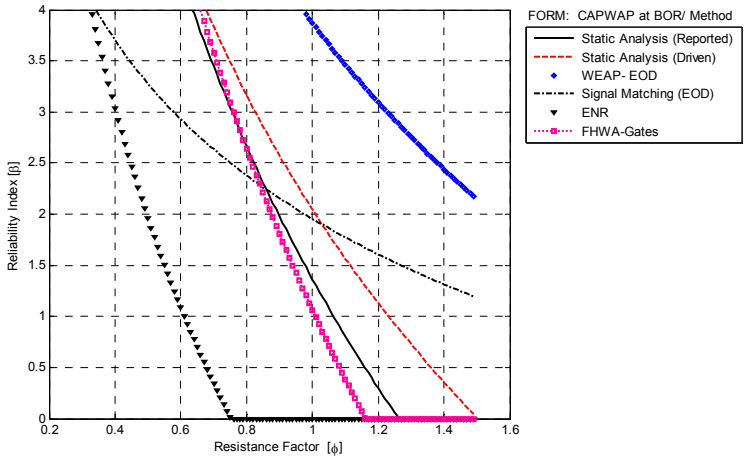

B.1 Resistance Factor versus Reliability Index for different Pile Analysis Methods referenced to BOR Capacity using FORM for the Statistics presented in Table 3-12.

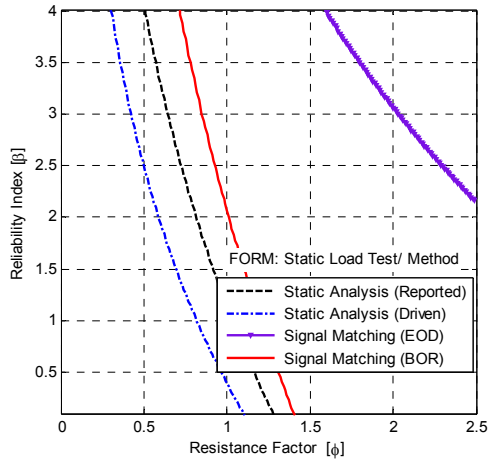

(a) SLT/Method

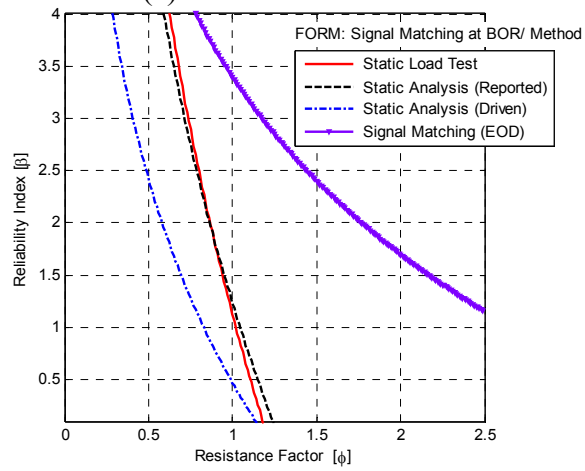

(b) CAPWAP-BOR/Method

B.2 Resistance Factor versus Reliability Index in Cohesive Soils based on FORM for the Statistics presented in Table 3-15.

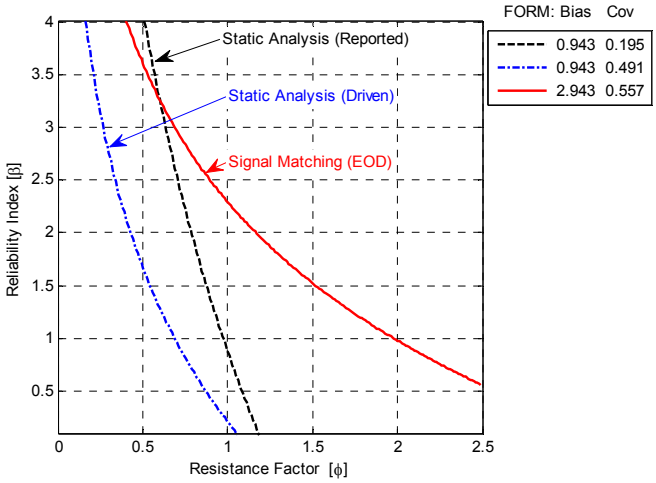

(a) Resistance Factors in Mixed Soils based on FORM for SLT/Method Statistics presented in Table 3-14.

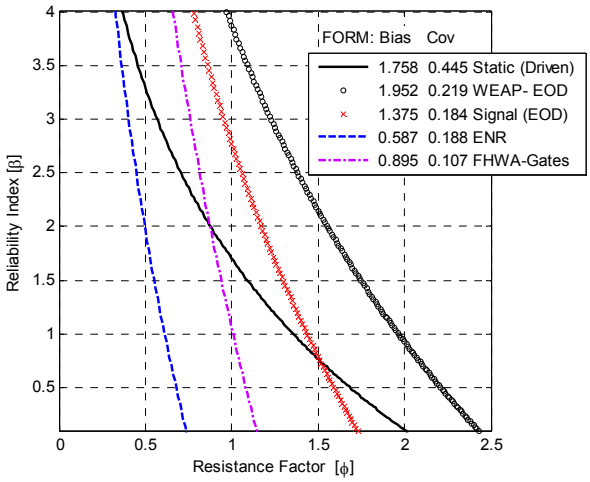

(b) Resistance Factors in Sands based on FORM for CAPWAP (BOR)/Method Statistics presented in Table 3-16.

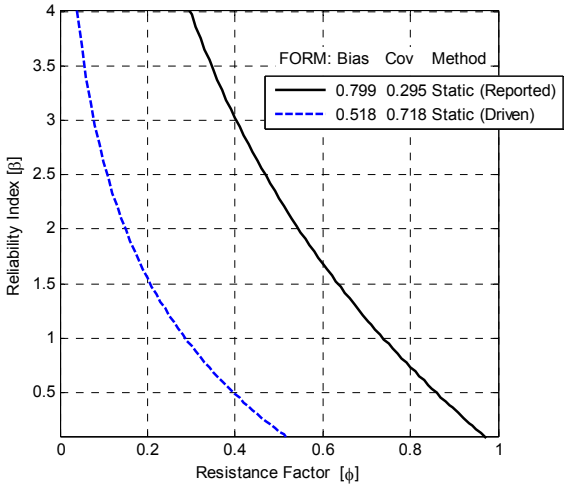

(c) Resistance Factors in Sands based on FORM for SLT/Method Statistics presented in Table 3-16.

B.3 Resistance Factor versus Reliability Index for different Pile Analysis Methods in Mixed Soil Layers and Non-Cohesive Soils based on First Order Reliability Method (FORM) for the Statistics presented in Table 3-14 and Table 3-16.

Appendix C Performance of Resistance Factors

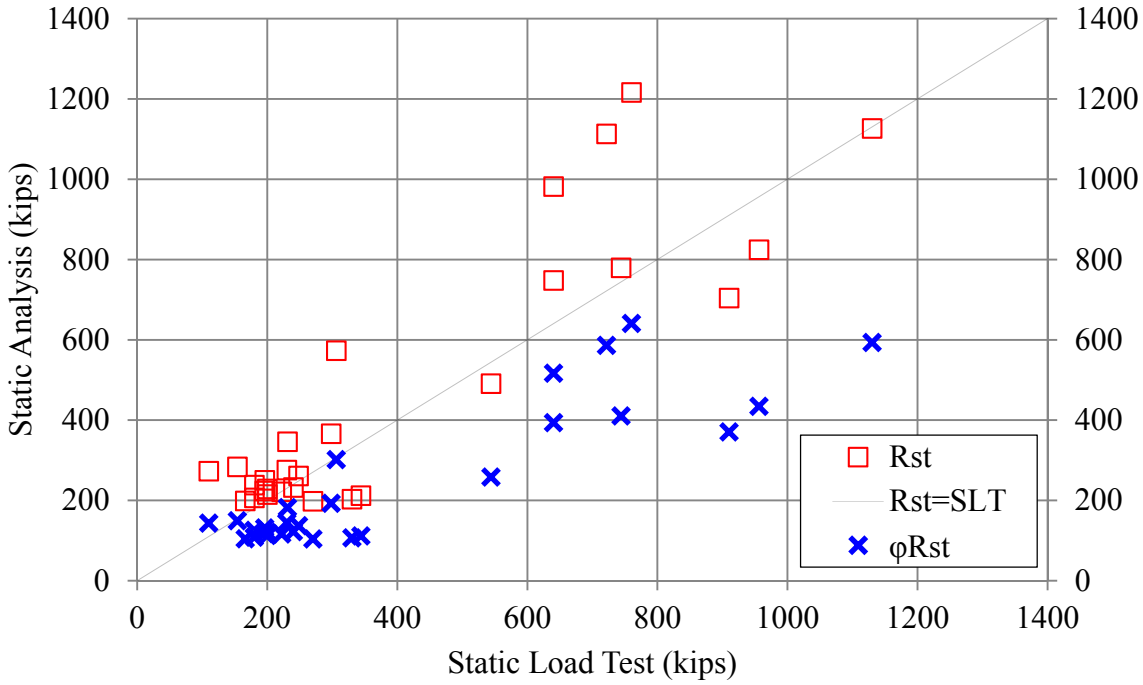

C.1 Davisson's Criterion versus Static Analysis Method: Nominal and Factored Capacities (β = 2.33, ϕ = 0.527, Cohesive Soils).

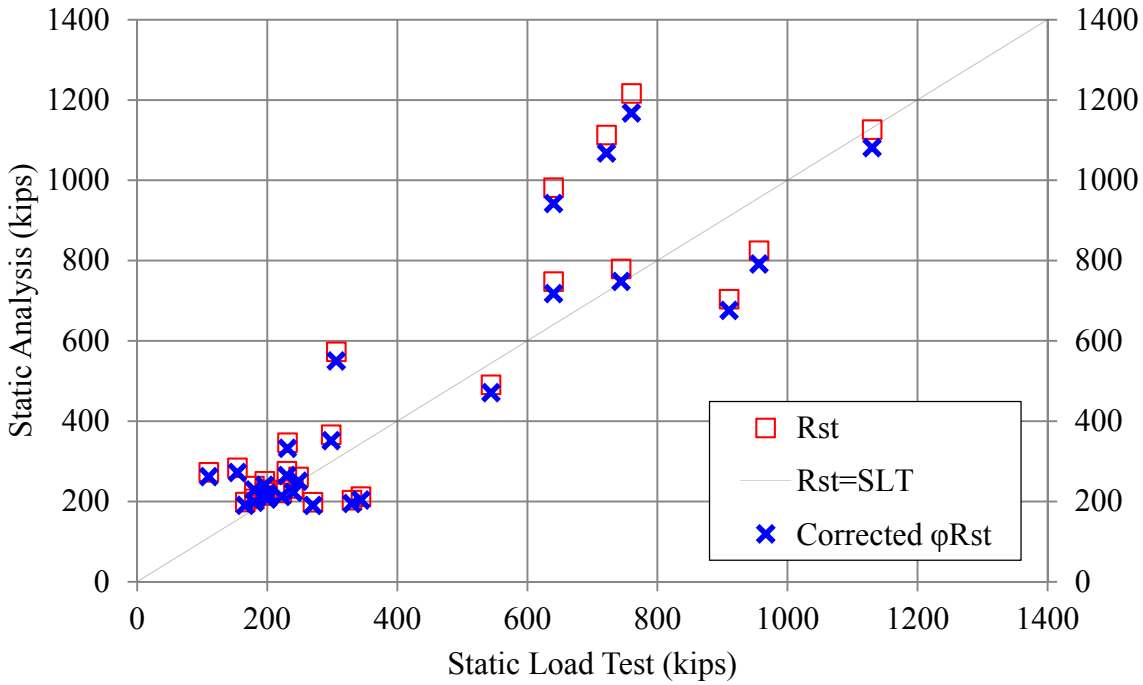

C.2 Davisson's Criterion versus Static Analysis Method by Incorporating Construction Control Method (β = 2.33, ϕ = 0.960, Cohesive Soils).

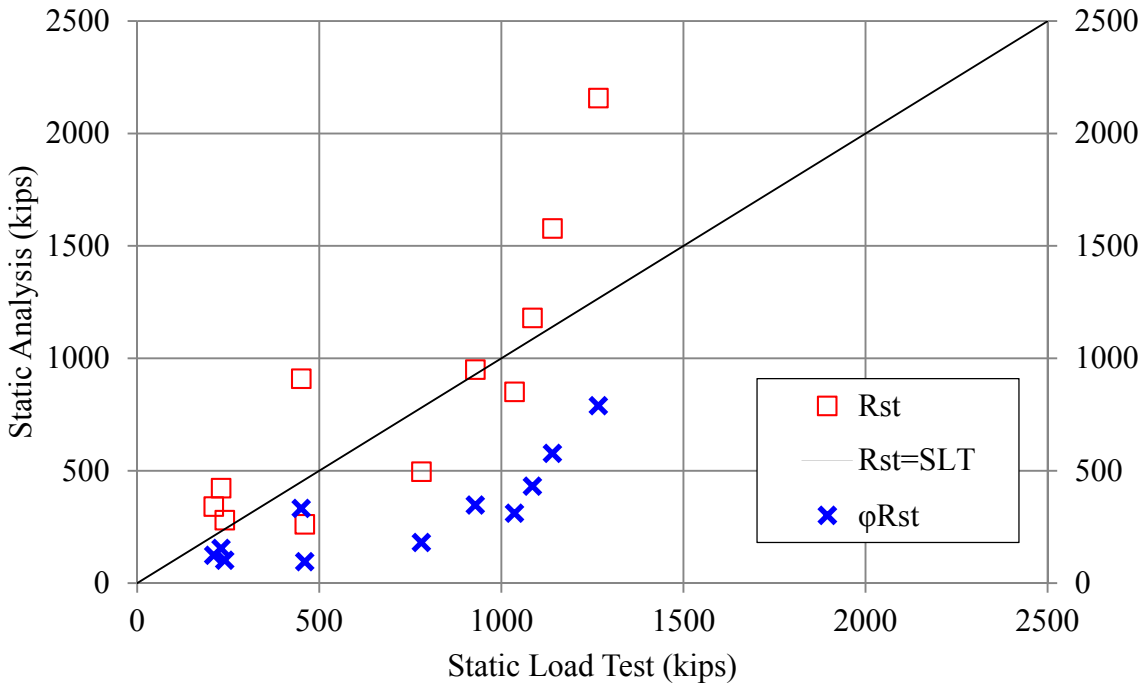

C.3 Davisson's Criterion versus Static Analysis Method: Nominal and Factored Capacities (β = 2.33, ϕ = 0.366, Mixed Soils).

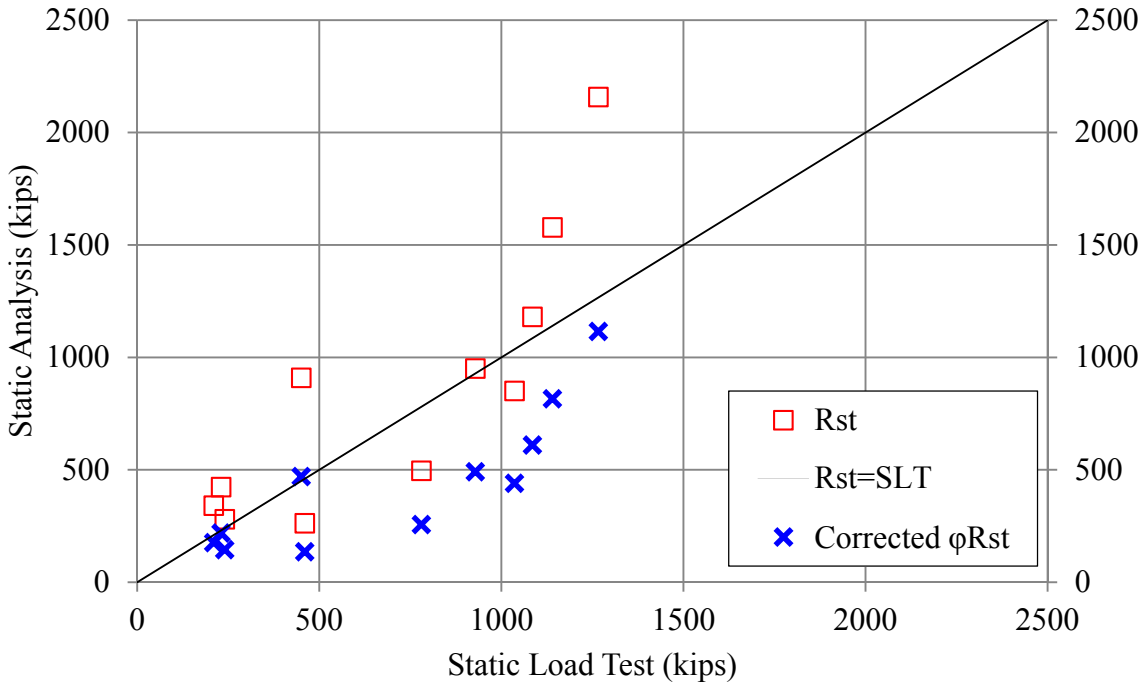

C.4 Davisson's Criterion versus Static Analysis Method by Incorporating Construction Control Method (β = 2.33, ϕ = 0.517, Mixed Soils).

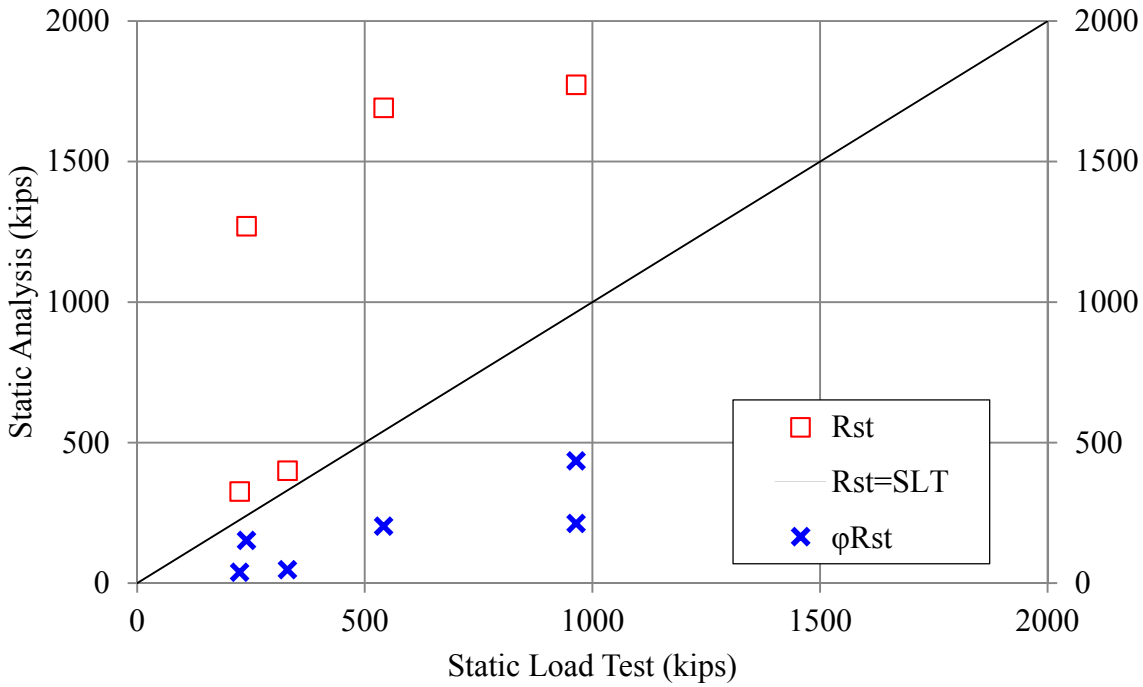

C.5 Davisson's Criterion versus Static Analysis Method: Nominal and Factored Capacities (β=2.33, ϕ=0.120, Cohesionless Soils).

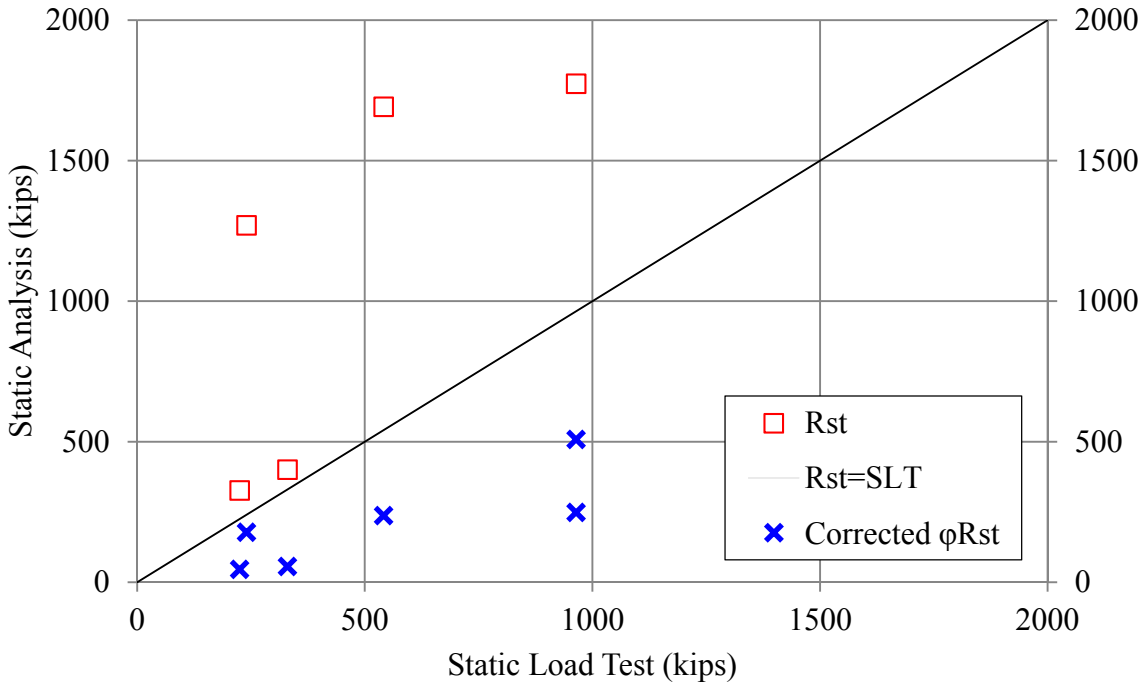

C.6 Davisson's Criterion versus Static Analysis Method by Incorporating Construction Control Method (β = 2.33, ϕ = 0.140, Cohesionless Soils).

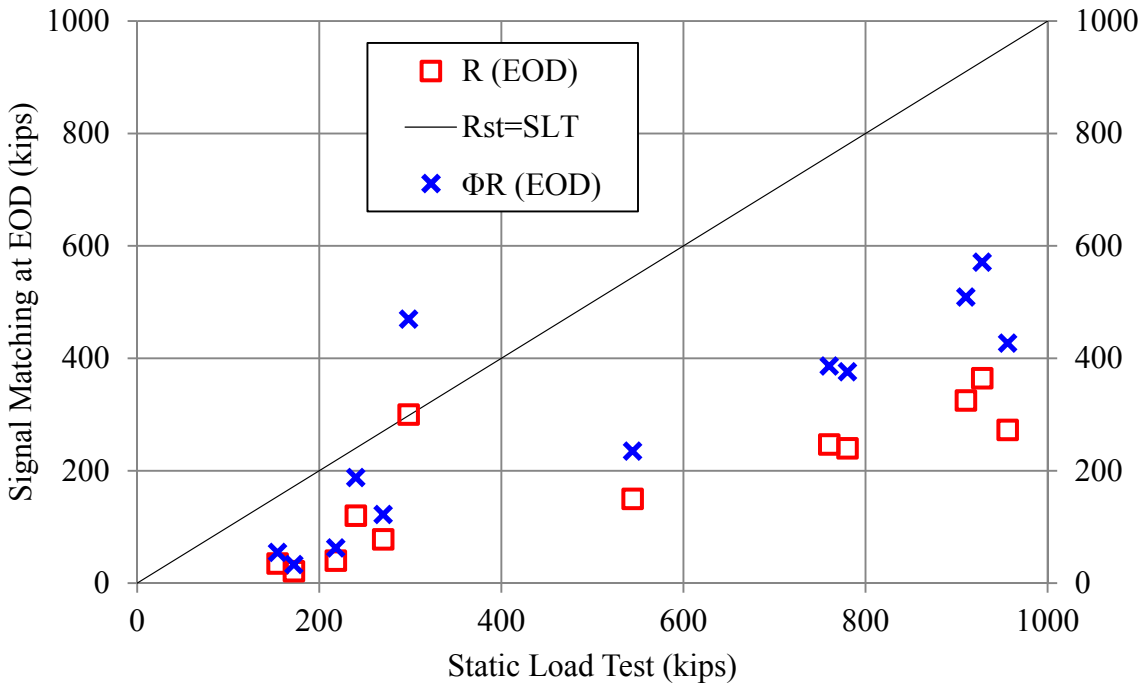

C.7 Davisson's Criterion versus Signal Matching at EOD: Nominal and Factored Capacities ($\beta = 2.33$, $\phi = 1.567$, All Soils).

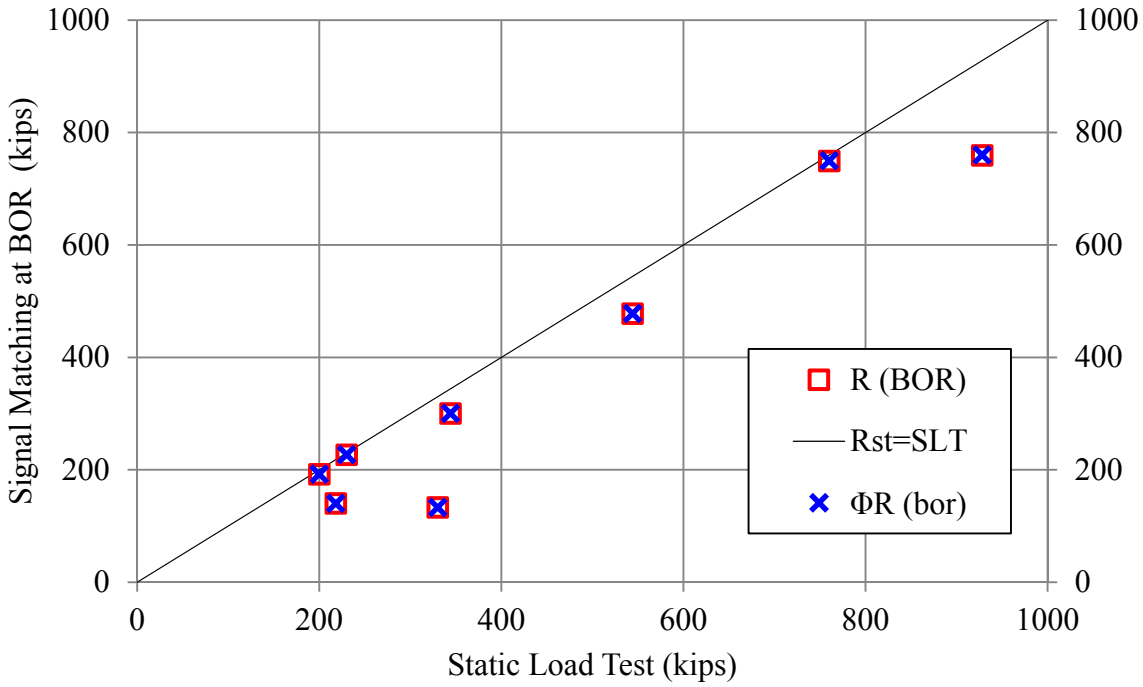

C.8 Davisson's Criterion versus Signal Matching at BOR: Nominal and Factored Capacities ($\beta = 2.33$, $\phi = 1.001$, All Soils).